UNIVERSIDADE DE LISBOA

FACULDADE DE FARMÁCIA

Targeting Neuroinflammation and Neurodegeneration in Parkinson's Disease

Sara Rodrigues Oliveira

Orientadores: Prof. Doutora Cecília Maria Pereira Rodrigues

Prof. Doutora Joana São José Dias Amaral

Prof. Doutor Félix Dias Carvalho

Tese especialmente elaborada para obtenção do grau de Doutor em Farmácia, especialidade em Biologia Celular e Molecular

2021

UNIVERSIDADE DE LISBOA

FACULDADE DE FARMÁCIA

Targeting Neuroinflammation and Neurodegeneration in Parkinson's Disease

Sara Rodrigues Oliveira

Orientadores: Prof. Doutora Cecília Maria Pereira Rodrigues

Prof. Doutora Joana São José Dias Amaral

Prof. Doutor Félix Dias Carvalho

Tese especialmente elaborada para obtenção do grau de Doutor em Farmácia, especialidade em Biologia Celular e Molecular

Júri:

Presidente: Doutor António José Leitão das Neves Almeida, Professor Catedrático e Presidente do Conselho Científico da Faculdade de Farmácia da Universidade de Lisboa

Vogais:

- Doutora Sandra Isabel Morais de Almeida Costa Cardoso, Professora Auxiliar da Faculdade de Medicina da Universidade de Coimbra;

- Doutor Hugo Miguel Vicente Miranda, Professor Auxiliar Convidado e Investigador Principal da Faculdade de Ciências Médicas da Universidade Nova de Lisboa;

- Doutor Joaquim José Coutinho Ferreira, Professor Associado da Faculdade de Medicina da Universidade de Lisboa;

- Doutor Rui Ferreira Alves Moreira, Professor Catedrático da Faculdade de Farmácia da Universidade de Lisboa;

- Doutora Joana São José Dias Amaral, Professora Auxiliar da Faculdade de Farmácia da Universidade de Lisboa, Orientadora.

2021

The studies presented in this thesis were performed at the Research Institute for Medicines (iMed.ULisboa), Faculty of Pharmacy, Universidade de Lisboa, under the supervision of Professor Cecília Maria Pereira Rodrigues, Professor Joana São José Dias Amaral and Professor Félix Dias Carvalho.

Sara Rodrigues Oliveira received a Ph. D. fellowship (PD/BD/128332/2017) from the PhD Programme in Medicines and Pharmaceutical Innovation (i3DU) Fundação para a Ciência e Tecnologia (FCT), Lisbon, Portugal. Part of these studies were funded by FEDER through the COMPETE programme and by FCT to CMPR (grants SAICTPAC/0019/2015 - LISBOA-01-0145-FEDER-016405 and PTDC/MED-FAR/29097/2017 - LISBOA-01-0145-FEDER-029097.

TABLE OF CONTENTS

List of Figures

List of Tables

PUBLICATIONS

The studies presented in this thesis were performed at the Research Institute for Medicines (iMed.ULisboa), Faculty of Pharmacy, Universidade de Lisboa, under the scientific supervision of Professor Cecília Maria Pereira Rodrigues, Professor Joana São José Dias Amaral and Professor Félix Dias Carvalho.

The research described in Chapters 2 and 3 is based on work that has been published in international peer-reviewed journals, as follows:

Oliveira SR, Dionísio PA, Brito H, Franco L, Rodrigues CAB, Guedes RC, Afonso CAM, Amaral JD, Rodrigues CMP. 2018. Phenotypic screening identifies a new oxazolone inhibitor of necroptosis and neuroinflammation. *Cell Death Discov*. 5:10

Oliveira SR, Dionísio PA, Gaspar MM, Ferreira MBT, Rodrigues CAB, Pereira RG, Estevão MS, Perry MJ, Moreira R, Afonso CAM, Amaral JD, Rodrigues CMP. 2021. Discovery of a necroptosis inhibitor improving dopaminergic neuronal loss after MPTP exposure in mice*. Int J Mol Sci.* 22(10):5289

Oliveira SR, Dionísio PA, Correia Guedes L, Gonçalves N, Coelho M, Rosa MM, Amaral JD, Ferreira JJ, Rodrigues CMP. 2020. Circulating inflammatory miRNAs associated with Parkinson's disease pathophysiology. *Biomolecules.* 10(6):945

Oliveira SR, Dionísio PA, Gaspar MM, Correia Guedes L, Coelho M, Rosa MM, Ferreira JJ, Amaral JD, Rodrigues CMP. 2021. miR-335 targets LRRK2 and mitigates inflammation in Parkinson's disease. *Front Cell Dev Biol.* 9:661461

The following manuscripts were also published during the period of this thesis:

Dionísio PA, **Oliveira SR**, Amaral JD, Rodrigues CMP. 2019. Loss of microglial parkin inhibits necroptosis and contributes to neuroinflammation. *Mol Neurobiol*. 56(4):2990-3004

Dionísio PA, **Oliveira SR**, Gaspar MM, Gama MJ, Castro-Caldas M, Amaral JD, Rodrigues CMP. 2019. Ablation of RIP3 protects from dopaminergic

neurodegeneration in experimental Parkinson's disease. *Cell Death Dis.* 10(11):84

ABBREVIATIONS

3’-UTR - 3’-untranslater region

4HB - four-helix bundle

6-OHDA - 6-hydroxydopamine

8-OHdG - 8-hydroxydeoxyguanosine

AADC - aromatic amino acid decarboxylase

AD - Alzheimer’s disease

AKT - protein kinase B

ALS - amyotrophic lateral sclerosis

ANK - ankyrin-like repeats

AP1 - activator protein 1

BBB - blood brain barrier

BCR-ABL - breakpoint cluster region-abelson leukemia

BDNF - brain-derived neurotrophic factor

Bim - Bcl-1-interacting mediator of cell death

CDC37 - cell cycle division cycle 37

cFLIP - cellular FLICE-like inhibitory protein

CHIP - carboxyl terminus of Hsp-70-interacting protein

CNS - central nervous system

COMT - catechol-O-methyltransferase

COR - carboxyl terminal of Ras of complex protein

COX - cyclo-oxygenase

CSF - cerebrospinal fluid

CYLD - cylindromatosis

DAMPs - damage-associated molecular patterns

DAT - dopamine transporters

DJ-1 - deglycase-1

DLP1 - dynamin-like protein 1

DR - death receptor

DRP1 - dynamic related protein 1

EOPD - early-onset Parkinson’s disease

ERK - extracelular-signal-regulated kinase

FADD - FAS-associated death domain protein

GBA - glucocerebrosidase

GDNF - glial-derived neurotrophic factor

GFAP - glial fibrillary acidic protein

GLUD1 - glutamine dehydrogenase 1

H&Y - Hoehn and Yahr

HD - Huntington's disease

HMGB1 - high-mobility group protein B1

HOIL-1 - hem-oxidized iron-regulatory protein 2 ubiquitin ligase-1

HOIP - HOIL-1L interacting protein

IAV - influenza A virus

IDO - indoleamine 2,3-dioxygenase

IFN-γ - interferon-γ

IL - interleukin

iNOS - inducible nitric oxide synthase

iPD - idiopathic Parkinson's disease

JNK - c-Jun N-terminal kinase

Ko - knock-out

LB - Lewy body

L-DOPA - levodopa

LPS - lipopolysaccharide

LRR - leucin-rich repeats

LRRK2 - leucine-rich repeat kinase 2

LUBAC - linear ubiquitin chain assembly complex

MAOB - monoamine oxidase B

MAPK - mitogen-activated protein kinase

MDS - movement disorder society

miRISC - miRNA-induced silencing complex

miRNA - microRNA

MLK - mixed-lineage kinase

MLKL - mixed lineage kinase domain-like protein

$MPDP^+$ - 1-methyl-4-phenyl-2,3-dihydropyridinium

MPP^+ - 1-methyl-4-phenylpiridinium ion

MPT - mitochondria pore transition

MPTP - 1-methyl-4-phenyl-1,2,3,6-tetrahydropyridine

mRNA - messenger RNA

MS - multiple sclerosis

mTOR - mammalian target of rapamycin

MyD88 - myeloid differentiation 88

Nec-1 - necrostatin-1

Nec-1s - Nec-1 stable

NEMO - NF-κB essential modulator

NF-κB - nuclear factor (NF)-κB

NLRP3 - nod-like receptor pyrin domain-containing 3

NO - nitric oxide

OGC - oxygen-glucose deprivation

PAMPs - pathogen-associated molecular patterns

PBMC - peripheral blood mononuclear cell

PD - Parkinson’s disease

PET - positron emission tomography

PGAM5 - phosphoglycerate mutase family member 5

PIP - phosphatidylinositol phosphate

Pre-miRNA - precursor miRNA

Pri-miRNA - primary miRNA

PRR - pattern recognition receptors

RCD - regulated cell death

RHIM - RIP homotypic interacting motif

RIP - receptor-interacting protein

ROC - Ras of complex protein

ROS - reactive oxygen species

SHARPIN - SHANK-associated RH domain-interacting protein

SN - substantia nigra pars compacta

SP1 - specificity protein 1

SPECT - single-photon emission computed tomography

TAK1 - transforming growth factor beta-activated kinase 1

TH - tyrosine hydroxylase

TIRAP - TIR-domain-containing adapter protein

TLR - toll-like receptor

TNFR1 - TNF receptor 1

TNF-α - tumour necrosis factor α

TRADD - TNFR1-associated death domain protein

TRAF2 - TNF-associated factor 2

TRAIL - TNF-related apoptosis-inducing ligand receptor

TRIF - TIR-domain-containing adapter-inducing interferon-β

UPDRS - unified Parkinson's disease rating scale

Wt - wild-type

zVAD-fmk - carbobenzoxy-valyl-alanyl-aspartyl-[O-methyl]- fluoromethylketone

zVAD - zVAD-fmk

α -syn - α-synuclein

ABSTRACT

Parkinson's disease (PD) is the second most common neurodegenerative disease worldwide, being mostly characterized by motor features correlating with dopaminergic neuronal degeneration in the *substantia nigra pars compacta* (SN) and striatum. Although predominantly sporadic, approximately 10% of all cases are classified as heritable forms of PD, with mutations in the leucine-rich repeat kinase 2 (*LRRK2*) gene being the most frequent known cause of familial PD. Necroptosis is a caspase-independent form of regulated cell death mediated by the strenuous action of receptor-interacting protein 3 (RIP3) and pseudokinase mixed lineage domain-like protein (MLKL), being also dependent on RIP1 kinase activity, according with the cellular context. Importantly, in the past few years, activation of necroptosis has been linked to PD, while necroptosis inhibition results in disease improvement, unveiling an alternative approach for therapeutic intervention. In turn, microRNAs (miRNAs or miRs), including miR-335, are small non-coding RNAs, whose deregulation has been associated with neurodegeneration and neuroinflammation in different neurodegenerative conditions, such as PD. Identification of deregulated miRNAs may serve as biomarkers for disease detection and prognosis prediction, can help in understanding the complex mechanism of neurodegenerative disease development, and their use in therapy may tackle several issues of aging and neurodegeneration.

The main objectives of this thesis were to extend the current knowledge on therapeutic approaches in PD, mostly focusing on the discovery of novel small molecule inhibitors of necroptosis, as well as miRNAs that could represent promising therapeutic strategies and/or biomarkers of disease.

In our first work, we phenotypically screened a library of 21 newly synthetized small compounds to identify novel inhibitors of necroptosis, using the BV2 murine microglial cell line treated with the well-known pan-caspase inhibitor, zVAD-fmk (zVAD). We identified one hit – compound Oxa12 – that strongly inhibited zVAD-induced necroptosis. Importantly, Oxa12 counteracted zVAD- and LPS-induced inflammation, by attenuating TNF-α and IL-1β expression. Moreover, Oxa12 negatively regulated JNK and p38 signalling pathways and NF-κB activation, thus suggesting an overall reduction of necroptosis-driven inflammation. In our second study, as a proof of concept, we evaluated the protective effect of Oxa12 *in vivo*, using the sub-acute 1-methyl-1-4-phenyl-

1,2,3,6-tetrahydripyridine hydrochloride (MPTP) PD-related mouse model. Importantly, we observed that Oxa12 protected from MPTP-induced dopaminergic neuronal loss in the SN and striatum. A combination of the analysis of whether Oxa12 was included in the CNS drug property space, using a CNS-multiparameter optimization (MPO) score and metabolic data indicated that Oxa12 has a good brain exposure and an estimated half-life of 13 minutes, turning this compound into a novel addition to the chemical toolbox of CNS-targeting anti-necroptotic compounds. Overall, Oxa12 is a good drug candidate for further optimization to attenuate PD pathogenesis.

Finally, we investigated the expression profile of a selected panel of miRNAs, previously linked to cell death and/or inflammatory pathways, in the serum of idiopathic PD (iPD) patients and patients carrying a mutation in the *LRRK2* gene (LRRK2-PD), and aged-matched healthy controls, and investigated its value as molecular marker of disease pathogenesis. We determined a differential pattern of miRNA expression between PD patients and age- and gender-matched healthy individuals, with a downregulation of miR-146a, miR-335-3p and miR-335-5p in PD patients in comparison with controls, and no significant alteration in miR-21, miR-34a, miR-34c and miR-155. Interestingly, miR-155 was significantly upregulated in the serum of LRRK2-PD patients versus iPD patients. Since miR-146a role in neurodegenerative diseases with an inflammatory component was already better known, and *in silico* studies pointed LRRK2 as a putative target of miR-335, we decided to dissect the protective role of miR-335 in experimental models of PD, during inflammatory and/or neurodegenerative events. Our results clearly demonstrated that miR-335 is downregulated in various PD-mimicking conditions, including LPS-stimulated and/or LRRK2wt-overexpressing BV2 microglia cells. These results were further confirmed in the serum of MPTP-injected mice. In terms of mechanism, we confirmed that miR-335 directly targets LRRK2 mRNA. More importantly, miR-335 overexpression clearly counteracted proinflammatory gene expression induced by LPS and LRRK2wt, in BV2 and N9 microglia cells. Further, miR-335 also reduced LPS-induced RIP1 and RIP3 proteins and activation of ERK1/2 and NF-κB cascade. In SH-SY5Y neuroblastoma cells, miR-335 reduced α-synuclein-triggered proinflammatory gene expression.

In conclusion, we identified one compound – Oxa12 – that strongly inhibits necroptosis *in vitro*, in the murine L929 fibroblast and BV2 microglia cell lines and protected from MPTP-driven dopaminergic neuronal loss *in vivo*, being therefore considered a strong drug candidate for further optimization to slow or attenuate PD pathogenesis. In addition, we identified different miRNA signatures between PD patients, including iPD and LRRK2-PD patients and healthy controls, and further unravelled novel roles for miR-335 in microglia and neuronal cells that halt chronic neuroinflammation effects induced by a classical inflammatory stimulus or even LRRK2wt overexpression. Overall, further characterization of the synergistic function of necroptosis inhibition and miRNA-based strategies may highlight their therapeutic potential for several neurodegenerative diseases with a strong neuroinflammatory component, such as PD.

Keywords: LRRK2; neuroinflammation; miRNAs; MPTP; necroptosis; Parkinson's disease.

RESUMO

A doença de Parkinson (DP) é a segunda doença neurodegenerativa mais comum a nível mundial. Devido à sua estreita correlação com o envelhecimento, é esperado que a prevalência da DP continue a aumentar juntamente com o aumento da esperança média de vida da população em países desenvolvidos. A DP é uma doença clinicamente heterogénea, de carácter crónico e debilitante e as suas atuais opções terapêuticas destinam-se somente ao tratamento sintomático da doença. No entanto, aquando do aparecimento dos característicos sintomas motores da DP, e diagnóstico final da doença, a deterioração cognitiva é já existente. Dessa forma, é de extrema importância o desenvolvimento de novas alternativas terapêuticas, de forma a reverter ou, pelo menos, atenuar, a progressão da doença. Os sintomas motores da DP resultam da neurodegenerescência dopaminérgica na *substantia nigra pars compacta* (SN) e no estriado. Apesar da DP ser predominantemente esporádica, aproximadamente 10% dos casos são classificados como formas hereditárias da doença, sendo que mutações no gene *leucine-rich repeat kinase* (*LRRK2*) constituem a forma mais frequente de DP familiar. Neste contexto, mutações que resultam no ganho de função da LRRK2 levam ao desenvolvimento de DP de forma autossómica dominante. De facto, a proteína LRRK2 tem sido bastante estudada ao longo dos últimos anos, parecendo ter um papel importante na disfunção mitocondrial, desregulação de vias autofágicas e, ainda, na neuroinflamação crónica e morte neuronal observada na DP.

A necroptose é um tipo de morte celular morfologicamente semelhante à necrose sendo, porém, regulada por mecanismos moleculares concretos. Dessa forma, o seu mecanismo de morte pode ser alvo de intervenção terapêutica. Em termos mecanísticos, a necroptose é um tipo de morte celular regulada, independente de caspases, que ocorre a jusante da ativação de recetores de morte celular, sendo o recetor do fator de necrose tumoral α (TNF-α) o mais bem estudado. A ativação dos recetores de morte pode resultar no recrutamento e consequente ativação das cinases *receptor interacting protein* 1 (RIP1) e 3 (RIP3), em condições em que a caspase-8 esteja ausente ou inibida. Consequentemente, a cinase RIP3, quando ativada, recruta e fosforila a proteína *mixed linease kinase domain-like* (MLKL) que, por sua vez, pode formar oligómeros capazes de interagir com a membrana celular e promover a sua permeabilização, com consequente libertação do conteúdo intracelular.

Recentemente, a ativação da necroptose tem sido descrita em várias doenças neurodegenerativas, incluindo na DP. De facto, a análise de amostras de cérebro de doentes com DP demonstrou a presença de níveis elevados de RIP1, RIP3 e MLKL na SN, o que sugere um papel importante da necroptose na progressão da doença. Um aspeto importante é o facto da inibição farmacológica da necroptose, através da inibição da atividade cinase da RIP1 pela necrostatina-1, demonstrar um papel protetor em diferentes modelos animais que mimetizam a DP.

Os microRNAs (miRNAs ou miRs) são pequenos RNAs conservados e não codificantes que contêm aproximadamente 21-25 nucleótidos e regulam negativamente a expressão genética após a transcrição. Durante os últimos anos, tem sido estudado o papel dos miRNAs como candidatos a biomarcadores de doença, incluindo da DP. De facto, os miRNAs podem ser facilmente detetados em diversos fluidos corporais, incluindo no sangue, saliva ou soro, o que os torna bastante interessantes como marcadores de diagnóstico. Para além disso, a investigação dos miRNAs como biomarcadores pode contribuir para que o diagnóstico de doença seja feito com recurso a técnicas menos invasivas, o que é especialmente importante na DP, na qual o diagnóstico é essencialmente baseado na avaliação de sintomas motores e cognitivos. Apesar dos miRNAs terem um papel biológico importante na manutenção das funções celulares fisiológicas, podem ainda assim assumir uma função patológica quando a sua expressão está desregulada. Nesse contexto, os miRNAs podem ser considerados bons candidatos para o diagnóstico e prognóstico de doença, assim como alvos promissores para intervenção terapêutica. O miR-335 é um exemplo que tem sido associado a processos de morte celular e inflamação em diversas doenças.

Os principais objetivos desta tese consistiram na identificação de novos inibidores de necroptose e, também, de miRNAs que pudessem ser estudados como potenciais estratégicas terapêuticas e/ou biomarcadores de doença, nomeadamente de DP.

No primeiro estudo, investigámos uma biblioteca de pequenos compostos de forma a identificar novos inibidores de necroptose, utilizando como modelo celular a linha celular de microglia BV2. Em primeiro lugar, verificámos que a inibição farmacológica de caspases com o pan-inibidor de caspases zVAD-fmk

(zVAD) resultou na indução de necroptose nas células de microglia. De seguida, identificámos um composto – Oxa12 – que inibiu em larga extensão a necroptose. Este resultado foi confirmado com a observação de que o composto Oxa12 diminuiu a presença da RIP1, RIP3 e MLKL fosforiladas nas frações proteicas insolúveis que representam a formação do necrosoma, o complexo que permite a ativação destes mediadores da necroptose. Para além desta função como inibidor de necroptose, verificámos que o composto Oxa12 diminuiu a inflamação induzida pela incubação das células de microglia com lipopolisacáridos (LPS), um componente das paredes celulares de bactérias Gram-negativas com elevado potencial inflamatório, o que foi observado pela diminuição dos níveis de expressão dos mediadores pró-inflamatórios TNF-α e IL-1β. Mais ainda, o composto Oxa12 foi capaz de regular negativamente a ativação das vias de sinalização *c-Jun N-terminal kinase* (JNK) e p38 *mitogen-activated protein kinase* (MAPK) e do fator de transcrição pró-inflamatório *nuclear factor-κB* (NF-κB). De seguida, como prova de conceito, avaliámos o papel protetor do composto Oxa12 em murganhos expostos a um regime sub-agudo de exposição à neurotoxina 1-metil-4-fenil-1,2,3,6-tetrahidropiridina (MPTP), que é habitualmente utilizada para induzir neurodegenerescência do circuito nigroestriatal em modelos experimentais da DP. Neste estudo, os murganhos expostos ao MPTP apresentaram um aumento significativo de perda neuronal na SN e no estriado. A administração terapêutica de Oxa12 por injeção intraperitoneal durante 30 dias protegeu da neurodegenerescência dopaminérgica neste modelo. Mais ainda, o composto Oxa12 apresentou uma boa exposição cerebral, indicado pela análise da pontuação de otimização de vários parâmetros do SNC, assim como um tempo de semivida de aproximadamente 13 minutos. De um modo geral, o composto Oxa12 demonstrou ser um bom candidato a futuras otimizações para atenuar a patogénese da DP.

De seguida, investigámos o perfil de expressão de um painel de miRNAs, anteriormente associados a vias de morte celular e/ou inflamação, em amostras de soro de doentes de Parkinson idiopáticos (iDP) e de doentes de Parkinson com mutação do gene *LRRK2* (LRRK2-DP) e indivíduos controlo, sem histórico de DP, de forma a determinar o seu papel na patogénese da DP. Neste estudo, observámos um perfil de expressão de miRNAs diferente entre doentes de

Parkinson e indivíduos controlo, sendo que observámos uma diminuição dos níveis de expressão dos miR-146a, miR-335-3p e miR-335-5p em doentes de Parkinson, enquanto os miR-21, miR-34a, miR-34c e miR-155 não apresentaram diferenças de expressão entre os grupos em estudo. Um aspeto interessante foi o facto de termos observado níveis elevados de expressão do miR-155 em doentes LRRK2-DP em comparação com doentes iDP.

Por último, decidimos aprofundar o potencial papel neuroprotetor do miR-335 em diferentes modelos experimentais de DP, durante processos inflamatórios e/ou de morte celular. Os nossos resultados demonstraram que os níveis de expressão do miR-335 estão claramente diminuídos em várias modelos celulares que mimetizam a DP, nomeadamente em células de microglia BV2 estimuladas com LPS e/ou com sobre-expressão da forma *wild-type* da LRRK2 (LRRK2wt). A diminuição dos níveis de expressão do miR-335 foi posteriormente confirmada no soro de murganhos expostos a um regime sub-agudo de exposição à neurotoxina MPTP em comparação com murganhos controlo. Em termos de mecanismo, o miR-335 tem como alvo direto o RNA mensageiro da LRRK2. Mais importante, o miR-335 contrariou claramente o aumento das proteínas RIP1 e RIP3 e da expressão de genes pró-inflamatórios induzido pela estimulação das células de microglia BV2 e N9 com LPS. Para além disso, o miR-335 diminuiu a ativação da via de sinalização ERK1/2 e do fator de transcrição NF-κB promovidos pela estimulação das células com LPS. Por último, o miR-335 é também capaz de reduzir a expressão de genes pró-inflamatórios que resultam da sobre-expressão da LRRK2wt em células de microglia BV2. Do mesmo modo, em células de neuroblastoma, SH-SY5Y, o miR-335 diminuiu a expressão de genes pró-inflamatórios induzidos pela sobre-expressão de α-sinucleína.

Em conclusão, os nossos estudos permitiram identificar uma nova molécula – Oxa12 – que inibe fortemente a morte celular por necroptose em células de microglia BV2 e, mais importante, diminui a neurodegenerescência dopaminérgica na SN e estriado em murganhos expostos à neurotoxina MPTP. Sendo assim, este composto pode ser considerado um forte candidato farmacológico para ser otimizado e utilizado em terapêuticas que atenuem a patogénese da DP. Mais ainda, identificámos um perfil de expressão de miRNAs que diferencia claramente doentes de Parkinson e indivíduos controlo.

Adicionalmente, desvendámos novos papeis para o miR-335, tanto em células de microglia como células neuronais, na diminuição da neuroinflamação crónica promovida por estímulos inflamatórios clássicos ou, até, pela sobre-expressão da LRRK2wt. Assim, uma caracterização mais profunda dos efeitos sinérgicos da inibição da necroptose juntamente com estratégias que tenham por base a modulação da expressão de miRNAs poderá elucidar acerca do seu potencial terapêutico em diversas doenças neurodegenerativas com uma preponderante componente inflamatória, tal como a DP.

Palavras-chave: Doença de Parkinson; neuroinflamação; LRRK2; miRNAs; MPTP; necroptose.

Chapter 1

GENERAL INTRODUCTION

1.1. Parkinson's disease

Parkinson's disease (PD) dates to 1817 when James Parkinson described in the monograph "An Essay on the Shaking Palsy" a disease that he called "*paralysis agitans*". Several years later, a French neurologist, Jean-Martin Charcot, named this disorder Parkinson's disease (PD) in memory of James Parkinson.

PD is the second most common progressive neurodegenerative disorder and the most prevalent movement disorder worldwide, affecting approximately 1-2% of people older than 65 years and 4-5% of people above 85 years of age (Lees 2007). Since PD onset is strongly linked to age, the prevalence of the disease is expected to continue to increase along with the increase in the lifespan of the population in develop countries.

Throughout the years, several studies have clarified the hallmarks of PD, as being the progressive loss of dopaminergic neurons in the *substantia nigra pars compacta* (SN) and consequent depletion of dopamine and axonal degeneration, as well as the presence of intracellular accumulation of protein aggregates composed of misfolded forms of α-synuclein (α-syn) in neuronal cell bodies, called Lewy bodies (LBs), and chronic neuroinflammation (**Figure 1.1**) (Dzamko, Geczy, and Halliday 2015; Poewe et al. 2017).

However, almost two centuries after PD first descriptions, there is still no effective cure and the knowledge of PD aetiology and development remains incomplete. Thus, it is of strong importance to clarify the basis of the neurodegenerative process to discover new efficient therapies for PD treatment.

1.1.1. Epidemiology

PD is the second most common neurodegenerative disease worldwide, with a prevalence of 1-2 per 1000 individuals in the general population and an incidence of approximately 15 new cases per 100 000 individuals each year (Tysnes and Storstein 2017). PD is rare before 50 years, but its incidence increases 5- to 10-fold in people older than 60 years of age, being mainly a disease of the elderly (Poewe et al. 2017). Classical PD is most common in people with 60 years or older (Halliday and McCann 2010), while people younger

than 40 years that develop PD are usually classified as early-onset PD (EOPD), whose are commonly linked to familial forms of the disease (Schrag and Schott 2006). Moreover, PD is twice more common in men than woman in most populations, suggesting sex-associated genetic factors, such as sex hormones, or sex-specific differences in terms of exposure to environmental risk factors (Poewe et al. 2017; Tysnes and Storstein 2017).

The continuous increase in life expectancy and consequently age-related disorders, such as PD, leads to a considerable pressure on primary care givers and consequently to an economical burden for any country (Kowal et al. 2013).

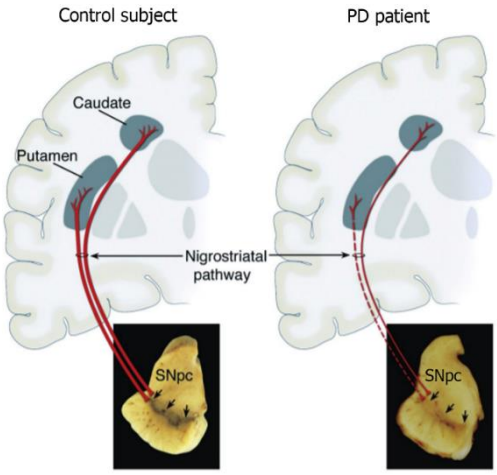

Figure 1.1. Neuropathological hallmarks of Parkinson's disease. The nigrostriatal pathway is composed by dopaminergic neurons whose cell bodies are situated in the substantia nigra pars compacta (SN). Dopaminergic neurons project to the basal ganglia and synapse in the striatum (formed by putamen and caudate nucleus). Throughout PD progression, the nigrostriatal pathway degenerates, leading to dopaminergic enervation loss and, consequently, to neuronal loss in the SN. Adapted from (Dauer and Przedborski 2003).

1.1.2. Clinical symptoms

PD is a clinical heterogenous disorder defined by motor manifestations, which are the cardinal symptoms of the disease, with the presence of bradykinesia associated with rigidity and/or rest tremor (Poewe et al. 2017; Postuma et al. 2015; Tolosa, Wenning, and Poewe 2006). Bradykinesia is one of

the main motor symptoms observed in PD, and it is characterized by a slowness of the movement, that could also be related to some secondary motor symptoms, such as hypophonia (soft speech), hypomimia (reduced facial expressions), micrographia (slow handwriting) and dysphagia (difficult in swallowing) (Jankovic 2008). Rest tremor, the most apparent symptom, normally presents asymmetrically, while rigidity is usually associated with pain (for instance, shoulder pain) (Sternberg et al. 2013). Currently, there are two major subtypes of PD regarding motor symptoms, tremor dominant or non-tremor dominant PD (Marras and Lang 2013). Non-motor symptoms such as autonomic problems (especially constipation), sensory deficits (mainly hyposmia) and sleep disorders are also well-established and may precede the appearance of motor symptoms by decades. Other symptoms including depression and dementia are associated to later stages of the disease (Chaudhuri and Schapira 2009; Poewe et al. 2017).

However, when typical cardinal symptoms appear and final diagnosis of the disease is achieved, there is already cognitive deterioration. In early stages of the disease, there is a selective and progressive loss of dopaminergic neurons in the ventrolateral SN, with relative sparing to other midbrain dopaminergic neurons (Damier et al. 1999; Fearnley and Lees 1991). This becomes more widespread in later stages of the disease, which leads to a consequent massive depletion of striatal dopamine. Another typical hallmark of PD is the presence of LBs that consist in abnormal deposition of α-syn in the cytoplasm of certain neurons in different brain regions. LB pathology occurs firstly in cholinergic and monoaminergic brainstem neurons and in neurons of the olfactory system, although it can appear in other brain areas, such as spinal cord (Iacono et al. 2015).

Nowadays, PD is not considered a disorder exclusively of the dopaminergic neurons of the SN. Even though PD onset and progression remain unclear, it is currently assumed that the disease occur in different brain regions and even outside the nervous system (Braak et al. 2003; Connolly and Lang 2014). In fact, the cumulative and progressive symptoms seem to confirm that PD is a multisystem disorder that needs to be approached from a broad perspective.

1.1.3. Aetiology

PD is a multifactorial disorder that in most cases (90-95%) occur sporadically, without a well-defined cause or correlation with patient lifestyle, being commonly defined as idiopathic PD (iPD). Although the major risk factor for PD is ageing, it is also widely assumed that both genetic and environmental factors (including cigarette smoking, caffeine, pesticides, herbicides, and heavy metals) play a key role on disease onset and development (Dauer and Przedborski 2003).

The discovery of familial genetic mutations linked to PD have led to the development of a variety of animal models, as an effort to clarify the molecular pathways involved in this disease (Thomas and Beal 2007; Dauer and Przedborski 2003). To date, several mechanisms have been implicated in PD pathogenesis, ranging from α-syn aggregation to abnormal protein clearance, mitochondrial dysfunction, oxidative damage and neuroinflammation. However, the underlying relation between different pathways are still not completely understood.

1.1.3.1. Environmental factors

Several lines of evidence indicate that continuous exposure to neurotoxins and chemical substances present in different pesticides can trigger the development of PD pathology. The first of such neurotoxins identified was 6-hydroxydopamine (6-OHDA), which increases the production of reactive oxygen species (ROS), leading to a selective neurodegeneration of catecholaminergic neurons (Ungerstedt 1968). In the beginning of the 80's, another neurotoxin, 1-methyl-4-phenyl-1,2,3,6-tetrahydropyridine (MPTP), was identified when a group of people start to develop all the classic motor PD-related symptoms after the consumption of a contaminant in illicit preparations of a potent synthetic opioid (Langston et al. 1983). In fact, these patients presented neurodegeneration in the SN and reduced tyrosine hydroxylase (TH) staining, a marker of dopaminergic neurons, in the striatum, in post-mortem analysis. Moreover, inflammatory glial activation was also observed at the time of death, suggesting that a time-limited exposure to MPTP could promote a self-perpetuating process of inflammation

and neurodegeneration (Langston et al. 1999). In terms of mechanism of action, MPTP, a highly lipophilic molecule, can cross the blood brain barrier (BBB). In the brain, astrocytic and serotonergic neuron monoamine oxidase B (MAOB) are responsible for the oxidation of MPTP to the intermediate 1-methyl-4-phenyl-2,3-dihydropyridinium ($MPDP^+$). This intermediate is then converted by auto-oxidation to 1-methyl-4-phenylpyridinium ion (MPP^+), the active neurotoxic metabolite, that is released into the extracellular space (Schildknecht et al. 2015; Ransom et al. 1987). Once in a critical concentration, MPP^+ is selectively uptake by dopamine transporters (DAT) and accumulates in synaptic vesicles and mitochondria of dopaminergic neurons (Dauer and Przedborski 2003; Javitch et al. 1985; Mayer, Kindt, and Heikkila 1986). In the mitochondria, MPP^+ inhibits complex I of the mitochondrial electron transport chain, impairing oxidative phosphorylation and leading to a decrease in ATP content, mostly in the striatum and midbrain, and to an increase in ROS production, instigating a vicious cycle of mitochondrial dysfunction and oxidative stress (Dauer and Przedborski 2003).

The key role of mitochondria in idiopathic PD has been elucidated since the recognition of MPTP as a mitochondrial toxin. In fact, several lines of evidence have implicated mitochondrial dysfunction as a central element in the pathogenesis of PD. For instance, activity of mitochondrial complex I is decreased in post-mortem SN of iPD patients (Schapira et al. 1990; Hattori et al. 1991). Importantly, oxidative stress, a consequence of mitochondrial dysfunction, is also increased in brain tissue of PD patients (Dias, Junn, and Mouradian 2013). In fact, nigral dopaminergic neurons are particularly sensible to metabolic and oxidative stress due to their long and unmyelinated axons with several synapses that require large amounts of energy (Pissadaki and Bolam 2013; Bolam and Pissadaki 2012), autonomous pacemaking activity (Surmeier et al. 2012; Surmeier, Obeso, and Halliday 2017), and toxic oxidative stress induced by the increased cytosolic dopamine levels and its metabolites (Mosharov et al. 2009; Lotharius and Brundin 2002).

Moreover, chronic exposure to pesticides, such as rotenone and paraquat are considered a potential risk factor to PD development. Rotenone, for instance, targets mitochondrial complex I, while paraquat, a widely used herbicide, is structurally similar to MPP^+ (Betarbet et al. 2000; Dauer and Przedborski 2003). Importantly, several studies have shown nigrostriatal degeneration induced by

these toxins in different animal models (Blesa and Przedborski 2014). However, the influence of toxins in PD development is still debatable, with studies showing presence or absence of correlation between environmental exposure due to rural living and PD incidence (Wan and Lin 2016; Nandipati and Litvan 2016; Dauer and Przedborski 2003). Interestingly, some reports also suggest that nicotine and caffeine could contribute to a reduced incidence of PD (Ross and Petrovitch 2001).

However, although extensive research correlating mitochondrial dysfunction and oxidative stress to PD pathogenesis, their exact role in disease aetiology is still largely unknown.

1.1.3.2. Genetic factors

Familial forms of PD account for only 5-10% of all cases (Tysnes and Storstein 2017). Although relatively rare, the study of the genetic forms of PD have been extremely useful to aid understanding on the pathophysiological processes involved in the disease (Tysnes and Storstein 2017). The discovery of familial forms of PD arises from a linkage analysis study in 1996 with an Italian family, where the α-syn-encoded gene was identified as the causative gene of PD (Polymeropoulos et al. 1997). So far, mutations in the genes SNCA (PARK1/4), that encodes α-syn, and LRRK2 (PARK8), which encodes the leucine-rich repeat kinase 2 (LRRK2), are associated with autosomal dominant forms of PD (Zimprich et al. 2004; Polymeropoulos et al. 1997); while mutations in the genes PRKN (PARK2), which encodes parkin, PINK1 (PARK6), that encodes PTEN-induced putative kinase 1 (PINK1), and PARK7, that encodes deglycase DJ-1, are associated with autosomal recessive forms of PD (Valente et al. 2004; Kitada et al. 1998; Bonifati et al. 2003). Rare mutations in other genes, such as ATP13A2, that encodes ATPase cation transporting 13A2, are also linked to autosomal recessive PD (Ramirez et al. 2006). In addition, genetic risk factors are involved in sporadic PD as well. For instance, genome-wide association studies (GWAS) have identified common variants in multiple loci as genetic risk factors for PD, where mutations in glucocerebrosidase (GBA) are the most frequent (Neumann et al. 2009). Moreover, also common variants in LRRK2 and SNCA confer a higher risk to develop PD (Satake et al. 2009). These and

other candidate genes have been commonly associated with pathways involving autophagy, endocytosis, inflammation, lysosomal activity, and mitochondria dysfunction (Nalls et al. 2014; Billingsley et al. 2018).

1.1.3.2.1. LRRK2

In 2002, a genetic linkage of the PARK8 locus on chromosome 12q12 with an autosomal dominant form of familial PD was first identified in a large Japanese family with multiple affected generations (Paisán-Ruíz et al. 2004; Zimprich et al. 2004). To date, more than forty LRRK2 variants have been reported, although only eight missense mutations are confirmed to be pathogenic, including Arg1441Cys, Arg1441Gly, Arg1441His, Asn1437His, Tyr1699Cys, Ile2020Thr and Gly2019Ser (**Figure 1.2**). Although almost all pathogenic variants are rare, Gly2019Ser (G2019S) mutation, which is the most frequent, account for approximately 4% of familial and 1% of sporadic PD worldwide. However, G2019S frequency varies across different populations, being especially high in genetically isolated populations, including North African individuals and Ashkenazi Jews, where it may account for up to 40% of total PD cases (Chien et al. 2014). This mutation presents high and incomplete penetrance and elevated age of onset variability, suggesting that a combination of environmental and genetic factors influence LRRK2-PD patients (Guo et al. 2007). Overall, LRRK2-PD patients present clinical similarities with iPD, including profound dopaminergic neuronal degeneration and gliosis in the SN, decreased levels of dopamine in the caudate putamen, and the appearance of LB pathology highlighting the relevance of understanding LRRK2 function to better comprehend both sporadic and familial forms of PD (Wang, Cai, et al. 2014; Marras and Lang 2013). However, G2019S LRRK2-PD is usually reported in patients slightly younger than in iPD, with a percentage of individuals whose onset is before 40 years higher in the first group (Nishioka et al. 2010; Healy et al. 2008). Interestingly, several studies have also suggested that the common male predominance in iPD is not observed in LRRK2-PD patients (Kestenbaum and Alcalay 2017; Gan-Or et al. 2015). Moreover, some cross-sectional studies have demonstrated that motor symptoms progression is slower in LRRK2-PD patients in comparison with iPD patients, while typical non-motor symptoms are commonly observed in both

groups (Gaig et al. 2014; Healy et al. 2008). Finally, most patients with G2019S LRRK2-PD develop typical LB pathology, although they also present other pathological changes including nonspecific cell loss without protein aggregation and abundant tau pathology (Vilas et al. 2018). Besides LRRK2 pathogenic mutations, some LRRK2 variants also influence the susceptibility to develop sporadic PD, which raises the possibility that LRRK2-targeting therapies may be interesting and beneficial to a larger number of PD patients (Healy et al. 2008).

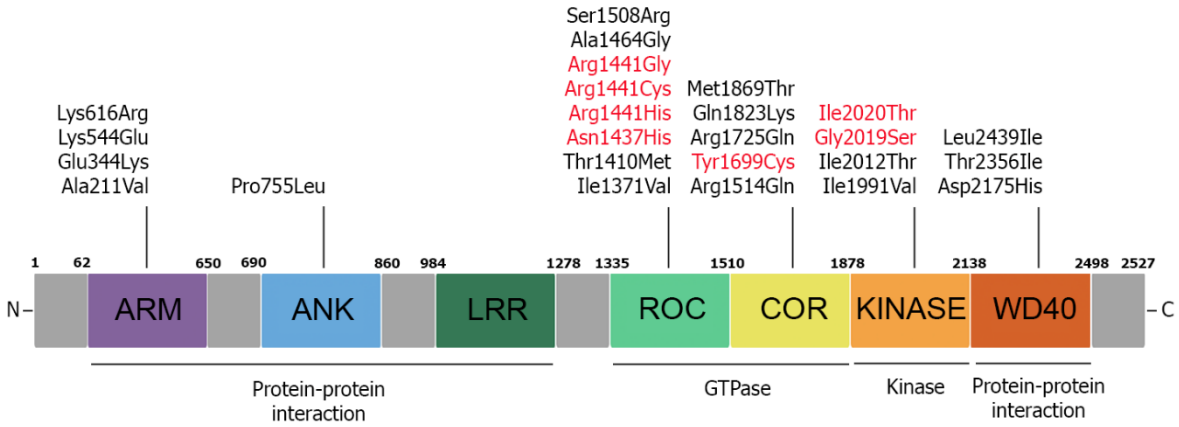

Figure 1.2. Domain architecture of LRRK2 with sites of pathogenic mutations shown. LRRK2 is constituted by seven domains, including four protein-protein interaction domains (ARM, ANK, LRR, and WD40), two GTPase domains (ROC and COR), and one kinase domain (KINASE). The LRRK2 variants are indicated according to their pathogenic (red) or probably pathogenic function (black). ARM – Armadillo repeat; ANK – Ankyrin repeat; LRR – Leucine-rich repeat; ROC – Ras-of-complex; COR – C-terminal of Ras-of-complex. Adapted from (Tolosa et al. 2020).

1.1.3.2.1.1. Structure and function

LRRK2, also known as dardarin, is a large multidomain protein composed by 2527 amino acids and with approximately 285 kDa of mass. LRRK2 belongs to the ROCO superfamily of proteins characterized by their unique structure containing central Ras of complex proteins (ROC)-type GTP-binding, and carboxyl terminal of ROC (COR) domains, flanked by various functional domains, including a serine/threonine protein kinase domain, and protein-protein interaction domains such as ankyrin-like repeats (ANK), leucin-rich repeats

(LRRs) at N-terminal and a β-propeller-like domain (WD40) at C-terminal (**Figure 1.2**) (Cookson 2010).

As a GTPase, LRRK2 binds to GTP by its ROC domain, which leads to a conformational alteration to facilitate GTP hydrolysis. Some pathogenic mutations are located within the GTPase domain, more concretely within the ROC (R1441G, R1441C, R1441H) and the COR (Y1699C) subdomains, and are associated with reduced LRRK2 GTPase enzymatic activity, thereby suggesting that GTPase activity plays a key role in the development of PD (Daniëls et al. 2011; Li et al. 2007). Moreover, mutations affecting GTP binding or that delete the GTPase domain lead to loss of kinase activity (Bardien et al. 2011). LRRK2 kinase domain is similar to mixed-lineage kinases (MLKs) and receptor-interacting protein kinases (RIPKs) (Mata et al. 2006) and the ROC and COR domains seem to be essential for control kinase activity (Greggio et al. 2008). In fact, several studies have suggested a potential intrinsic regulatory mechanism between GTPase and kinase domains (Gilsbach and Kortholt 2014; Anand and Braithwaite 2009; Biosa et al. 2012). Importantly, it is described that LRRK2 exists in an oligomeric complex with minimal kinase activity that, upon GTP binding, dissociates to form an intermediate substrate, which auto-phosphorylates and forms a homodimer with kinase activation (Webber and West 2009). G2019S, the most frequent LRRK2 mutation lies in the activation loop of the kinase domain, which stabilizes the enzyme in its active form, leading to a 2-3-fold gain-of-function of the protein (Greggio et al. 2008; Mata et al. 2006). Still in the kinase domain, the effect of I2020T mutation is far from being understood, with studies suggesting that this mutation led to an increase, decrease or null effect on the kinase activity of the protein (Reichling and Riddle 2009; Gloeckner et al. 2006). The WD40 domain appears to be essential to LRRK2 intrinsic phosphotransferase activity, while the function of the ARM, ANK and LRR domains are still not well understood, although the presence of these protein-protein interaction domains strongly suggest that LRRK2 may act as a scaffold for several other proteins with important roles in cellular signalling (Mata et al. 2006).

The different LRRK2 mutations promote a wide range of neuropathology traits in PD. In fact, several post-mortem studies have discovered a pleomorphic neuropathology linked to different LRRK2 mutations, or even to the same

mutation, thus suggesting that LRRK2 may influence different signalling pathways involved in cellular survival (Zimprich et al. 2004).

Physiologically, LRRK2 is expressed in many tissues, with the highest expression in the brain, lung, and kidney (Giasson et al. 2006). LRRK2 is also present in biofluids, such as urine, cerebrospinal fluid (CSF) and blood, where it is found in peripheral blood mononuclear cells (PBMCs), including monocytes and lymphocytes (Biskup et al. 2007). In the brain, LRRK2 is ubiquitously expressed, although earlier studies have described that its expression is lower in regions rich in dopaminergic neurons, including the SN and the ventral tegmental area of the midbrain (Taymans et al. 2006; Higashi et al. 2007; Biskup et al. 2007), and higher in the striatum (Davies et al. 2013). However, recent studies showed LRRK2 expression in both SN and striatum, the most PD-affected regions (Sharma et al. 2011; Miklossy et al. 2006; Higashi et al. 2007). In terms of subcellular distribution, LRRK2 is thought to be a cytosolic protein, although it may also be associated with cellular membranes, including the plasma membrane, endoplasmic reticulum, Golgi complex, mitochondrial membrane and lipid rafts, as well as vesicular structures such as endosomes, lysosomes and synaptic vesicles (Hatano et al. 2007; Alegre-Abarrategui et al. 2009).

1.1.3.2.1.2. Cell signalling

Since the discovery of LRRK2 pathogenic mutations, many efforts have been done to identify the physiological roles of LRRK2 and which signalling pathways are involved.

The mitogen-activated protein kinase (MAPK) was one of the first pathways studied as potentially linked to LRRK2. In fact, the LRRK2 kinase domain is closely related to MLKs, which mediate cellular responses by activating p38 MAPKs and c-Jun N-terminal kinases (JNKs) through their upstream kinases, MKK3/6 and MKK4/7, respectively (Gallo and Johnson 2002). Several studies have demonstrated that LRRK2 binds to and phosphorylates MAPK kinases (MKKs) through the COR and kinase domains (Takekawa et al. 2005; Hsu et al. 2010). Importantly, in G2019S transgenic mice, G2019S LRRK2 mutation was shown to promote MKKSer257 hyper-phosphorylation and, consequently, degeneration of SN dopaminergic neurons, suggesting that dopaminergic

neuronal death induced by G2019S mutation may be mediated by JNK-c-Jun signalling pathway (Chen et al. 2012). Also, MEK1 and MEK2, other members of the MAPK pathway, were recently associated with LRRK2. In fact, some authors demonstrated that G2019S mutation activates MEK1/2, leading to a hyper-phosphorylation of their effectors, extracellular-signal-regulated kinase 1 (ERK1) and ERK2, which seems to be responsible for the G2019S-LRRK2-mediated increase in basal autophagy (Bravo-San Pedro et al. 2012). Interestingly, others have demonstrated that over-expression of wild-type (wt) LRRK2 may specifically activate ERKs in human embryonic kidney (HEK293) and human neuroblastoma (SH-SY5Y) cells. In fact, in both cell lines, LRRK2wt appears to have a neuroprotective role against oxidative stress that is mediated by ERK1/2 (Liou et al. 2008).

The role of LRRK2 in mitochondrial dysfunction has also been suggested. For instance, fibroblasts from G2019S-LRRK2-PD patients present abnormal mitochondrial morphology (Mortiboys et al. 2010). Likewise, G2019S transgenic mice show accumulation of damaged mitochondria (Ramonet et al. 2011). In SH-SY5Y cells, overexpression of LRRK2wt also induce mitochondrial fragmentation, which is exacerbated by R1441C and G2019S mutations. In addition, G2019S mutation promote mitochondrial uncoupling, reduce membrane potential and increase oxygen consumption (Wang et al. 2012; Papkovskaia et al. 2012). Further, recruitment of dynamin-like protein 1 (DLP1), a protein involved in mitochondrial fission, to the mitochondria, after LRRK2 overexpression *in vitro* was also demonstrated, which may indicate a role for LRRK2 in mitochondria homeostasis and quality control, probably via DLP1 (Wang et al. 2012). However, it is still unknown whether mitochondrial dysfunction is a primary pathogenic event induced by LRRK2 mutations, or if it is a secondary event induced by LRRK2-mediated toxicity.

In the past few years, some GWAS studies have identified LRRK2 as one of the genes causing susceptibility for developing leprosy and Crohn's disease, two diseases with a strong inflammatory component (Wang et al. 2014). Since that, numerous studies have been trying to explore the role of LRRK2 in microglia cells, the resident macrophages of the brain, as well as the impact of LRRK2 mutations in PD-associated neuroinflammation. Recent studies have demonstrated that LRRK2 is increased in several immune cells, including

microglia and astrocytes (Moehle et al. 2012; Marker et al. 2012; Berwick et al. 2019), but also in PBMCs (B cells, dendritic cells, and macrophages) (Thévenet et al. 2011; Hakimi et al. 2011). Importantly, some studies showed that inflammatory stimuli, such as LPS or interferon-γ (IFN-γ), increase LRRK2 phosphorylation and its recruitment to the membrane, in both microglia cells from mouse SN or striatum and microglial cell cultures (Gillardon et al. 2012; Moehle et al. 2012), thereby suggesting that LRRK2 may be required during an inflammatory response, although the exact signalling pathways involved are still unknown. Concordantly, LRRK2 inhibition or downregulation in murine microglia cells present reduced proinflammatory mRNA and protein levels, including tumour-necrosis factor α (TNF-α), interleukin-1β (IL-1β), IL-6 and inducible nitric oxide synthase (iNOS) (Kim et al. 2012; Moehle et al. 2012). Moreover, decreased nuclear factor-κB (NF-κB), following toll-like receptor (TLR)-induced activation by LPS, is also observed after LRRK2 knockdown in microglia (Kim et al. 2012). Interestingly, other authors have demonstrated that R1441C LRRK2 microglia cells present a basal sensitization toward a proinflammatory phenotype, as gene profiling in unstimulated conditions reveal increased levels of cytokines, chemokines and membrane receptors involved in microglia activation (Kim et al. 2012). Moreover, conditioned medium from LPS-stimulated R1441C LRRK2 microglia increases primary cortical neuronal death, as compared with LPS-stimulated LRRK2wt microglia (Kim et al. 2012). Furthermore, the proinflammatory role of LRRK2 has been suggested in different neuroinflammatory animal models, where LRRK2 kinase activity being an inflammatory driver. For instance, increased microgliosis and astrogliosis have been observed in α-syntg mice in the presence of G2019S LRRK2 (Lin et al. 2009). In accordance, others also showed elevated microglial activation in the SN of G2019S LRRK2tg mice, after a recombinant adeno-associated viral vector (rAAV)-mediated α-syn overexpression, which was accompanied by dopaminergic neuronal degeneration (Daher et al. 2015). More recently, some studies also demonstrated increased microglial activation and consequent TNF-α and IL-6 expression in microglia isolated from G2019S LRRK2 mice injected with recombinant α-syn fibrils (Bieri et al. 2019). Importantly, LRRK2 genetic ablation was shown to be protective against LPS-induced dopaminergic

neurodegeneration and rAAV-based α-syn overexpression-driven neuroinflammation and neurodegeneration (Daher et al. 2014).

Overall, LRRK2 appears to be a relevant contributor, not only to neuronal death in PD, but also to neuroinflammation, by shifting the balance between neuroprotection and neurotoxicity of microglia. Thus, understanding the intricate relation between LRRK2 and microglia may pave the way to the discovery of novel pathways for therapeutic intervention.

Also, LRRK2 have been implicated in other cellular processes, such as vesicle trafficking, dopamine homeostasis and dopamine receptor activation, synaptogenesis, miRNA processing and cytoskeletal remodelling (Migheli et al. 2013; Paisán-Ruiz et al. 2013).

1.1.4. Animal models

Throughout the years, the development of animal models of PD has allowed a better understanding of the pathophysiological features of the disease, as well as the discovery of new therapeutic approaches to control and reduce motor symptoms. Even so, none of the existing PD models present all the clinical and neuropathological features of the disease. Currently, PD animal models can be classified into toxin models and genetic models.

1.1.4.1. Toxin-based models

Several pharmacological and toxin agents have been used to model PD, including dopaminergic neurotoxins (6-OHDA, MPTP, rotenone and paraquat), and inflammatory agents such as lipopolysaccharide (LPS). However, the most frequently used are still the classical 6-OHDA in rats and MPTP in mice and monkeys (Bové and Perier 2012; Ogata et al. 1997; Qin et al. 2007). The neurotoxin-based models are usually specific to the nigrostriatal circuit, similarly to PD, inducing preferential loss of dopaminergic terminals in the putamen that result into motor deficits (Bové and Perier 2012; Blesa and Przedborski 2014). However, neurodegeneration in dopaminergic neurons occurs rapidly in a few days and animals do not present typical LB pathology (Blesa and Przedborski 2014; Bové and Perier 2012). MPTP is the gold standard choice to investigate

the mechanisms underlying dopaminergic neuronal death in PD. To date, several administration regimens and methods have been used in mouse and primates and can be divided in acute, sub-acute, sub-chronic and chronic models (Porras, Li, and Bezard 2012; Blesa and Przedborski 2014; Jackson-Lewis et al. 1995; Meredith et al. 2011). More concretely, acute models usually consist in 4 intraperitoneal (i.p.) injections of 20-30 mg/kg MPTP, 2 h separately, and result in rapid and severe reduction of dopamine in the striatum by approximately 90%, and consequent dopaminergic neurodegeneration that reaches a peak after 4 days (Huang et al. 2017; Liu et al. 2015; Jackson-Lewis et al. 1995). A sub-acute regimen involves 4 i.p. injections of 15-25 mg/kg MPTP at 6 or 12 h intervals, within 2 days, and typically leads to ~80% loss of TH-positive fibers and ~40% of dopaminergic neurodegeneration one day after the last injection (Liu al. 2015; Huang et al. 2017). The sub-chronic model consists in 1 i.p. injections of 20-30 mg/kg MPTP daily during 5-10 sequential days and leads to a depletion of dopamine in the striatum of approximately 50% along with 30-40% dopaminergic neuronal loss that peaks within 4 days after last injection (Tatton and Kish 1997; Jackson-Lewis et al. 1995; Bové and Perier 2012; Meredith et al. 2011).

The presence and evaluation of motor deficits in MPTP mouse models is somehow controversial (Meredith et al. 2006; Meredith et al. 2011). MPTP administration in mice has been described to induce a broad range of motor alterations that can be stable or transient. These differences depend mainly on MPTP regimen, time of behavioural testing, training previous to testing, mice strain and age (Meredith et al. 2006; Tillerson et al. 2003). As example, some authors reported that mice subjected to sub-acute and chronic MPTP models present decreased locomotion, stride length and rearing, while others demonstrated that sub-acute and acute MPTP models do not alter locomotion or even induce hyperactivity (Fornai et al. 2005; Fredriksson et al. 1994; Tomac et al. 1995; Tillerson et al. 2003; Meredith et al. 2006; Meredith et al. 2011). These disparate results indicate that a full battery of properly standardized tests, along with previous training and measurements performed at well-defined time-points, should be systematically employed in research involving MPTP mouse models.

1.1.4.2. Genetic models

Genetically engineered mice lacking or expressing PD-related genes have been created throughout the years to better simulate the mechanisms underlying genetic forms of PD. However, in most of these models, the pathological and behavioural phenotypes are very distinct from human condition (Blesa and Przedborski 2014). For instance, different α-syn transgenic mice have been developed and although they present α-syn accumulation and consequent inflammation, no significant nigrostriatal neurodegeneration is found in most of these mice (Paumier et al. 2013; Watson et al. 2012; Blesa and Przedborski 2014). Moreover, mice deficient in or expressing specific PD-related genes, such as PARK2/PRKN, PINK1, LRRK2 or DJ-1 have also been described and lack relevant dopamine-related behavioural deficits and nigrostriatal degeneration (Kitada et al. 1998; Blesa and Przedborski 2014). LRRK2 knock-out (ko) mice are viable and have intact nigrostriatal dopaminergic pathway until two years of age; however, they present α-syn or ubiquitin accumulation (Tong et al. 2010; Andres-Mateos et al. 2009; Hinkle et al. 2012). Throughout the years, numerous transgenic mouse models for LRRK2 disease-causing mutations have been developed (Chen et al. 2017; Li et al. 2010; Li et al. 2009; Ramonet et al. 2011; Liu, Sgobio, et al. 2015; Karuppagounder et al. 2016). However, overexpression of G2019S LRRK2tg mice is the most studied mouse model, due to its widespread prevalence in PD patients (Xu et al. 2012). Overall, G2019S LRRK2 mutant mice present a mild progressive and selective degeneration of dopaminergic neurons in the SN. However, although no alteration in dopamine striatal levels and locomotor activity is observed, these mice show defective dopaminergic transmission, which strongly correlates with the dysfunctional dopaminergic system observed in PD patients, especially in early stages of the disease (Xu et al. 2012; Ramonet et al. 2011; Chen et al. 2012). Moreover, others also demonstrated that G2019S LRRK2tg mice present autophagic and mitochondrial dysfunction (Ramonet et al. 2011). However, in aged mice, G2019S LRRK2 fails to influence striatal dopamine (Ramonet et al. 2011). By contrast, aged R1441C LRRK2tg mice show a progressive impairment of locomotor activity, as well as accumulation of autophagic vacuoles in the cortex and decreased levels of cortical catecholamines (Ramonet et al. 2011).

Interestingly, LRRK2wt or mouse LRRK2 overexpression show no PD-relevant phenotype, thus indicating the crucial role of mutated LRRK2 to drive pathological toxicity (Xu et al. 2012). Recently, some authors observed that G2019S LRRK2tg mice injected with MPTP present increased dopaminergic neuronal loss in the SN, along with dopaminergic loss in the striatum and impaired dopamine synthesis in the SN, in comparison with MPTP-injected LRRK2wt mice. Curiously, these pathological features did not translate into a worse behavioural phenotype (Karuppagounder et al. 2016). Importantly, LRRK2ko mice do not show any differences in terms of sensitivity to MPTP-induced neurodegeneration (Andres-Mateos et al. 2009), which suggests that the enhanced neurotoxicity is most likely due to a specific G2019S LRRK2-related gain of function.

Although both neurotoxic and genetic mouse models have been contributing to the understanding of PD pathology, none of these models totally reproduce human PD pathological features. Thus, attempts must be made to merge the strengths of each type of model to better mimic PD characteristics, namely progressive nigrostriatal degeneration, and LB pathology (Blesa and Przedborski 2014).

1.1.5. Diagnosis and therapy

PD diagnosis is defined by the presence of cardinal motor symptoms, more specifically, bradykinesia and rigidity and/or rest tremor, in combination with additional supporting and exclusion criteria (Tolosa et al. 2006; Poewe et al. 2017). More specifically, different rating scales may be used to determine disease stage of PD. The most common rating scales used in clinic are the Hoehn and Yahr (H&Y) and the Unified Parkinson's Disease Rating Scale (UPDRS). The H&Y scale, originally described in 1967, divides PD into five stages of disease progression. Briefly, stage I is characterized only by unilateral involvement, normally with minimal or no function impairment; stage II already involves bilateral or midline impairment, without impairment of balance. In stage III, the first sign of impaired righting reflexes appears. Functionally, patient disability is mild to moderate and they are capable of leading independent lives. In stage IV, severely clinical disability is fully developed; however, patients are still able to work and stand without assistance, although they are significantly incapacitated. Finally,

stage V is characterized by confinement to bed or wheelchair unless aided. However, some patients may never reach to stage five due to related mortality (Hoehn and Yahr 1967). Moreover, the most recent version of UPDRS sponsored by the movement disorder society (MDS), called MDS-UPDRS, contains four parts, related to intellectual function, activity of daily living, motor examination, and motor complications, respectively. Patients are scored in each part, using zero for no problems, one for minimal, two for mild, three for moderate, and four for severe problems (Goetz et al. 2007). Importantly, diagnostic criteria for PD only allow for the identification of already manifested disease, which occurs several years after the neurodegenerative process begin (Poewe et al. 2017). Align to this, misdiagnosis frequency is high due to the amount of overlapping parkinsonian disorders (Tolosa et al. 2006). There are several techniques able to detect structure and function abnormalities in brain regions of PD patients, including magnetic resonance imaging and transcranial B-mode sonography that detect modified brain structures, as well as single-photon emission computed tomography (SPECT) and positron emission tomography (PET) scans (Emamzadeh and Surguchov 2018; Barber et al. 2017). However, these techniques are expensive, involve radiation exposure and are not specific for PD. In this context, and in order to provide better clinical intervention and treatment at the early stages of disease, it is of strong importance to find accurate biomarkers for diagnosis and monitoring of disease progression. In fact, the discovery of sensitive and selective biomarkers that can identify PD patients in the prodromal phase is essential.

Potential biochemical biomarkers of PD have been extensively investigated in body fluids and tissues with several examples already identified in blood, saliva, CSF and biopsies. For instance, the levels of urate, an important physiological antioxidant present in all body fluids, have been identified as molecular predictor for the risk, diagnosis and prognosis of PD (Cipriani et al. 2010). Uniquely, higher urate levels in plasma or CSF were linked to both a lower risk of developing PD and to a slower rate of disease progression in numerous prospective epidemiological and clinical cohorts enrolling over 1600 early cases of PD (Schwarzschild et al. 2008; Ascherio et al. 2009). Moreover, some authors also studied protein DJ-1, whose mutations are a familial cause of PD, as a potential biomarker. In fact, some studies showed an increase in DJ-1 levels in

CSF or plasma of PD patients when compared to control subjects (Waragai et al. 2007), as well as a positive correlation between DJ-1 levels and H&Y scores (Waragai et al. 2007). 8-Hydroxydeoxyguanosine (8-OHdG), a DNA oxidation product, was also reported elevated in CSF of PD patients as compared with controls (Gmitterová et al. 2009). Others also demonstrated that urinary 8-OHdG levels are increased in PD patients in comparison with controls and are linked to H&Y stage (Sato et al. 2005; Hirayama et al. 2011). Besides biochemical biomarkers, abnormal protein accumulation and aggregation may also be used as potential biomarkers of PD. Of note, altered levels of total or modified forms of α-syn was already reported, with higher amounts found in the CSF of PD patients as compared with control subjects (Mollenhauer et al. 2011, Parnetti et al. 2014, Parnetti et al. 2019). Moreover, others also showed a negative correlation between α-syn levels in CSF and H&Y stage, thus reflecting disease severity (Tokuda et al. 2006). Importantly, an increase in oligomeric forms of α-syn, apparently related to α-syn toxicity, was also observed in PD and the ratio of α-syn oligomeric/total protein was described as an effective manner to differentiate PD patients from controls (Tokuda et al. 2010). In addition, a microRNA (miRNA) panel for early PD diagnosis was demonstrated to have high predictive accuracy, which was reinforced by the inclusion of α-syn data (Dos Santos et al. 2018; Emamzadeh and Surguchov 2018). In fact, the combination of different biomarkers is critical to guaranty high sensitivity and specificity of diagnosis. miRNAs, and in particular circulating miRNAs, have been extensively studied as candidate biomarkers for PD in the past few years (Roser et al. 2018), a subject that will be discussed in more detail in section 1.2.1.

Over the past half century, a huge progress was made in the therapies available for PD. However, until now, these therapies only relief PD symptomatology without any effect on disease progression. Levodopa (L-DOPA) is still the major treatment used to control PD symptoms, being able to replace DA levels (Jankovic and Aguilar 2008). Current L-DOPA preparations also include inhibitors of aromatic amino acid decarboxylase (AADC), such as pergolide and rotigotine, which may prevent peripheral metabolism and increase L-DOPA bioavailability. Inhibitors of catechol-O-methyltransferase (COMT) could also enhance L-DOPA half-life and bioavailability and are a first-line treatment for PD patients as well (Jankovic and Aguilar 2008). Moreover, MAOB inhibitors,

such as selegiline and rasagiline, can also be used to increase and prolong synaptic dopamine levels (Jankovic and Aguilar 2008). Adenosine A2A antagonists have been investigated as potential non-dopaminergic compounds for PD treatment that are able to modulate striato-pallidal output improving motor disability. These compounds have been studied since caffeine, an antagonist of this receptor, seem to reduce the risk of PD development (Kachroo and Schwarzschild 2012). Although some A2A antagonists including preladenant and tozadenant have failed in clinical trials, istradefylline has be proven to be effective and well tolerated in fluctuating PD patients (Torti et al. 2018). Interestingly, although oxidative stress is reported as a main feature of PD pathology, administration of free radical scavenger, such as coenzyme Q_{10}, or antioxidants, including α-tocopherol and vitamin E, showed no improvement of motor deficits in clinical trials (Devos et al. 2014). Finally, deep brain stimulation in specific brain regions may also improve motor deficits. However, this procedure is normally used only when patients do not respond to conventional therapy, since it has a 3- to 6-month waiting period required for optimal results and the possibility to develop brain infection (Stefani et al. 2019; Emamzadeh and Surguchov 2018).

Although drugs that relieve PD motor symptoms are moderately effective, these treatments are less useful to treat advanced disease. Until now, there are no disease-modifying therapies that slow or halt PD progression. In that regard, several drugs have reached clinical trials, including molecules that modulate α-syn aggregation and concentration, agents that modulate glucocerebrosidase function, and LRRK2 kinase inhibitors. For instance, a new drug discovered by Neuropore Therapies, NPT200-11, entered in phase I clinical trials, being able to inhibit α-syn oligomerization (Emamzadeh and Surguchov 2018). Moreover, LRRK2 kinase inhibitors, DNL-151 and DNL-201, have successfully completed phase 1 and phase 1b clinical trials in healthy volunteers and PD patients, respectively (Emamzadeh and Surguchov 2018). In addition to LRRK2-PD patients, LRRK2 kinase activity has also been reported in the pathogenesis of iPD patients, suggesting that a larger population of PD patients may value from these treatments.

1.2. Neuroinflammation

One of the major hallmarks of PD is chronic neuroinflammation, and evidence shows that it exacerbates PD pathology, in both familial and sporadic cases (Ishikawa and Takahashi 1998; Farrer et al. 2001). Indeed, emerging data suggests that glial cell activation, T cell infiltration, and sustained inflammatory responses, along with high levels of proinflammatory mediators, such as TNF-α, IL-6, IL-1β, IFN-γ, iNOS and cyclo-oxygenase (COX)-1 and COX-2, are commonly present in human PD patients and animal models of PD, playing key roles in dopaminergic neuronal degeneration (McGeer et al. 1988; Hirsch et al. 2012). Moreover, PET studies have indicated microglial activation in different PD brain regions, including in the putamen and basal ganglia, which is associated with dopaminergic neuronal loss and, consequently, motor symptoms (Ouchi et al. 2005; Gerhard et al. 2006). Finally, activation of microglia in the SN and striatum in several PD animal models, and consequent dopaminergic neuronal degeneration further confirm the role of chronic neuroinflammation in PD progression (Kurkowska-Jastrzebska et al. 1999; Dzamko et al. 2015; Lee et al. 2019). Importantly, peripheral inflammation seems to play a key role in PD, as well, as suggested by the elevated levels of proinflammatory cytokines present in the serum and CSF of PD patients (Dobbs et al. 1999; Scalzo et al. 2010).

Microglia, the brain resident macrophages, are the main line of innate immune defence in the central nervous system (CNS). These cells are originated from progenitor erythromyeloid cells from the embryonic yolk sac that colonize the CNS during foetal development, being maintained by self-renewal (Gomez Perdiguero et al. 2015). In humans, microglia represent about 10% of the CNS cellular population and have crucial functions in both physiological and pathological conditions (Streit et al. 2004). Normally, microglia exist in an inactive or resting stage characterized by a ramified morphology, with long branching processes and a small soma. In this stage, microglia cells are able to monitor the surrounding micro-environment in efforts to maintain tissue homeostasis and appropriate synaptic function (Le et al. 2016). However, under pathological situations, microglia become activated, assuming a hypertrophic ameboid morphology and higher phagocytic activity to rapidly clear pathogens and cell debris (Tang and Le 2016). Microglia express several pattern recognition

receptors (PRRs) that allow for their immune surveillance functions (**Figure 1.3**). These receptors recognize conserved motifs of microbial and viral-derived molecules, such as LPS, which are commonly classified as pathogen-associated molecular patterns (PAMPs). Some of these receptors, including TLRs, can also recognize distinct molecules released from endogenous compartments or modified in structure, such as abnormal protein aggregates, that constitute damage-associated molecular patterns (DAMPs), culminating in the activation of downstream inflammatory signalling pathways or phagocytosis (Le et al. 2016; Kouli et al. 2019). Microglia activation leads to altered expression of specific surface receptors and key enzymes, ranging from two different activation stages, classical activation (M1 activation) and alternative activation (M2 activation). Classical microglia activation is usually associated with disease stages and leads to an increased production of proinflammatory cytokines such as TNF-α, IL-6, IL-1β, chemokines such as IL-8, and release of ROS, nitric oxide (NO) and prostaglandins (**Figure 1.3**). On the other hand, alternative microglia activation is associated with inflammation resolution and tissue repair, and triggers the production of anti-inflammatory cytokines, such as IL-10, IL-4 and IL-13, and phagocytosis (Tang and Le 2016). Upon ligand binding, TLRs recruit Toll/interleukin-1 receptor (TIR) domain-containing adapter protein (TIRAP) at the plasma membrane and bind to myeloid differentiation 88 (MyD88), which leads to activation of NF-κB and MAPKs and consequently to an increase of proinflammatory gene expression. In addition, TLR4 can also recruit TIR domain-containing adapter-inducing interferon-β (TRIF), leading to late-phase NF-κB and MAPKs activation (Kawai and Akira 2010; Kouli et al. 2019).

The causes underlying neuroinflammation in PD have been largely investigated and include the release of molecules, such as α-syn or β-amyloid, from damaged or dying neurons (Kouli et al. 2019). In fact, microglia and neurons communication may potentially damage brain tissue, which as limited capacity to regenerate and repair. Several researchers have showed that primary microglia is activated by aggregated α-syn oligomers *in vitro* and, importantly, in primary neuron-glia co-cultures, α-syn-activated microglia is neurotoxic towards mesencephalic neurons (Zhang et al. 2005; Su et al. 2008). Other studies demonstrated that α-syn-induced microglial activation involves activation of TLRs, including TLR2, TLR4, P2X7 and Fc-gamma receptor (FcγR), which leads

to proinflammatory signalling activation and phagocytosis (Béraud et al. 2011; Kouli et al. 2019; Jiang et al. 2015). Accordingly, TLR2 and TLR4 are commonly increased in different brain regions and peripheral tissues from PD patients (Cao et al. 2012; Kouli et al. 2019). Overall, these studies suggest that there is a driving cycle between neuroinflammation and dopaminergic degeneration in PD, in which extensive microglial activation and consequent cytokine production exacerbates oxidative damage and dopaminergic death, which in turn also release proinflammatory molecules to perpetuate inflammation.

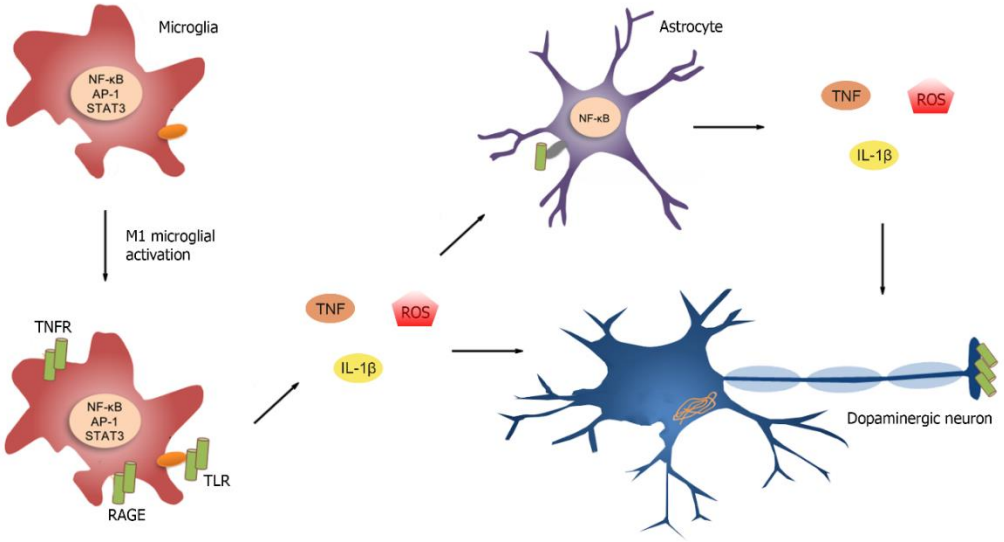

Figure 1.3. Neuroinflammation in Parkinson's disease. In a pathological condition, microglial cells become activated and express several families of pattern recognition receptors (PRRs), including TLRs and RAGE. Classical microglia activation (M1 activation) is related to disease stages and leads to production of proinflammatory mediators, such as cytokines TNF and IL-1β, and reactive oxygen species (ROS). These proinflammatory mediators can be damaging to dopaminergic neurons, and stimulate astrocytes, amplifying proinflammatory signals, inducing dopaminergic neuronal toxicity. Adapted from (Hirsch et al. 2012).

Regarding astrocytes, their role during nigrostriatal degeneration remains highly controversial. Astrocytes are the most abundant type of glial cells in the CNS, and they present important functions in maintaining neuronal health by providing metabolic and structural support, and regulating synaptic transmission, ionic homeostasis, and BBB maintenance (Booth et al. 2017; Refolo and Stefanova 2019). Astrocytes are also responsible for the production of

neurotrophic molecules, such as brain-derived neurotrophic factor (BDNF) and glial-derived neurotrophic factor (GDNF), that are crucial for dopaminergic neuronal development and survival (Lin et al. 1993; Schaar et al. 1993). Nevertheless, astrocytes can also contribute and amplify inflammatory responses initiated by microglia, by upregulating the expression of some intermediate filament proteins, including glial fibrillary acidic protein (GFAP) and vimentin, further feeding the production of proinflammatory mediators (Refolo and Stefanova 2019). In addition, although astrocytic uptake of α-syn and consequent decrease of extracellular α-syn toxic species could be a protective mechanism, astrocytes may also be activated after α-syn binding to TLR4 and induce ROS and proinflammatory cytokine production (Lindström et al. 2017; Loria et al. 2017; Huang et al. 2017). This proinflammatory activation of astrocytes mainly relies on microglial activation, but it is damaging towards dopaminergic neurons (**Figure 1.3**) (Yun et al. 2018). Importantly, emerging evidence has revealed that astrocytic disruption is implicated in dopaminergic neuronal degeneration in PD. However, others have also found no alterations in astrocytic phenotypes in PD brains, despite profound microgliosis (Liddelow et al. 2017; Refolo and Stefanova 2019). Therefore, additional studies are needed to deeply understand and clarify the role of astrocytes in nigrostriatal degeneration during PD progression.

1.3. Regulated cell death

Throughout the years, multicellular organisms developed a self-demise machinery to remove damaged cells and guarantee that the whole body could survive. Since the first description of regulated cell death (RCD) in 1965, the continuous investigation and concomitant development of models and technologies have granted a better understanding of its involvement in several diseases. Traditionally, regulated cell death was classified as apoptosis or passive necrosis, centred on morphological features. However, today there is a widely consensus about the existence of multiple forms of genetically encoded RCD pathways, that have gained relevance due to their role in disease pathogenesis (Galluzzi et al. 2018). Interestingly, these cell death pathways can exist at the same time in a tissue and pathological environment, with some of them sharing common mechanisms that can be a backup strategy to guarantee

tissue homeostasis (Galluzzi et al. 2018). For instance, in neurodegenerative diseases, including PD, it is assumed that different RCD pathways are involved in neuronal loss during disease progression (Perier et al. 2012). Overall, RCD is a form of cell death resulting from the activation of one or more signal transduction modules, that can be modulated pharmacologically or genetically. RCD it is not unique to multicellular life forms, which constitutes a clearly advantage for organismal homeostasis in physiological and pathological settings (Galluzzi et al. 2018; Fuchs and Steller 2011). Importantly, programmed cell death (PCD) is a type of RCD that occurs in specific physiological conditions, and it is not related to perturbations of homeostasis. Therefore, PCD does not occur in the context of failing adaptation to stress (Galluzzi et al. 2018).

Originally described in 1972, apoptosis is the most common and well-known form of RCD (Kerr et al. 1972). Apoptosis performs key roles in physiological processes during embryonic and post-natal development, as well as in the adult tissue homeostasis, defence against pathogen infection and genotoxic stress. Nevertheless, in several pathological conditions, such as neurodegenerative diseases, apoptosis could be extensively activated (Galluzzi et al. 2018). Apoptotic activation is an extremely regulated process that involves caspase activation, an evolutionarily conserved family of cysteine aspartases, and can be initiated by two different pathways that share similar mechanisms of cell death: the intrinsic pathway, mediated by mitochondria, and the extrinsic pathway, mediated by death receptor activation (Galluzzi et al. 2018). Importantly, this type of cell death has been widely described in postmortem studies of PD patient brains, through the observation of cell shrinkage, chromatin condensation and DNA fragmentation, typical morphological features of apoptosis (Perier et al. 2012; Mochizuki et al. 1996; Anglade et al. 1997; Tatton et al. 1998). In addition, in experimental models of PD, including in the MPTP mouse model, the same apoptotic markers have been identified (Perier, Bové, and Vila 2012).

1.3.1. Necroptosis

Necrosis was first described as a pure accidental and passive form of cell death resulting from external injury. This type of cell death leads to a rapid

cytoplasmic and organelle swelling, along with plasma membrane permeabilization and release of DAMPs (Berghe et al. 2010; Galluzzi et al. 2018). However, accumulating evidence shows that necrosis can also occur in a regulated manner triggered by extrinsic or intrinsic stimuli. In that regard, several types of regulated necrosis have been described, including mitochondria pore transition (MPT)-dependent necrosis, necroptosis, ferroptosis, parthanatos or pyroptosis. Of note, these necrotic pathways can be activated by specific mechanisms engaged during pathological conditions and can be pharmacologically or genetically modulated (Galluzzi et al. 2018). The term regulated necrosis was suggested in 1988 after the discovering that TNF was able to induce both apoptosis and necrosis depending on cell type (Laster et al. 1988). Several years later, in 2005, the term necroptosis was proposed to reveal a nonapoptotic cell death pathway initiated by death receptor (DR) activation upon caspase inhibition, which could potentially be inhibited by necrostatin-1 (Nec-1), a common inhibitor of receptor interacting protein (RIP1) (also known as RIPK1) kinase activity (Degterev et al. 2005). More recently, according to the Nomenclature Committee on Cell Death, necroptosis was classified as a RCD resulting from extracellular or intracellular alterations that depend on RIP3 and pseudokinase mixed lineage kinase domain-like protein (MLKL), being also dependent on RIP1 kinase activity in some situations (Galluzzi et al. 2018).

1.3.1.1. Necroptosis activation

Necroptosis can be triggered during specific conditions after ligand stimulation of cell surface DR, including TNF receptor 1 (TNFR1) and TNF-related apoptosis-inducing ligand receptors (TRAILRs), or PRRs, more specifically TLRs, such as TLR3 and TLR4 (Choi et al. 2019). Moreover, some studies have shown that necroptosis may also be instigated by a variety of extracellular and intracellular stimuli that induce DR expression and/or activation (Upton et al. 2012).

Necroptosis activation by ligand-dependent stimulation of DR depends on the recruitment and kinase activity of RIP1 (**Figure 1.4**) (Yuan et al. 2019). Although necroptosis can be activated through different DR, such as Fas and

TRAILRs, necroptotic signalling downstream of TNFR1 activation is still the most well-studied (Seo et al. 2019). At the molecular level, after TNF binding to TNFR1, RIP1 ubiquitination regulates whether a cell survive or dies by apoptosis or necroptosis. In fact, following TNFR1 activation, two different complexes can be formed, with opposite signalling. The complex I, a pro-survival complex, comprises the adaptor protein TNFR1-associated death domain protein (TRADD), RIP1, TNF-associated factor 2 (TRAF2), E3-ubiquitin ligases cIAP-1, cIAP2 and the linear ubiquitin chain assembly complex (LUBAC), that is formed by hem-oxidized iron-regulatory protein 2 ubiquitin ligase-1 (HOIL-1), HOIL-1L interacting protein (HOIP) and SHANK-associated RH domain-interacting protein (SHARPIN) (Haas et al. 2009). In this complex, E3 ligases LUBAC and cIAP1 promote RIP1 Met1-linear and Lys63-linked polyubiquitinations, that support the recruitment of NF-κB essential modulator (NEMO) and transforming growth factor beta-activated kinase 1 (TAK1), key mediators of NF-κB and MAPK pathways, respectively, thus promoting cell viability and inflammation (O'Donnell et al. 2011). In contrast, RIP1 deubiquitination by cylindromatosis (CYLD) induces apoptosis or necroptosis through the formation of complex II, a cytoplasmic death-inducing signalling complex (Hitomi et al. 2008). Here, TNFR1 is internalized in the endosome, along with recruitment of caspase-8, FAS-associated death domain protein (FADD), TRADD, and cellular FLICE-like inhibitory protein (cFLIP), which leads to the formation of complex IIa. This complex trigger apoptosis by activating caspase-3 and -7, and inhibits necroptosis through RIP1, RIP3, and CYLD cleavage by FADD and caspase-8 (O'Donnell et al. 2011). FADD or caspase-8 genetic deletion promotes early embryonic lethality in mice, that can be rescued by RIP3 co-deletion (Yeh et al. 1998; Dillon et al. 2012). Oppositely, in conditions where caspase-8 recruitment is prevented, RIP1 and RIP3 accumulate and phosphorylate, forming the complex IIb, called necrosome, which initiates necroptosis (**Figure 1.4**) (Zhang et al. 2009). Thus, caspase-8 inhibition is a crucial factor for RIP1-dependent necroptosis, which can be accomplished genetically or pharmacologically. In fact, several studies have demonstrated that the widely used pan-caspase inhibitor zVAD-fmk (zVAD) sensitizes various cell types to DR-induced necroptosis (Vercammen et al. 1998). For instance, murine fibroblast-like cell line, L929, undergoes necroptosis after treatment with zVAD, and that was later proved to

be mediated, at least partially, by TNF-α secretion (Wu et al. 2011). Importantly, defective caspase-8 activation was already detected in cortical lesions of multiple sclerosis (MS) patients and animal models, which could promote disease progression by restricting caspase-8 activity and cleaving proteins involved in necroptosis (Ofengeim et al. 2015).

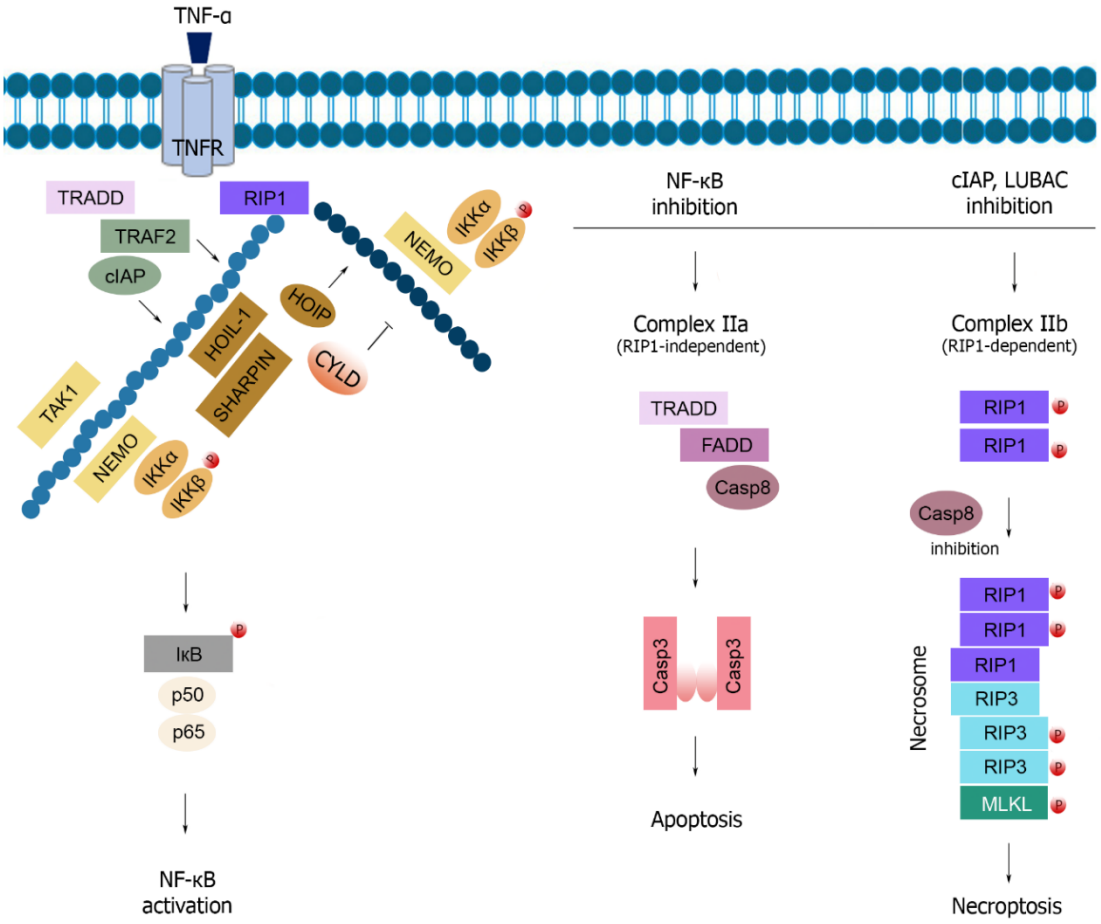

Figure 1.4. TNF-α signalling pathways downstream of TNFR. Upon binding of TNF to TNFR, TRADD and RIP1 are recruited by death domain interactions to initiate the formation of complex I. in this complex, TRADD binds to TRAF2 and recruits cIAPs, leading to K63 poly-ubiquitination of RIP1. LUBAC complex is recruited to perform K11 poly-ubiquitination of RIP1. Deubiquitination enzyme CYLD is recruited along with LUBAC to complex I. RIP1 polyubiquitination mediates the recruitment of signalling complexes, including TAK1 and NEMO/IKKLα/IKKβ. In normal conditions, activated IKKs and TAK promote NF-κB activation and transcription of proinflammatory and pro-survival genes, leading to the suppression of caspase-8 and RIP1 activation. However, in conditions where NF-κB activation is prevented, a cytosolic complex called complex IIa is formed. Caspase-8 is then activated and cleaves RIP1, leading to RIP1-indepdendent

apoptosis. Inhibition or depletion of cIAPs, LUBAC or TAK1 leads to rapid RIP1 homodimerization through death domain interactions and transphosphorylation, activating its kinase activity and forming complex IIb, which could lead to RIP1 kinase-dependent apoptosis. However, when caspase-8 is inhibited or depleted, active RIP1 can heterodimerize with RIP3, forming the necrosome, an amyloid-like structure. In the necrosome, active RIP3 recruit and phosphorylate MLKL, promoting MLKL oligomerization and consequent translocation to plasma membrane to induce necroptosis. Adapted from (Seo et al. 2019).

TLR3/TLR4 signals have also been shown to initiate necroptosis in different cell types via downstream TRIF signalling, in conditions where caspase-8 is inhibited. In fact, LPS- or dsRNA/polyinosinic-polycytidylic acid (poly I:C)-mediated activation of TLR4 and TLR3, respectively, promote the interaction between TRIF and RIP1 and/or RIP3 through their RIP homotypic interacting motif (RHIM) domains (He et al. 2011; Kaiser et al. 2013; Kim and Li 2013). In physiological conditions, recruitment and poly-ubiquitination of RIP1 is necessary to induce TRIF-dependent NF-κB activation (Meylan et al. 2004; Cusson-Hermance et al. 2005; Moriwaki and Chan 2017). However, in conditions where caspase-8 activation is prevented, RIP1 and RIP3 are cleaved, which results in necroptosis activation (Kaiser and Offermann 2005; Feoktistova et al. 2011). Interestingly, RIP1 kinase activity seems to contribute to TLR3/TLR4-mediated necroptosis in macrophages and microglia, although it is not necessary in other cell lines (Fricker et al. 2013; Kaiser et al. 2013; Kim and Li 2013; Kearney et al. 2015). Moreover, TLR3- and TLR4-mediated necroptosis in microglia was further proved to be facilitated by TRIF, RIP3 and JNK, and reactive oxygen species (ROS) (Kim and Li 2013). More specifically, when caspase-8 is inhibited, TRIF/RIP3 complex promotes a downstream ROS accumulation which then activates necroptosis independently of NF-κB activation (He et al. 2011).

1.3.1.2. Effectors of necroptosis

Originally described as an NF-κB and apoptosis regulator, it was only in 2009 that the key role of RIP3 in TNF-α-mediated necroptosis after caspase

inhibition was reported (Kasof et al. 2000; Sun et al. 1999; Cho et al. 2009; Zhang et al. 2009). RIP3 is a 528 amino acid protein which contains an active Ser/Thr kinase domain in the N-terminus and a RHIM domain near to the C-terminus, both essential for RIP3 necroptotic activity (Cho et al. 2009). In RIP1-dependent necroptosis, RIP1 further recruit RIP1 and RIP3 by their RHIM domain interactions, which leads to their phosphorylation and oligomerization, forming a large hydrophobic amyloid-like complex, called necrosome, that is a key event in the necroptotic signalling cascade (Li et al. 2012; Wu et al. 2014; Mompeán et al. 2018). Of note, heat shock protein 90 (Hsp90) and its co-chaperone cell division cycle 37 (CDC37) also control necrosome formation by increasing the stability of their component proteins (Li et al. 2015; Zhao et al. 2016). Importantly, RIP1/RIP3 heterodimers are not able to induce necroptosis by themselves, therefore requiring subsequent formation of RIP3/RIP3 homodimers. In fact, after homodimerization, RIP3 kinase domains induce RIP3 activation by cis-autophosphorylation of T231/S232 in mouse, and S227 in human RIP3, thus eliciting necroptosis (Sun et al. 2012; Xie et al. 2013; Wu et al. 2014; Raju et al. 2018). Hence, it is plausible to assume that RIP3 dimerization is most likely the key point of necroptosis induction. Moreover, under specific cellular settings, RIP3 increased levels or overexpression of a RIP3 phospho-mimetic mutant can elicit necroptosis in the absence of RIP1, which further highlights RIP3 as a master regulator of necroptotic cell fate (Upton et al. 2010; Zhang et al. 2009).

All aspects of RIP1 and RIP3 steady-state levels are intensely regulated, including their transcriptional activity, stability of expressed molecules and degradation. For instance, both proteins are regulated by the E3-ubiquitin ligase carboxyl terminus of Hsp70-interacting protein (CHIP), that ubiquitinates and targets them for lysosomal degradation (Seo et al. 2016). Concordantly, cIAPs can also poly-ubiquitinate RIP3 and promote its proteasomal degradation (Bertrand et al. 2011).

After activation, RIP3 kinase domain can effectively bind to MLKL C-terminal domain and phosphorylates T357/S358 in human MLKL or S345 in mouse MLKL, which is a crucial event for necroptosis induction (Sun et al. 2012; Xie et al. 2013; Rodriguez et al. 2016). Importantly, cells and mice lacking MLKL are completely protected from necroptosis (Murphy et al. 2013; Wu et al. 2013). In terms of structure, human and mouse MLKL have a similar composition,

consisting in a carboxy-terminal pseudokinase domain, linked to an amino-terminal four-helix bundle (4HB) domain by a two-helix linker. The 4HB domain functions as a cell death executer domain that is maintained in an inactive state by the pseudokinase domain (Tanzer et al. 2016; Petrie et al. 2019; Petrie et al. 2018). Interestingly, although human and mouse MLKL orthologs exhibit different mechanisms of activation, MLKL full-length protein and killer constructs are insignificant inducers of necroptotic cell death when expressed in MLKL-deficient cells from other species (Tanzer et al. 2016). Moreover, RIP3-mediated phosphorylation at S345 of mouse MLKL is enough to completely activate this protein, since MLKL phosphomimetic mutants may induce necroptosis in RIP3-deficient cells (Tanzer et al. 2016; Jacobsen et al. 2016; Petrie et al. 2019). Human MLKL, in the other hand, is more tightly regulated, with RIP3 playing an obligate role in MLKL activation. In fact, it was already demonstrated that MLKL phosphomimetic mutants for T357/S358, which prevents RIP3 action, totally negates necroptosis in MLKL-deficient human cells, thus suggesting that RIP3 recruitment is a key step in the necroptotic signalling activation (Petrie et al. 2019; Petrie et al. 2018). Furthermore, recent evidence has suggested the existence of regulatory mechanisms downstream MLKL activation that could regulate necroptosis (Petrie et al. 2019; Tanzer et al. 2016). For instance, ATP binding to human MLKL pseudokinase domain appears to destabilize MLKL oligomerization, thus indicating that ATP depletion, an event that occurs during cell death, allow MLKL activation (Petrie et al. 2018). In addition, others have also showed that HSP90 is critical for human and mouse MLKL oligomerization and consequently translocation to plasma membranes, despite its role in necrosome stabilization (Jacobsen et al. 2016; Zhao et al. 2016; Bigenzahn et al. 2016). Finally, TRAF2 can also prevent necroptosis through its association with MLKL, which is reverted during TNF-α-mediated necroptosis through CYLD-dependent TRAF2 deubiquitination (Petersen et al. 2015).

The presence of phosphorylated MLKL oligomers at the plasma membrane is considered a hallmark of cells undergoing necroptosis. However, some authors have shown that there is a time lag between phosphorylated MLKL oligomers translocation to the plasma membrane and consequent membrane rupture and cell death (Dondelinger et al. 2014; Wang et al. 2014; Tanzer et al. 2016; Petrie et al. 2019). The precise mechanisms by which MLKL induces

membrane rupture following MLKL oligomerization are still controversial (Davies et al. 2018; Petrie et al. 2018; Petrie et al. 2019). After RIP3 phosphorylation, p-MLKL translocates to the inner leaflet of the plasma membrane by low-affinity phosphatidylinositol phosphate (PIP)-binding sites present in the MLKL 4HB domain and exposes its high-affinity PIP-binding sites that allow a strong interaction between MLKL oligomers and the plasma membrane (Dondelinger et al. 2014; Quarato et al. 2016). Accordingly, several studies have proposed that MLKL mainly functions by directly or indirectly permeabilizing the plasma membrane (Sun et al. 2012; Zhao et al. 2012). In fact, it was already shown that MLKL oligomers can disrupt the plasma membrane by partial or whole insertion, which leads to the formation of pores or cation channels, allowing for Ca^{2+} and Na^{+} influx and consequent loss of ionic and osmotic homeostasis, culminating in cell lysis and release of intracellular contents, such as DAMPs (Dondelinger et al. 2014; Hildebrand et al. 2014; Wang et al. 2014; Xia et al. 2016; He and Wang 2018). Melastatin-related transient receptor potential 7 channel (TRPM7), a nonselective cation channel that is involved in maintaining Ca^{2+} and Mg^{2+} homeostasis, was also reported as necessary for necroptosis execution (Cai et al. 2014). However, other authors have recently suggested that MLKL can form plasma membrane nanopores that induce plasma membrane permeabilization independently of Ca^{2+} influx and that calcium oscillations in necroptosis are mainly due to the efflux from intracellular reservoirs (Ros et al. 2017; Ousingsawat et al. 2017).

Regarding the role of ROS as critical mediators of necroptosis, data published so far remains controversial as they seem to be unnecessary for necroptosis in some cell types (He et al. 2009; Tait et al. 2013; Zhang et al. 2017; Yang et al. 2018). Yet, it has been shown that TNF-α induces ROS production leading to necrosome assembly and consequently necroptotic cell death (Schenk and Fulda 2015). Importantly, necrosomal RIP3 seems to be essential for ROS production during necroptosis in FADD-deficient Jurkat cells, while MLKL silencing prevents cell death and only moderately protects from ROS production (Schenk and Fulda 2015; Zhang et al. 2009). Concordantly, the use of different antioxidants totally protects L929 and FADD-deficient Jurkat cells from necroptosis (Schenk and Fulda 2015; Zhang et al. 2017). ROS sequestration by antioxidants also attenuate necroptosis in several CNS cell types, including

microglia, oligodendrocytes, and neurons (Li et al. 2009; Kim et al. 2013; Iannielli et al. 2018).

Mitochondria are commonly described as a major mediator of ROS production during necroptosis, although other mechanisms are also reported (Kim et al. 2007; Zhang et al. 2017; Yang et al. 2018). Earlier studies indicated that the complex I of the electron transport chain is responsible for ROS production during TNF-α-induced necroptosis (Schulze-Osthoff et al. 1992; Goossens et al. 1999). In fact, mitochondrial complex I inhibition reduces TNF-α-dependent necroptosis in L929 cells (Schulze-Osthoff et al. 1992; Goossens et al. 1999; Yang et al. 2018; Zhang et al. 2017). Interestingly, during TNF-α/zVAD-induced necroptosis in NIH/3T3 murine fibroblasts, there is a depletion in mitochondria by mitophagy that reduces ROS production, thereby indicating a role for mitochondria in necroptotic-mediated ROS production (Tait et al. 2013). Concordantly, L929 cells depleted of mitochondria are partially protected from TNF-α/zVAD-induced necroptosis (Zhang et al. 2017; Yang et al. 2018). Several evidence also indicate that, upon stimulation, RIP1, RIP3 and MLKL may translocate to the mitochondria in several cell types (Zhang et al. 2009). After translocation, RIP3 may interact with and stimulate the activity of several metabolic enzymes, such as mitochondrial protein glutamate dehydrogenase 1 (GLUD1). In fact, GLUD1 knockdown partially prevents TNF-α-induced ROS production and cell death in NIH/3T3 cells (Zhang et al. 2009). Moreover, RIP3 can also directly phosphorylate pyruvate dehydrogenase complex E3 subunit, which enhances aerobic respiration and mitochondrial ROS production (Yang et al. 2018). Finally, others also demonstrated that upon translocation to the mitochondria, the necrosome can interact with and activate mitochondrial phosphoglycerate mutase family member 5 (PGAM5), described as a key executioner of necroptosis downstream of RIP3 activation through activation of mitochondrial fission dynamin-related protein 1 (DRP1) (Wang et al. 2012). Nevertheless, recent studies refuted this hypothesis, by performing genetic deletion or silencing of both proteins. In fact, some authors demonstrated that wild-type and PGAM5-/- primary MEFs treated with TNF, zVAD and smac mimetic, BV6 showed similar levels of necroptosis commitment. Moreover, in macrophages, LPS and zVAD-induced necroptosis independent of the inflammasome or autocrine TNF production. While RIP1-/- and RIP3-/-

macrophages were refractory to LPS and zVAD-dependent necroptosis, PGAM5-/- and wild-type macrophages have a similar response to LPS and zVAD-induced necroptosis, thus suggesting that PGAM5 may be dispensable for cell death triggered by classical necroptosis activators (Moriwaki and Chan 2017; Remijsen et al. 2014).

1.3.1.3. Necroptosis-based proteins and inflammation

Necroptosis is generally considered a proinflammatory type of cell death. During necroptosis, the intracellular components, or DAMPs, such as cytokines, ATP, high-mobility group protein B1 (HMGB1) and heat shock proteins, are released to the extracellular space, where innate immune cells are present, thus eliciting an inflammatory response (Moriwaki et al. 2014; Davidovich et al. 2014). Although the role of RIP1 and RIP3 in necroptosis-mediated inflammation has been widely described, there is now evidence that these necroptosis-related proteins may also regulate inflammatory signalling in response to TNFR and TLR activation in a necroptosis-independent manner (Ofengeim et al. 2013; Christofferson et al. 2012).

Notably, RIP1 mediates the crosstalk between cell survival or death by apoptosis or necroptosis, especially due to its scaffolding functions downstream receptor activation (Degterev et al. 2019). Several studies have described that, particularly in macrophages and microglia, RIP1 activation can mediate proinflammatory gene expression independently of cell death, with or without RIP3 recruitment and without MLKL involvement (Christofferson et al. 2012; Ito et al. 2016; Najjar et al. 2016; Ofengeim et al. 2017; Saleh et al. 2017; Zhu e tal. 2018; Degterev et al. 2019). In fact, RIP1 can regulate inflammatory responses downstream of TLR3 and TLR4 activation, which comprises activation of two parallel pathways mediated by MyD88 and TRIF (Cusson-Hermance et al. 2005; Meylan et al. 2004; Degterev et al. 2013). Regulation of inflammatory gene expression is thought to rely on MAPKs activation, particularly p38, ERK1/2 and JNK, and downstream activation of transcription regulators including activator protein 1 (AP1), specificity protein 1 (Sp1), NF-κB and interferon regulatory factors (IRFs). However, the precise molecular mechanisms involved in RIP1 and/or RIP3 modulation of inflammatory events are still mainly unknown

(Christofferson et al. 2012; Ito et al. 2016; Najjar et al. 2016; Zhu et al. 2018; Cao et al. 2018). Importantly, in mouse models of Alzheimer's disease (AD) and amyotrophic lateral sclerosis (ALS), RIP1 genetic or pharmacological inhibition diminishes inflammation, mostly due to reduced microglial M1 activation and proinflammatory gene expression, thus suggesting that RIP1 has a crucial role in regulating microglia-driven neuroinflammation (Ito et al. 2016; Ofengeim et al. 2017).

Conversely, several studies have suggested that RIP3 may also modulate inflammation independently of necroptosis (Moriwaki et al. 2014). Although earlier studies have shown that RIP3 could either activate or inhibit NF-κB (Kasof et al. 2000; Meylan et al. 2004; Sun et al. 1999; Yu et al. 1999), more recent findings demonstrate that RIP3 is a cell type-specific NF-κB activator (Moriwaki et al. 2014). In fact, RIP3ko mice-derived dendritic cells have a diminished proinflammatory response after LPS exposure, which is in part due to an incomplete NF-κB signalling downstream of IκB degradation. Moreover, in a colitis model, the production of proinflammatory cytokines, such as IL-1β, IL-23 and IL-22 is compromised in RIP3ko mice-derived dendritic cells, which leads to tissue repair (Moriwaki et al. 2014). Importantly, while mice expressing RIP3 lacking the RHIM domain present a phenotype similar to RIP3ko mice, mice expressing a $RIP3^{K51A}$ catalytically inactive form are similar to wt mice, therefore suggesting that the protective effect of RIP3 in the expression and production of proinflammatory cytokines depends on RHIM interactions, and not on RIP3 kinase activity or necroptosis (Moriwaki et al. 2017b). RIP3 deletion provides protection in a large variety of mouse models of disease, including TNF-α stimulation, IL-1β-dependent arthritis, renal ischemia-reperfusion injury, *Staphylococcus aureus* infection, sepsis-induced acute kidney injury and metastatic tumour, which suggests that, besides its function during necroptosis, RIP3 also plays a role in non-necroptotic pathways, particularly in inflammation (Lawlor et al. 2015; Kitur et al. 2016; Newton et al. 2016; Hänggi et al. 2017; Sureshbabu et al. 2018).

Furthermore, several studies have suggested that RIP1, RIP3, MLKL and caspase-8 downstream TLR3/4-TRIF activation may engage inflammasome in immune cells, including dendritic cells and macrophages, without the involvement of cell death (Lawlor et al. 2015; Kang et al. 2015; Conos et al. 2017).

Inflammasomes are multiprotein complexes that are formed upon proinflammatory stimuli exposure, ultimately leading to pro-IL-1β cleavage and maturation into IL-1β. More concretely, mature IL-1β secretion requires a two-step process. This process begins with the NF-κB-dependent *de novo* synthesis of pro-IL-1β, followed by inflammasome activation, that consists in the assembly of a sensor protein such as nod-like receptor pyrin domain-containing 3 (NLRP3), an adaptor protein ASC, and the IL-1β converting enzyme (ICE; caspase 1), in which effector caspase-1 is activated to cleave pro-IL-1β into the mature cytokine. Interestingly, pro-IL-1β processing may also be mediated by a caspase-8-activating complex, containing RIP1, RIP3 and FADD under specific conditions (Lawlor et al. 2015; Moriwaki et al. 2017). In fact, some studies have shown that upon LPS stimulation of dendritic cells, RIP3 can promote mature IL-1β secretion by interacting with caspase-8. However, in some cases, caspase-8 may also have an inhibitory role on RIP3/MLKL-mediated inflammasome activation and IL-1β maturation (Lawlor et al. 2015; Kang et al. 2013). As example, under conditions that caspase-8 is suppressed, the necrosome (RIP3/MLKL) is enough to promote NLRP3 activation and IL-1β processing, after TLR stimulation in C57BL/6 mouse macrophages (Kang et al. 2013). Additionally, others have also demonstrated that in the absence of cIAPs in macrophages, TLR4 stimulation mediate NLRP3 inflammasome activation through RIP3 recruitment and consequent kinase activity-independent activation of caspase-8, which leads to NLRP3-caspase-1 activation by a mechanism independent of MLKL. However, concomitant inhibition of cIAPs and caspase-8 leads to TLR-induced NLRP3 activation in a RIP3/MLKL-dependent manner, thus suggesting that MLKL-mediated inflammasome activation is limited by caspase-8 (Lawlor et al. 2015). Conversely, in dendritic cells, caspase-8 deficiency has shown to facilitate NLRP3 inflammasome activation after TLR4 stimulation, which is prevented by MLKL silencing (Kang et al. 2013; Gutierrez et al. 2017). Moreover, MLKL activation is sufficient to trigger K^+ efflux and the consequent NLRP3 inflammasome assembly, thus leading to caspase-1-dependent IL-1β processing. MLKL can also contribute to inflammasome activation by NLRP3 and pro-IL-1β transcriptional regulation in a cellular and context dependent manner (Zhang et al. 2016).

1.3.1.4. Physiological roles of necroptosis

Throughout the years, necroptosis has evolved as a fighting mechanism against viral infections that are capable of terminating apoptosis in the host cell. Importantly, necroptosis, as a proinflammatory type of cell death, not only finishes viral replication in infected cells but also promotes the release of proinflammatory molecules, such as cytokines, DAMPs and PAMPs, thus eliciting an immune response against the invading pathogen (Dondelinger et al. 2016). In fact, a combination of necroptosis activation and proinflammatory cytokine production signals the immune system to clear potentially harmful pathogens from the organism (Dondelinger et al. 2016). Recently, some authors showed that necroptotic cells can prolong *de novo* synthesis of cytokines and chemokines after membrane permeabilization and irreversibly commitment to cell death, which clearly contribute to necroptotic cell immunogenicity (Orozco et al. 2019). Evidence has indicated that some DNA viruses, such as poxviruses, can target and inhibit caspase-1 and caspase-8 and thus promote necroptosis. In fact, cellular infection with poxvirus vaccinia virus leads to the expression of the viral pan-caspase inhibitor B13R/Spi2, which inhibits caspase-8, thus inducing TNF-α-dependent necroptosis (Cho et al. 2009). Moreover, infection with others virus, such as influenza A virus (IAV), can also induce necroptosis. For instance, in macrophages and epithelial cells, NS1 protein of human IAV interacts with MLKL and increases its oligomerization and translocation to plasma membrane, thus inducing necroptotic cell death. In addition, NS1/MLKL interaction also leads to NLRP3 inflammasome activation and consequent increase in IL-1β processing and secretion (Gaba et al. 2019). Contrarily, several other viruses, including murine cytomegalovirus and human herpes simplex virus type 1 (HSV-1) and type 2 may also have anti-necroptotic mechanisms (Guo et al. 2015; Upton et al. 2012). For instance, HSV-1/2 can inhibit necroptotic and apoptotic pathways through ICP6 or ICP10 expression, that can bind to caspase-8 and RIP1/3 (Guo et al. 2015). However, in murine cells, ICP6/10 can promote RIP3-dependent necroptosis, thus emphasizing that RIP3 and MLKL are poorly conserved among mammalian species (Wang et al. 2014; Dondelinger et al. 2016). Interestingly, some poxviruses can also avoid necroptosis in mouse and human cells, by expressing a homologous MLKL pseudokinase able to sequester RIP3 (Petrie et

al. 2019). Finally, the recently identified severe acute respiratory syndrome coronavirus 2 (SARS-CoV-2), responsible for the coronavirus disease 2019 (COVID-19) pandemic, was also shown to activate caspase-8 and trigger apoptosis and inflammatory cytokine processing in the lung epithelial cells. The processed inflammatory cytokines are released through the virus-induced necroptosis pathway. SARS-CoV-2 infection was shown to promote a dual mode of cell death pathways, apoptosis, and necroptosis, as well as activation of inflammatory responses, which were observed in the infected HFH4-hACE2 transgenic mouse model and in post-mortem lung sections of fatal COVID-19 patients (Li et al. 2020).

Moreover, several bacterial species have mechanisms to induce necroptosis in some cell types, such as macrophages, to avoid engulfment and clearance (Robinson et al. 2012; González-Juarbe et al. 2015). For instance, keratinocytes infected with *Staphylococcus aureus* can recruit necroptosis to clear bacteria from cells. Interestingly, while MLKL-deficient mice are not able to decrease bacterial load, RIP3ko mice have higher staphylococcal clearance and reduced inflammation, which could be due to a reduced IL-1β maturation and apoptosis activation (Kitur et al. 2016).

Several studies also described that necroptosis may be important in the immunogenicity and immune system activation against cancer cells. In fact, DAMPs released by necroptotic cells into the tissue microenvironment provide antigens and inflammatory cytokines to dendric cells, which allows for antigen cross-priming and consequent activation of cytotoxic CD8+ T lymphocytes, promoting tumour cell elimination (Aaes et al. 2016; Yang et al. 2016; Gong et al. 2019; Yatim et al. 2015). Moreover, during necroptosis, RIP1 and NF-κB activation are crucial for begin CD8+ T cell adaptive immune response, while RIP3 is described to mediate natural killer T (NKT) cell function and anti-tumour immune response through PGAM5 activation (Gong et al. 2019; Yatim et al. 2015; Aaes et al. 2016). Importantly, it is widely described that several key molecules of the necroptotic pathway, including RIP3, are downregulated in different types of cancer cells, thus indicating that cancer cells may avoid necroptosis upon gain resistance to apoptosis to survive (Gong et al. 2019; Koo et al. 2015).

Furthermore, in physiological conditions where apoptosis is inhibited, necroptosis may also occur. For instance, mice with a deficiency in Bcl-2-

interacting mediator of cell death (Bim), an important pro-apoptotic BH3-only Bcl-2 family member, present lymphoproliferative disorder and autoimmunity due to inadequate apoptosis activation in T cells. Importantly, caspase-8 deletion in these cells partially reverts this phenotype through necroptosis activation (Bohgaki et al. 2011). Of note, although mice deficient in both FADD or RIP3 and caspase-8, and MLKL are viable and fertile, they present a profound lymphoproliferative disorder over time and accumulation of T lymphocytes (Dillon et al. 2012; Kaiser et al. 2011; Newton et al. 2014; Oberst et al. 2011). Conversely, these conditions are also observed in mice and humans with mutations in FAS or FASL, therefore indicating that MLKL and FADD may have key roles in preventing lymphoproliferative disease (Zhang et al. 2016). Surprisingly, although necroptosis is widely described as a proinflammatory type of cell death, other studies suggested that RIP3 and MLKL can also be negative regulators of TNF-α- and LPS-induced inflammation. In fact, *in vitro* and *in vivo* studies demonstrated that TNF-α- and LPS-induced necroptosis resulted in a dramatic reduction of the production of proinflammatory cytokines and chemokines, which is not compensated by the intracellular DAMPs release. Moreover, RIP3ko not only inhibited necroptosis but also re-established proinflammatory cytokine production (Kearney et al. 2015; Li et al. 2019).

1.3.1.5. Necroptosis in central nervous system diseases

The pathological relevance of necroptosis has been extensively described in a variety of paradigms. Necroptosis has emerged as a key event in the pathogenesis of multiple diseases with an inflammatory component, including acute and chronic neurodegenerative diseases (Choi et al. 2019; Yuan et al. 2019). Importantly, enhanced protein levels of RIP1 and RIP3, two critical necroptotic mediators, are frequently observed in several pathological conditions (Vitner et al. 2014). Importantly, in the CNS, caspase-8 inhibition was shown to protect neurons in an inflammatory neuronal loss model, by specifically inducing necroptosis in activated microglia (Fricker et al. 2013). However, both microglial and neuronal necroptosis has been described in several neurodegenerative diseases, including AD, ALS and PD (Ito et al. 2016; Iannielli et al. 2018; Caccamo et al. 2017; Oñate et al. 2020).

Necroptosis has been studied in a wide range of diseases, including adult ischemic or hemorrhagic stroke (Degterev et al. 2005), neonatal hypoxic-ischemic damage (Northington et al. 2011), and neurodegenerative diseases (Caccamo et al. 2017; Iannielli et al. 2018; Ofengeim et al. 2015; Oñate et al. 2020). Several of these studies commonly use Nec-1, a tryptophan-based molecule that acts as an allosteric type III RIP1 inhibitor, as potent necroptosis inhibitor. Nec-1 was firstly used in an ischemia brain injury mouse model, in which intracerebroventricular administration of this molecule considerably decreased infarct volume following middle cerebral artery occlusion (Degterev et al. 2005). Later studies demonstrated that Nec-1 administration inhibited necroptosis of hippocampal neurons following oxygen-glucose deprivation (OGC). Moreover, in a haemorrhagic stroke rat model, Nec-1 administration protected from BBB disruption (Chen et al. 2019). Others have also suggested that Nec-1 protective role may be due to a decrease in RIP1/RIP3 interaction in the brain and consequent mitigation of necroptotic cell death and inflammation (Su et al. 2015; Lule et al. 2017). Importantly, RIP3 or TNF-α inhibition also showed protection through downregulation of necroptosis markers (Yuan et al. 2019). Furthermore, in a model of neonatal hypoxia-ischemia, Nec-1 treatment also reduced RIP1/RIP3 necrosome formation and inflammation, and this protection seemed to rely on the improvement of mitochondrial complex I activity and in the reduced mitochondrial structural deficits in both neurons and astrocytes (Northington et al. 2011; Chavez-Valdez et al. 2012).

Importantly, necroptosis has also been reported during neurodegeneration and neuroinflammation associated to several chronic neurodegenerative diseases (Yuan et al. 2019). For instance, Nec-1 has been reported to effectively inhibit necroptosis in animal models of Huntington's disease (HD) (Zhu et al. 2011). Activation of necroptosis mediators, RIP1, RIP3 and MLKL, along with defective caspase-8 activation have been observed in human MS cortical lesions. In fact, TNF-α-mediated necroptosis is reported as responsible for oligodendrocyte degeneration. Importantly, Nec-1s, a more stable variant of Nec-1, as well as RIP3 deficiency decrease motor deficits, myelin loss and microglial activation in animal models of MS, thereby protecting oligodendrocyte from cell death (Ofengeim et al. 2015). Similarly, some studies have described increased activation of RIP1, RIP3, and MLKL, and therefore necroptosis in spinal cords of

superoxide dismutase 1 (SOD1)^{G93A} transgenic mouse model of ALS, as well as in the optineurin (OPTN)$^{-/-}$ mice, whose loss-of-function gene mutations are linked to ALS (Ito et al. 2016). Importantly, in both mouse models, Nec-1s and RIP3 deficiency can prevent oligodendrocyte cell death, as well as M1-microglial activation and consequent axonal degeneration (Ito et al. 2016). Moreover, RIP1, RIP3, and MLKL activation was also observed post-mortem in the spinal cord of ALS patients, particularly in oligodendrocytes and microglia present in demyelinated while matter, thus indicating that necroptosis may be involved in ALS pathogenesis (Ito et al. 2016). Similarly, in a humanized *in vitro* model of ALS, astrocytes obtained from sporadic ALS patients, induced necroptotic neuronal death in neurons differentiated from human embryonic stem cells (Re et al. 2014). In contrast, a recent study showed no variations in RIP1 protein levels in ALS patient spinal cords (Dermentzaki et al. 2019). Moreover, these authors also reported that RIP3 deficiency did not offer protection in the SOD1^{G93A} transgenic mouse model (Dermentzaki et al. 2019). In AD, activation of necroptotic mediators RIP1, RIP3, and MLKL was observed in human AD brains, particularly in neurons and microglia, and their levels seem to positively correlate with Braak disease stage (Caccamo et al. 2017; Ofengeim et al. 2017). Importantly, in a transgenic mouse expressing five human familial AD mutations, Nec-1s reduced p-MLKL recruitment and neurodegeneration associated with necroptosis (Ofengeim et al. 2017). Moreover, Nec-1s or RIP1^{D138N} kinase death mutation decreased β-amyloid plaque burden, as well as microglial presence near plaques and proinflammatory cytokine expression in the APP/PS1 mice (Ofengeim et al. 2017).

In PD, necroptosis has also emerged as a possible contributor to dopaminergic neurodegeneration. Analysis of post-mortem brain tissue from PD patients revealed the increased levels of RIP1, RIP3, and p-MLKL in the SN (Oñate et al. 2020; Iannielli et al. 2018; Hu et al. 2019). Moreover, others have shown the involvement of necroptosis in the acute MPTP mouse model of PD (Lin et al. 2020), as well as in mice injected with 6-OHDA (Oñate et al. 2020). Importantly, Nec-1s administration attenuated dopaminergic neurodegeneration in the sub-chronic MPTP mouse model as well as axonal degeneration and loss of TH-positive neurons in the SN of 6-OHDA-injected mice (Oñate et al. 2020; Iannielli et al. 2018). In accordance, RIP3- and MLKL-deficient mice were

protected from MPTP deleterious effects in the nigrostriatal circuit and showed reduced proinflammatory cytokine expression in the midbrain (Lin et al. 2020). Interestingly, a recent study demonstrated that in the sub-chronic MPTP mouse model, treatment with a miR-425 mimic confers protection from increased RIP1 and p-MLKL levels in TH-positive neurons and that this protection positively correlates with higher TH-fiber density in the striatum, dopaminergic neurons, and decreased neuroinflammation (Hu et al. 2019).

Overall, necroptosis has demonstrated to be relevant in several neurodegenerative diseases. However, besides its key role in necroptosis, RIP1 is also involved in other signalling pathways, including apoptosis and inflammation. In addition, RIP1 scaffold is important for cell and animal survival, since $RIP1^{-/-}$ mice present systemic inflammation and cell death in several tissues and die during the postnatal phase (Rickard et al. 2014; Dannappel et al. 2014). Conversely, inhibition of RIP1 kinase activity appears to be more beneficial than RIP3 or MLKL deficiency in different CNS pathologies. In fact, RIP1 kinase inhibition has no deleterious effects *in vivo*, being described as an important therapeutic target for the treatment of chronic inflammatory neurodegenerative diseases (Yuan et al. 2019).

1.3.1.6. Necroptosis as a therapeutic target

As mentioned above, in 2005, the first RIP1 kinase inhibitor was identified in a phenotypic screening for small molecule inhibitors of TNF-α-induced necroptosis in human monocyte U937 cells (Degterev et al. 2005; Degterev et al. 2008). Nec-1 is an allosteric type III RIP1 inhibitor that stabilizes RIP1 kinase domain in an inactive conformation (**Figure 1.5**) (Degterev et al. 2008; Degterev et al. 2019; Takahashi et al. 2012).

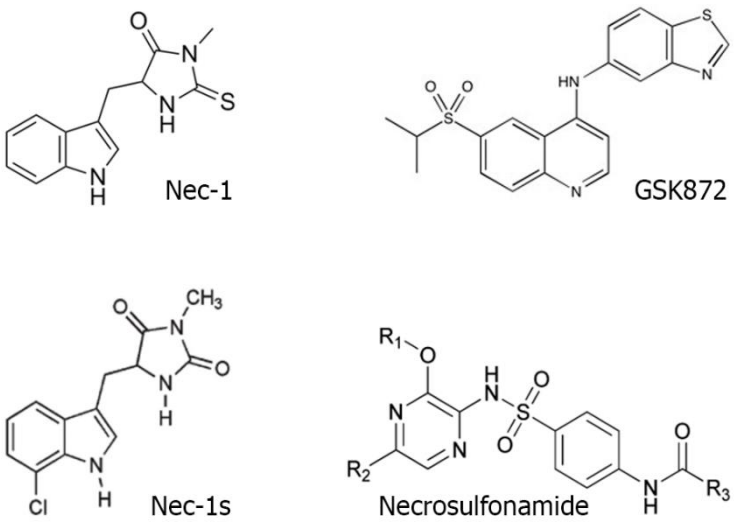

Figure 1.5. Chemical structure of RIP1, RIP3 and MLKL inhibitors. Chemical structure of RIP1 inhibitors, Nec-1 and Nec-1; RIP3 inhibitor, GSK872; and MLKL inhibitor, necrosulfonamide. Adapted from (Zhuang et al. 2020).

Nec-1 is considered a strong necroptosis inhibitor, and although the original Nec-1 has a short *in vivo* half-life (~5 minutes) and non-specific activity against other proteins, such as indoleamine 2,3-dioxygenease (IDO) that is involved in inflammatory responses, chemical optimization of this compound has led to commonly used derivatives with a half-life of approximately 1 h in mouse microsomal assay (Vandenabeele et al. 2013; Degterev et al. 2013). Later, others demonstrated that Nec-1s, which has better specificity and pharmacokinetic properties than Nec-1, still holds a poor half-life *in vivo*, thus suggesting the huge need for the development of better RIP1 inhibitors (Ofengeim et al. 2015). In that regard, other RIP1 inhibitors were developed, including GSK2982772, which targets the same allosteric pocket as Nec-1s, and is currently in phase II clinical trials for the treatment of inflammatory diseases, specifically psoriasis, rheumatoid arthritis and ulcerative colitis (Harris et al. 2017). 7-Oxo-2,4,5,7-tetrahydro-6H-pyrazolo[3,4-c]pyridine derivatives were also recently developed by Takeda Pharmaceuticals as novel potent, orally available and brain penetrant type III RIP1 inhibitors, that present great pharmacokinetic profiles and capacity to ameliorate disease progression in a MS mouse model (Yoshikawa et al. 2018). More recently, DNL747, a highly selective brain RIP1 inhibitor developed by Denali Therapeutics, also reached into phase I clinical trials for AD and ALS,

while DNL788 is currently in preclinical development and appears to have higher preclinical therapeutic window in comparison with DNL747, enabling the development for several medical indications, such as AD, ALS and MS (Yuan et al. 2019). Moreover, anti-leukemic agents and breakpoint cluster region-abelson leukemia (BCR-ABL) inhibitors pazopanib and ponatinib were approved as type I and type II RIP1 inhibitors, respectively. However, both molecules present poor specificity (Degterev et al. 2019; Fauster et al. 2015). Some RIP3 inhibitors were also reported, including GSK840, GSK843, GSK872 and GW39B (**Figure 1.5**). However, these compounds showed to induce RIP1-dependent apoptosis, while can also target other RIP family members, such as RIP2 (Mandal et al. 2014; Newton et al. 2014). Furthermore, a recent study identified GSK074 as a new class of necroptosis inhibitors with dual targeting for RIP1 and RIP3. Although this molecule showed structural similarity to GSK843, an already established RIP3 inhibitor, it does not present cytotoxicity event at high doses in contrast to GSK843 (Zhou et al. 2019). Thus, dual inhibitors may have the advantage of inhibiting both RIP1-dependent and -independent necroptosis, as well as inhibition of non-necroptotic RIP3 kinase-dependent roles (Zhou 2019). Finally, necrosulfonamide can also inhibit necroptosis by blocking MLKL (**Figure 1.5**). However, this molecule only blocks human MLKL and not the mouse ortholog, thus invalidating testing in preclinical mouse models of disease (Sun et al. 2012). Overall, RIP1 stands out as a prime candidate for therapeutic intervention, due to its structural characteristics and functions dependent or independent of necroptosis, thus allowing for the development of highly specific type III inhibitors.

1.4. MicroRNAs

MicroRNAs are a class of endogenous conserved small non-coding RNAs of approximately 21-25 nucleotides that regulate gene expression at the post-transcriptional level (Bartel 2004; Lin and Gregory 2015). miRNA biogenesis involves a sequence of highly regulated processing steps that begin with the formation of a primary miRNA (pri-miRNA) from miRNA genes. Still in the nucleus, the pri-miRNA is processed by Drosha, a class 2 RNase III enzyme, to form a precursor miRNA (pre-miRNA) that is then exported to the cytoplasm by

Exportin-5. In the cytoplasm, pre-miRNAs are processed by Dicer, another RNase III, to produce double-stranded mature miRNAs that are loaded onto the Argonaute protein to produce the effector miRNA-induced silencing complex (miRISC). Mature miRNAs are then responsible for binding miRISC to target messenger RNAs (mRNAs) leading to gene silencing by translational repression and/or mRNA deadenylation and degradation. Target recognition involves sequence complementarity between the 5' end of the miRNA, called the seed region, and the 3'-untranslated regions (3'-UTR) of the mRNA (**Figure 1.6**) (Bartel 2004; Wahid et al. 2010). Importantly, each miRNA can bind to a multiplicity of targets, allowing its action on different signalling pathways. Moreover, different miRNAs may also target the same mRNA, leading to a tight regulation of the gene expression network (Friedman et al. 2009).

1.4.1. MicroRNAs as biomarkers of disease

During the past few years, circulating miRNAs have been described as promising biomarker candidates for PD, as they have small size and great stability, mostly due to the binding to RNA-binding proteins and/or package into exosomes (Etheridge et al. 2011). In addition, miRNAs can also be easily detected in a multiplicity of human specimens, ranging from frozen and formalin-fixed paraffin-embedded tissues, to biofluids, such as amniotic fluid, breast milk, cerebrospinal and peritoneal fluid, plasma, serum, saliva and urine (Scian et al. 2011; Shigehara et al. 2011; Weber et al. 2010). Moreover, there are several established methods to detect and quantify miRNA expression, including RNA sequencing, microarray and quantitative RT-PCR (Ferracin et al. 2015). Alterations in miRNAs expression have been associated with PD-relevant pathophysiological processes, turning them into promising body fluid-derived biomarkers for PD diagnosis and progression. One of the first studies profiling miRNAs expression in the plasma of PD patients identified miR-222, miR-626 and miR-505-3p as a set of miRNAs able to predict PD development. miR-222 and miR-505 are possible targets for PARK2 by TargetScan Human, an *in silico* platform for targeting prediction, while miR-626 is a possible target for LRRK2 and PARK2 (Khoo et al. 2012). Since then, several miRNAs have been highlighted, such as miR-124-3p and miR-30a-5p, that are decreased and

increased, respectively, in the serum of PD patients in comparison with control subjects (Schwienbacher et al. 2017). Of note, miR-30a-5p may target AKR Serine/Threonine Kinase 1 (AKT1), epidermal growth factor receptor (EGFR), and ABL proto-oncogene 1, non-receptor tyrosine kinase (ABL1) that are involved in the EGFR/PI3K/AKT pathway, which is mostly activated by oxidative stress (Schwienbacher et al. 2017; Wang et al. 2000). Curiously, some PD-related genes, including parkin, PINK1 or DJ-1 that are involved in the mitochondrial dynamic regulation, are also related with this pathway (Klinkenberg et al. 2012). Importantly, others have also demonstrated that miR-29a-3p, miR-29c-3p, miR-19a-2p, and miR-19b-3p were decreased in the serum of iPD and LRRK2-PD patients comparing to healthy individuals (Botta-Orfila et al. 2014). In contrast, other studies profiled miRNA expression in PBMCs and proposed that miR-29a-3p, miR-29c-3p, miR-30b-5p, and miR-424-5p were increased in these cells in PD patients (Pasinetti 2012; Serafin et al. 2015). Interestingly, miR-29 have been associated to insulin resistance, a process possibly linked to PD neurodegeneration (Herrera et al. 2010; Trajkovski et al. 2011; Aviles-Olmos et al. 2013). Moreover, one of the candidate targets of miR-29a-3p is DJ-1, which has a role in protecting cells against oxidative stress and death. Cell division control protein (CDC)-42, a PD-candidate gene involved in neuronal death, was also identified as a potential target of miR-29a-3p and miR-103a-3p (Serafin et al. 2015). Importantly, most of these studies determined the diagnostic accuracy of the miRNAs identified by performing ROC curve analysis, and indicated values between 63% and 97%, which are usually improved by combining multiple miRNAs (Botta-Orfila et al. 2014; Gui et al. 2015).

In sum, an ideial biomarker needs to be objectively measured and evaluated and is an indicator of a physiological or pathological biological process or of a pharmacological reaction to therapy (Ziemssen, Akgün, and Brück 2019). Moreover, a good biomarker is generally safe for the patient, easy to detect, and the analytical detection method should be highly accurate and reproducible, as well as simple, fast, and cost-effective (Sahab, Semaan, and Sang 2007; Ziemssen, Akgün, and Brück 2019). Finally, the result of the analytical method should not be influenced either by sample collection, sample processing or sample storage (Teunissen et al. 2014; Ziemssen, Akgün, and Brück 2019). Overall, dysregulated miRNAs that are present in body fluids can potentially be

used as diagnostic markers for several diseases, including PD. In fact, miRNA biomarker research could lead to more accurate disease diagnosis using less invasive techniques, which is particularly important in PD, where diagnosis is mainly based on symptomatic and cognitive examinations rather than through more objective tests.

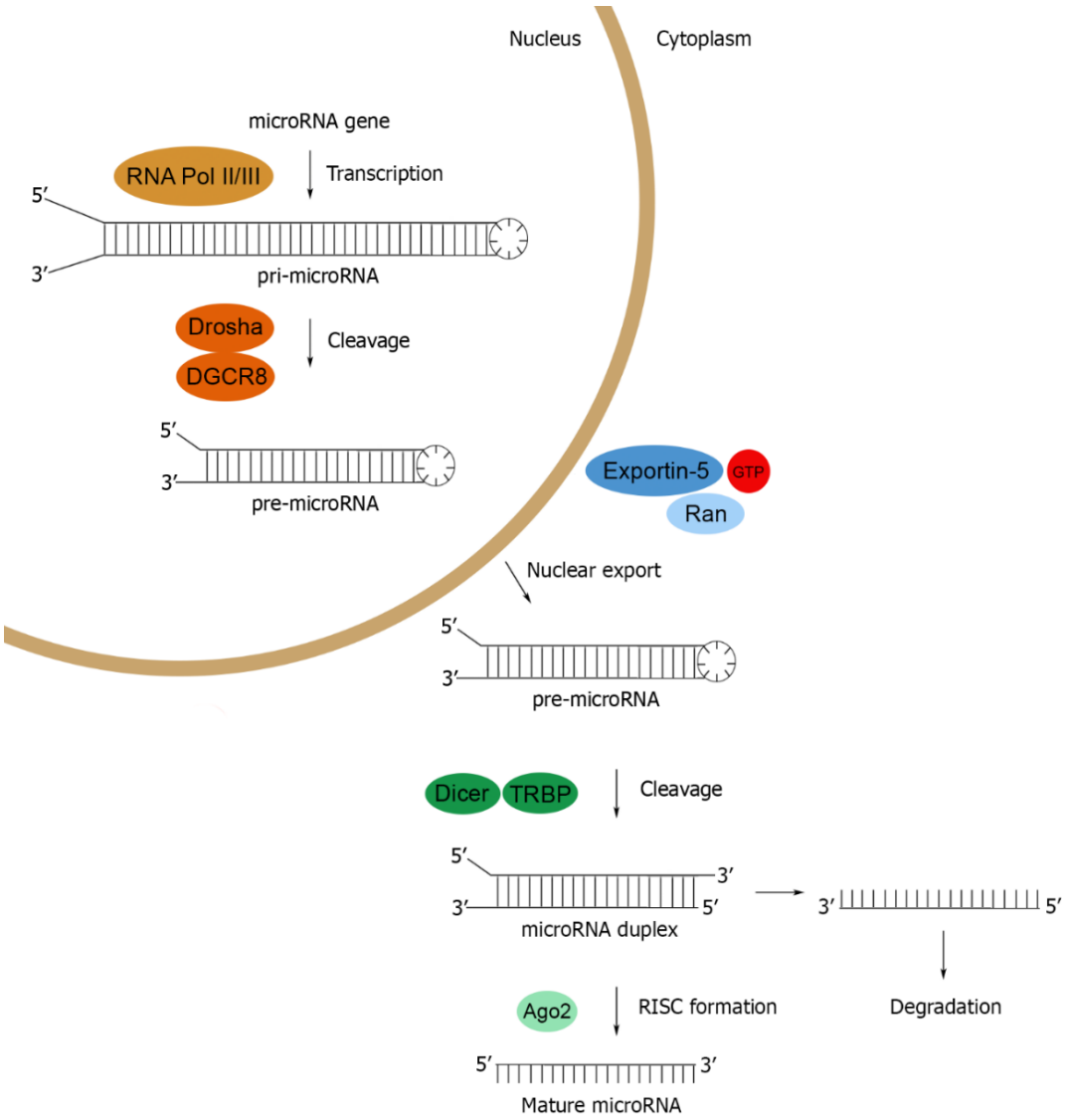

Figure 1.6. Canonical pathway of microRNA biogenesis. MicroRNA canonical maturation begins in the nucleus with the formation of the primary miRNA transcript (pri-miRNA) by RNA polymerase II or III. The pri-miRNA is then cleaved by the complex Drosha-DGCR8. The resultant precursor hairpin, pre-miRNA, is exported to the cytoplasm by Exportin-5-Ran-GTP. In the cytoplasm, the pre-miRNA is cleaved into its mature length by the RNase Dicer in complex with TRBP, a double-stranded RNA-binding protein. Then, the functional strand of the mature miRNA is loaded along with

Argonaute (Ago2) proteins into the RNA-induced silencing complex (RISC), leading to silencing of target mRNAs. Adapted from (Winter et al. 2009).

1.4.2. MicroRNAs as a therapeutic approach

MiRNAs have also shown to regulate several important biological processes involved in the maintenance of normal cellular functions, such as cell death, proliferation and differentiation (Satterlee et al. 2007). However, if dysregulated, they can assume a pathological function therefore contributing to disease pathogenesis. In fact, dysregulated miRNAs are key candidate molecules for diagnosis and prognosis of disease, as well as promising targets for therapeutic intervention (Gaudet et al. 2018; Leung et al. 2010; Shivdasani 2006). In that regard, it is extremely important to discover the mechanism(s) underlying miRNAs dysregulation due to their great potential for the discovery and development of novel therapeutic regimens. As such, alterations in miRNA content using synthetic oligos may alter the underlying mechanisms of neurodegenerative diseases, including PD.

Growing evidence suggests that miRNAs have a key role in controlling α-syn accumulation in apoptotic neurons (Doxakis 2010; Choi et al. 2014). In fact, some PD-downregulated miRNAs could contribute to α-syn accumulation and consequently to dopaminergic neuronal loss (Gao et al. 2011). For instance, miR-7 is reduced in specific brain regions of PD mice models, including in the SN and midbrain of MPTP-injected mice (Saba et al. 2008; Junn et al. 2009). Of note, miR-7 was already proved to directly target the 3'-UTR region of α-syn mRNA, which leads to α-syn accumulation and further neuronal loss (Junn et al. 2009; Doxakis 2010; Fragkouli and Doxakis 2014; Kabaria et al. 2015). Moreover, mir-7 and miR-153 targeting of α-syn has been shown to affect signalling by modulating BDNF expression and protein kinase B (AKT) activity (Yuan et al. 2010; Chung et al. 2011). Importantly, miR-7 and miR-153 overexpression protects neurons from death in the MPP^+ *in vitro* model of PD (Titze de Almeida et al. 2018; Doxakis 2010; Fragkouli and Doxakis 2014). Moreover, overexpression of these miRNAs significantly upregulated mammalian target of rapamycin (mTOR) complex downstream signalling (Fragkouli and Doxakis

2014), suggesting their role in mTOR activation. overall, this data suggest that miR-7 and miR-153 overexpression protect neurons from MPP^+-induced toxicity by upregulating mTOR downstream targets (Fragkouli and Doxakis 2014). Importantly, intra-striatal injection of miR-7 mimics in MPTP-exposed mice also decreases dopaminergic neuronal loss, microglial activation, and therefore the proinflammatory cytokine content (Zhou et al. 2016).

Regarding miR-124, one of the most abundant miRNAs in the adult brain, it is involved in the maintenance of neuronal identity and synaptic plasticity (Cheng et al. 2009; Åkerblom et al. 2012; Yu et al. 2008; Visvanathan et al. 2007). miR-124 has been reported as downregulated in the SN of MPTP-treated mice and in dopaminergic neurons *in vitro* and was further proved to target 3'-UTR α-syn mRNA. Importantly, miR-124 overexpression reverts cell death, being therefore suggested as a potential therapeutic target in PD (Kanagaraj et al. 2014). MiR-34c-5p is described as depleted in the amygdala, frontal cortex, SN and cerebellum of PD patients, and its altered expression also influences α-syn accumulation (Miñones-Moyano et al. 2011). A decrease in the levels of miR-34c-5p starts early in premotor stages and continues in later stages of disease suggesting a role for this miRNA during the gradual and progressive loss of dopaminergic neurons even before the motor symptoms emerge (Miñones-Moyano et al. 2011). Other studies have also reported that miR-34c-5p directly targets α-syn 3'-UTR mRNA, leading to an accumulation of this protein, affecting neuronal viability, oxidative stress, and mitochondrial dysfunction in SH-SY5Y cells (Miñones-Moyano et al. 2011).

Further, miRNAs targeting genes involved in neuroinflammation have also been described. For instance, some authors showed several miRNAs either up- (let-7b, miR-103, miR-155, miR-16-5p, miR-17, miR-204, miR-27, and miR-98) or downregulated (let-7a, miR-128, miR-145, miR-181a, miR-23a, miR-23b, and miR-320a) in TNF-α-treated SH-SY5Y cells (Prajapati et al. 2015). In addition, they also suggested that miR-155 and miR-27 target ATP5G3, a subunit of F1-ATP synthase, whose expression is reduced in the presence of TNF-α. Concordantly, SH-SY5Y cells transfected with antago-miR-155, that inhibits miR-155 expression, showed a decrease in TNF-α-induced cell death (Prajapati et al. 2015). MiR-155 role in the regulation of inflammatory processes was formerly suggested, as it inhibits FADD, SOC1, and IKK, thus increasing the production of

proinflammatory cytokines (IL-1, IL-6, TNF-α) and iNOS (Louafi et al. 2010; Liu and Abraham 2013; Ponomarev et al. 2013; Thome et al. 2016). Moreover, miR-7 has also been reported to directly regulate NLRP3 inflammasome, which is activated in the serum and midbrain of PD patients, leading to a reduction of proinflammatory cytokine content *in vitro* in the BV2 cell line and in MPTP-treated mice (Zhou et al. 2016).

A few years ago, miRNAs able to directly regulate LRRK2 expression were also discovered. Of note, some authors showed an increase in LRRK2 expression levels in frontal cortex of PD patients in comparison with control subjects and a concordant decrease in miR-205 levels, which was further proved to directly target the 3'-UTR LRRK2 mRNA (Cho et al. 2013). Accordingly, miR-205 overexpression in neuronal primary cultures led to a LRRK2 reduction, which prevent its harmful effects (Cho et al. 2013). Recently, miR-335 has also been associated with PD, with studies showing a downregulation or an upregulation in PD patients comparing with control subjects, and LRRK2 was further confirmed as a direct target of this miRNA (Martins et al. 2011; Yılmaz S et al. 2016; Patil et al. 2019). Moreover, some LRRK2 pathogenic mutations, such as the G2019S mutation, have been reported to upregulate the expression of E2F transcription factor 1 (E2F1), leading to neuronal death, by inhibiting expression of let-7 and miR-184-3p. In contrast, let-7 and miR-184-3p overexpression reverted mutant LRRK2 neurotoxic effects (Gehrke et al. 2010), suggesting that LRRK2 may have a role in PD pathogenesis through miRNA modulation, which highlights new possible routes for PD treatment.

OBJECTIVES

Parkinson's disease is a complex multifactorial disorder, mostly instigated by dopaminergic neuronal loss in the *substantia nigra*, and whose underlying causes and mechanisms are still not completely understood. Nowadays, PD diagnosis only rely on clinical observations and the gold standard for the treatment of PD is still a pharmacological approach directed to alleviate motor symptoms of the disease. As such, PD remains without a definitive cure.

During several years, apoptosis was assumed as the main cell death pathway involved in PD neuronal loss. However, recent findings suggest that other cell death mechanisms may be involved, including necroptosis. Thus, targeting necroptosis has emerged as a promising therapeutic strategy in neurodegenerative diseases, especially PD. Furthermore, miRNAs dysregulation underlies altered expression of target genes, impacting neuronal dysfunction and disease pathogenesis. In that regard, miRNAs appeared in the past few years as potential biomarkers of disease and possible therapeutic strategies in several pathological conditions, including PD.

Therefore, the main objectives of this thesis were deepening the current knowledge on therapeutic approaches in PD, mainly focusing on the discovery of novel necroptosis inhibitors, as well as in miRNAs that might be used as promising therapeutic strategies and/or biomarkers of disease. Specifically, we established the following objectives:

1. Discover novel necroptosis inhibitors through compound screening using an *in vitro* model based on the murine BV2 microglia cell line.
2. Validate hit compounds in the sub-acute MPTP mouse model of PD.
3. Compare miRNA expression profiles in the serum of PD patients and age-matched healthy controls.
4. Assess how dysregulated miRNAs regulate inflammatory and cell death pathways in the context of PD.

Chapter 2

NECROPTOSIS IN PARKINSON'S DISEASE

Reprinted, with minor modifications, from Oliveira SR *et al.* 2018. Phenotypic screening identifies a new oxazolone inhibitor of necroptosis and neuroinflammation. *Cell Death Discov.* 10;4:10
doi: 10.1038/s41420-018-0067-0,

Phenotypic screening identifies a new oxazolone inhibitor of necroptosis and neuroinflammation

Sara R. Oliveira, Pedro A. Dionísio, Hugo Brito, Lídia Franco, Catarina A. B. Rodrigues, Rita C. Guedes, Carlos A. M. Afonso, Joana D. Amaral and Cecília M. P. Rodrigues

Research Institute for Medicines (iMed.ULisboa), Faculdade de Farmácia, Universidade de Lisboa, Portugal

2.1.1. Abstract

Necroptosis is a regulated form of necrosis, which may be critical in the pathogenesis of neurodegenerative diseases. Neuroinflammation, characterized by the activation of glial cells such as microglia, is closely linked with neurodegenerative pathways and constitutes a major mechanism of neural damage and disease progression. Importantly, inhibition of necroptosis results in disease improvement, unveiling an alternative approach for therapeutic intervention. In the present study, we screened a small library of new molecules, potentially inhibitors of necroptosis, using two cellular models of necroptosis. A new oxazolone, Oxa12, reduced tumour necrosis factor α (TNF-α)-induced necroptosis in mouse L929 fibrosarcoma cells. Notably, Oxa12 strongly inhibited zVAD-fmk-induced necroptosis in murine BV2 microglial cells. Moreover, Oxa12 blocked phosphorylation of mixed-lineage kinase domain-like protein (MLKL), and interfered with necrosome complex formation, indicating that Oxa12 targets components upstream of MLKL. In fact, *in silico* molecular docking studies revealed that Oxa12 is occupying a region similar to the 1-aminoisoquinoline type II kinase inhibitor inside the receptor-interacting protein 1 (RIP1) kinase domain. Finally, in microglial cells, Oxa12 attenuated zVAD-fmk- and lipopolysaccharide (LPS)-induced inflammatory processes, as revealed by a marked decrease of TNF-α and/or IL-1β expression. More specifically, Oxa12 negatively targeted c-Jun N-terminal kinase (JNK) and p38 mitogen-activated protein kinase (MAPK) pathways, as well as NF-κB activation. Overall, we identified a strong lead

inhibitor of necroptosis that is also effective at reducing inflammation-associated events. Oxa12 is a promising candidate molecule for further development to target disease states dependent on RIP kinase activity.

2.1.2. Introduction

Neurodegenerative diseases are a group of chronic disorders characterized by progressive neuronal dysfunction and loss in specific areas of the nervous system. Neuroinflammation has also emerged as a critical mechanism contributing to neuronal damage and fuelling disease progress.

Necrosis has historically been considered an accidental and passive cell death mechanism (Miura 2011; Zhou and Yuan 2014). However, evidence now reveals that a subtype of necrosis, necroptosis, can be molecularly controlled (Vandenabeele et al. 2010), and viewed as an appealing target for therapeutic intervention. Necroptosis is a caspase independent form of cell death that can be activated by death receptors, particularly tumour necrosis factor receptor 1 (TNFR1), as well as Toll-like receptor 3 (TLR3), and TLR4 (Kaiser et al. 2013; Schworer et al. 2014). Downstream signalling involves auto- and trans-phosphorylation of receptor-interacting protein 1 (RIP1) and 3 (RIP3), converging on the assembly of an amyloid-like structure, named necrosome (Li et al. 2012). RIP3 then recruits and phosphorylates pseudokinase mixed lineage kinase domain-like (MLKL), which in turn triggers membrane rupture, resulting in necroptotic cell death (Dondelinger et al. 2014; Sun et al. 2012; Wang et al. 2014).

The role of necroptosis in disease was first investigated in ischemic brain injury (Degterev et al. 2005). Since then, necroptosis has emerged as a critical event in the pathogenesis of other diseases, namely inflammatory diseases such as pancreatitis (He et al. 2009), skin inflammation (Bonnet et al. 2011), and liver injury (Afonso et al. 2015), but also neurodegenerative diseases. Indeed, necroptosis has been reported in Huntington's disease (Vandenabeele et al. 2010), amyotrophic lateral sclerosis (Re et al. 2014), multiple sclerosis (Ofengeim et al. 2015), Alzheimer's disease (Caccamo et al. 2017) and Parkinson's disease (Iannielli et al. 2018), while both genetic and chemical inhibition of necroptosis results in disease improvement.

Pharmacological targeting of necroptosis has been attempted using necrostatin-1 (Nec-1), a strong inhibitor of RIP1 kinase activity (Degterev et al. 2005). Other molecules targeting components of the necroptotic signalling pathway have been described (Sun et al. 2012; Mandal et al. 2014); however, none is available for clinical use. Here, we propose a robust *in vitro* model to screen for necroptosis inhibitors based on the murine BV2 microglial cell line. Oxa12 was identified as a potent inhibitor of necroptosis in BV2 cells and further confirmed in L929 cells. Moreover, Oxa12 attenuated neuroinflammation, highlighting the potential benefit of necroptosis inhibitors to halt neurodegenerative diseases.

2.1.3. Materials and methods

2.1.3.1. Cell culture and reagents

BV2 murine microglia cells (kindly provided by Elsa Rodrigues, University of Lisbon) were cultured in RPMI 1640 medium (GIBCO® Life Technologies, Inc. Grand Island, USA), supplemented with 10% heat inactivated foetal bovine serum (FBS), 1% antibiotic/antimycotic solution and 1% GlutaMAX™ (GIBCO). Throughout experiments, the culture media was replaced by RPMI supplemented with 1% antibiotic/antimycotic solution, 1% insulin-transferrin-selenium (RPMI/ITS) and 1 mg/mL bovine serum albumin (BSA; GIBCO). The L929 murine fibrosarcoma cell line (kindly provided by Junying Yuan, Harvard Medical School) was cultured in DMEM (GIBCO) supplemented with 10% FBS and 1% GlutaMAX™. Cells were maintained at 37 °C in a humidified atmosphere of 5% CO2. Other chemicals used were as follows: LPS from Escherichia coli 055:B5 (#437625; Calbiochem, San Diego, CA, USA), Nec-1 (Sigma-Aldrich, St. Louis, MO, USA), dimethyl sulfoxide (DMSO; SigmaAldrich), Z-Val-Ala-Asp-fluoromethylketone (zVADfmk) pan- caspase inhibitor (Enzo Life Sciences, Farmingdale, NY, USA), and recombinant murine TNF-α (PeproTech EC Ltd., London, UK). A small in-house library of potential inhibitors of necroptosis was tested, including Oxa 12 ((Z)-4-(4-((E)-2-(1H-benzo[d]imidazol2-yl)vinyl) benzylidene)-2-phenyloxazol-5(4H)-one) that was synthetized accordingly to a reported method (Rodrigues et al. 2012, 2013).

2.1.3.2 Viability assay

BV2 cells were plated in 96-well plates at 5 x 10^3 cells/ well. After 24 h of cell plating, media was replaced by fresh RPMI/ITS containing 100 ng/mL LPS, or no addition, and cells were incubated for additional 24 h. Then, BV2 cells were exposed to 25 µM zVAD-fmk for additional 24 h. Nec-1 (30 µM) was added 1 h before zVADfmk. Cellular metabolic activity was measured using the CellTiter 96® Aqueous Non-Radioactive Cell Proliferation (MTS) Assay (Promega, Madison, WI, USA). Changes in absorbance were measured at 490 nm using GloMax® Multi Detection System (Sunnyvale, CA, USA).

2.1.3.3. General cell death assays

Cell membrane integrity was evaluated using the lactate dehydrogenase (LDH) Cytotoxicity Kit^{PLUS} (Roche Diagnostics GmbH, Mannheim, Germany). Briefly, 50 µL of cell supernatants were incubated with 50 µL of assay substrate for 10–30 min, at room temperature, protected from light. Absorbance readings were measured at 490 nm, with 620 nm reference wavelengths using a BioRad Model 680 microplate reader. Further, cell death was also determined using the ToxiLight^{TM} BioAssay Kit (Lonza Walkersville Inc., Walkersville, MD, USA), according to the manufacturer's instructions. The release of adenylate kinase enzyme from damaged cells was determined using 10 µL each of cell supernatants and bioluminescent cytolysis assay in the microplate reader.

2.1.3.4. Drug screening

Drug screening was performed using BV2 and L929 cell lines. BV2 cells were seeded in 96-well plates at 7 x 10^3 cells/well; necroptosis was induced using 25 µM zVADfmk and compounds were incubated at a final concentration of 30 µM. Cell viability and death were assessed 24 h later by MTS and LDH assays. For the L929 cell line, cells were seeded in 384-well plates at 1 × 10^3 cells/well, necroptosis was induced using 30 µM TNF-α, and compounds were incubated at a final concentration of 30 µM. Cell death was assessed 8 h later using the ToxiLight™ BioAssay Kit. All measurements were performed in duplicate. A percentage of control was calculated to normalise for variability across different plates. Half-maximum effective concentration (EC_{50}) at inhibiting necroptosis and

half maximal inhibitory concentration (IC_{50}) were calculated for the selected hits in both cell lines, using the GraphPad Prism Software version 5.00 (GraphPad Software, Inc., San Diego, CA, USA) with the log (inhibitor) vs. response (variable slope) function.

2.1.3.5. Docking studies

Non-covalent molecular docking calculations were used to understand compound activity against RIP1. 3D structure coordinates of RIP1 were obtained from five different crystal structures at the Protein Data Bank (PDB), 4ITI, 4ITH, 4ITJ, and 4NEU, with a resolution in the range 1.80–2.89 Å. Co-crystallized inhibitors and all crystallographic waters were removed. Hydrogen atoms were then added, and the protonation states were correctly assigned using the Protonate-3D tool within the Molecular Operating Environment (MOE) 2016.08 software package. All the compounds tested were built and energy minimized using Amber forcefield implemented in MOE 2016.08 software.

Molecular docking studies were then performed using the GoldScore scoring function from GOLD 5.2 software package and each ligand was subjected to 1000 docking runs. For all five structures, the docking protocol was validated using crystallographic ligands; poses were reproducible with RMSD´s lower than 1 Å. In addition, an extra validation of the receptor structure was performed with 10 established RIP1 inhibitors, including Nec-1 and derivatives, GSK962, GSK963, and ponatinib. Significant differences were observed between final poses and scores obtained using 4ITI, 4ITH, 4ITJ, and 4NEU. The 4NEU structure was able to reproduce the experimental activities, while all other structures showed severe penalties in scores due to a very tight active centre. Results presented here were obtained with the 4NEU prepared structure.

2.3.6. Total and soluble/insoluble protein extraction

For total protein extraction, BV2 cells were plated in 60 mm culture dishes at 4 x 10^5 cells/dish, and L929 cells were plated in 6-well plates at 2.5 x 10^5 cells/well. Floating and adherent cells were collected directly in nonyl phenoxypolyethoxylethanol (NP-40) lysis buffer (1% NP-40, 20 mM Tris–HCl pH 7.4, 150 mM NaCl, 5 mM EDTA, 10% glycerol, 1 mM dithiothreitol, and 1× Halt

Protease and Phosphatase Inhibitor Cocktail EDTA-free (Pierce, Thermo Fisher Scientific, Rockford, IL, USA), followed by sonication and centrifugation at 3200 g during 10 min at 4 °C. Total protein extracts were recovered and stored at −80°C. Protein concentration was determined by the colorimetric Bradford method (Bio-Rad). BSA (Sigma-Aldrich) was used as standard, and absorbance measurements were performed at 595 nm using the microplate reader (Bio-Rad). To isolate the soluble and detergent-insoluble proteome of BV2 cells, floating and adherent cells were collected in phosphate-buffered saline (PBS)/EDTA, centrifuged at 600 g for 5 min at 4 °C, and the pellet homogenized in NP-40 lysis buffer. Then, cell lysates were rotated for 30 min at 4 °C and centrifuged at 16,000 g for 20 min at 4 °C. Supernatants were recovered and used as the soluble fractions. To remove carryovers, the pellet was washed with NP-40 lysis buffer and centrifuged again at 16,000 g for 10 min at 4 °C. Urea sodium dodecyl sulphate (SDS) buffer composed by 8 M urea and 3% SDS in NP-40 lysis buffer was used to resuspend the pellet and followed by sonication. Lysates were then spun at 16000 g for 20 min at 4 °C, and the supernatants recovered and used as the detergent insoluble fractions. To determine protein concentration, the bicinchoninic acid (BCA) assay (Thermo Fisher Scientific) was used, according to the manufacturer's recommendations.

2.1.3.7. Immunoblot analysis

Equal amounts of total, insoluble or soluble protein extracts were electrophoretically resolved on 8% SDS polyacrylamide gels and transferred onto nitrocellulose membranes. Then, transient staining with 0.2% Ponceau S (Merck, Darmstadt, Germany) was used to confirm protein loading and transfer. Following blocking with 5% milk solution in Tris-buffered saline (TBS), blots were incubated overnight at 4 °C with primary rabbit polyclonal antibodies reactive to RIP1, RIP3, Akt, p-Akt (Ser473), NF-κB p65 and IκBα (#7881, #135170, #8312, #7985, #372, and #371; Santa Cruz Biotechnology, Santa Cruz, CA, USA), MLKL (#M6697; Sigma Aldrich), p-MLKL (Ser358) and p-NF-κB p65 (Ser536) (#196436, #131109; Abcam, Cambridge, UK), p-p38 (Thr180/Tyr182) (#9211; Cell Signalling, Danvers, MA, USA); and with primary mouse monoclonal antibodies reactive to JNK, p-JNK (Thr183/Tyr185),and p38α/β (#7345, #6254, #7972; Santa Cruz Biotechnology) and p-IκBα (Ser32/36) (#9246; Cell Signalling), and finally with

secondary goat anti-mouse or anti-rabbit IgG antibody conjugated with horseradish peroxidase (Bio-Rad Laboratories) diluted 1:5000 in blocking solution for 1 h at room temperature. Membranes were processed for protein detection using Immobilon™ Western (Merck Millipore, Burlington, MA, USA) or SuperSignal substrate (Pierce, Thermo Fisher Scientific). β-actin (AC-15; Sigma-Aldrich) was used as endogenous control. Densitometric analysis was performed with the Image Lab Software version 5.1 Beta (Bio-Rad).

2.1.3.8. Quantitative RT-PCR

BV2 cells were plated in 12-well plates at 8 x 10^5 cells/ well for real-time RT-PCR analysis. Briefly, total RNA was extracted using TRIzol™ reagent (Invitrogen, Grand Island, USA). RNA was quantified using a Qubit™ 2.0 fluorometer (Invitrogen) and then converted into cDNA using NZY Reverse Transcriptase (NZYTech, Lisbon, Portugal). RT-PCR was performed in an Applied Biosystems 7300 System (Thermo Fisher Scientific). The following primer sequences were used: COX2 gene, 5′-C AGCCAGGCAGCAAATCCTT (forward) and 5′-A GTCCGGGTACAGTCACACT (reverse); IL-6 gene, 5′-G ACGATACCACTCCCAACAGACC (forward) and 5′-A AGTGCATCATCGTTGTTCATACA (reverse); NRLP3 gene, 5′-AGAGCCTACAGTTGGGTGAAATG (forward) and 5′-CCACGCCTACCAGGAAATCTC (reverse); and TNF-α gene, 5′-AGGCACTCCCCCAAAAGATG (forward) and 5′-TGAGGGTCTGGGCCATAGAA (reverse). Two independent reactions for each primer set were performed in a total volume of 12.5 µL containing 2× Power SYBR Green PCR master mix (Thermo Fisher Scientific) and 0.3 µM of each primer. The relative amounts of each gene transcript were calculated based on the standard curve normalized to the level of hypoxanthine-guanine phosphoribosyltransferase (HPRT) and expressed as fold-change from control cells.

2.1.3.9. Enzyme-linked immunosorbent assay (ELISA)

Sandwich ELISA kits (PeproTech) were used to determine TNF-α concentration in culture media. First, the plates were covered with a capture

antibody specific for TNF-α overnight at room temperature, followed by removal of the liquid and washing 4 × with washing buffer (0.05% Tween-20 in PBS). Then, blocking buffer (1% BSA in PBS) was added for 1 h at room temperature to block non-specific binding, followed by the same cycle of washes. Afterwards, 100 µL of BV2 cell supernatants were added to each well and incubated for 2 h at room temperature, followed by additional four washes. The detection antibody was then added to each well and incubated for 2 h at room temperature, followed by four washes as before. Avidin peroxidase was finally incubated during 30 min at room temperature, followed by four washes as before. Addition of a peroxidase substrate solution then allows the colourless substrate to convert into a soluble blue coloured product. Colour intensity is proportional to the quantity of TNF-α contained in each sandwich structure. Samples were then incubated at room temperature until green colour was visually detectable (±30 min), followed by absorbance reading at 450 nm, with 590 nm reference wavelengths using a Bio-Rad Model 680 microplate reader. TNF-α concentration (pg/mL) was calculated from standard curves.

2.1.3.10. Immunofluorescence

NF-κB p65 nuclear translocation in BV2 cells was examined by immunocytochemistry. Briefly, BV2 cells were incubated with zVAD-fmk in the presence or absence of Nec-1 or Oxa12 for 24 h. Then, cells were fixed with 4% paraformaldehyde in PBS for 20 min at room temperature, followed by two washes with PBS. Nonspecific binding was blocked with 10% normal donkey serum for 1 h at room temperature. Next, cells were incubated with primary mouse monoclonal anti-NF-κB p65 antibody (1:50, Santa Cruz Biotechnology) overnight at 4 °C. Cells were then washed three times with PBS, followed by incubation with Alexa Fluor 568-conjugated donkey anti-rabbit IgG (1:150, Life Technologies) for 2 h at room temperature. Nuclei were stained with Hoechst 33258 (Sigma-Aldrich) and mounted on Mowiol mounting medium (Sigma-Aldrich). Images were taken using a fluorescence microscope.

2.3.11. Image analysis

BV2 and L929 cells morphology was evaluated by phase-contrast microscopy using a Primo Vert microscope and fluorescence images were captured using an Axio ScopeA.1 fluorescent microscope (Carl Zeiss MicroImaging GmbH, Gottingen, Germany). At least 8 images per condition were acquired using an AxioCam 105 Color camera with the Zen lite 2012 (both from Carl Zeiss MicroImaging GmbH). Quantification of p65 NF-κB signal was performed using ImageJ v3.91 software, by selecting a region of interest according to the localization of the nucleus and measurement of fluorescence intensity in the same region.

2.3.12. Statistical analysis

All data are presented as mean ± standard error the mean (SEM) of at least three independent experiments. Comparison between groups was made by one-way analysis of variance (ANOVA) followed by post hoc Bonferroni's test. Analysis and graphical presentation were performed with the GraphPad Prism Software version 5.00. The statistical significances were achieved when $p < 0.05$.

2.1.4. Results

2.1.4.1. zVAD-fmk induces necroptosis in BV2 microglia cells

Previous studies have demonstrated that primary microglia undergo RIP1/RIP3-dependent necroptosis after treatment with LPS or other TLR ligands, when caspases are inhibited (Fricker et al. 2013; Kim and Li 2013). Other authors showed that the pan- caspase inhibitor zVAD-fmk induces necroptosis in the L929 fibrosarcoma cell line by a mechanism that depends on autocrine production of TNF-α (Christofferson et al. 2012; Wu et al. 2011). Here, we anticipated a new *in vitro* model for the study of microglial necroptosis, based on the murine BV2 microglial cell line. Exposure of BV2 cells to LPS for 48 h did not induce cell death, as detected by MTS metabolism and LDH release (Fig. 2.1.1a). However, when cells were exposed to LPS for 24 h followed by incubation with zVAD-fmk for additional 24 h, cell viability was reduced by ~80% ($p < 0.001$) with a concomitant increase in cell death. Importantly, the presence of zVAD-fmk alone was sufficient to induce high levels of cell death ($p < 0.001$). Addition of

Nec-1, a RIP1-specific kinase inhibitor, fully reverted cell death to control levels in all conditions tested ($p < 0.001$), thus implicating RIP1-dependent necroptosis as the mechanism of cell death.

Necroptosis activation requires assembly of RIP1 and RIP3 in an insoluble amyloid-like complex called necrosome (Li et al. 2012). Exposure of cells to zVAD-fmk for 24 h, triggered RIP1 and RIP3 sequestration in the insoluble fraction (Fig. 2.1.1b), corroborating the viability data, thus confirming functional necrosome assembly and necroptosis activation. Addition of Nec-1 abolished RIP1 and RIP3 sequestration in the insoluble fraction. Taking these results into account, BV2 cells exposed to zVAD-fmk represent a robust *in vitro* model of microglial necroptosis, which is fully reverted when RIP1 kinase activity is inhibited by Nec-1.

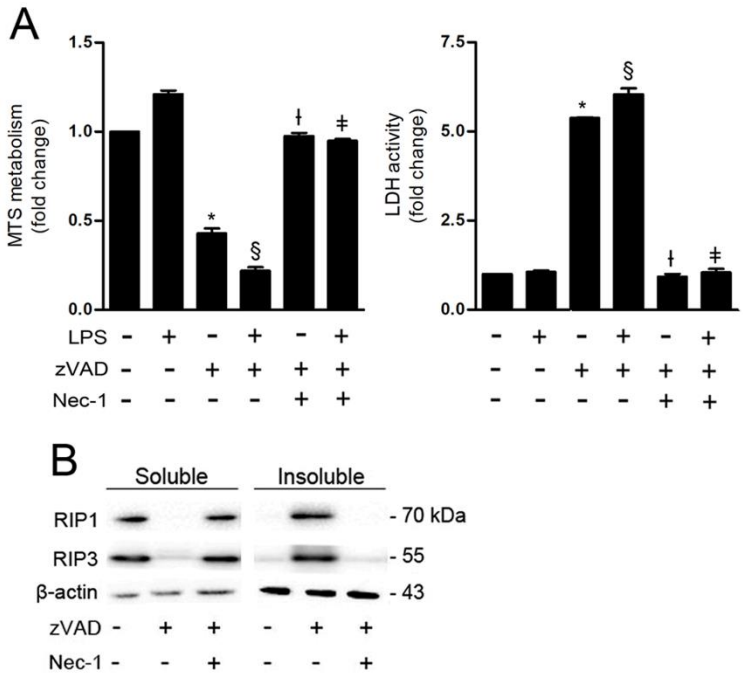

Figure 2.1.1 zVAD-fmk induces necroptosis in BV2 cells at 24 h of incubation. (A) BV2 cells were pre-exposed to 100 ng/mL LPS for 24 h and then incubated with the pan-caspase inhibitor zVAD-fmk (25 µM) for additional 24 h. Nec-1 (30 µM) was added 1 h before zVAD-fmk. Cell metabolic activity was determined by the MTS metabolism assay and cell membrane integrity by the LDH activity assay. Results are presented as the mean value ± SEM of three independent experiments performed in duplicates and normalized to control cells. *$p < 0.001$ vs. control; §$p < 0.001$ vs. LPS; ŧ$p < 0.001$ vs. zVAD-fmk; ǂ$p < 0.001$ vs. LPS/zVAD-fmk. (B) BV2 cells were co-incubated with zVAD-

fmk (25 µM) plus Nec-1 (30 µM) for 24 h. Detergent soluble and insoluble fractions were prepared for Western blot analysis of RIP1 and RIP3. β-actin was used as loading control. Representative immunoblots are presented.

2.1.4.2. Screening for potential inhibitors of necroptosis

To identify novel inhibitors of necroptosis, we screened a small library of new compounds for their ability to block zVAD-fmk-induced necroptosis using the BV2 cell line model (Fig. 2.1.2a). Among the compounds tested, one potential hit was identified that significantly rescued BV2 cell viability ($p < 0.05$) (Fig. 2.1.2b). As proof-of-concept, we used a well-described model where L929 cells undergo TNF-α-induced necroptosis, which in turn is fully reverted by Nec-1 (Fig. 2.1.3a). In L929 cells, four compounds were able to revert TNF-α-induced cell death ($p < 0.05$) (Fig. 2.1.3b). We proceeded with our studies using compound Oxa12 (Fig. 2.1.2c) that showed effects similar to Nec-1 in both cell lines. Three different batches of Oxa12 were tested, showing the same ability to inhibit necroptosis in both cell models (data not shown).

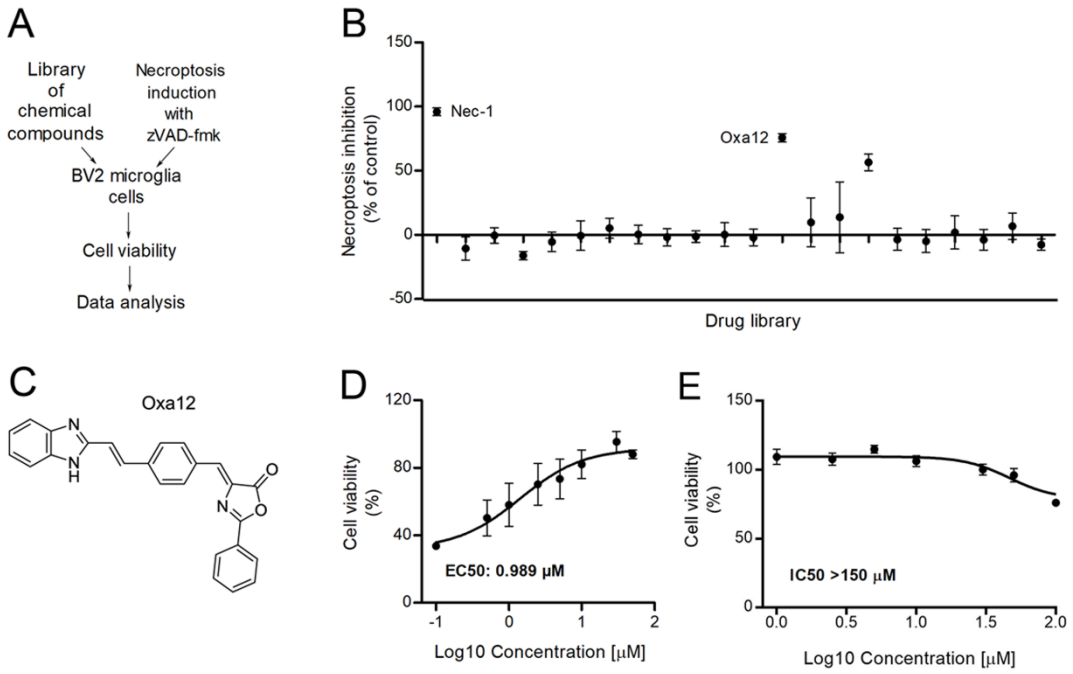

Figure 2.1.2. Drug screening identifies Oxa12 as necroptosis inhibitor in BV2 microglia cells. (A) Schematic overview of the drug screening workflow. (B) Normalized necroptosis inhibition values depicted as percentage of control (DMSO) for compounds

(30 µM) tested on BV2 cells exposed to 25 µM zVAD-fmk for 24 h. Results are presented as the mean value ± SEM of at least three independent experiments performed in duplicates. (C) Oxa12 chemical structure. (D) BV2 cells were incubated with Oxa12 (0.1–50 µM) plus zVAD-fmk (25 µM) for 24 h. e BV2 cells were incubated with Oxa12 (1–150 µM) for 24 h. Cell viability was determined by the MTS metabolism assay. The results are presented as the mean value ± SEM of three independent experiments performed in duplicates and normalized to vehicle control (DMSO).

To further characterize Oxa12 activity and confirm the screening data, we performed dose–response studies and quantitatively assessed its inhibitory potency. The half maximal effective concentration (EC_{50}) of Oxa12 for inhibiting necroptosis was determined to be 0.989 µM in BV2 cells (Fig. 2.1.2.d) and 0.398 µM in L929 cells (Fig. 2.1.3c). Drug toxicity was also assessed by determining the half maximal inhibitory concentration (IC_{50}) in BV2 and in L929 cells. Notably, Oxa12 displayed no cytotoxicity throughout the whole range of concentrations in both cell lines (Figs. 2.1.2e and 2.1.3d), with IC_{50} values greater than 150 µM, highlighting the wide window of opportunity for inhibiting necroptosis with this compound.

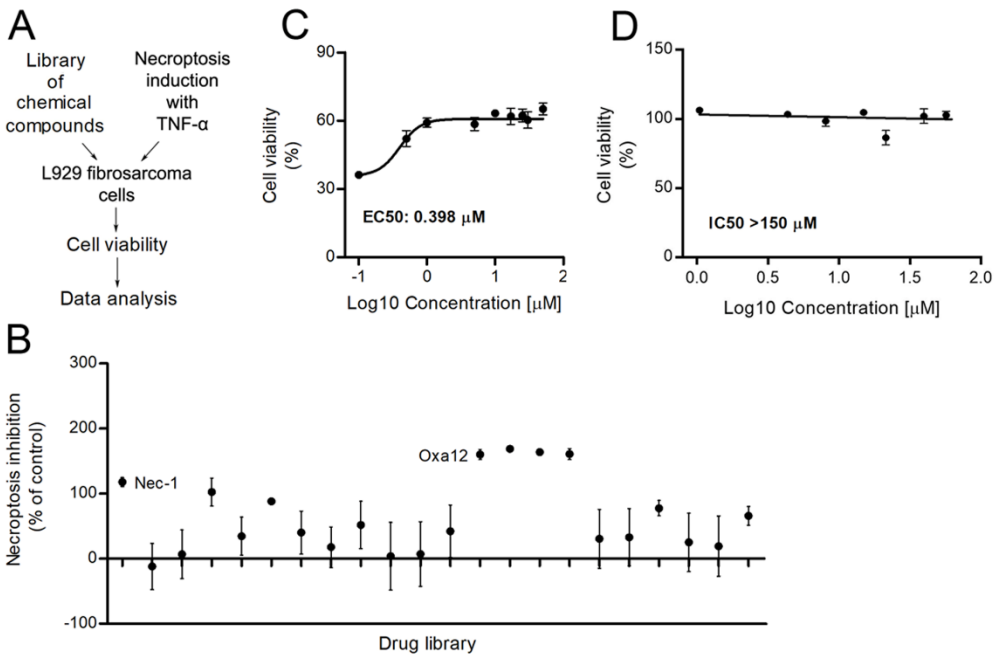

Figure 2.1.3. Drug screening identifies Oxa12 as necroptosis inhibitor in L929 cells. (A) Schematic overview of the drug screening workflow. (B) Normalized necroptosis inhibition values depicted as percentage of control (DMSO) for compounds (30 µM)

tested on L929 cells exposed to 30 µM TNF-α for 8 h. Results are presented as the mean value ± SEM of at least three independent experiments performed in duplicates. (C) L929 cells were incubated with Oxa12 (0.1 to 50 µM) plus TNF-α (30 µM) for 24 h. (D) L929 cells were incubated with Oxa12 (1–150 µM) for 24 h. Cell viability was determined by the MTS metabolism. The results are presented as the mean value ± SEM of three independent experiments performed in duplicates and normalized to vehicle control (DMSO).

Motivated by these results and to get further insight into the mechanism of action of Oxa12 at the molecular level, we performed *in silico* molecular docking calculations for Oxa12 inside the RIP1 kinase domain using the 4NEU X-ray structure obtained for this enzyme complexed with 1-aminoisoquinoline type II kinase inhibitor. Our results revealed that without any constrain, Oxa12 is occupying a region similar to the co-crystallized inhibitor, with the phenyl rings from both compounds almost overlapped, suggesting a similar interaction pattern (Fig. 2.1.4a). Oxa12, however, is slightly rotated in the binding pocket when compared with the crystallographic ligand, being close to Asp156, Leu157, Met67, and Met95, which may enable important hydrogen bonds and π interactions. Oxa12 showed slightly increased interaction distances in comparison to the crystallographic inhibitor (Fig. 2.1.4b).

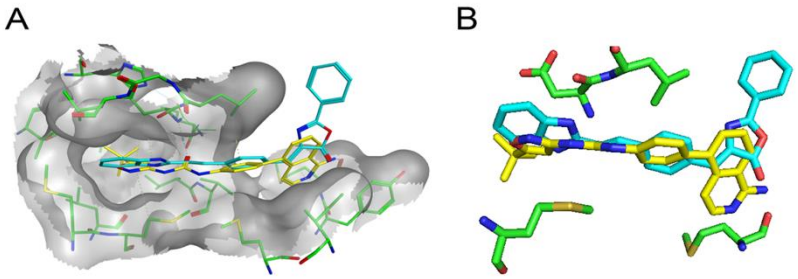

Figure 2.1.4. *In silico* molecular docking calculations for Oxa12. (A) Optimal poses obtained inside RIP1 active site (grey) for compound Oxa12 (represented in stick model and coloured blue) compared with crystallographic ligand 1-aminoisoquinoline inhibitor (PDBID: 4NEU) (yellow). (B) Compound Oxa12 and 4NEU co-crystallized inhibitor interacting with Asp156, Leu157, Met67, and Met95. Docking calculations were performed using the X-ray structure obtained for RIP1 complexed with 1-

aminoisoquinoline inhibitor at resolution of 2.57 Å, PDBID: 4NEU, by the GOLD 5.2 software.

2.1.4.3. Oxa12 is a potent inhibitor of necroptosis

To determine the effect of Oxa12 in the necroptotic signalling pathway, we co-incubated BV2 cells with zVAD-fmk and Oxa12 for 24 h and evaluated necrosome assembly and MLKL phosphorylation in the detergent insoluble proteome. During necroptosis, MLKL is phosphorylated at Thr357/Ser358 residues (p-MLKL) by RIP3 kinase. Once phosphorylated, MLKL oligomerizes and ultimately induces cell membrane disruption, being an excellent marker of necroptosis commitment15. Exposure of BV2 cells to zVAD-fmk promoted the sequestration of all key components of the necroptosis machinery, RIP1, RIP3, and p-MLKL, in the insoluble fraction ($p < 0.01$) (Fig. 2.1.5a, b). Nec-1 abrogated both necrosome assembly and MLKL phosphorylation ($p < 0.01$). Importantly, Oxa12 also abolished all necroptosis-associated changes ($p < 0.05$).

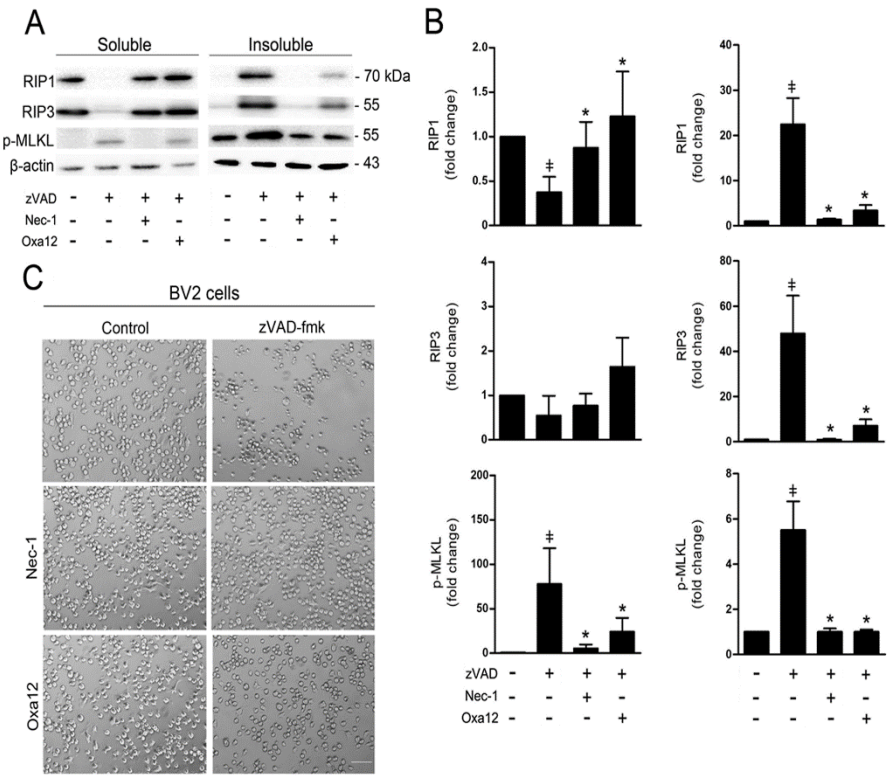

Figure 2.1.5. Oxa12 inhibits necroptosis in a murine microglial cell line. (A) BV2 cells were incubated with zVAD-fmk (25 µM), zVAD-fmk (25 µM) plus Nec1 (30 µM), or zVAD-fmk (25 µM) plus Oxa12 (30 µM) for 24 h. Detergent soluble and insoluble protein

fractions were prepared for Western blot analysis of RIP1, RIP3, MLKL, and p-MLKL. Representative immunoblots are presented. β-actin was used as loading control. (B) Densitometric analysis. Values are expressed as mean ± SEM of three independent experiments. ǂ $p < 0.05$ vs. control; *$p < 0.05$ vs. zVAD-fmk. (C) Bright-field microscopic images of BV2 cells incubated with zVAD-fmk (25 µM) in the presence of absence of Nec-1 (30 µM) or Oxa12 (30 µM) for 24 h. Microscopy photographs were taken at ×100 with a Primo Vert microscope. Scale bar=100 µm.

Microscopy analysis of cell morphology was consistent with the previous results, showing evident cell death after zVAD-fmk treatment and improvement of this phenotype when Nec-1 or Oxa12 were added to BV2 (Fig. 2.1.5c). Of note, neither Nec-1 nor Oxa12 alone affected cell morphology. The effect of Oxa12 was further confirmed in L929 cells, in which Oxa12 prevented TNF-α-induced increase of p-MLKL ($p < 0.05$) and preserved cell morphology (Fig. S2.1.1a and b). Taken together, these results implicate Oxa12 as a strong inhibitor of necroptosis.

2.1.4.4. Oxa12 reduces TNF-α gene expression and secretion

Necroptosis is a proinflammatory type of cell death that culminates in the release of intracellular components to the extracellular space (Moriwaki and Chan 2013). Moreover, zVADfmk-induced necroptosis in L929 cells is dependent on the production and autocrine secretion of TNF-α (Wu et al. 2011). To determine whether Oxa12-mediated inhibition of necroptosis may also contribute to decrease necroptosis-associated inflammation, we analysed mRNA levels of proinflammatory genes, including cyclooxygenase 2 (COX2), interleukin-6 (IL-6), nucleotide-binding oligomerization domain-like receptor (NLR) pyrin domain containing 3 (NLRP3), and TNF-α, as well as TNF-α protein secretion to the culture medium. COX2 and NLRP3 did not show any significant variation, with either zVAD-fmk alone or in combination with Nec-1/Oxa12, while IL-6 was barely detectable in all conditions tested (data not shown). In contrast, exposure of BV2 cells to zVAD-fmk for 24 h resulted in a significant increase of TNF-α gene expression ($p < 0.001$) and protein secretion levels ($p < 0.05$) (Fig. 2.1.6a). Importantly, at the mRNA level, this increase was significantly reduced upon Nec-1 and Oxa12 incubation ($p < 0.05$). Similarly, Nec-1 completely abolished zVAD-

fmk-induced TNF-α secretion, while Oxa12 diminished TNF-α levels in the culture medium by about 70% ($p < 0.05$). These results suggest that, similarly to what was described for L929 cells, the autocrine secretion of TNF-α is a key step in zVAD-fmk-induced necroptosis in BV2 microglia cells, and Oxa12 appears to counteract this proinflammatory condition.

To determine if Oxa12 could play a role in protecting BV2 microglia cells from an inflammatory stimulus, per se, we investigated TNF-α and IL-1β gene expression after stimulation of BV2 cells with LPS. As expected, exposure of BV2 cells to LPS significantly increased TNFα and IL-1β gene expression ($p < 0.001$), an effect exacerbated by LPS/zVAD-fmk co-incubation ($p < 0.001$) (Fig. 2.1.6b). Moreover, Nec-1 robustly reduced TNF-α and IL-1β mRNA levels ($p < 0.001$), which is in accordance with previous studies (Huang et al. 2018; Northington et al. 2011; Liu et al. 2017). Notably, Oxa12 partially reverted LPS- and LPS/zVAD-fmk-induced TNF-α and IL-1β gene expression ($p < 0.001$), thus highlighting the anti-inflammatory potential of this compound.

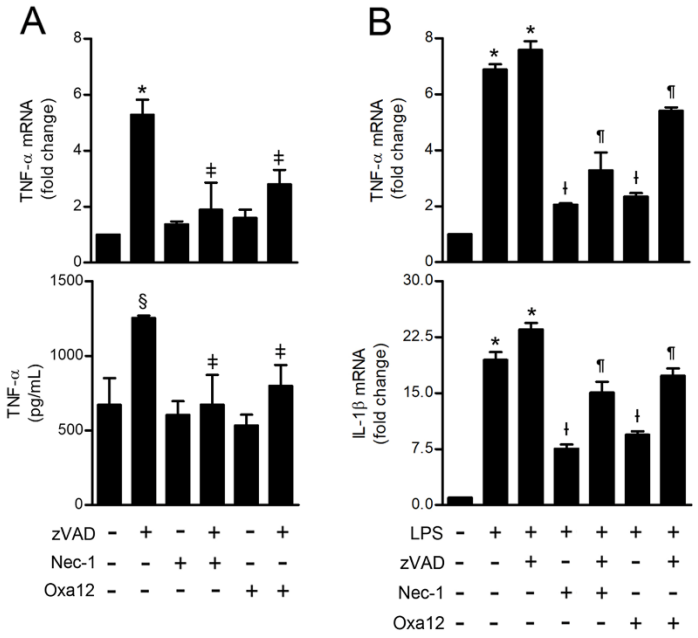

Figure 2.1.6. Oxa12 decreases TNF-α gene expression and protein secretion levels. (A) BV2 cells were incubated with zVAD-fmk (25 µM) in the presence or absence of Nec-1 (30 µM) or Oxa12 (30 µM) for 24 h. TNF-α mRNA levels were measured by qRT-PCR and secreted TNF-α by ELISA. Results are expressed as mean ± SEM from three independent experiments. *$p < 0.001$ vs. control; ǂ$p < 0.001$ vs. zVAD-fmk. (B) BV2 cells were incubated with 100 ng/mL LPS, LPS plus zVAD-fmk (25 µM) in the presence or

absence of Nec-1 (30 µM) or Oxa12 (30 µM) for 24 h. TNF-α and IL-1β mRNA levels were measured and results are expressed as mean ± SEM from three independent experiments. *p < 0.001 vs. control; łp < 0.001 vs. LPS; ¶p < 0.001 vs. LPS/ zVAD-fmk.

2.1.4.5. Oxa12 inhibits zVAD-fmk-induced JNK, p38 MAPK and NF-κB activation

To further dissect which inflammatory pathways Oxa12 specifically targets, we evaluated JNK (Thr183/ Tyr185) and p38 (Thr180/Tyr182) phosphorylation, two classic MAPK inflammatory signalling pathways. We also evaluated phosphorylation of protein kinase B, also known as Akt (Ser473). Indeed, others have shown that JNK and Akt, when activated, have important roles in necroptosis, being involved in the production and autocrine secretion of TNF-α (Christofferson et al. 2012). Incubation of BV2 cells with zVAD-fmk for 24 h induced a significant increase in JNK and p38 phosphorylation, thus suggesting activation of these two signalling pathways (Fig. 2.1.7a, b). In contrast, Nec-1 completely abolished JNK and p38 phosphorylation, while treatment with Oxa12 markedly reduced their activation. No significant changes were observed for Akt activation under these experimental conditions (Fig. 2.1.7c).

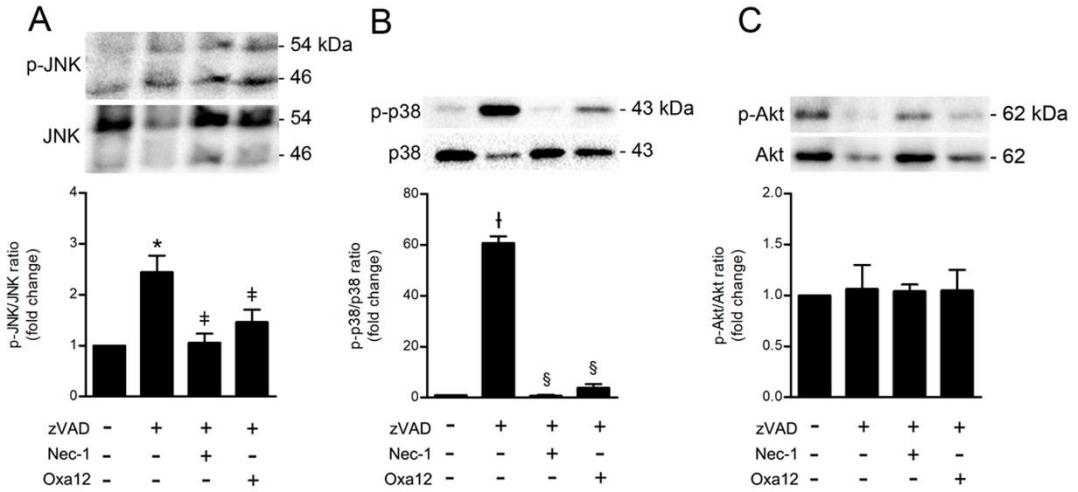

Figure 2.1.7. Oxa12 decreases zVAD-fmk-induced JNK and p38 MAPK activation in BV2 cells. BV2 cells were treated with zVAD-fmk (25 µM) in the presence or absence of Nec-1 (30 µM) or Oxa12 (30 µM) for 24 h. Representative immunoblots are presented, together with the respective densitometric analysis of the p-JNK/JNK, p-p38/p38 and p-Akt/Akt ratios. (A) p-JNK (Thr183/Tyr185) and total JNK. (B) p-p38 (Thr180/Tyr182) and

total p38. (C) p-Akt (Ser473) and total Akt. Results are expressed as mean ± SEM of three independent experiments. *$p < 0.001$ vs. control; ǂ$p < 0.05$ vs. zVADfmk; łp < 0.01 vs. control; §$p < 0.001$ vs. zVAD-fmk.

NF-κB has long been considered a pivotal mediator of inflammatory responses, largely based on its activation by proinflammatory cytokines such as TNF-α. We investigated whether NF-κB signalling was activated in BV2 cells after exposure to zVAD-fmk. No significant differences were observed in NF-κB steady-state levels upon exposure of BV2 cells to zVAD-fmk (Fig. 2.1.8a). However, IκB was markedly decreased ($p < 0.01$) with a concomitant increase of the NF-κB/IκB ratio ($p < 0.01$), suggesting that zVAD-fmk treatment induced NF-κB activation (Fig. 2.1.8a). Importantly, NF-κB activation was further confirmed by immunofluorescence. BV2 cells treated with zVAD-fmk for 5 h showed a marked increase of NF-κB p65 subunit in the nucleus (Fig. 2.1.8b). In contrast, both Nec-1 and Oxa12 strongly suppressed zVAD-fmk-driven NF-κB activation ($p < 0.01$).

2.1.5. Discussion

Neurological disorders ranked as the leading cause group of disability, and the second-leading cause of mortality worldwide (GBD 2017). Globally, the burden of neurodegenerative diseases is expected to increase over the next years, mostly because of the expanding population and ageing. Currently, the treatments available are ineffective. Therefore, interventions that slow or stop neurodegeneration are an urgent, unmet need. Although apoptosis is frequently implicated in neurodegeneration, necroptosis has been recently described as a prominent player in neurodegenerative disease pathobiology (Vandenabeele et al. 2010). In fact, the role of necroptosis has been studied in the pathogenesis of a broad spectrum of diseases, including neurodegenerative diseases, where inhibition of necroptosis is considered a beneficial event (Re et al. 2014; Ofengeim et al. 2015; Caccamo et al. 2017; Iannielli et al. 2018). Neuroinflammation is also a pathological hallmark of neurodegenerative diseases, where microglia have a fundamental role in regulating innate and adaptive immune responses (Xu et al. 2007; Rubio-Perez et al. 2012). Recently

it was shown that in certain pathological conditions, such as multiple sclerosis, microglia present defective caspase-8 activation, which may promote inflammation through activation of necroptosis, thus contributing to disease progression (Ofengeim et al. 2015). Others have also shown that necroptosis in retina microglia triggers neuroinflammation and exacerbates retinal neural damage and degeneration in mice (Huang et al. 2018). In these cases, targeting the necroptotic machinery has been proven to be useful to attenuate microglia-mediated neuroinflammation and ameliorate neural injury.

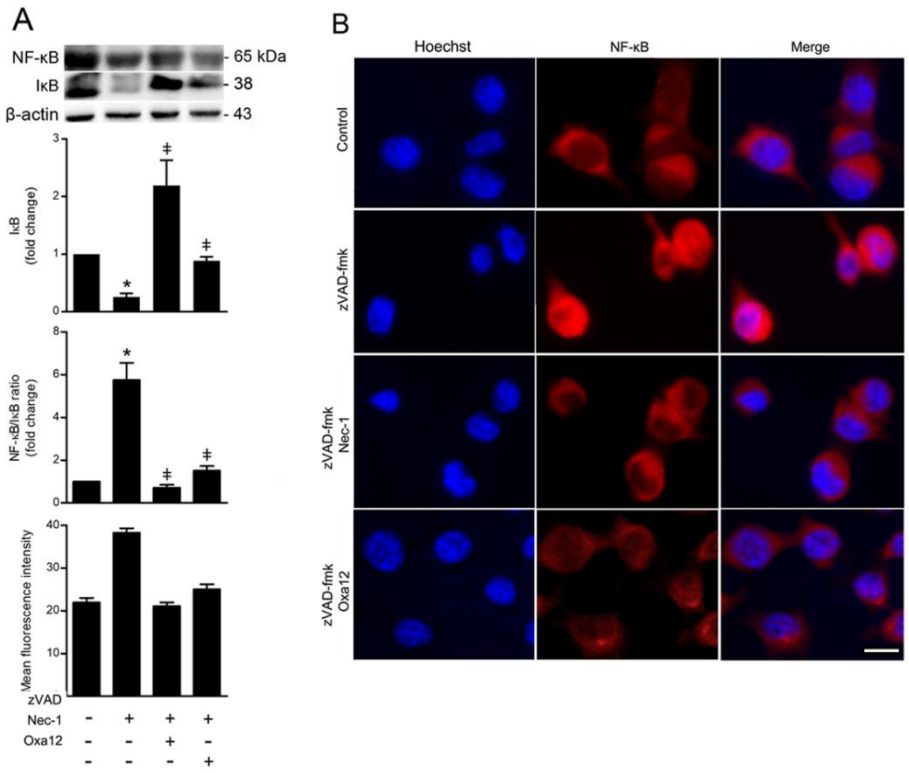

Figure 2.1.8. Oxa12 reduces NF-κB/IκB ratio and NF-κB p65 nuclear translocation when compared to zVAD-fmk-treated cells. (A) BV2 cells were incubated with zVAD-fmk (25 μM) in the presence or absence of Nec-1 (30 μM) or Oxa12 (30 μM) for 24 h. Representative immunoblots of total NF-κB are presented together with the respective densitometric analysis of NF- κB/IκB ratio. β-actin was used as loading control. Results are expressed as mean ± SEM from three independent experiments. *$p < 0.05$ vs. control; ǂ$p < 0.05$ vs. zVAD-fmk. (B) Representative images of immunofluorescence staining showing NF-κB p65 (red) nuclear translocation in BV2 cells treated with zVAD-fmk (25 μM) in the presence or absence of Nec-1 (30 μM) or Oxa12 (30 μM) for 5 h, and

quantification of mean fluorescence intensity. Cell nuclei were detected by Hoechst (blue). Scale bar=1 µm.

Here, we used the murine BV2 microglia cell line as a new and robust cellular model to screen for potential small molecule modulators of microglial necroptosis. Our results showed that BV2 cells undergo necroptosis after 24 h incubation with the pan-caspase inhibitor, zVAD-fmk, which is in agreement with previous studies reporting that zVAD-fmk induces necroptosis in L929 cells (Christofferson et al. 2012; Wu et al. 2011). Nec-1, a RIP1 kinase inhibitor here used as positive control of necroptosis inhibition, fully reverted cell death to control levels, thus implicating RIP1- dependent necroptosis as the death mechanism. Interestingly, pre-incubation with LPS, a well-known TLR4 agonist, accelerated the death mechanism, thus linking necroptosis to this inflammatory context. Indeed, we observed a further decrease of ~30% in MTS metabolism when cells were pre-incubated with LPS for 24 h and then, incubated with zVAD-fmk for additional 24 h, while no differences were observed in LDH activity. These results suggest that cell membrane permeabilization and leakage of intracellular components, such as LDH, may be an initial step in the necroptotic cascade, while mitochondria dysfunction appears to contribute indirectly to late-stage necroptosis (Wang et al. 2014; Chen et al. 2014). In addition, we observed that zVAD-fmk alone induced necrosome assembly after 24 h. It is known that zVAD-fmk triggers the production of TNF-α at the transcriptional level, and subsequently the autocrine secretion of this cytokine, which in turn may activate TNFR to induce necroptosis (Wu et al. 2011). Reversion of necrosome formation induced by Nec-1 further confirmed the importance of this molecular platform as the cell death inducer in this model. Overall, BV2 cells exposed to zVAD-fmk represent a robust *in vitro* model of microglial necroptosis, along with full reversion of all necroptotic processes when RIP1 kinase activity is inhibited by Nec-1.

Since the discovery of Nec-1 as the first inhibitor of necroptosis (Degterev et al. 2005), other inhibitors have been described, including RIP1, RIP3 and MLKL inhibitors. Nonetheless, all compounds identified so far show several limitations. Nec-1 itself is highly effective in inhibiting necroptosis; however, it has inadequate pharmacokinetic properties including very short *in vivo* half-life of ~1 h, reduced solubility (Teng et al. 2005), and presents off-target activity against

indoleamine-pyrrole 2,3-dioxygenase (IDO), a modulator of the innate and adaptive immune system (Takahashi et al. 2012; Vandenabeele et al. 2013), serine/threonine-protein kinase 1 (PAK1) and cAMP-dependent protein kinase catalytic subunit α (PKAcα). Later, Nec-1 optimizations led to the identification of Nec-1s (Nec-1 stable), also known as 7-Cl-O-Nec-1, which is a selective RIP1 kinase inhibitor with low toxicity. However, this molecule has also poor pharmacokinetic properties (Vandenabeele et al. 2013; Takahashi et al. 2012). Regarding RIP3 inhibitors, all compounds described so far also induce apoptosis (Mandal et al. 2014). Necrosulfonamide (NSA), a well-known MLKL inhibitor, inhibits necroptosis by blocking human MLKL phosphorylation, but not the rodent homolog, thus invalidating pharmacological, pharmacokinetic and toxicity preclinical testing (Sun et al. 2012). In sum, although tool compounds blocking necroptosis have previously been developed, no necroptosis inhibitors are in clinical use to date. Therefore, the discovery of new specific and potent pharmacologic inhibitors of necroptosis is relevant and of utmost importance.

In this study, we screened a library of new compounds that potentially modulate necroptosis. We identified one hit, Oxa12, that inhibits necroptotic cell death in BV2 cells (EC_{50} = 0.989 µM) and L929 cells (EC_{50} = 0.459 µM) without cytotoxicity associated. Further, Oxa12 inhibited necroptosis-associated events in murine BV2 cells, including necrosome assembly and MLKL S358 phosphorylation, two key markers of necroptosis commitment. Importantly, the docking pose of Oxa12 inside RIP1 kinase active site is similar to that of the co-crystallized 1-aminoisoquinoline RIP1-specific inhibitor, thus highlighting the potential of Oxa12 as a RIP1 inhibitor.

To further characterize the mechanism of action of Oxa12 and because necroptosis is an inflammatory type of cell death, we hypothesized that necroptosis inhibition by Oxa12 could also result in decreased inflammation. Our results showed that BV2 cells exposed to zVAD-fmk presented increased levels of TNF-α gene expression and cytokine secretion. These findings were in accordance with previous studies reporting the production and autocrine secretion of TNF-α as a crucial factor in zVADfmk-induced necroptosis (Wu et al. 2011; Hitomi et al. 2008). No differences were detected in COX2 and NLRP3 transcription levels, which might be explained by the involvement of these two proteins in later stages of the inflammatory cascade, being extensively regulated

by other proteins and signalling pathways (Abderrazak et al. 2015; Latz et al. 2013). Similarly to what happens with Nec-1, treatment of BV2 cells with Oxa12 reduced TNF-α gene expression and cytokine secretion levels, suggesting that RIP1 kinase activity is required for TNF-α production, as previously reported (Christofferson et al. 2012).

After confirming the involvement of necroptosis-associated inflammation in our cellular model and its concomitant reduction by Oxa12, we further investigated if Oxa12 could protect BV2 microglial cells from a classic inflammatory stimulus, independent of necroptosis activation. Therefore, we used LPS, a specific ligand of TLR4 that activates downstream pro-inflammatory signalling cascades without eliciting cell death. As expected, treatment of BV2 cells with LPS for 24 h induced TNF-α and IL-1β gene expression. Curiously, Nec-1 counteracted the effect of LPS implicating RIP1 in the production of proinflammatory cytokines, unrelated to necroptosis. In fact, this was not the first time that an anti-inflammatory role was reported for Nec-1, independently of its activity as necroptosis inhibitor (Jie et al. 2016). Similarly, Oxa12 strongly inhibited LPS-induced TNF-α and IL-1β mRNA levels, thus revealing the potential of this molecule not only as an inhibitor of necroptosis, but also as an agent with ability to resolve established inflammation. Exposure of LPS-stimulated BV2 cells to zVAD-fmk further potentiated the transcription of proinflammatory TNF-α and IL-1β, suggesting that caspase blockade sensitizes cells to LPS challenge. Nonetheless, both Nec-1 and Oxa12 were still capable of reducing LPS/zVAD-fmk-induced proinflammatory mediators.

To better understand which inflammatory pathways Oxa12 specifically targeted, we evaluated the activation of two MAPK signalling pathways, JNK and p38, as well as the activation of Akt. Importantly, activated MAPK signalling pathways are described in the pathogenesis of neurodegenerative diseases, including Alzheimer's disease and Parkinson's disease as contributors of inflammation and neuronal death (Hashimoto et al. 2003; Rawal et al. 2007; Tortarolo et al. 2003). Deregulation of Akt pathway is also reported in brains from Alzheimer's and Parkinson's disease patients (Rickle et al. 2004). Recent studies have reported that JNK activation plays an important role during zVAD-fmk-induced necroptosis in L929 cells downstream to RIP1 kinase, promoting TNF-α gene expression (Wu et al. 2011; Christofferson et al. 2012). Increased TNF-α

transcription may translate into elevated levels of this cytokine, which could induce necroptosis through TNFR activation (Wu et al. 2011). Our results are in line with these studies, since exposure of BV2 cells to zVAD-fmk induced high levels of JNK activation, which may be related with the increase observed in TNF-α gene expression and cytokine secretion levels. By contrast, Nec-1 and Oxa12 abolished both JNK activation and TNF-α gene expression and cytokine secretion levels, thus confirming the involvement of this signalling pathway in zVAD-fmk-induced necroptosis. Regarding p38, while some authors reported that this signalling pathway is not activated during necroptosis in L929 cells (Wu et al. 2009), others show that pharmacological inhibition of TNF-α-induced necroptosis in L929 cells resulted in p38 activation (Ye et al. 2011). Here, we show that treatment of BV2 cells with zVAD-fmk induced a marked increase in p38 phosphorylation, which is fully reverted by Nec-1 and Oxa12, suggesting activation of this signalling pathway during zVAD-fmk-mediated necroptosis in BV2 microglial cells. It is well known that JNK and p38 MAPK pathways are activated by several inflammatory mediators in different cell lines, being involved in stress responses and inflammation (Dhillon et al. 2007), being possible that the intracellular components released by necroptotic cells may induce JNK and p38 MAPK activation.

The role of Akt in necroptosis has also been demonstrated. Akt is linked to necroptosis in L929 cells, where it plays a key role in mediating TNF-α synthesis (Liu et al. 2014). Inhibition of Akt protected L929 cells from TNF-α-induced necroptosis and triggers autophagy instead (Liu et al. 2014; Jin et al. 2007). In contrast, others showed that zVAD-fmk alone is capable of inducing Akt activation, with this activation being dependent of Thr308 phosphorylation, with no alterations observed in Akt Ser473 phosphorylation (McNamara et al. 2013). In the present study, we evaluated Akt Ser473 phosphorylation as a marker of Akt activation, which may explain the absence of significant differences between the conditions tested.

In the nervous system, evidence supports a dual role of NF-κB in neurodegenerative diseases. In general, it appears that activation of NF-κB in neurons protects against degeneration, whereas activation in glial cells mediates pathological inflammatory processes (Camandola and Mattson 2007). Taking this into account, we were not surprised by the activation of NF-κB in BV2 cells treated

with zVAD-fmk. In contrast, Nec-1 and Oxa12 strongly abrogated this activation, which highlights their potential at reducing inflammation-associated events. Altogether, our findings suggest that zVAD-fmk induces the expression of inflammatory target genes at early time-points, thus promoting the downstream activation of important inflammatory signalling pathways. Further, longer incubation times will activate necroptosis, which has also a prominent role on inflammation (Pasparakis and Vandenabeele 2015).

Overall, we established a robust *in vitro* model of microglia necroptosis, based on the murine BV2 microglial cell line and identified a strong lead inhibitor of this type of regulated cell death. Oxa12 is efficient at decreasing necroptosis-driven inflammation, as well as activation of important signalling pathways including JNK, p38 MAPK and NF-κB. Thus, Oxa12 can now be considered a promising candidate molecule for targeting pathologies-dependent on RIP1-kinase activity.

2.1.6. Supplementary figures

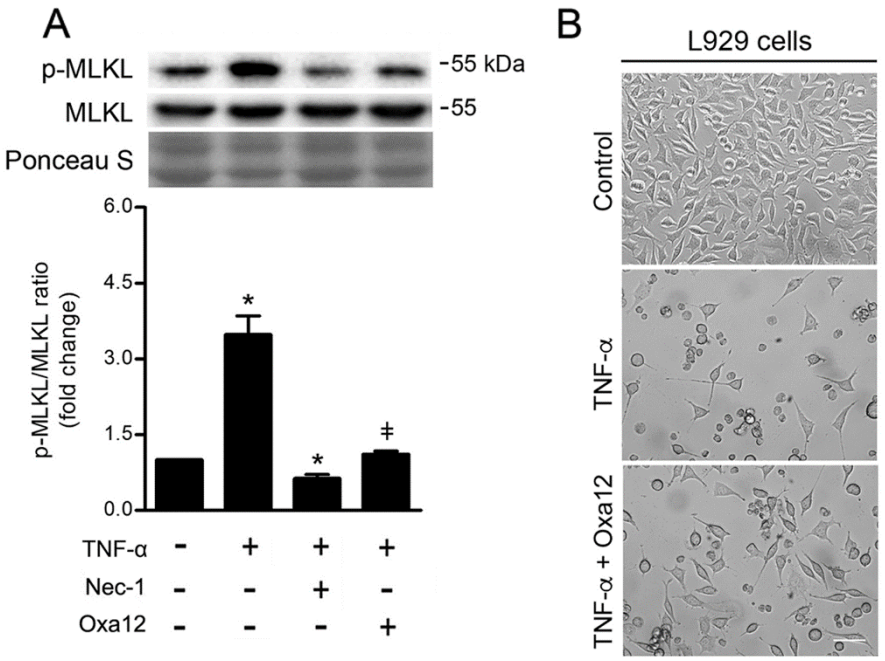

Figure S2.1.1. Oxa12 reduces MLKL phosphorylation in the murine L929 cell line. (A) L929 cells were incubated with 30 µM each of TNF-α, TNF-α plus Nec-1, or TNF-α plus Oxa12 for 5 h. Total protein lysates were prepared for Western blot analysis of p-MLKL and MLKL. Representative immunoblots are presented with the respective densitometric analysis. Blots were normalized to Ponceau S staining. Values are expressed as mean ± SEM of three independent experiments. **p* < 0.05 vs control; ‡*p* < 0.05 vs TNF-α. (B) Bright-field microscopic images of L929 cells incubated with 30 µM each of TNF-α, TNF-α plus Nec-1 or TNF-α plus Oxa12 for 24 h. Microscopy images were taken at 100x with a Primo Vert microscope. Scale bar, 100 *µ*m.

Reprinted, with minor modifications, from Oliveira SR *et al.* 2021. Discovery of a necroptosis inhibitor improving dopaminergic neuronal loss after MPTP exposure in mice. *Int J Mol Sci.* 22(10), 5289
doi: 10.3390/ijms22105289, Copyright © 2021

Discovery of a necroptosis inhibitor improving dopaminergic neuronal loss after MPTP exposure in mice

Sara R. Oliveira, Pedro A. Dionísio, Maria M. Gaspar, Maria B. T. Ferreira, Catarina A. B. Rodrigues, Rita G. Pereira, Mónica S. Estevão, Maria J. Perry, Rui Moreira, Carlos A. M. Afonso, Joana D. Amaral and Cecília M. P. Rodrigues

Research Institute for Medicines (iMed.ULisboa), Faculdade de Farmácia, Universidade de Lisboa, Portugal

2.2.1. Abstract

Parkinson's disease (PD) is the second most common neurodegenerative disorder, mainly characterized by motor deficits correlated with progressive dopaminergic neuronal loss in the substantia nigra pars compacta (SN). Necroptosis is a caspase-independent form of regulated cell death mediated by the concerted action of receptor-interacting protein 3 (RIP3) and the pseudokinase mixed lineage domain-like protein (MLKL). It is also usually dependent on RIP1 kinase activity, influenced by further cellular clues. Importantly, necroptosis appears to be strongly linked to several neurodegenerative diseases, including PD. Here, we aimed at identifying novel chemical inhibitors of necroptosis in a PD-mimicking model, by conducting a two-step screening. Firstly, we phenotypically screened a library of 31 small molecules using a cellular model of necroptosis and, thereafter, the hit compound effect was validated *in vivo* in a sub-acute 1-methyl-1-4-phenyl-1,2,3,6-tetrahydropyridine hydrochloride (MPTP) PD-related mouse model. From the initial compounds, we identified one hit - Oxa12 - that strongly inhibited necroptosis induced by the pan-caspase inhibitor zVAD-fmk in the BV2 murine microglia cell line. More importantly, mice exposed to MPTP and further treated with Oxa12 showed protection against MPTP-induced dopaminergic neuronal loss in the SN and striatum. In conclusion, we identified Oxa12 as a hit compound that represents a new chemotype to tackle necroptosis. Oxa12 displays *in vivo*

effects, making this compound a drug candidate for further optimization to attenuate PD pathogenesis.

2.2.2. Introduction

Parkinson's disease (PD) is the second most common neurodegenerative disorder worldwide. PD is pathologically defined by the progressive dysfunction of the nigrostriatal pathway, which culminates in the loss of dopaminergic neurons in the substantia nigra pars compacta (SN) and depletion of dopaminergic enervation in the striatum (Poewe et al. 2017; Kordower et al. 2013). Of note, degeneration of dopaminergic neurons in the SN precedes the first motor deficits afflicting PD patients (Kordower et al. 2013).

The pathological mechanisms causing PD are thought to stimulate a cascade of events that activate regulated cell death (RCD) pathways, which are responsible for neuronal death (Levy et al. 2009; Venderova and Park 2012). Recent evidence has shown that necroptosis, a type of regulated necrosis, plays crucial pathogenic roles in several human diseases, including neurodegenerative diseases, such as PD, while holding high potential for clinical targeting (Conrad et al. 2016). Necroptosis is a caspase-independent type of RCD commonly executed after RIP1 and RIP3 kinase activation. Typically, this type of cell death is initiated following cell death transmembrane receptor stimulation, with tumor necrosis factor (TNF) receptor 1 (TNFR1) being the most well-studied example (He et al. 2009; Bonnet et al. 2011). In conditions where caspase-8 activation is genetically or pharmacologically prevented, RIP1 and RIP3 are not cleaved and accumulate in the so-called necrosome complex (Grootjans et al. 2017). Then, activated RIP3 recruits and phosphorylates pseudokinase mixed lineage domain-like protein (MLKL), which further translocates to the plasma membrane, inducing membrane disruption and necroptosis execution (Conrad et al. 2016). Importantly, necroptosis has already been associated with neuronal death induced by the neurotoxin 1-methyl-4-phenyl-1,2,3,6-tetrahydropyridine (MPTP), a PD-mimicking neurotoxin, in both *in vivo* and *in vitro* rodent models, as well as in PD human samples (Iannielli et al. 2018; Lin et al. 2020).

Importantly, the first necroptosis inhibitors were identified back in 2005 through a phenotypic screening for chemical inhibitors of necroptosis induced by TNF and zVAD-fmk in human monocytic U937 cells. This led to the identification of necrostatin-1 (Nec-1) and its optimized derivative necrostatin-1 stable (Nec-1s), later confirmed to be RIP1 kinase inhibitors (Wang et al. 2008; Christofferson et al. 2012; Degterev et al. 2005). Additional studies regarding Nec-1 properties pointed to off-target activity and limited metabolic stability in mice, while Nec-1s presented higher activity as a necroptosis inhibitor, along with no nonspecific cytotoxicity and reasonable pharmacokinetic properties. However, Nec-1s still presents a short *in vivo* half-life. (Declercq et al. 2009; Wang et al. 2008; Xie et al. 2013; Brenner et al. 2015; Teng et al. 2005). Of note, Nec-1s identification proved that RIP1 inhibition is beneficial in several diseases (Degterev et al. 2005; Caccamo et al. 2017; Lin et al. 2020; Iannielli et al. 2018). Moreover, molecules targeting other components of necroptotic signaling pathway, such as RIP3 or MLKL, have also been proposed (Sun et al. 2012; Mandal et al. 2014). However, none of the compounds discovered so far reached the expectation of clinical application, which has led researchers to unceasingly screen new drugs with better selectivity and potency.

In this study, we phenotypically screened a library of 31 new molecules to discover novel inhibitors of necroptotic cell death with structural novelty. Although target-based drug discovery has been the dominant approach to drug discovery in the past decades, there has been a recent reawakening interest in phenotypic drug discovery approaches, based on their potential to address the complexity of only partially understood diseases and their promise of delivering first-in-class drugs, in parallel with major advances in cell-based phenotypic screening tools. In addition, prioritized hits from the primary screen were further evaluated for *in vivo* proof-of-concept using an MPTP PD-mimicking mouse model. We identified a potential hit, Oxa12, that significantly inhibited zVAD-fmk-induced necroptotic cell death in the BV2 microglial cell line, with a half-maximal effective concentration (EC50) of ~1 µM. Importantly, Oxa12 showed to protect dopaminergic neuronal cells from death induced by MPTP *in vivo*, in the SN and striatum, which highlights the potential benefits of discovering and optimizing new molecules with mechanisms of action that affect disease-relevant pathways, such as necroptosis.

2.2.3. Materials and Methods

2.2.3.1. Cell culture and reagents

The BV2 murine microglia cell line was gently provided by Dr. Elsa Rodrigues, University of Lisbon. BV2 microglia cells were cultured in RPMI 1640 medium (GIBCO® Life Technologies, Inc. Grand Island, USA) supplemented with 10% heat inactivated foetal bovine serum (FBS), 1% antibiotic/antimycotic (A/A) solution and 1% GlutaMAX^{TM} (GIBCO). During the experiments, culture media was substituted by RPMI supplemented with 1% A/A, 1% insulin-transferrin-selenium (RPMI/ITS) and 1 mg/mL bovine serum albumin (BSA; GIBCO). Cells were maintained at 37ºC in a humidified atmosphere of 5% CO_2. Chemicals used were Nec-1 (Sigma-Aldrich, St. Louis, MO, USA), dimethyl sulfoxide (DMSO; Sigma-Aldrich) and Z-Val-Ala-Asp-fluoromethylketone (zVAD-fmk) pan-caspase inhibitor (Enzo Life Sciences, Farmingdale, NY, USA).

2.2.3.2. Chemical synthesis and analysis

The oxazol-5-(4H)-ones (Oxas) and the precursors aldehydes were synthesized following a general synthetic reported route: A mixture of the corresponding aldehyde (30 – 600 µmol scale, 1 equiv.), hippuric acid or derivatives (1 equiv.), sodium acetate (1 equiv.) and acetic anhydride (3 equiv.) in a round-bottom flask was heated under magnetic stirring at 110ºC for 2 hours (Rodrigues et al. 2013). Then, the reaction mixture was cooled to room temperature and the obtained solid was washed with distilled water (2x) and MeOH (4x) and dried under vacuum. If further purification was needed, some of the compounds were recrystallized in a suitable solvent. The purity and structural identification were performed by ^{1}H, ^{13}C NMR and mass spectrometry analyses.

2.2.3.3. Screening of necroptosis inhibitors

BV2 cells were plated in 96-well plates at 7 x 10^3 cells/well and after 24 h, necroptosis was induced by adding 25 µM zVAD-fmk in RPMI/ITS. Test compounds or Nec-1 (positive control of necroptosis inhibition) were incubated along with zVAD-fmk at a final concentration of 30 µM for 24 h. DMSO was used as vehicle control. Cell viability was determined based on measurement of MTS metabolism using the CellTiter 96® Aqueous Non-Radioactive Cell Proliferation

(MTS) Assay (Promega, Madison, WI, USA). Differences in absorbance were measured at 490 nm using GloMax® Multi Detection System (Sunnyvale, CA, USA).

2.2.3.4. EC_{50} determination

To quantitatively determine the effective potency in BV2 cells, the compound half maximal effective concentration (EC_{50}) was determined by a dose-response curve. In brief, BV2 cells were plated in 96-well plates as described above and treated with increasing concentrations of compound Oxa12 (from 0,1 to 50 µM), using Nec-1 as positive control and DMSO as vehicle control. Following 24 h of incubation, cell viability was determined based on measurement of MTS, as previously described.

2.2.3.5. RIP1 and RIP3 kinase activity assays

Oxa12 were tested at 5 µM for RIP1 kinase activity by a radiometric-binding assay using myelin basic protein as substrate (Eurofins, France) as before (Brito et al. 2020).

2.2.3.6. Microsomal stability assay

In the microsomal stability assay, an analytical high-performance liquid chromatography (HPLC) system was used with the following condition: column, Merck Lichrospher 100 RP18 125 mm 4.6 mm (5 µm); mobile phase A = 0.1% trifluoroacetic acid in water, B = 0.1% trifluoroacetic acid in acetonitrile, isocratic; flow rate, 1 mL/min; detection, UV at 400 nm injection, 20 µL; column temperature, ambient. The metabolic stability assays were carried out using the cosolvent method, appropriate for assessing the metabolic stability of compounds poorly soluble in aqueous medium (Di et al. 2006). For the cosolvent method, a 0.5 mM DMSO stock solution of Oxa12 was prepared. Then, a diluted solution of the compound was prepared by adding 50 µL of the previous 0.05 mM solution with 200 µL of acetonitrile, to make a 0.1 mM solution of Oxa12 in 20% DMSO/80% acetonitrile. Cosolvent assay conditions were: substrate concentration, 1 µM; microsomal protein, 0.5 mg/mL; organic solvents, 0.2% DMSO, 0.8% acetonitrile; incubation time, 30 min; number of assays, duplicates

for T0 and T30 min. Time 0 and time 30 batches, after quenching with acetonitrile, were centrifuged at 11,000 g for 5 min and the supernatants were analyzed by HPLC, in order to quantify compound Oxa12.

2.2.3.7. MPTP mouse model

Animal studies were performed according to the animal welfare of the Faculty of Pharmacy, University of Lisbon, and approved by the competent national authority Direção Geral de Alimentação e Veterinária (DAGV) and in accordance with the EU Directive (2010/63/UE), Portuguese laws (DR 113/2013, 2880/2015 and 260/2016) and all relevant legislation. To evaluate the neuroprotective effect of our hit compound - Oxa12 - in the sub-acute MPTP mouse model, male 13-week-old C57BL/6N wild-type (wt) mice (Charles River Laboratories, Wilmington, MA, USA) were injected intraperitoneally (i.p.) with a unique dose of MPTP-HCl (40 mg/kg; Sigma Aldrich, St Louis, MO, USA), dissolved in sterile 0.9% saline, or vehicle only (control group). One hour after MPTP administration, mice were intraperitoneally injected with 10 mg/kg Oxa12 solubilized in 1% DMSO (Sigma-Aldrich) and 30% 2-hydroxypropyl-beta-cyclodextrin (Sigma-Aldrich) or 10 mg/kg Nec-1s (Focus Biomolecules, Plymouth Meeting, PA, USA) solubilized in 1% DMSO, 4% 2-hydroxypropyl-beta-cyclodextrin (Sigma-Aldrich), in PBS (Dionísio et al. 2019; Castro-Caldas et al. 2009; Saporito, Thomas, and Scott 2000). Oxa12 and Nec-1s injections were administered once every day for 30 days. Oxa12 dosage and regimen of administration were selected based on published protocols for Nec-1s (Iannielli et al. 2018; Ofengeim et al. 2015). Seven animal per group were used. After 30 days, mice were sacrificed in a CO_2 chamber followed by transcardiac perfusion with ice-cold PBS. Brains were then excised, and one hemisphere was used to isolate the midbrain region, containing the SN, and the striatum, as previously described (Dionísio et al. 2019; Castro-Caldas et al. 2009), which was rapidly frozen in liquid nitrogen and stored at −80 ˚C until processing for protein extraction. The other hemisphere was fixed in 4% paraformaldehyde for 48 h and then stored in 20% sucrose/PBS and 0.025% sodium azide, at 4 ˚C, for further immunohistochemistry analyses.

2.2.3.8. Immunohistochemistry

Hemispheres previously fixed in paraformaldehyde were cryoprotected in 20% sucrose/PBS and embedded in gelatin. Then, sequential coronal brain sections (8 µm thick) near the midstriatum (Bregma 1.00) and SN (Bregma -3.20) were obtained by cryostat sectioning and mounted on SuperFrost-Plus glass slides (Thermo Fisher Scientific). Afterwards, sections were incubated in warm PBS at 37 ºC during 15 min, followed by two washes in PBS, to remove gelatin. Then, sections were blocked in Tris buffered saline (TBS) containing 10 % (v/v) normal donkey serum (Jackson ImmunoResearch Laboratories Inc., West Grove, PA, USA) and 0.1 % (v/v) Triton X-100 (Sigma-Aldrich) for 1 h. Subsequentially, to stain dopaminergic neurons, sections were incubated with primary rabbit polyclonal anti-tyrosine hydroxylase (TH) antibody (#ab112; Abcam, Cambridge, UK, 1:700), overnight at 4 ºC. After several washes with PBS, anti-TH primary antibody was detected with diluted (1:200) Alexa Fluor 488 (anti-rabbit) conjugated secondary antibody (Invitrogen – Thermo Fisher Scientific) during 2 h at room temperature. After extensive rinsing, sections were counterstained with Hoechst 33258 (Sigma-Aldrich) and mounted on Mowiol 4-88 (Sigma-Aldrich).

2.2.3.9. Image analysis

Images were obtained by an Axioskop fluorescence microscope (Carl Zeiss GmbH, Hamburg, Germany). Images were captured from six region-matched sections for nigral and striatal regions for each animal and converted into a gray scale with an 8-bit format using the ImageJ software (National Institute of Health, Bethesda, USA). A threshold optical density was determined for each staining. Areas occupied by positive staining were quantified in thresholded images, normalized to the total area of interest region and calculated as percentage of total area.

2.2.3.10. Protein isolation

For total protein isolation, tissues obtained from dissected midbrains and striata were homogenized in radio-immunoprecipitation assay (RIPA) buffer (50 nM Tris/HCl, pH 8; 150 nM NaCl; 1% NP-40; 0.5% sodium deoxycholate; 0.1% SDS) and 1x Halt Protease and Phosphatase Inhibitor Cocktail (Pierce, Thermo

Fisher Scientific) with a moto-driven Bio-vortexer (No 1083; Biospec Products, Bartlesfield, UK). Lysates were maintained on ice during 30 min and were then sonicated and centrifuged at 10000 g for 10 min. Supernatants were collected and used as total protein extracts. Protein concentrations were determined by using the Bio-Rad protein assay kit, according to the manufacturer's instructions.

2.2.3.11. Western blot

Equal amounts of total protein extracts were electrophoretically resolved on 8% SDS-PAGE. Resolved proteins were then transferred onto nitrocellulose membranes and blocked with a 5% milk solution in Tris-buffered saline (TBS). Then, membranes were incubated with primary antibody rabbit polyclonal TH (#ab112, Abcam) overnight at 4 °C. After washing with TBS/0.2% Tween 20 (TBS-T), membranes were incubated with secondary goat anti-rabbit IgG antibody conjugated with horseradish peroxidase (Bio-Rad Laboratories) during 2 h at room temperature. Membranes were processed for protein detection using Immobilon^{TM} Western (Millipore). β-actin (AC-15) (#A5441, Sigma-Aldrich) was used as loading control. Densitometric analysis was performed using the Image Lab Software version 5.1 Beta (Bio-Rad).

2.2.3.12. Statistical analysis

All data are presented as mean ± standard error of the mean (SEM). Data analysis were performed with one-way analysis of Variance (ANOVA) followed by post hoc Bonferroni's test. Analysis and graphical presentation were conducted with the GraphPad Prim Software version 8 (GraphPad Software Inc., San Diego, CA, USA). Statistically significance was achieved when $p < 0.05$.

2.2.4. Results

2.2.4.1. Phenotypic screening for hit selection

To identify novel necroptosis inhibitors, we performed a cell-based phenotypic screening assay to select hit compounds that strongly inhibit necroptotic cell death (Figure 2.2.1A).

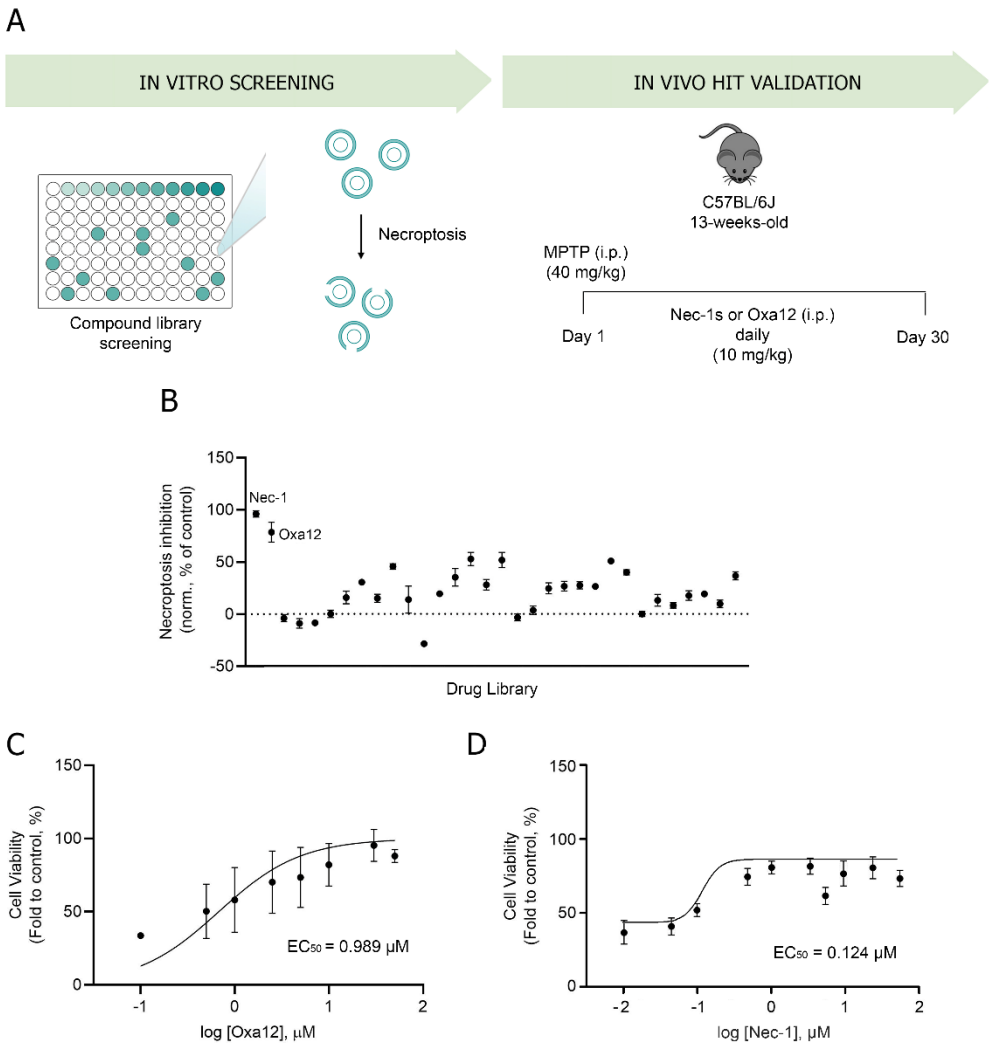

Figure 2.2.1. A cell-based phenotypic screening identifies Oxa12 as a necroptosis inhibitor. (A) Schematic overview of the two-step screening workflow. (B) Determination of compound ability to inhibit necroptosis. Cell metabolic activity is depicted as percentage of control (DMSO = 0; Nec-1 at 30 µM) for compounds at 30 µM tested in BV2 murine microglia cells exposed to 25 µM zVAD-fmk for 24 h. (C) Half-maximal effective concentration (EC_{50}) determination in BV2 murine microglia cells in a dose-response concentration (0.1 to 50 µM Oxa12) plus 25 µM zVAD-fmk for 24 h. (D) Half-maximal effective concentration (EC_{50}) determination in BV2 murine microglia cells in a dose-response concentration (0.1 to 50 µM Oxa12) plus 25 µM zVAD-fmk for 24 h.

Previous studies have demonstrated that the pan-caspase inhibitor zVAD-fmk induces necroptosis in different cellular models, including in the L929 fibrosarcoma and in the BV2 murine microglial cell lines, by a mechanism that most likely depends on TNF autocrine secretion (Christofferson et al. 2012; Wu et al. 2011; Oliveira et al. 2018). Here, we used BV2 cells incubated with zVAD-fmk as an *in vitro* model of necroptosis and screened a total of 31 small compounds potentially inhibitors of this type of cell death. These compounds are part of a larger in-house library containing mainly the heterocyclic core of 4-methylene-2-aryloxazol-5(4H)-one and are represented in Figure 2.2.2. The remaining compounds have been tested in previous papers (Christofferson et al. 2012; Oliveira et al. 2018; Wu et al. 2011). Cells were incubated with 25 µM zVAD-fmk alone or in combination with 30 µM test compounds for 24 h. BV2 cells treated with DMSO were used for data normalization. BV2 cells co-incubated with zVAD-fmk and Nec-1, a well-known RIP1 kinase inhibitor, were used as positive control of necroptosis inhibition (Figure 2.2.1B). As expected, treatment with Nec-1 almost completely rescued zVAD-fmk-induced decrease in cell viability ($p < 0.001$) (Figure 2.2.1B), as assessed by MTS metabolism. More importantly, we identified one hit that significantly protected cells from zVAD-fmk-mediated necroptosis by ~70% ($p < 0.01$) (Figure 2.2.1B). Importantly, RIP1 kinase activity inhibitory potential of Oxa12 was determined using radiometric binding-based assays. The results show that Oxa12 at 5 µM inhibits RIP1 activity by ~15%, which confirms RIP1 as a possible target. The anti-necroptotic effects, however, may not be solely dependent on this target. These results are in line with our previous work, where we showed the sequestration of key necroptosis mediators, RIP1, RIP3, and p-MLKL, in the insoluble fraction in zVAD-fmk-treated BV2 cells, while Oxa12 abolished necrosome assembly and MLKL phosphorylation (Oliveira et al. 2018). Moreover, Oxa12 strongly rescued zVAD-fmk-induced cell death, as observed by microscopy analysis of cell morphology (Oliveira et al. 2018). Furthermore, our previous *in silico* molecular docking calculations for Oxa12 inside the RIP1 kinase domain demonstrated that Oxa12 is occupying a region similar to the co-crystallized inhibitor, suggesting a similar interaction pattern and indicating that Oxa12 most likely targets RIP1 to some extent (Oliveira et al. 2018)

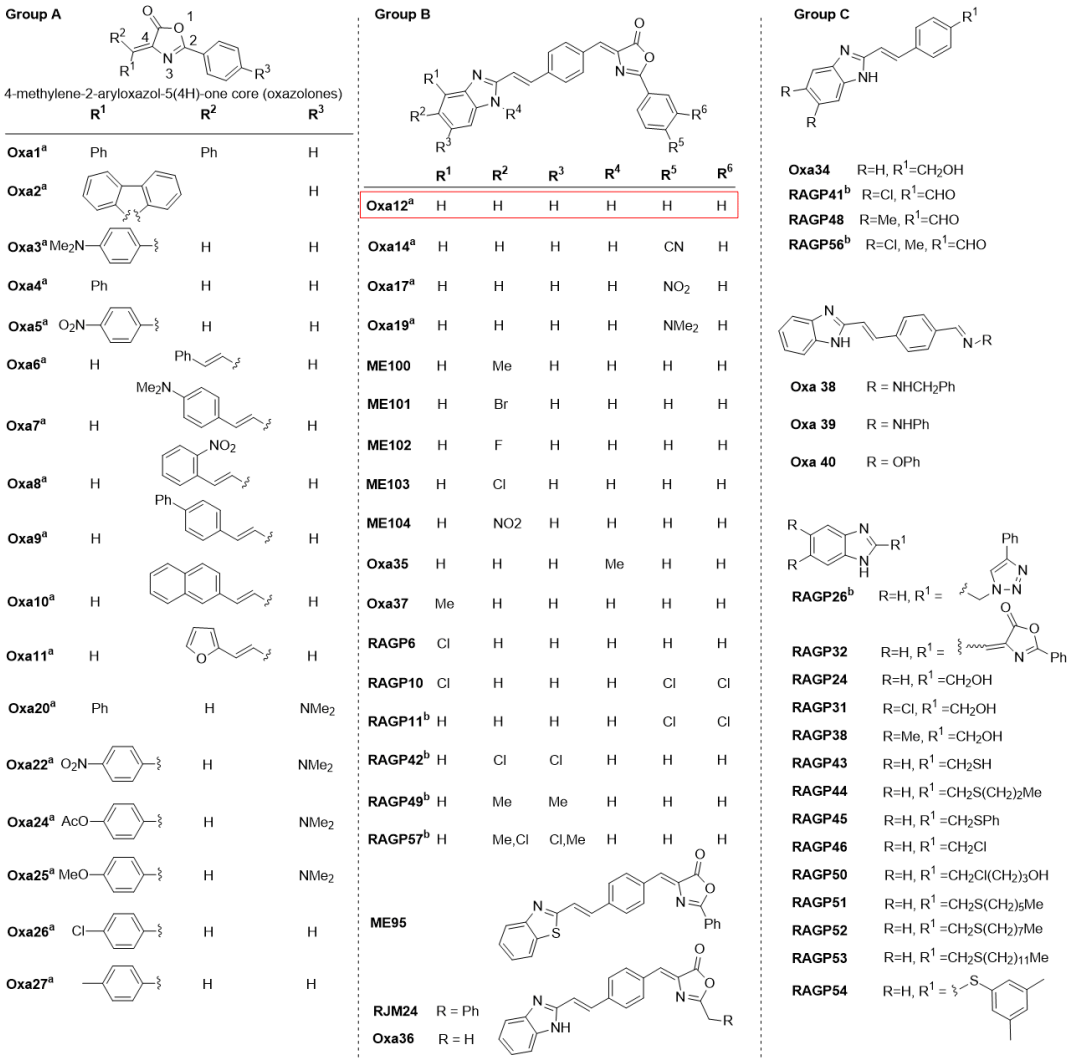

Figure 2.2.2. Structures of the tested synthesized small-molecule library compounds based on the 4-methylene-2-aryloxazol-5(4H)-one core (oxazolones). Group A includes oxazolones containing substituted aryl and aromatic heterocyclic attached to the 4-methylene position. Group B consists of extended oxazolones containing terminal fused heterocycles. Group C includes additional compounds without the oxazolone core or the 4-methylene side chain.

[a]Synthesized compounds evaluated in a previous paper (22). [b]Compounds not evaluated due to insoluble properties at the tested concentration.

To further characterize Oxa12 activity, we the EC_{50}, a pharmacologic parameter commonly used as a measure of compound potency, which here indicates 50% of compound maximal potency to inhibit necroptosis, by

performing a dose-response study. BV2 cells were incubated with zVAD-fmk along with Oxa12 at a range of concentrations (0.1-50 µM) during 24 h and the EC_{50} calculated. Our results showed that Oxa12 presented an EC_{50} value of 0.989 µM, comparable with 0.124 µM of Nec-1, thus indicating its effectiveness as a necroptosis inhibitor (Figure 2.2.1C, D).

We next found that Oxa12 met stringent criteria on activity, chemical tractability, and structural novelty, including a low chemical similarity with Nec-1 and its analogues, as measured by Tanimoto's index. Moreover, we analysed whether Oxa12 was included in the central nervous system (CNS) drug property space, using a CNS multiparameter optimization (MPO) approach, a prospective design tool and a widely utilized predictor for ADME and safety properties suitable for CNS targeting (Wager et al. 2010). CNS MPO utilizes a set of six physicochemical descriptors to calculate a score, between 0 and 6. A higher score represents the optimal chemical space possessing alignment of key drug properties for CNS therapeutic agents. Generally, a CNS MPO score ≥ 4 is desired, although there are drugs active on the CNS with lower score, with the range 3-4 being still acceptable (Wager et al. 2016). Here, we observed that Oxa12 has a value of 3.6, while being lower than the CNS MPO score of 5 calculated for Nec-1, the value for Oxa12 is similar to that determined for several well-known CNS drugs, suggesting a good brain exposure (Table 2.2.1).

Finally, we also determined the extent of Oxa12 metabolism in human liver microsomes. Using our medium-throughput drug metabolism platform, we observed that 20% of Oxa12 was detected by HPLC after incubation for 30 min in mouse liver microsomes, which corresponds to an estimated half-life of 13 min, a liability that negatively impacts the systemic and brain exposure of Oxa12. These results allowed us to calculate a clearance Clint *in vitro* of 0.99 mL/min/mg protein and a predicted hepatic extraction ratio of 0.76. of note, although the original Nec-1 has a half-life of < 5 min, chemical optimization of this compounds has led to commonly used derivatives with a half-life of about 1 h in mouse microsomal assays (Degterev et al. 2013). Thus, a combined analysis of the CNS MPO score and metabolic data confirms that Oxa12 is a novel addition to the chemical toolbox of CNS-targeting anti-necroptotic compounds.

2.2.4.2. *In vivo* efficacy of Oxa12 in the sub-acute MPTP mouse model

To determine if our identified hit compound was effective *in vivo*, we used a sub-acute MPTP mouse model. MPTP is the most widely used neurotoxin to mimic PD-related nigrostriatal degeneration, since it can be easily administered systemically, and human exposure to MPTP has been associated with severe parkinsonism, which reinforces the relevance of MPTP animal models (Meredith et al. 2011; Langston 2017). Mechanistically, MPTP can rapidly cross the blood–brain barrier and, once in the brain, it is mostly oxidized to an intermediate, which then diffuses to the extracellular space and converts to the active toxic metabolite, 1-methyl-4-phenylpyridinium (MPP^+) (Ransom et al. 1987; Schildknecht et al. 2015). Then, dopaminergic neurons selectively uptake MPP^+. In mitochondria, MPP^+ inhibits the complex I of the respiratory chain, leading to decreased ATP generation along with the production of reactive oxygen species (ROS), and ultimately cell death (Schildknecht et al. 2015; Dauer and Przedborski 2003). In this regard, several studies have already demonstrated that necroptosis is involved in neuronal death induced by MPTP and that Nec-1/Nec-1s administration is neuroprotective in multiple MPTP exposure regimens (Iannielli et al. 2018; Lin et al. 2020).

Here, we used a sub-acute MPTP regimen consisting of a single dose of MPTP (40 mg/kg), or vehicle, intraperitoneally injected in 13-week-old mice. Then, 10 mg/kg of Oxa12 or Nec-1s was administered 1 h after MPTP and then once every day for 30 days. As expected, we observed a significant reduction of approximately ~50% in TH-positive staining, a marker of dopaminergic neurons, in the SN and in the striatum of MPTP-exposed animals (Figure 2.2.3A,B), while no differences were observed in mice injected with Oxa12 or Nec-1s alone (Figure 2.2.3A,B).

Importantly, treatment with Oxa12 or Nec-1s partially protected cells from MPTP-induced dopaminergic cell death, in the SN (Oxa12, $p = 0.05$; Nec-1s, $p = 0.12$) and striatum (Oxa12, $p = 0.06$; Nec-1s, $p = 0.08$), as observed by the rescue of TH-positive staining in comparison with MPTP-treated animals (Figure 2.2.3A,B).

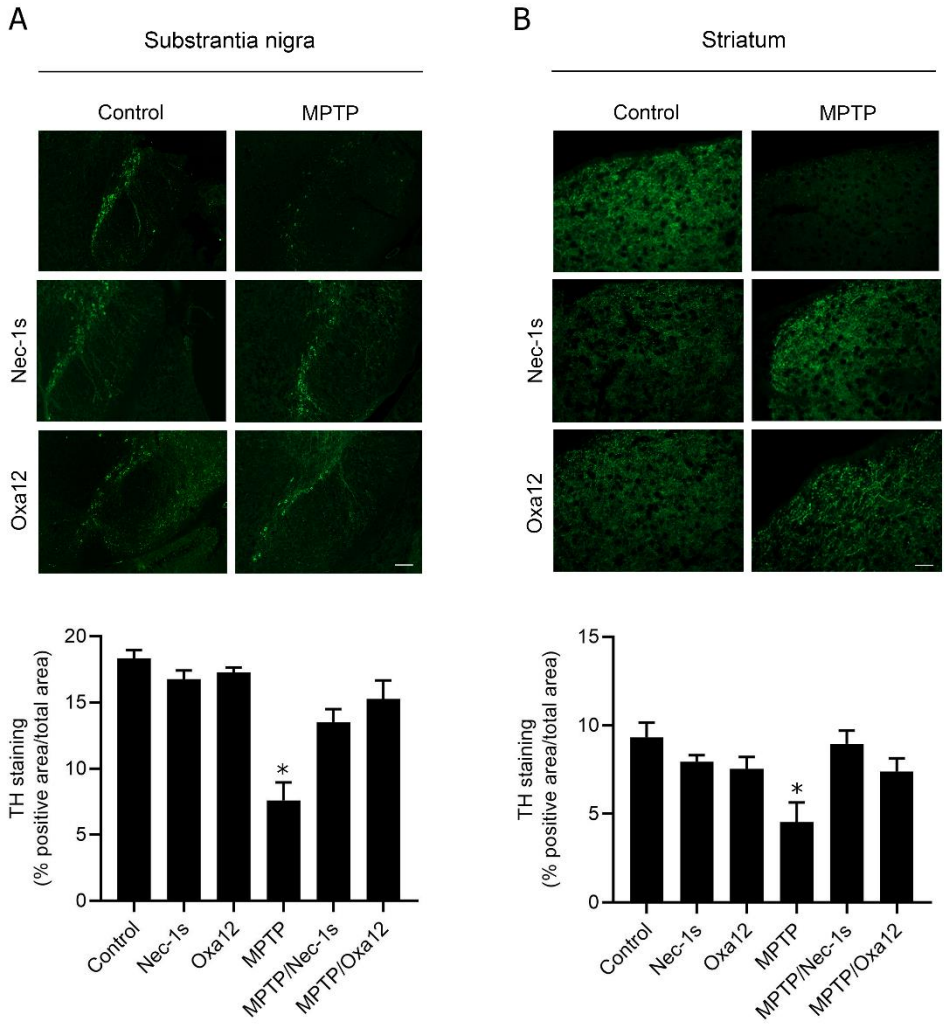

Figure 2.2.3. Oxa12 protects from MPTP-driven dopaminergic neuronal loss. Representative images of TH-positive immunostaining from control- and MPTP-injected mice treated with vehicle, Nec-1s or Oxa12 in the SN (A) and the striatum (B), and respective quantification. *Scale bar*, 100 µm. *$p < 0.05$ vs. control mice.

In accordance, exposure to MPTP significantly reduced TH protein levels in the SN, while Oxa12 and Nec-1s treatment alone did not alter TH levels (Figure 2.2.4). Notably, Oxa12 significantly rescued TH reduced protein levels induced by MPTP treatment by ~30% ($p < 0.05$), while Nec-1s showed a ~10% difference (Figure 2.2.4). The challenging dissection of SN-enriched midbrain sections, which include other dopaminergic structures, may account for the less significant rescue of TH in the SN by western blot as compared with immunofluorescence. Our results show that Oxa12 reveals a propensity to protect neuronal cells from

MPTP-induced cell loss, with the potential to be explored as a new chemotype to tackle necroptosis. Nevertheless, careful examination of target engagement, including RIP1 and MLKL sequestration in insoluble fractions, a strong indicator of necrosome assembly and, therefore, of necroptosis commitment (Ransom et al. 1987), deserves further investigation upon using appropriate antibodies.

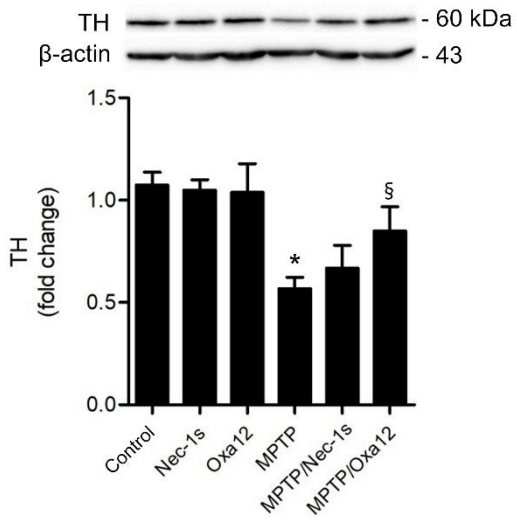

Figure 2.2.4. Oxa12 protects dopaminergic neurons from MPTP-induced cell death. Representative western blot of TH protein levels from control- and MPTP-injected mice treated with vehicle, Nec-1s or Oxa12 in the SN, and respective densitometric analysis. β-actin was used as loading control. Values are expressed as mean ± SEM of three independent experiments. *p < 0.05 vs. control mice; §p < 0.05 vs. MPTP mice. TH, tyrosine hydroxylase.

Finally, MPTP mice models normally develop an inflammatory response that initiates in the striatum, with astrogliosis developing later than microgliosis and being sustained for a longer period of time (Schildknecht et al. 2015; Dauer and Przedborski 2003). Concordantly, we observed an increase in GFAP immunostaining and GFAP protein levels in MPTP-treated mice, thus suggesting a prolonged astrogliosis in these animals (data not shown). However, no significant differences were observed in mice treated with Oxa12 or Nec-1s.

2.2.5. Discussion

In the present study, a two-step screening workflow was performed to identify novel necroptosis inhibitors from a small-molecule library of 31 compounds. In a first step, we conducted an *in vitro* phenotypic screening to identify hit compounds that strongly inhibited zVAD-fmk-induced necroptotic cell death in the murine BV2 microglial cell line. In a second step, the ability of our hit molecule to protect against dopaminergic neuronal cell loss was determined *in vivo* using the sub-acute MPTP mouse model of PD.

As a strategy for the first step, we initially screened a range of diverse heterocyclic functionalized compounds collected from different developed synthetic methodologies. From this preliminary screening, several existing compounds containing the 4-methylene-2-aryloxazol-5(4H)-one (oxazolones) core were identified as bioactive (Rodrigues et al. 2013). Furthermore, we also synthesized a range of oxazolones containing diverse substituents at the 4-methylene and 2-aryl positions (Groups A and B) and by replacing the oxazolone core (Group C) as well as by inclusion of longer phenylmethylene spacer and additional structural tuning on the attached fused heterocycles (Group B). Importantly, we identified one molecule - Oxa12 - that strongly inhibited necroptosis in the zVAD-fmk-treated BV2 microglia cells, and this effect was further demonstrated *in vivo*. Oxa12 tended to protect dopaminergic neuronal cells from MPTP-induced cell death, thus suggesting the potential of this compound in ameliorating PD pathogenesis.

Since the discovery of Nec-1 as the first necroptosis inhibitor, several other studies were performed and new inhibitors for RIP1, RIP3 and MLKL were identified. However, the therapeutic potential of all these inhibitors is restricted by low potency or reduced selectivity. In fact, so far, there is no compound that reached the prospects of clinical application, which has led to the continuous screening of new molecules with higher selectivity and potency. Despite its strongness at inhibiting necroptosis, Nec-1 is a far-from-ideal drug due to its short *in vivo* half-life of approximately 1 hour, as well as its off-target effects, including inhibitory binding to indoleamine 2,3-dioxygenase (IDO), a protein involved in inflammation (Vandenabeele et al. 2013). Nec-1s presents higher specificity and improved pharmacokinetics properties; however still holds poor *in vivo* half-life

(Ofengeim et al. 2015). Thus, Nec-1s represents a better choice for *in vivo* experiments. Other RIP1 inhibitors, including GSK'481, GSK'963 and GSK'772 also demonstrate similar limitations (Berger et al. 2015; Harris et al. 2013; Harris et al. 2017). RIP3 inhibitors, such as GSK'872, have also been studied; however, while inhibiting necroptosis, they may also promote apoptosis (Mandal et al. 2014). Thus, considering the limitations of all known RIP1 and RIP3 inhibitors, the development of novel and potent small compounds able to specifically attenuate necroptosis continues to be of strong need.

Here, we used the BV2 murine microglia cell line treated with the pan-caspase inhibitor, zVAD-fmk, as a model of necroptosis execution. In fact, we and others already demonstrated that zVAD-fmk strongly induces necroptotic cell death in both L929 fibrosarcoma and BV2 murine microglia cells (Christofferson et al. 2012; Wu et al. 2011 Oliveira et al. 2018). Importantly, the pharmacological relevance of the *in vitro* phenotypic screening was guaranteed by using a well-established necroptosis inhibitor. Here, Nec-1, which inhibits RIP1 kinase activity, was used as positive control throughout the *in vitro* screening and demonstrated to be a strong necroptosis inhibitor. To identify novel necroptosis inhibitors, an in-house library of 31 small compounds were screened at a concentration of 30 µM, which allowed us to filter new necroptosis inhibitor scaffolds with potential to be further modified chemically. We identified one hit - Oxa12 - that strongly inhibited necroptosis in the BV2 microglia cells by ~70%. To further characterize Oxa12 potency *in vitro*, dose-response curves were performed, where Oxa12 showed an EC_{50} value of 0,989 µM, thus reflecting its potential to be tested *in vivo*.

Throughout the years, MPTP mouse models have been widely used due to their specific and reproducible neurotoxic effect on the nigrostriatal system, being considered a convenient model of dopaminergic neurodegeneration to study therapeutic interventions. However, these models do not fully reproduce the human condition, and behavioral abnormalities are still a challenging question (Harris et al. 2017). Moreover, previous studies have already demonstrated the involvement of necroptosis in the acute and sub-chronic MPTP mouse model of PD, where Nec-1/Nec-1s administration attenuated dopaminergic neurodegeneration (Iannielli et al. 2018; Lin et al. 2020). Here, we used a sub-acute regimen of MPTP exposure, consisting of a single injection of MPTP (40 mg/kg) and still observed a significant increase in dopaminergic

neurodegeneration in the SN and the striatum, while Nec-1s administration showed a tendency to protect cells from MPTP-induced dopaminergic cell death (Langston 2017; Pong et al. 2001; Dionísio et al. 2019). Importantly, Oxa12 alone did not induce neuronal toxicity, but it was able to protect dopaminergic neurons from MPTP-induced cell death in both SN and striatum. This experimental observation together with the MPO value suggest that Oxa-12 can cross the BBB, at least to some extent. Medicinal chemistry optimization of Oxa-12 should tackle issues such as solubility and be followed by extensive *in vivo* characterization of a more advanced lead compound, including by evaluating BBB penetration, half-life and target engagement. The role for inhibiting necroptosis deserves further exploitation (Brito et al. 2020).

Overall, these results indicate that Oxa12 has reasonable potency, associated with an apparent lack of toxicity, which makes this compound fit for additional chemistry optimization. Therapies using small molecules targeting key components of dopaminergic neuron cell death could evolve as a potential therapeutic approach for ameliorating PD progression.

Chapter 3

MiRNAs IN PARKINSON'S DISEASE

Reprinted, with minor modifications, from Oliveira SR *et al.* 2020. Circulating inflammatory miRNAs associated with Parkinson's disease pathophysiology. *Biomolecules*. 23;10(6):945.
doi: 10.3390/biom10060945,

Circulating Inflammatory miRNAs Associated with Parkinson's Disease Pathophysiology

Sara R. Oliveira[1], Pedro A. Dionísio[1], Leonor Correia Guedes[2,3], Nilza Gonçalves[2], Miguel Coelho[2,3], Mário M. Rosa[2,3,4], Joana D. Amaral[1], Joaquim J. Ferreira[2,4] and Cecília M. P. Rodrigues[1]

[1]Research Institute for Medicines (iMed.ULisboa), Faculdade de Farmácia, Universidade de Lisboa, Portugal
[2]Instituto de Medicina Molecular João Lobo Antunes, Faculdade de Medicina, Universidade de Lisboa, Portugal
[3]Department of Neuroscience and Mental Health, Neurology, Hospital de Santa Maria, Centro Hospitalar Universitário Lisboa Norte, Portugal
[4]Laboratory of Clinical Pharmacology and Therapeutics, Faculdade de Medicina, Universidade de Lisboa, Portugal

3.1.1. Abstract

Parkinson's disease (PD) is the second most common neurodegenerative disease worldwide, being largely characterized by motor features. MicroRNAs (miRNAs) are small non-coding RNAs, whose deregulation has been associated with neurodegeneration in PD. In this study, miRNAs targeting cell death and/or inflammation pathways were selected and their expression compared in the serum of PD patients and healthy controls. We used two independent cohorts (discovery and validation) of 20 idiopathic PD patients (iPD) and 20 healthy controls each. We also analyzed an additional group of 45 patients with a mutation in the leucine-rich repeat kinase 2 (LRRK2) gene (LRRK2-PD). miRNA expression was determined using Taqman qRT-PCR and their performance to discriminate between groups was assessed by receiver operating characteristic (ROC) curve analysis. We found miR-146a, miR-335-3p, and miR-335-5p downregulated in iPD and LRRK2-PD patients versus controls in both cohorts. In addition, miR-155 was upregulated in LRRK2-PD compared to iPD patients

showing an appropriate value of area under the ROC curve (AUC=0.80) to discriminate between the two groups. In conclusion, our study identified a panel of inflammatory related miRNAs differentially expressed between PD patients and healthy controls that highlight key pathophysiological processes and may contribute to improve disease diagnosis.

3.1.2. Introduction

Parkinson's disease (PD) is the second most common neurodegenerative disorder worldwide, affecting 1–2% of people older than 65 years. Although mostly sporadic, around 10% of all cases are now considered to be related to heritable forms of PD (Pringsheim et al. 2014). Mutations in leucine-rich repeat kinase 2 (LRRK2) gene are the most frequent known cause of monogenic PD, especially G2019S, which is associated with a toxic gain-of-function of LRRK2 protein kinase domain. Interestingly, LRRK2 mutations account not only for 5–6% of familial PD, but also for 1–2% of sporadic cases (Healy et al. 2008), due to incomplete penetrance. Frequency varies considerably among different regions, being higher in South European Countries, such as Portugal and Spain, and even higher in Jewish and North African Arab populations, where mean frequencies are around 40% and 33% of familial and sporadic PD cases, respectively (Correia Guedes et al. 2010).

PD is clinically characterized by parkinsonism, with the presence of bradykinesia associated with rest tremor and/or rigidity, and additionally associated with other motor and nonmotor symptoms, such as hyposmia and sleep disorders, and dysautonomic symptoms, such as constipation, postural hypotension, pain, fatigue, psychiatric problems, and impaired cognition (Postuma et al. 2015; Chaudhuri and Odin 2010). Currently, PD diagnosis during life is based on clinical diagnosis criteria (Postuma et al. 2015), with relatively significant limitation in specificity. Definite diagnosis is only possible post-mortem by neuropathological studies, where neurodegeneration of dopaminergic cells of the substantia nigra pars compacta and the accumulation of neuronal cytoplasmatic inclusions known as Lewy bodies (LBs), composed of misfolded forms of α-synuclein (ASYN), are usually present (Poewe et al. 2017).

The identification of new biomarkers of degeneration associated with PD could improve diagnosis certainty in life and contribute to the identification of individuals at risk for developing the disease in early stages of the neurodegenerative process before motor symptoms emerge. It is known that, when typical motor symptoms allowing clinical diagnosis emerge, there is already 30–70% of dopaminergic neuronal loss in the substantia nigra pars compacta (Kordower et al. 2013). This population of individuals in early pre-clinical or prodromal stages of the disease would benefit the most from future, and still unavailable, disease modifying treatments.

MicroRNAs (miRNAs or miRs) are small non-coding RNAs of approximately 18–25 nucleotides that negatively regulate gene expression at post-transcriptional level by targeting the 30 untranslated region of messenger RNAs (mRNAs). It is well known that miRNAs have key roles in different biological processes, such as cell fate determination, embryonic development, cell proliferation, differentiation, and apoptosis (Satterlee et al. 2007). In the past few years, miRNA deregulation has been implicated in several neurodegenerative diseases, such as Alzheimer's disease (Danborg et al. 2014; Van den Hove et al. 2014), amyotrophic lateral sclerosis (Butovsky et al. 2012; Hoye et al. 2017), multiple sclerosis (Junker et al. 2009; Moore et al. 2013), and PD (Martins et al. 2011; Miñones-Moyano et al. 2011; Patil et al. 2019), where it contributes to neurodegeneration and disease progression. In PD, some miRNAs have been associated with neuroinflammation, thereby worsening disease pathogenesis (Leggio et al. 2017; Nuzziello and Liguori 2019). miR-21 and miR-34a have revealed a key role in resolving or prompting inflammatory conditions, respectively, by modulating inflammatory pathways (Nuzziello and Liguori 2019; Bhattacharjee et al. 2014). Moreover, miR-146a and miR-155, two classical inflammatory miRNAs, have been extensively associated with neuronal inflammation in neurodegenerative diseases, including PD (Caggiu et al. 2018). miR-34b and miR-34c are also reported as deregulated in the brain of PD patients, where they may be implicated in key hallmarks of the disease (Miñones-Moyano et al. 2011). Finally, miR-335 might have a role in PD pathogenesis, most likely by targeting LRRK2 (Patil et al. 2019). Mounting evidence has also shown that extracellular circulating miRNAs can be detected in biological fluids such as blood, urine, serum, plasma, and cerebrospinal fluid and have a proven high

chemical stability (Chen et al. 2008; Gallo et al. 2012). For instance, some studies have identified differential expression levels of miR-34a (plasma) (Bhattacharjee, Zhao, and Lukiw 2014), miR-146a and miR-155 (PBMCs) (Chen et al. 2008), and miR-335 (PBMCs and serum) in PD (Martins et al. 2011; Patil et al. 2019). Therefore, miRNAs have emerged as novel candidate non-invasive biomarkers for diagnosis, prognosis, and treatment response for neurodegenerative diseases, particularly in PD (Danborg et al. 2014).

In the present study, we investigated the profile of a selected set of inflammatory miRNAs, miR-21-5p, miR-34a-5p, miR-34b-5p, miR-34c-5p, miR-146a-5p, miR-155-5p, miR-335-3p, and miR-335-5p- in the serum of idiopathic PD (iPD) patients and patients carrying a mutation in the LRRK2 gene (LRRK2-PD), and of age-matched healthy controls, and explored its value as molecular markers of disease pathogenesis.

3.1.3. Materials and methods

3.1.3.1. Study population

We designed 2 case-control studies comparing iPD patients versus control individuals with no known neurological disorder or family history of PD. The first case-control is identified as the “discovery cohort” and the second as the “validation cohort”. Cases were randomly selected from a cohort of 867 iPD patients included at the Movement Disorders biobank of the Instituto de Medicina Molecular, Lisbon. Healthy controls were selected from a randomized cohort of 287 controls of the same biobank and matched age at sample collection and gender with each case. The iPD patients and controls of each cohort did not overlap. An additional group composed by 45 LRRK2-PD patients was also studied and results compared with the groups of iPD patients and healthy controls. Of those, 40 patients carry a mutation in G2019S, while the remaining 5 carry a mutation in R1441H. All participants were recruited at the Movement Disorders outpatient clinic of the Hospital de Santa Maria (Lisbon, Portugal). PD patients and healthy controls were evaluated by neurologists with expertise in Movement Disorders. The Hoehn and Yahr scale was used to evaluate disease stage (Hoehn and Yahr 1967). Informed consent for inclusion was given before participation in the study. The study was conducted in accordance with the

Declaration of Helsinki, and the protocol was approved by the Ethics Committee of Hospital de Santa Maria.

3.1.3.2. Serum isolation

Blood samples were collected in appropriate tubes without anticoagulant. Samples were spun at 2000 g for 10 min at room temperature to isolate the serum, which was then carefully transferred to a new Cryotube to avoid disturbing the buffy coat. Serum samples were gradually frozen and stored at −80 ◦C until miRNA extraction.

3.1.3.3. miRNA extraction

Total miRNA extraction was performed using miRCURY™ RNA Isolation Kit—Biofluids (Exiqon, Vedbaek, Denmark) from 200 µL of serum, according to manufacturer's instructions. A final volume of 50 µL of the eluate was collected. To normalize for the miRNA content, 1 µL (1.6×10^8 copies/µL working solution) of synthetic Caenorhabditis elegans miR-39-3p (cel-miR-39-3p) (Sigma-Aldrich, Saint Louis, MO, USA) was added to each sample.

3.1.3.4. Reverse transcription and quantitative real-time PCR

Total miRNA (5 µL) was used to synthesize cDNA using TaqMan MicroRNA Reverse Transcription Kit (Thermo Fisher Scientific, Rockford, IL, USA). Then, serum miRNA expression levels were quantified using TaqMan Universal Master Mix II no UNG (Thermo Fisher Scientific) and the 7500 Sequence Detection System (Applied Biosystems, Foster City, CA, USA) according to the manufacturer's instructions. All reactions were performed in duplicates. Relative expression levels of each subject were calculated using the comparative ΔΔCt method with cel-miR-39-3p (Thermo Fisher Scientific, Rockford, IL, USA) as the normalization control. miRNA expression levels of each patient were then normalized to the mean value of controls. The miRNAs investigated in this study were: hsa-miR-21-5p, hsa-miR-34a-5p, hsa-miR-34b-5p, hsa-miR-34c-5p, hsa-miR-146a-5p, mmu-miR-155-5p, hsa-miR-335-3p, and hsa-miR-335-5p (Thermo Fisher Scientific).

3.1.3.5. Data analysis

Data were described using descriptive statistics. Continuous variables are presented as mean ± standard error of the mean (SEM), and categorical variables as absolute and relative frequencies. Statistical tests were used to compare values between study groups (non-parametric when the assumption of normality was not achieved), namely t-test and ANOVA with Bonferroni test for post hoc comparisons. ROC curves were estimated to each miRNA to identify sensitivity (true positive rate) and specificity (true negative rate) against the study groups. Area under the ROC curve (AUC) was estimated to measure how well the miRNA can distinguish between the study groups. Correlation analysis was performed between miRNA values and clinical outcome measures (Spearman's rank correlation when normality assumption was not observed). Correlation analysis between different miRNAs was assessed by Spearman's rank correlation coefficient. All analysis was achieved for a 0.05 significance level. Statistical analysis was performed using RStudio.

3.1.4. Results

3.1.4.1. Patient population

The first case-control study (discovery cohort) included 20 iPD patients and 20 age- and gender-matched healthy individuals; the second case-control study (validation cohort) included 20 iPD and 20 healthy controls. The additional LRRK2-PD cohort included 45 patients. The main demographic and clinical characteristics of controls, iPD patients and LRRK2-PD patients included in this study are summarized in Table 3.1.1. Patients covered the full spectrum of early to advanced PD, characterized by Hoehn & Yahr stage (1–5). All patients were taking antiparkinsonic medication at the time of sample collection. Age and gender balance were guaranteed between the three groups.

3.1.4.2. Serum levels of miR-146a, miR-335-3p and miR-335-5p are reduced in idiopathic PD patients

An initial panel of miRNAs was selected from the literature, suggested as potential molecular markers for PD or other neurodegenerative diseases in general. Further, by submitting our miRNA panel to the target prediction program

TargetScan version 7.2 and to the microTCDS software from the DIANA online platform (Paraskevopoulou et al. 2013), we filtered those miRNAs with predicted targets linked to cell death and/or inflammatory pathways, including miR-21, miR-34a, miR-34b, miR-34c, miR-146a, miR-155, miR-335-3p, and miR-335-5p.

miR-34b showed undetectable levels in all serum samples, being excluded from further analysis. Moreover, miR-21, miR-34a, miR-34c, and miR-155 expression levels did not change between iPD patients and healthy controls (Figure 3.11). Importantly, miR-146a, miR-335-3p, and miR-335-5p were significantly decreased in iPD patients versus controls ($p < 0.05$).

To further determine the accuracy of miRNAs that statistically differed between iPD and healthy controls, ROC curves were generated, and the AUC values derived. As observed in Figure 2, miR-146a, miR-335-3p, and miR-335-5p showed good sensitivity and specificity to differentiate between iPD and healthy controls (AUC = 0.74, AUC = 0.74, and AUC = 0.71, respectively) (Figure 3.1.2).

Table 3.1.1. Clinical characteristics of patients and controls in each cohort. Data are presented as mean ± standard deviation. iPD, idiopathic Parkinson's disease; LRRK2-PD, *LRRK2* mutation Parkinson's disease.

	Discovery Cohort		Validation Cohort		
Patients Characteristics	Controls (*n* = 20)	iPD (*n* = 20)	Controls (*n* = 20)	iPD (*n* = 20)	LRRK2-PD (*n* = 45)
Age (years)	69.5 ± 8.08	71.6 ± 9.17	65.3 ± 8.3	69.2 ± 11.3	70.0 ± 9.0
Gender (F/M)	10/10	10/10	10/10	10/10	31/14
Age at symptom onset (years)	-	59.7 ± 11.4	-	56.7 ± 13.9	56.4 ± 11.9
Disease duration (years)	-	11.9 ± 8.9	-	12.6 ± 9.4	13.6 ± 7.8
Hoehn & Yahr	-	2.3 ± 0.6	-	2.6 ± 1.1	2.7 ± 1.0
Family history of PD (%)	-	10	-	25	63.4

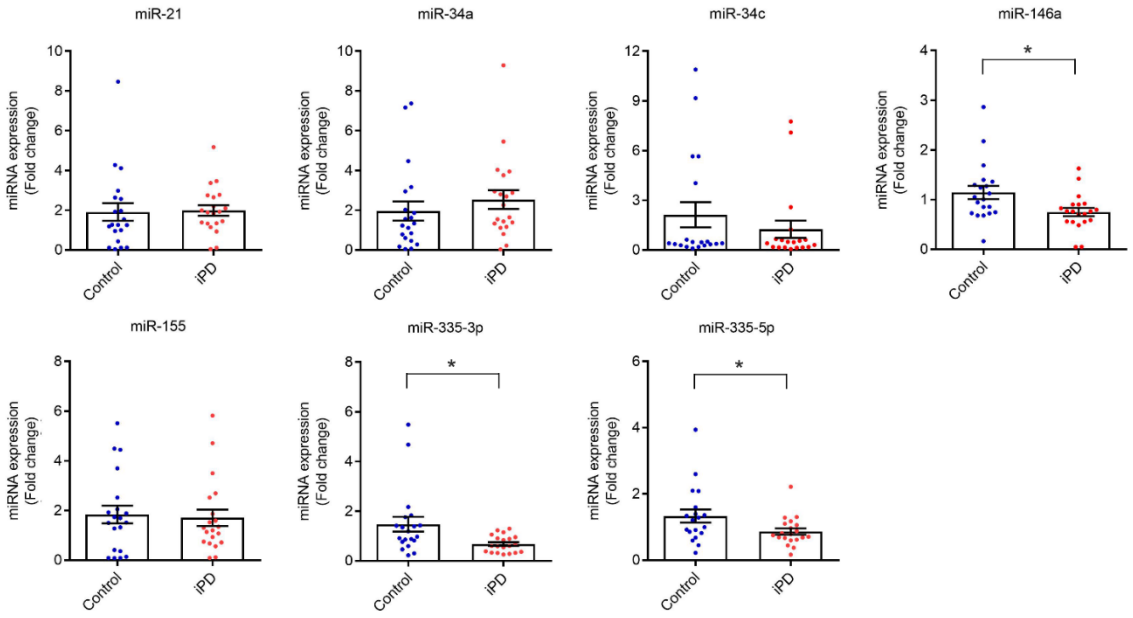

Figure 3.1.1. Relative expression values of miRNA in the serum of iPD patients and controls in the discovery cohort. Data are presented as the mean ± SEM. Cel-miR-39-3p was used as spike-in external control. Values were normalized relative to the mean of control healthy individuals. Differences were analysed by Student's *t*-test. *$p < 0.05$ vs. control.

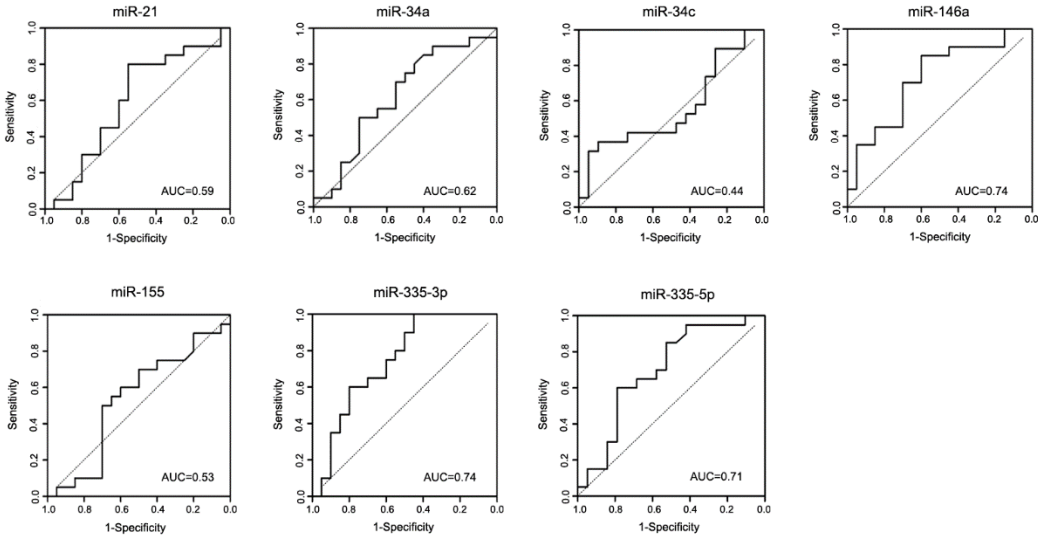

Figure 3.1.2. Receiver operating characteristic (ROC) curves of miRNAs in the discovery cohort, discriminating between iPD patients and controls. The true positive rate (sensitivity %) is plotted as a function of the false positive rate (100% - specificity) for the seven miRNAs individually. Area under the curve (AUC) values are indicated in each plot.

3.1.4.3. Validation of the discovery data in an independent cohort

To validate the findings of the discovery cohort, we determined the expression levels of the same miRNAs using an independent cohort, composed by 20 control subjects and 20 iPD patients. Six controls and three iPD patients were excluded from further analysis due to sample haemolysis. Consistent with data from the discovery cohort, miR-21, miR-34a, miR-34c, and miR-155 showed no significant differences between iPD patients and healthy controls. Importantly, miR-146a ($p < 0.01$), miR-335-3p ($p < 0.05$), and miR-335-5p ($p < 0.01$) were significantly reduced in the serum of iPD patients as compared with controls (Figure 3.1.3). Moreover, ROC curves showed that miR-146a, miR-335-3p, and miR-335-5p have moderate ability to discriminate between iPD patients and controls in this cohort (AUC = 0.62, AUC = 0.67, and AUC = 0.59, respectively), while miR-155 has great sensitivity and specificity to discriminate between the two groups, with an AUC = 0.85 (Figure 3.1.4).

Combining both discovery and validation cohorts, miR-146a, miR-335-3p, and miR-335-5p demonstrate moderate ability to discriminate between iPD patients and healthy controls (AUC = 0.68, AUC = 0.70, and AUC = 0.66, respectively) (Figure 3.1.5A). Additionally, binary logistic regression analysis was used to investigate if a combination of different miRNAs could improve their diagnostic accuracy. We created a model in which miRNAs found differentially expressed between iPD patients and controls (miR-146a, miR-335-3p, and miR-335-5p) were combined. We observed a slight increase in AUC value (AUC = 0.72) (Figure 3.1.5B).

3.1.4.4. miR-146a, miR-155, and miR-335 are differentially expressed in the serum of LRRK2-PD patients

Then, a different group composed by 45 patients carrying a mutation in the LRRK2 gene (LRRK2-PD) was also analysed, from which four samples were excluded due to sample haemolysis. No significant differences were found in the expression of miR-21, miR-34a, and miR-34c between LRRK2-PD patients and controls or between LRRK2-PD and iPD patients (Figure 3.1.6). Importantly, miR-146a and miR-335-5p were significantly decreased in LRRK2-PD patients in

comparison with healthy controls ($p < 0.01$), while no differences were observed between LRRK2-PD and iPD patients. miR-335-3p was also decreased in LRRK2-PD patients versus controls, although not significantly. Interestingly, miR-155 was significantly increased in LRRK2-PD patients as compared with iPD patients ($p < 0.01$) (Figure 3.1.6). ROC curves were also created to determine the discriminatory capacity of miRNAs between iPD and LRRK2-PD patients and miR-155 showed great ability to discriminate between the two groups, with AUC = 0.80 (Figure 3.1.7). Moreover, miR-146a and miR-335-5p showed AUC values of 0.69 and 0.66, respectively (Supplementary Materials, Figure S3.1.1a), while combining these two miRNAs did not alter this value (AUC = 0.68) (Figure S3.1.1b).

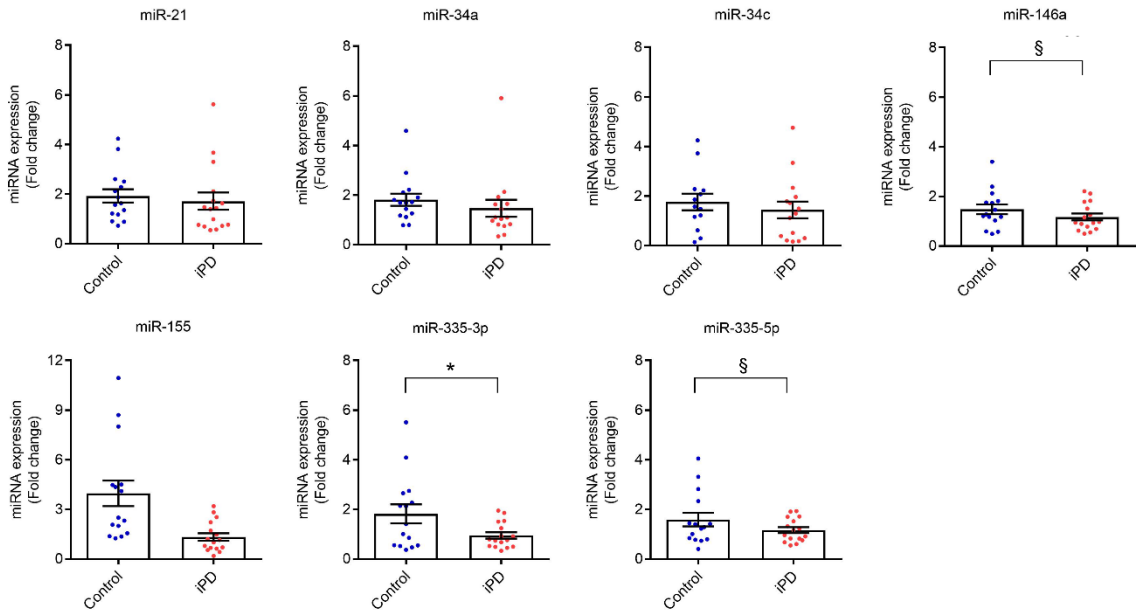

Figure 3.1.3. Relative expression values of miRNA in the serum of iPD patients and controls in the validation cohort. Data are presented as the mean ± SEM. Cel-miR-39-3p was used as spike-in external control. Values were normalized relative to the mean of control healthy individuals. Differences were analyzed by Student's *t*-test. *$p < 0.05$ versus control; § $p < 0.01$ versus control.

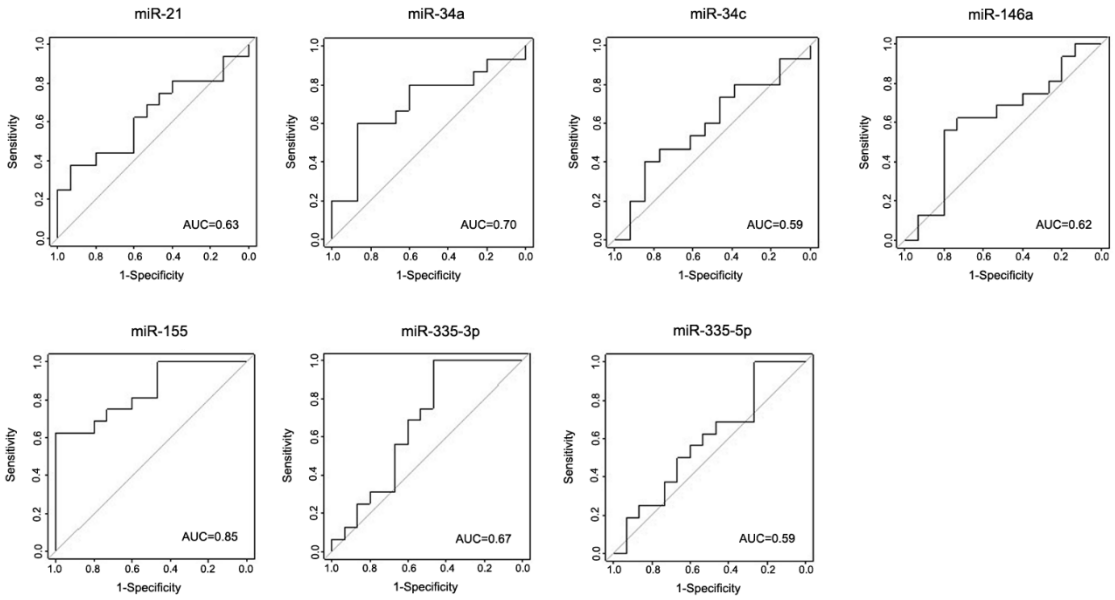

Figure 3.1.4. Receiver operating characteristic (ROC) curves of miRNAs in the validation cohort, discriminating between controls and iPD patients. The true positive rate (sensitivity %) is plotted as a function of the false positive rate (100% - specificity) for the seven miRNAs individually. Area under the curve (AUC) values are indicated in each plot.

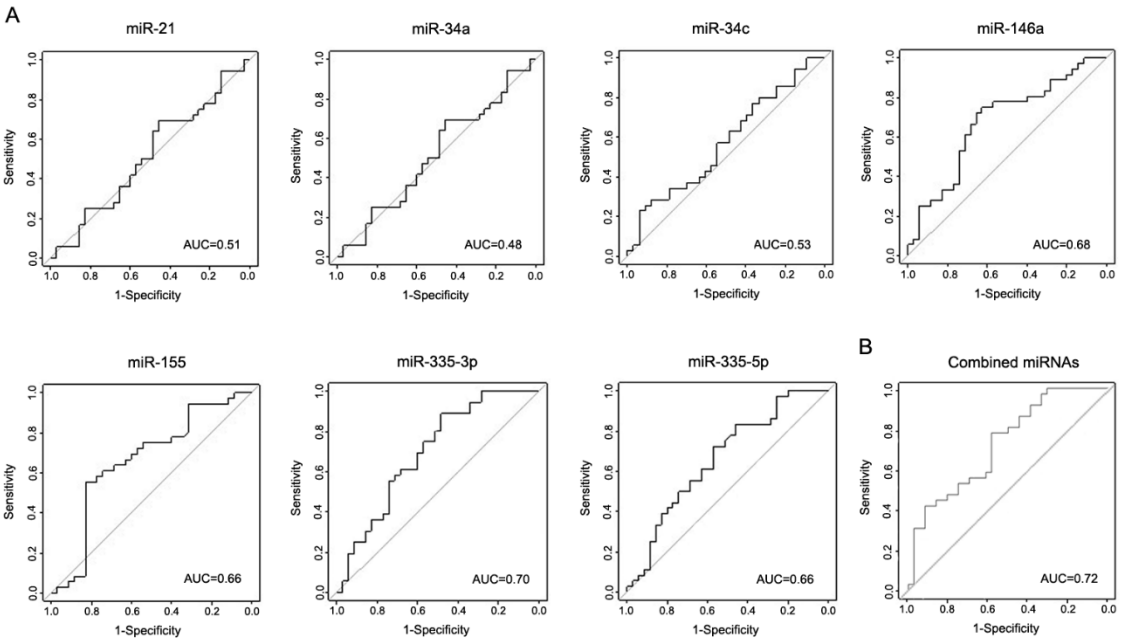

Figure 3.1.5. (A) ROC curves of combined miRNAs in discovery and validation cohorts, discriminating between controls and iPD patients. (B) ROC curves of models created from binary logistic regression to improve discrimination between the two groups. AUC values are indicated in each plot.

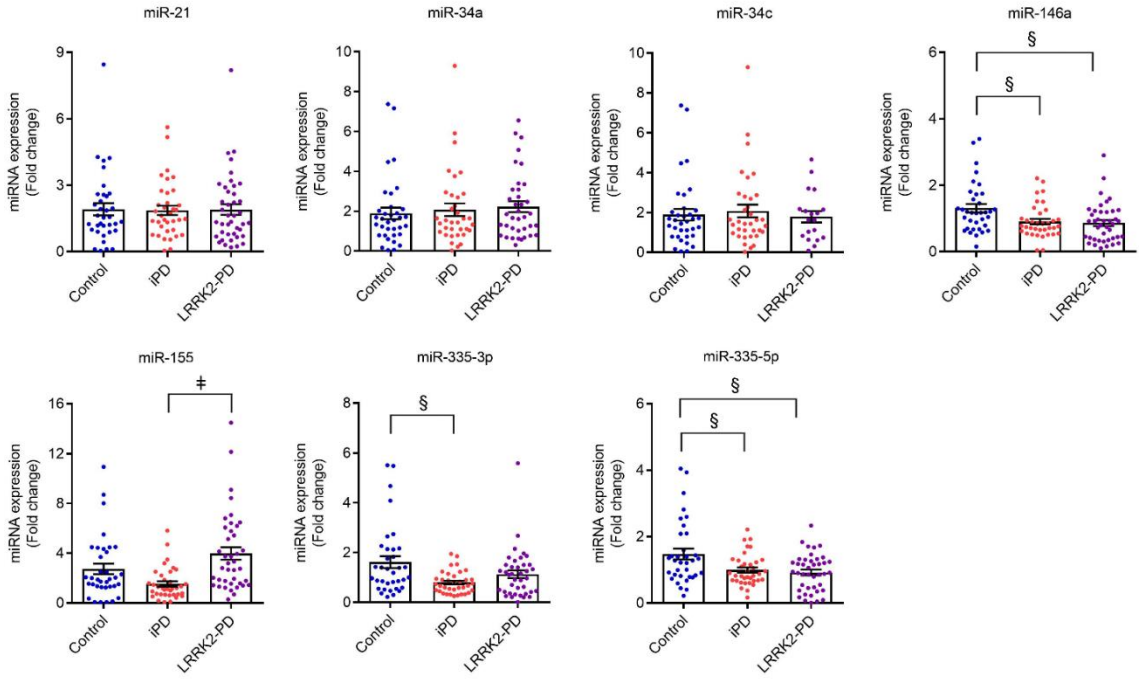

Figure 3.1.6. Relative expression levels of miRNA in the serum of iPD patients, LRRK2-PD patients and controls in the discovery and validation cohorts. Data are presented as the mean ± SEM. Cel-miR-39-3p was used as spike-in external control. Values were normalized to the mean of control healthy individuals. Differences were analyzed by ANOVA with Bonferroni test for post hoc comparisons. $p < 0.01$ versus control; ‡$p < 0.01$ versus iPD.

3.1.4.5. Correlation analysis

As expected, according to the study design, no significant differences were found for age at inclusion or gender between all groups in the discovery cohort (50% male, p = 1.000; age control: 69.5 ± 8.08; and age iPD: 71.6 ± 9.17, p = 0.4469) or in the validation cohort (46.6% male, p = 0.499; age control: 65.3 ± 8.3; age iPD: 69.2 ± 11.3; and age LRRK2-PD 70.0 ± 9.0, p = 0.271). Correlations between miRNA expression and clinical parameters (age, age at symptom onset, disease duration, Hoehn & Yahr stage, dyskinesias, motor fluctuation, and tremor predominant at onset) were determined for both cohorts. However, no significant correlations were observed after controlling for age and sex (Tables S3.1.1 and S3.1.2). Moreover, to determine if there was a correlation between the expression levels of the different miRNAs, a correlation analysis was also performed. Overall,

in the discovery cohort, we observed ten significant positive correlations between miRNAs, of which the most prominent were between miR-21 and miR-34a ($r = 0.81$, $p < 0.001$) and between miR-146a and miR-335-3p ($r = 0.80$, $p < 0.001$) (Figure 3.1.8). In accordance, in the validation cohort, the same prominent correlations were observed (Figure S3.1.2), while, in the combination of discovery and validation cohorts, six positive correlations were observed, being the most prominent also between miR-21 and miR-34a ($r = 0.80$, $p < 0.001$) and between miR-146a and miR-335-3p ($r = 0.64$, $p < 0.001$) (Figure S3.1.3).

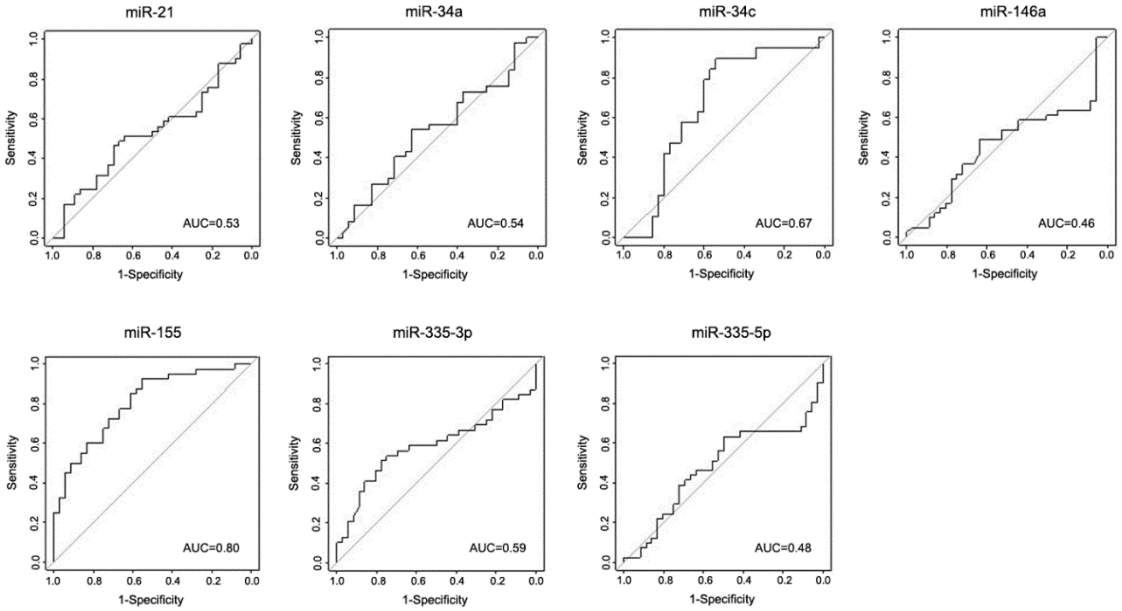

Figure 3.1.7. Receiver operating characteristic (ROC) curves of miRNAs in discovery and validation cohorts, discriminating between iPD and LRRK2-PD patients. The true positive rate (sensitivity %) is plotted as a function of the false positive rate (100% - specificity) for the seven miRNAs individually. Area under the curve (AUC) values are indicated in each plot.

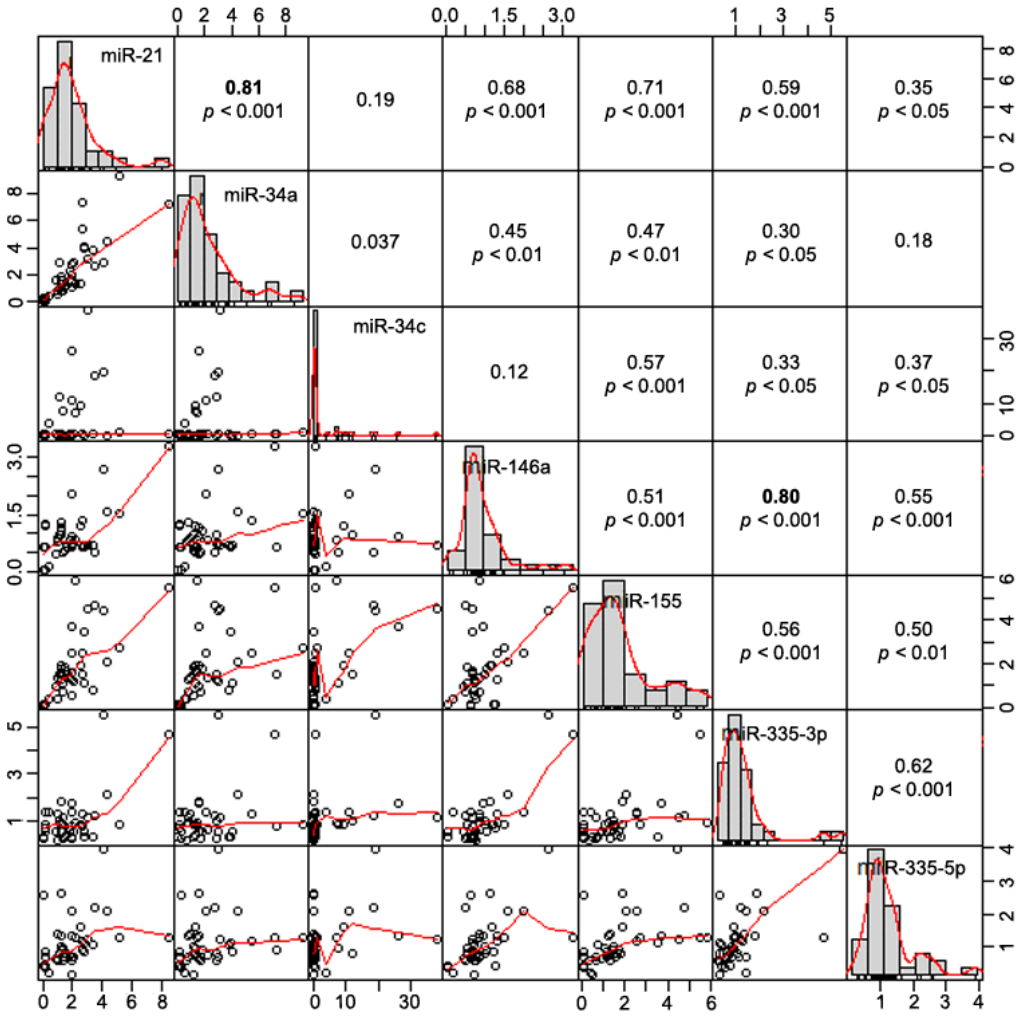

Figure 3.1.8. Correlation analysis between each two different miRNAs among iPD patients and healthy control groups in the discovery cohort. Statistically significant correlation ($p < 0.05$) and Spearman's rank correlation coefficient values are indicated in the graphs.

3.1.5. Discussion

Our study aimed at identifying a panel of miRNAs whose expression is either altered or remain unaffected between PD-diagnosed patients and control subjects, which may become a relevant diagnosis tool to differentiate PD patients as well as contribute to further comprehend PD pathophysiology. A panel of miRNAs (miR-21, miR-34a, miR-34b, miR-34c, miR-146a, miR-155, miR-335-3p, and miR-335-5p) was selected from the literature, previously described to be involved in inflammatory and/or cell death pathways and deregulated in PD or

other neurodegenerative diseases. We identified a differential pattern of miRNA expression between PD patients, including iPD and LRRK2-PD patients, and age- and gender-matched healthy controls, with a downregulation of miR-146a, miR-335-3p, and miR-335-5p in PD patients versus controls and no significant variation in the other miRNAs under investigation.

miR-146a is commonly described as downregulated in neurodegenerative diseases, including Alzheimer's disease and PD. miR-146a negatively regulates inflammation, immunity, and cell survival by targeting interleukin-1 receptor-associated kinase 1 (IRAK1) and TNF receptor associated factor 6 (TRAF6), attenuating proinflammatory responses (Taganov et al. 2006; Li et al. 2011). Our results are in line with these studies, as we observed significantly reduced levels of miR-146a in PD patients versus controls, including iPD and LRRK2-PD patients, which may suggest an overall inflammatory condition in these patients. Furthermore, circulating levels of miR-335 are associated with PD susceptibility (Yılmaz S et al. 2016) and were found decreased in whole blood and PBMCs of PD patients (Yılmaz S et al. 2016; Martins et al. 2011). However, a recent study showed an upregulation of miR-335-5p in serum of PD patients (Patil et al. 2019). These differences may be attributed to different clinical samples used for miRNA extraction and analysis. Importantly, miR-335 was predicted to target LRRK2 gene *in silico* and further confirmed *in vitro* (Patil et al. 2019). Here, miR-335-3p and miR-335-5p were significantly reduced in iPD patients and miR-335-5p was also significantly decreased in LRRK2-PD patients in comparison with aged-matched healthy controls. Therefore, it is plausible that miR-335 decreased levels may contribute to PD pathogenesis due to an increase in LRRK2 protein content. In fact, LRRK2 was already described to have a key role in PD pathogenesis in both iPD and LRRK2-PD patients (Li et al. 2014; Di Maio et al. 2018). miR-155 is a proinflammatory miRNA that can recruit macrophages and bind to suppressor of cytokine signalling 1 (SOCS1) and SOCS3 mRNAs, thereby increasing proinflammatory cytokine secretion (Wang et al. 2010; Cardoso et al. 2012). Importantly, in microglia cells, miR-155 is upregulated in the presence of a proinflammatory stimuli, thereby suggesting that, despite its contribution to harmful conditions, its regulation may have a role in protective immunity (Cardoso et al. 2012). Of note, numerous studies indicate miR-155 as upregulated in inflammatory conditions, including amyotrophic lateral sclerosis and PD (Caggiu

et al. 2018; Koval et al. 2013). Here, we did not find significant differences between PD patients and controls; however, we observed an upregulation of miR-155 in LRRK2-PD patients when compared with iPD patients. Although iPD and LRRK2 G2019S-PD patients are described as clinically and pathologically similar (Healy et al. 2008), some studies showed that LRRK2-PD patients may differ from iPD patients regarding growth factor concentrations and interleukin 8 (IL-8) levels in CSF (Dzamko et al. 2016). Of note, mounting evidence suggests a role for LRRK2 in modulating inflammatory processes in immune cells of the brain, particularly in microglia (Dzamko et al. 2015; Moehle et al. 2012). Therefore, it is plausible that increased LRRK2 activation in LRRK2-PD patients could lead to an overall inflammatory response that, in turn, increases miR-155 expression levels, which has also a role on inflammation.

Finally, although some studies have already shown that miR-21 (Junker et al. 2009), miR-34a (Bhattacharjee et al. 2014), and miR-34b/c (Miñones-Moyano et al. 2011) are deregulated in some neurodegenerative diseases, here, we did not observe any significant differences between groups. However, there are several factors that can account for the variability across different miRNA studies, such as methodological heterogeneity, conditions of sample collection and storage, differences in miRNA normalization strategies, purification protocols, and different body fluids. Moreover, we cannot discard an effect of antiparkinsonian medication in the peripheral miRNA expression, which may further increase the variability among untreated/treated PD patients and healthy controls (Alieva et al. 2015). Interestingly, a statistically significant positive correlation between miR-146a and miR-335-3p was observed while, despite the absence of significant differences, miR-21 and miR-34a also positively correlate with each other. In fact, miR-146a and miR-335-3p appear to have similar anti-inflammatory properties (Patil et al. 2019; Li et al. 2011), while miR-21 and miR-34a are commonly associated with impaired cell death pathways (Alvarez-Erviti et al. 2013; Cosín-Tomás et al. 2017).

3.1.6. Conclusions

miRNAs are evolving as important molecular tools for discovery and development of novel innovative diagnosis and therapeutic strategies. Here, we clearly demonstrate a pattern of miRNA expression that differs between PD patients and age-matched healthy controls, in which miR-146a, miR-335-3p, and miR-335-5p are significantly downregulated in PD patients as compared with controls, while miR-21, miR-34a, miR-34c, and miR-155 expression levels are not affected. Moreover, we evidently showed that LRRK2-PD and iPD patients can be distinguished by an upregulation of miR-155 in the first group, and no alterations in the other miRNAs in study. Overall, this work suggests that these miRNAs may regulate important cellular mechanisms implicated in PD pathogenesis, such as inflammation. However, additional confirmation is necessary in larger cohorts, and functional relevance of the newly identified miRNAs in the context of disease needs to be further clarified. Finally, deciphering unsuspected roles of target modulation by miRNAs may also pave the way to a deeper understanding of PD pathogenesis.

3.1.7. Supplementary figures

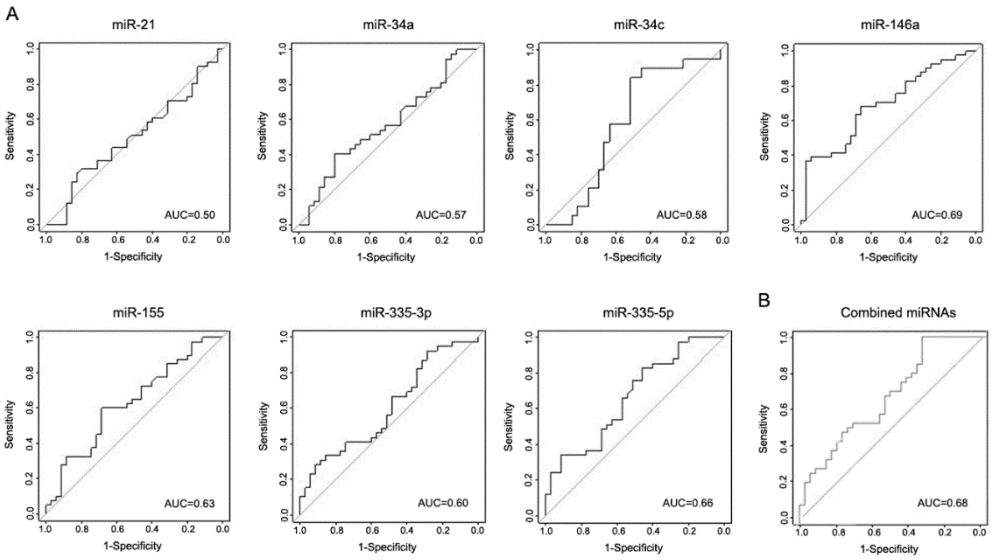

Figure S3.1.1. (A) ROC curves of miRNAs in discovery and validation cohorts, discriminating between LRRK2-PD patients and controls. (B) ROC curves of models created from binary logistic regression to improve discrimination between the two groups. AUC values are indicated in each plot.

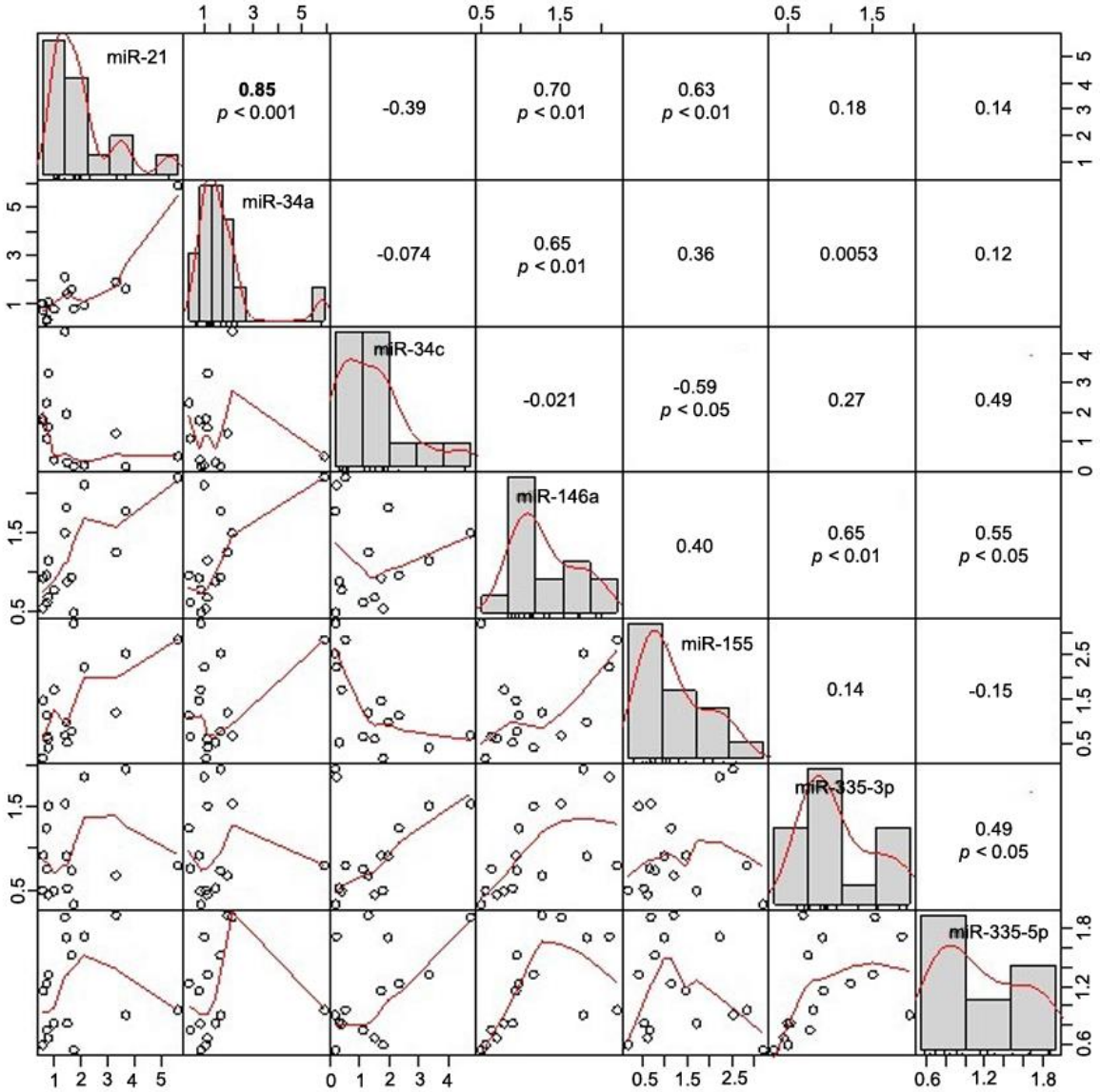

Figure S3.1.2. Correlation analysis of all miRNAs among iPD patients and healthy control groups in the validation cohort. Statistically significant correlation ($p < 0.05$) and Spearman's rank correlation coefficient values are indicated in the graphs.

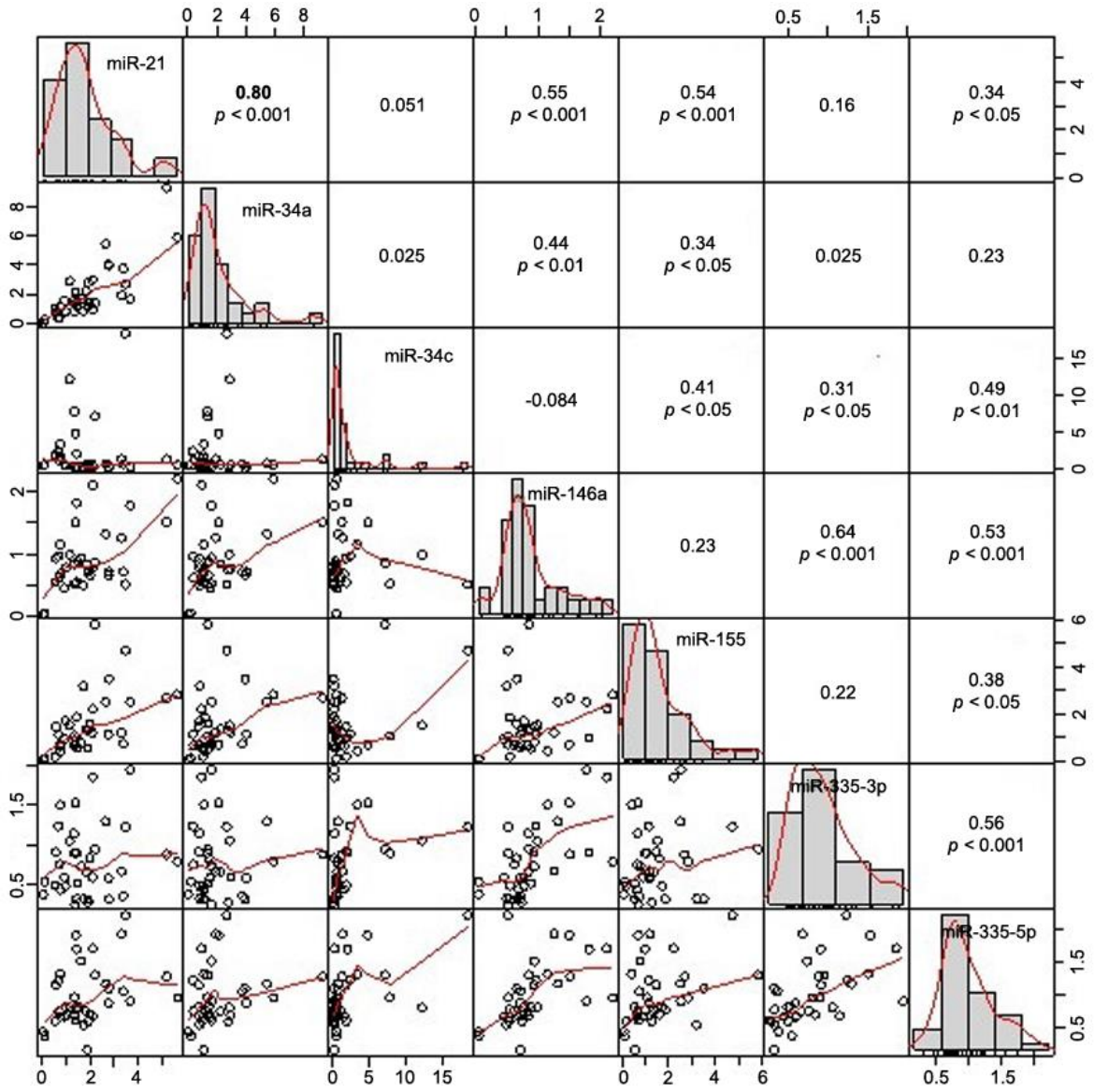

Figure S3.1.3. Correlation analysis of all miRNAs among iPD patients and healthy control groups in discovery and validation cohorts. Statistically significant correlation ($p < 0.05$) and Spearman's rank correlation coefficient values are indicated in the graphs.

Table S3.1.1. Correlation analysis between miRNA expression and clinical parameters in discovery and validation cohorts of iPD patients. Correlation coefficient is indicated in the table.

	iPD patients					
	Tremor at onset	No tremor at onset	History of dyskinesia	No history of dyskinesia	History of motor fluctuation	No history of motor fluctuation
miR-21	1.85	2.16	1.80	2.20	1.96	2.14
miR-34a	2.05	3.13	2.60	2.60	2.89	2.11
miR-34c	4.36	0.42	2.00	2.50	1.39	3.90
miR-146a	0.62	0.80	0.80	0.60	0.760	0.620
miR-155	1.910	1.450	1.70	1.70	1.550	2.060
miR-335-3p	0.640	0.720	0.900	0.600	0.710	0.590
miR-335-5p	0.800	0.920	0.800	0.900	0.820	0.920

Table S3.1.2. Correlation analysis between miRNA expression and clinical parameters of iPD and LRRK2-PD patients in discovery and validation cohorts. Correlation coefficient is indicated in the table.

	iPD patients				LRRK2-PD patients			
	Age	Age at symptom onset	Disease duration	H&Y	Age	Age at symptom onset	Disease duration	H&Y
miR-21	0.178	0.004	0.194	0.237	-0.030	-0.142	0.181	0.114
miR-34a	0.111	-0.065	0.215	0.278	-0.204	-0.344	0.321	-0.035
miR-34c	0.110	0.181	-0.128	-0.120	-0.008	-0.066	0.086	0.073
miR-146a	-0.057	-0.173	0.176	0.211	-0.416	-0.417	0.153	0.147
miR-155	0.234	0.078	0.155	0.025	-0.083	-0.090	0.041	0.106
miR-335-3p	-0.054	-0.105	0.085	0.022	-0.265	-0.131	-0.097	-0.267
miR-335-5p	-0.081	-0.220	0.214	0.006	-0.255	-0.243	0.075	-0.086

H&Y, Hohen and Yahr.

Reprinted, with minor modifications, from Oliveira SR *et al.* 2021. miR-335 targets LRRK2 and mitigates inflammation in Parkinson's disease. Front Cell Dev Biol. 9:661461.
doi: 10.3389/fcell.2021.661461

miR-335 targets LRRK2 and mitigates inflammation in Parkinson's disease

Sara R. Oliveira[1], Pedro A. Dionísio[1], Maria M Gaspar[1], Leonor Correia Guedes[2,3], Miguel Coelho[2,3], Mário M Rosa[2,3,4], Joaquim J Ferreira[2,4], Joana D. Amaral[1], and Cecília M. P. Rodrigues[1]

[1]Research Institute for Medicines (iMed.ULisboa), Faculdade de Farmácia, Universidade de Lisboa, Portugal

[2]Instituto de Medicina Molecular João Lobo Antunes, Faculdade de Medicina, Universidade de Lisboa, Lisbon, Portugal

[3]Department of Neuroscience and Mental Health, Neurology, Hospital de Santa Maria, Centro Hospitalar Universitário Lisboa Norte, Lisbon, Portugal

[4]Laboratory of Clinical Pharmacology and Therapeutics, Faculdade de Medicina, Universidade de Lisboa, Lisbon, Portugal

3.2.1. Abstract

Parkinson's disease (PD) is mainly driven by dopaminergic neuronal degeneration in the substantia nigra pars compacta accompanied by chronic neuroinflammation. Despite being mainly sporadic, approximately 10% of all cases are defined as heritable forms of PD, with mutations in the leucine-rich repeat kinase (LRRK2) gene being the most frequent known cause of familial PD. MicroRNAs (miRNAs or miRs), including miR-335, are frequently deregulated in neurodegenerative diseases, such as PD. Here, we aimed to dissect the protective role of miR-335 during inflammation and/or neurodegenerative events in experimental models of PD. Our results showed that miR-335 is significantly downregulated in different PD-mimicking conditions, including BV2 microglia cells stimulated with lipopolysaccharide (LPS) and/or overexpressing wild-type LRRK2. Importantly, these results were confirmed in serum of mice injected with 1-methyl-1-4-phenyl-1,2,3,6-tetrahydripyridine hydrochloride (MPTP), and further validated in patients with idiopathic PD (iPD) and those harboring mutations in LRRK2 (LRRK2-PD), thus corroborating potential clinical relevance.

Mechanistically, miR-335 directly targeted LRRK2 mRNA. In the BV2 and N9 microglia cell lines, miR-335 strongly counteracted LPS-induced proinflammatory gene expression, and downregulated receptor interacting protein 1 (RIP1) and RIP3, two important players of necroptotic and inflammatory signaling pathways. Further, miR-335 inhibited LPS-mediated ERK1/2 activation. LRRK2-Wt-induced proinflammatory gene expression was also significantly reduced by miR-335 overexpression. Finally, in SH-SY5Y neuroblastoma cells, miR-335 decreased the expression of pro-inflammatory genes triggered by α-synuclein. In conclusion, we revealed novel roles for miR-335 in both microglia and neuronal cells that strongly halt the effects of classical inflammatory stimuli or LRRK2-Wt overexpression, thus attenuating chronic neuroinflammation.

3.2.2. Introduction

Parkinson's disease (PD) is the second most common neurodegenerative disorder worldwide, mainly instigated by dopaminergic neurodegeneration in the substantia nigra pars compacta (Poewe et al. 2017). The etiology of PD is complex and involves chronic neuroinflammation, mitochondrial dysfunction and oxidative stress (Poewe et al. 2017). Even though mostly sporadic, about 10% of all cases are currently estimated to be related to monogenic forms of PD (Poewe et al. 2017; Henn et al. 2005). Pathogenic mutations in the leucine-rich repeat kinase 2 (LRRK2) gene are the most frequent known cause of monogenic PD and are usually associated with a toxic gain-of-function of LRRK2 kinase activity (Zimprich et al. 2004; Healy et al. 2008). Importantly, the most frequent LRRK2 mutation, G2019S, can be relatively common depending on the ethnic group, with frequencies of 35.7% in sporadic and 42% in familial cases, in specific populations (Healy et al. 2008; Mata et al. 2006).

Although the role of LRRK2 is still not completely understood, LRRK2 pathogenic mutations are associated with dopaminergic neuronal cell death, inflammatory responses, and oxidative damage (Mata et al. 2006; Tsika and Moore 2012). For instance, LRRK2 seems to be involved in the regulation of survival/inflammatory signaling pathways, such as mitogen activated protein kinase (MAPK) pathways, whose activation may eventually lead to neuronal death (Chen et al. 2012). Interestingly, it has also been suggested that, in specific

conditions, wild-type (wt) LRRK2 overexpression may protect SH-SY5Y cells from death, by selectively activating ERK1/2 signaling (Liou et al. 2008). Moreover, an exacerbation of LRRK2 levels in different immune cells, such as microglia or macrophages, has been reported in response to inflammatory stimuli, such as lipopolysaccharide (LPS) or interferon-γ (IFN-γ), thereby perpetuating inflammation (Gardet et al. 2010; Gillardon et al. 2012). The discoveries that both pharmacological and genetic inhibition of LRRK2 can be neuroprotective in preclinical models of PD (West 2017; Chen et al. 2018; Chan and Tan 2017; Zhao et al. 2017) have placed LRRK2 at the center of disease modifying PD strategies. In addition, recent findings also suggest that LRRK2 plays a role in the pathogenesis of PD, indicating that LRRK2-targeted therapies might, therefore, be beneficial in both subtypes of PD (Tolosa et al. 2020).

Throughout the years, several experimental models have been developed to mimic PD, including the systemic administration of animals with 6-hydroxydopamine (6-OHDA) and 1-methyl-1-4- phenyl-1,2,3,6-tetrahydripyridine hydrochloride (MPTP) (Dauer 2003). However, the neurotoxin MPTP has been the most widely used to mimic PD-associated nigrostriatal degeneration, since it can be systemically administered and human exposure to MPTP induces severe parkinsonism (Meredith and Rademacher 2011; Langston 2017).

MicroRNA (miRNA or miR) dysregulation can also contribute to the development and progression of a wide variety of human diseases, including PD, where miRNAs have been associated with neuroinflammation (Martins et al. 2011; Miñones-Moyano et al. 2011; Patil et al. 2019). In this regard, miR-335 has recently been involved in PD. The results are somehow contradictory with some authors suggesting that miR-335 is downregulated in peripheral blood mononuclear cells (PBMCs) and sera of PD patients, while others have found increased levels of miR-335 in PD serum samples (Yılmaz S et al. 2016; Patil et al. 2019; Oliveira et al. 2020). Importantly, some authors also demonstrated that miR-335 upregulation reduces inflammation and reactive oxygen species (ROS) in a sepsis mouse model (Gao et al. 2018). In accordance, miR-335 downregulation appears to affect mitochondrial dynamics, autophagy and apoptosis in SH-SY5Y neuronal cells (De Luna et al. 2020). Interestingly, *in silico* and *in vitro* studies point LRRK2 mRNA as a target of this miRNA (Martins et al. 2011; Yılmaz S et al. 2016; Patil et al. 2019; Oliveira et al. 2020).

Thus, our main hypothesis is that miR-335 regulates key inflammatory events by targeting LRRK2. In the present study, we demonstrated that miR-335 is reduced in experimental models of PD and in serum of idiopathic PD (iPD) and LRRK2- associated PD (LRRK2-PD) patients vs. healthy individuals, corroborating its clinical relevance during PD progression. In addition, miR-335 overexpression protected microglial cells from LPS-induced inflammation, by reducing RIP1 and RIP3 protein levels, proinflammatory cytokine expression and ERK1/2 activation. On a functional level, miR-335 directly targeted LRRK2 and reduced wild-type LRRK2-driven inflammation. The combination of novel miRNA strategies with LRRK2 inhibition may translate into promising and innovative therapeutic approaches to tackle PD.

3.2.3. Materials and methods

3.2.3.1. Cell culture and reagents

The BV2 and N9 murine microglial cell lines, kindly provided by Elsa Rodrigues (University of Lisbon), were cultured in RPMI 1640 medium (GIBCO Life Technologies, Inc. Grand Island, United States), supplemented with 10% heat inactivated fetal bovine serum (FBS), 1% antibiotic/antimycotic solution and 1% GlutaMAX™ (GIBCO). The SH-SY5Y human inducible WT α-synuclein (α-syn) cell line was cultured in RPMI 1640 medium, supplemented with 10% FBS, 1% penicillin (100 U/mL) (GIBCO), 100 mg/mL streptomycin (GIBCO), 250 µg/mL G418 (Thermo Fisher Scientific, Rockford, IL, United States) and 50 µg/mL hygromycin B (Thermo Fisher). α-synuclein expression was switched off by adding doxycycline (2 µg/mL) (Vekrellis K, 2009). Cells were maintained at 37◦C in a humidified atmosphere of 5% CO2. LPS was from Escherichia coli 055:B5 (#437625; Calbiochem, San Diego, CA, United States).

3.2.3.2. MPTP animal model

Animal experiments were performed according to the animal welfare organ of the Faculty of Pharmacy, University of Lisbon, approved by the competent national authority Direção-Geral de Alimentação e Veterinária (DAGV) and in accordance with the EU Directive (2010/63/UE), Portuguese laws (DR 113/2013, 2880/2015, and 260/2016) and all relevant legislation. We performed a sub-acute

MPTP mouse model in 13-week-old male C57BL/6N wild-type (Wt) obtained from the Charles River Laboratories (Wilmington, MA, United States). Mice were intraperitoneally (i.p.) injected with a single dose of MPTP HCl (40 mg/kg; Sigma-Aldrich, St. Louis, MO, United States), dissolved in sterile 0.9% saline, or vehicle only (control group); seven animals per group were used (Dionísio et al. 2019; Saporito, Thomas, and Scott 2000). After 30 days, mice were sacrificed in a CO2 chamber followed by transcardiac perfusion with ice-cold phosphate buffered saline (PBS). Serum was collected and stored at −80˚C.

3.2.3.3. miRNA expression in human serum

We analyzed serum samples from 40 iPD, 45 LRRK2-PD patients and 40 control individuals with no known neurological disorder or family history of PD. Cases were selected from a randomized cohort of 867 iPD patients included at the Movement Disorders biobank (Instituto de Medicina Molecular, Lisbon, Portugal). Healthy controls were selected from a randomized cohort of 287 individuals of the same biobank. The LRRK2-PD group included 40 patients that carried the G2019S mutation and 5 patients that carried the R1441H mutation. All participants were recruited at the Movement Disorders outpatient clinic of the Hospital de Santa Maria (Lisbon, Portugal). Consent for inclusion in the study was obtained before participation and the study was performed in accordance with the Declaration of Helsinki and the protocol approved by the Ethics Committee of Hospital de Santa Maria. Serum isolation and miRNA extraction was performed as previously reported (Oliveira et al. 2020). miRNA expression was determined using TaqMan Universal Master Mix II no UNG (Thermo Fisher Scientific) and the 7500 Sequence Detection System (Applied Biosystems, Foster City, CA, United States), according to the manufacturer's recommendations. Relative miR-335-3p expression levels of each subject were determined by the comparative 11Ct method using the spike-in cel-miR-39- 3p (Thermo Fisher Scientific, Rockford, IL, United States) as the normalization control. miR-335 expression levels of each PD patient were normalized to the mean value of healthy controls.

3.2.3.4. Cell transfection

BV2, N9, and SH-SY5Y cells were transfected with 40 nM of a specific miR-335-3p precursor (pre-miR-335-3p; Ambion, Thermo Fisher Scientific, Inc.) or a pre-miR negative control (pre-miR-Control; Ambion, Thermo Fisher Scientific, Inc.) 24 h after plating. To evaluate the targeting of LRRK2 by miR335-3p, BV2, and SH-SY5Y cells were co-transfected with 150 ng of a reporter plasmid driven by the SV40 basal promotor, harboring the LRRK2 30 untranslated region (UTR) (HmiT002101-MT06, Tebu-bio, Lisbon, Portugal), or a negative control region (CmiT000001-MT06, Tebu-bio), upstream of the humanized firefly luciferase gene, in combination with the pre-miR-335-3p/pre-miR-Control or anti-miR-335-3p/antimiR-Control (Ambion, Thermo Fisher Scientific, Inc.), for 24 h. For normalization, expression of the Renilla luciferase gene, contained in the reported plasmid, was used. Reporter assays were performed using Dual-Luciferase® Reporter Assay (Promega Corp.), according to the manufacturer's instructions. In LRRK2 overexpression experiments, BV2 or SH-SY5Y cells were transfected with 500 ng of pDEST53-LRRK2-WT DNA plasmid, gift from Mark Cookson (#25044, Addgene, Watertown, MA, EUA) (Greggio 2006) or empty-vector for 24 h, before further treatments. Moreover, BV2 cells were transfected with 250 ng of a plasmid encoding a constitutively active form of mitogen-activated protein kinase (MEK1*) (pCMB-deltaN3- MEK1), kindly provided by Dr. Roger J. Davis (Howard Hughes Medical Institute) or empty vector for 24 h before further treatments. All transfections were performed with Lipofectamine 3000™ (Invitrogen, Thermo Fisher Scientific, Inc.), according to the manufacturer's recommendations.

3.2.3.5. Cell viability/death assays

BV2 cells were plated in 96-well plates at 5 x 10^3 cells/well and transfected the next day for 24 h before exposure to 100 ng/mL LPS for additional 24 h. SH-SY5Y cells, with or without overexpression of α-syn, were plated in 96-well plates at 4 x 10^4 cells/well and transfected the next day for 24 h. Cellular metabolic activity was determined using CellTiter 96® Aqueous Non-Radioactive Cell Proliferation (MTS) Assay (Promega, Madison, WI, United States). Alterations in absorbance were measured at 490 nm using GloMax® Multi Detection System (Sunnyvale, CA, United States). Cell membrane integrity was determined using

the lactate dehydrogenase (LDH) Cytotoxicity Kit^{PLUS} (Roche Diagnostics GmbH, Mannheim, Germany). Absorbance was measured at 490 nm, with 620 nm reference wavelengths, using a BioRad Model 680 microplate reader.

3.2.3.6. Protein extraction and immunoblotting analysis

BV2 and N9 cells were plated in 35-mm dishes at 1.1 x 10^5 cells/dish and transfected the next day for 24 h before treatment with 100 ng/mL LPS for additional 24 h. SH-SY5Y cells, with or without overexpression of α-syn, were plated in 35-mm dishes at 12 x 10^5 cells/dish and transfected the next day for 24 h. Cells were collected in nonyl phenoxypolyethoxylethanol (NP-40) lysis buffer [1% NP-40, 20 mM Tris–HCl pH 7.4, 150 mM NaCl, 5 mM EDTA, 10% glycerol, 1 mM dithiothreitol, and 1x Halt Protease and Phosphatase Inhibitor Cocktail EDTA-free (Pierce, Thermo Fisher Scientific, Rockford, IL, United States)], followed by sonication and centrifugation at 3200 g for 10 min at 4˚C. Total protein extracts were recovered and stored at −80˚C. Protein concentration was calculated using the colorimetric Bradford method (Bio-Rad), according to the manufacturer's recommendations. Equal amounts of protein (40 μg) were denatured and electrophoretically resolved on 6–8% SDS-polyacrylamide gels and transferred onto nitrocellulose membranes. Transient staining was performed with 0.2% Ponceau S (Merck, Darmstadt, Germany) to confirm protein loading and transfer. Membrane blocking was performed using 5% non-fat dried milk in Tris-buffered saline (TBS) for 1 h. Then, membranes were incubated overnight at 4˚C with the following primary rabbit antibodies: RIP1 (#3493, Cell Signaling, MA, United States), RIP3 (#135170, Santa Cruz Biotechnology), p-MLKL (Ser358) (#196436, Abcam; Cambridge, Unite Kingdom), MLKL (#M6697, Sigma-Aldrich), IkB (#135170, Santa Cruz Biotechnologies), p-p38 (Thr180/Tyr182) (#9211, Cell Signaling), Erk1/2 (#4695, Cell Signaling), and with the following primary mouse monoclonal antibodies: JNK, p-JNK (Thr183/Tyr185), p38α/β, p-Erk1/2 (Tyr204) (#7345, #6254, #7972, #7383, Santa Cruz Biotechnologies) and p-IkB (Ser32/36) (#9246, Cell Signaling) and LRRK2 (#133474, Abcam) and finally with goat secondary antibodies conjugated with horseradish peroxidase anti-mouse or anti-rabbit (Bio-Rad Laboratories, Hercules, CA, United States) for 2 h at room temperature. Membranes were then processed for protein detection using Immobilon^{TM} Western (Merck Millipore,

Burlington, MA, United States) or SuperSignal™ West Femto Maximum Sensitivity Substrate (Pierce, Thermo Fisher Scientific). β-Actin (AC-15, Sigma Aldrich) was used as endogenous control. Densitometric analysis was performed with the Image Lab Software version 5.1 Beta (Bio-Rad).

3.2.3.7. Quantitative real time-PCR

BV2 and N9 cells were plated in 12-well plates at 4 x 10^4 cells/well and transfected the next day for 24 h before treatment with 100 ng/mL LPS for additional 24 h. SH-SY5Y cells, with or without overexpression of α-syn, were plated in 12-well plates at 5 x 10^5 cells/well and transfected in the following day for 24 h. Total RNA was extracted using TRIzol™ reagent (Invitrogen, Grand Island, United States) and quantified using a Qubit™ 2.0 fluorometer (Invitrogen). RNA was then converted into cDNA using NZY Reverse Transcriptase (NZYTech, Lisbon, Portugal). qRT-PCR was performed in the QuantStudio™ 7 Flex Real-Time PCR System (Thermo Fisher Scientific Inc.). The following primer sequences were used: COX2 gene, 5' -CAGCCAGGCAGCAAATCCTT (forward) and 5' -AGTCCGGGTACAGTCACACT (reverse); HPRT gene, 5' -GGTGAAAAGGACCTCTCGAAGTG (forward) and 5' -TA GTCAAGGGCATATCCAACAACA (reverse); IL-1β gene, 5' -TG CCACCTTTTGACAGTGATG (forward) and 5' -TGATGTGC TGCTGCGAGATT (reverse); IL-6 gene, 5' -ATGAACTCCTTC TCCACAAGC (forward) and 5' -GTTTTCTGCCAGTGCCTGT TTG (reverse); NLRP3 gene, 5' -GAGCCTACAGTTG GGTGAAATG (forward) and 5' -CCACGCCTACCAGGAAA TCTC (reverse); and TNF-α gene, 5' -AGGCACTCCCC CAAAAGATG (forward) and 50 -TGAGGGTCTGGGCCATA GAA (reverse). Two independent reactions for each primer set were performed in a final volume of 12.5 µL comprising 2x Power SYBR green PCR master mix (Thermo Fisher Scientific, Inc.) and 360 nM of each primer. The relative expression levels of each gene of interest were determined based on the standard curve normalized to the level of the housekeeping gene hypoxanthine-guanine phosphoribosyltransferase (HPRT). For miR-335-3p, TaqMan R Gene Expression Assay (Thermo Fisher Scientific, Inc.) was used. U6 or cel-miR-39-3p were used as normalization control for cell extracts or serum samples, respectively. Relative amount of miR-335-3p was calculated by the threshold cycle ($2^{-\Delta\Delta Ct}$) method.

3.2.3.8. Statistical analysis

Data analysis were performed with t-test and one-way analysis of variance (ANOVA) followed by post hoc Bonferroni's test. Statistically significance was achieved when values of $p < 0.05$. Analysis and graphical presentation were presented with the GraphPad Prism software Version 8 (GraphPad Software Inc., San Diego, CA, United States). Results are showed as mean ± standard error of the mean (SEM).

3.2.4. Results

3.2.4.1. Patient characterization

In this study, we included 40 iPD patients, 45 LRRK2-PD patients and 40 age- and gender-matched healthy controls. The major demographic and clinical features of patients and controls are presented in Table 3.2.1. Of note, patients covering the full spectrum of early to advanced PD, characterized by Hoehn and Yahr stage (1–5) were included. Further, at the time of sample collection, all patients were under treatment with antiparkinsonic medication. Age and gender equilibrium were assured between the three groups.

Table 3.2.1. Clinical features of patients and controls.

Patient Characteristics	Controls (n = 40)	iPD (n = 40)	LRRK2-PD (n = 45)
Age (years)	67.4 ± 8.19	70.4 ± 10.2	70.0 ± 9.0
Gender (F/M)	20/20	20/20	31/14
Age at symptom onset (years)	-	58.2 ± 12.7	56.4 ± 11.9
Disease duration (years)	-	12.3 ± 9.1	13.6 ± 7.8
Hoehn & Yahr	-	2.5 ± 0.9	2.7 ± 1.0
Family history of PD (%)	-	35.0	63.4

Data are presented as mean ± standard deviation. iPD, idiopathic Parkinson's disease; LRRK2-PD, LRRK2 mutation Parkinson's disease.

3.2.4.2. miR-335 is reduced in experimental models of PD and in the serum of PD patients

Recent studies have shown that the expression of miR-335 is altered in PD (Martins et al. 2011; Patil et al. 2019; Oliveira et al. 2020). Moreover, LRRK2 was pointed as a potential target of miR-335 (Martins et al. 2011). Here, we decided to further dissect the role of miR-335 in PD pathogenesis. We started by analyzing the expression pattern of miR-335 in several experimental models of PD. As an in vitro model of PD, we used the BV2 murine microglia cell line transiently transfected with a plasmid encoding wild-type LRRK2 (LRRK2-Wt), or empty vector, followed by LPS stimulation. Our results showed that LRRK2-Wt overexpression and/or cell incubation with LPS for 24 h significantly reduced miR-335 expression levels (Figure 3.2.1A). *In vivo*, we used 13-week-old male, injected intraperitoneally with a single dose of MPTP, or vehicle, and euthanized 30 days later, as a more clinically relevant model. This PD mouse model displays stable nigrostriatal dopaminergic neurodegeneration at 30 days, which is in accordance with the notion that dopaminergic neurodegeneration in PD patients majorly precedes the development of motor symptoms (Saporito et al. 2000; Kordower et al. 2013; Dionísio et al. 2019). We observed that MPTP-injected mice presented a significant reduction of miR-335 in the serum, when compared to control mice (Figure 3.2.1B). Finally, we determined the expression levels of miR-335 in serum samples of 40 iPD patients, 45 LRRK2-PD patients and 40 healthy controls, and confirmed that miR-335 was significantly reduced in the sera of iPD and LRRK2-PD patients in comparison with control subjects (Figure 3.2.1C). Although miR-335 levels were not significantly reduced in iPD patients in comparison with LRRK2-PD patients, a slight tendency of miR-335 to be reduced in iPD patients was observed, which could suggest that the role of LRRK2 in reducing miR-335 levels contributes to PD pathology in combination with several other mechanisms. Overall, these results indicate that miR-335 is reduced both *in vitro* and *in vivo* experimental models of PD, and most importantly, in the sera of PD patients, which highlights the potential of modulating miR-335 to alleviate PD pathogenesis.

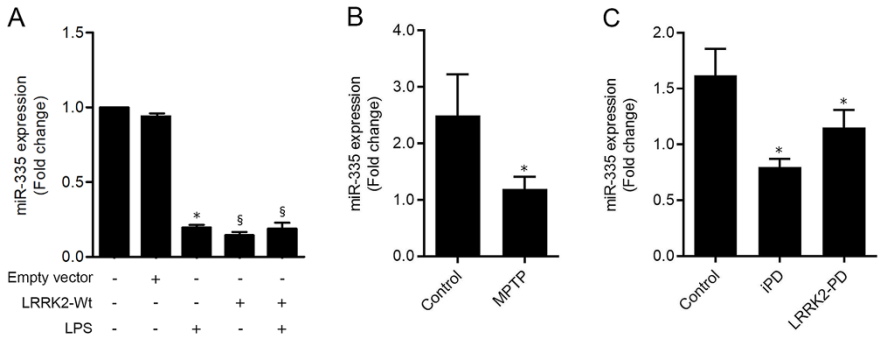

Figure 3.2.1. miR-335 is reduced in *in vitro* and *in vivo* experimental models of PD and in the sera of PD patients. (A) qRT-PCR analysis of miR-335 in BV2 microglial cells transfected with LRRK2-Wt overexpression plasmid, or empty vector, for 24 h and then stimulated with 100 ng/mL LPS for additional 24 h. (B) qRT-PCR analysis of miR-335 in the sera of MPTP-injected mice or control mice, euthanized at 30 days after MPTP injection. Values were normalized to the mean of control mice. (C) qRT-PCR analysis of miR-335 in the serum of iPD and LRRK2-PD patients and control individuals. Values were normalized to the mean of control healthy individuals. Results are expressed as mean ± SEM. **p* < 0.05 vs. Control; §*p* < 0.05 vs. control Empty vector.

3.2.4.3. miR-335 overexpression reduces LPS-mediated RIP1 and RIP3 increased levels

Emerging evidence suggest a role of miR-335 in regulating inflammation in different experimental models of disease. Moreover, several authors have proposed that key necroptosis mediators such as RIP1 and RIP3 are involved in inflammatory responses, especially in macrophages and microglia, without necroptosis commitment (Christofferson et al. 2012; Ito et al. 2016; Degterev et al. 2019; Ofengeim et al. 2017). Here, to determine the involvement of RIP1 and RIP3 in the inflammatory response, we used BV2 and N9 microglia cells transfected with pre-miR-335, or pre-negative control (NC), for 24 h, followed by stimulation with LPS for additional 24 h; and SH-SY5Y neuroblastoma cells, with or without α-syn overexpression, transfected with pre-miR-335 or NC for 24 h. In both microglia and neuroblastoma cells, transfection with pre-miR-335 significantly increased miR-335 expression levels, thus confirming miRNA transfection efficiency (Fig. S3.2.1A and B). In addition, as expected, stimulation of BV2 cells with LPS or α-syn overexpression in SH-SY5Y cells did not induce

cell death in MTS and LDH release assays (Fig. S3.2.1C and D). Similarly, miR-335 overexpression did not affect cell viability in both cell lines (Fig. S3.2.1C and D). However, LPS stimulation in BV2 and N9 cells significantly increased RIP1 and RIP3 protein levels, thus indicating that LPS-induced protein expression of RIP1 and RIP3 may be related to inflammatory events (Fig. 3.2.2A and B). Importantly, miR-335 overexpression per se did not influence RIP1 and RIP3 levels, while concomitant LPS stimulation and miR-335 overexpression significantly reduced LPS-induced RIP1 and RIP3 protein expression, further suggesting a role for this miRNA in decreasing inflammation (Fig. 3.2.2A and B). In agreement, a marker of necroptosis commitment such as the p-MLKL/MLKL ratio showed no significant differences (Fig. 3.2.2.A and B). Moreover, no differences were observed in RIP1 and RIP3 protein levels in BV2 cells overexpressing LRRK2-Wt (Fig. S3.2.2A). In SH-SY5Y cells with or without α-syn overexpression and/or miR-335 overexpression, no differences were observed in RIP1, RIP3, and MLKL protein levels (Fig. S3.2.2B).

3.2.4.4. miR-335 overexpression attenuates LPS- or α-syn-mediated proinflammatory mediators and LPS-induces ERK1/2 activation

Some authors have already proposed that miR-335 downregulation may have a deleterious effect by increasing the production of proinflammatory mediators in an inflammatory sepsis mouse model (Gao et al. 2018). To further determine the role of miR-335 in modulating inflammatory events, BV2 and N9 microglia cells were transfected with a pre-miR-335 or NC for 24 h, and further incubated with LPS for additional 24 h. Similarly, SH-SY5Y neuroblastoma cells with or without α-syn overexpression were transfected with a pre-miR-335 or NC for 24 h.

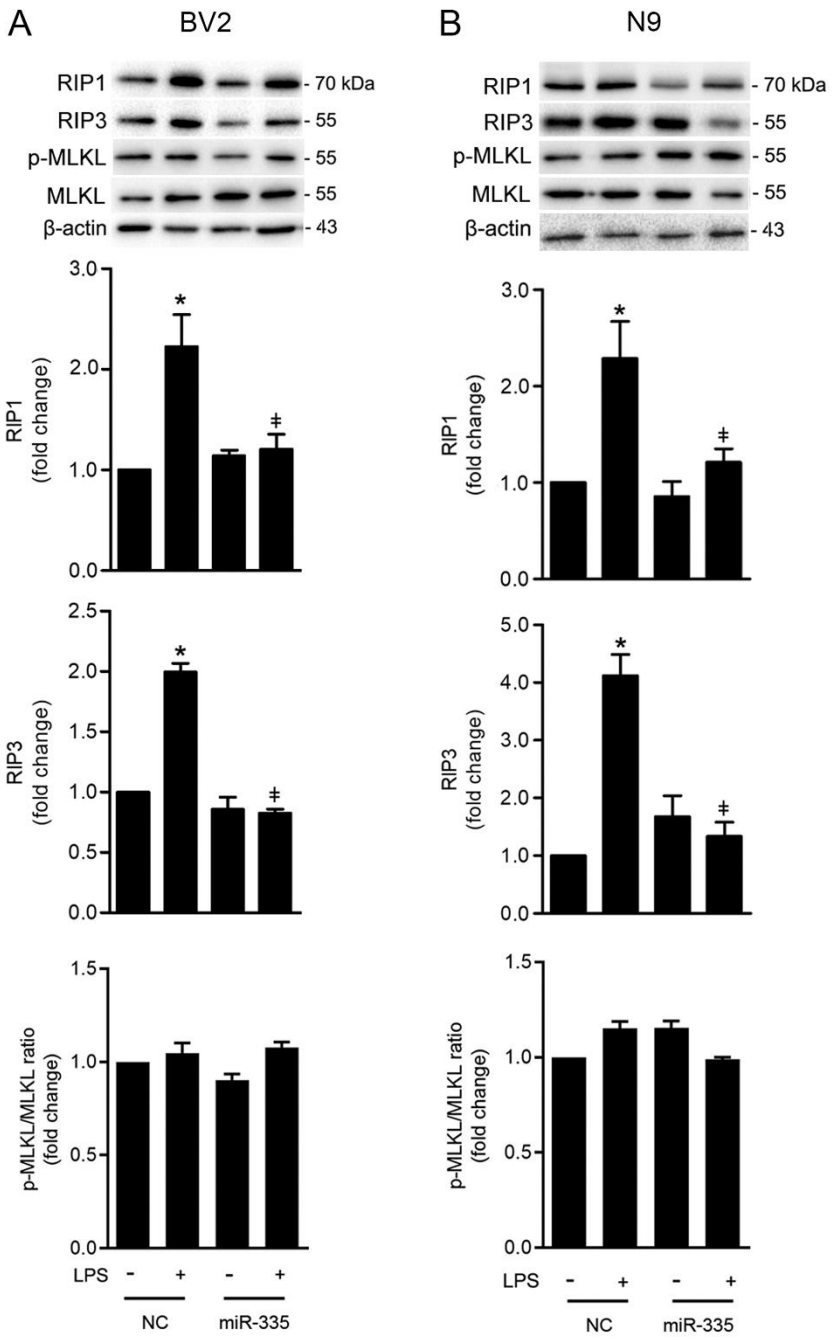

Figure 3.2.2. Modulation of LPS-induced protein expression of RIP1 and RIP3 by miR-335. BV2 microglial cells (A) and N9 microglial cells (B) were transfected with pre-miR-335 or negative control (NC) for 24 h and then stimulated with LPS for additional 24 h. Total protein extracts were prepared for Western blot analysis of RIP1, RIP3 and p-MLKL/MLKL ratio. Representative immunoblots are presented. β-actin was used as loading control. Values are expressed as mean ± SEM of three independent experiments. *$p < 0.05$ vs. NC; ǂ$p < 0.05$ vs. NC exposed to LPS.

Our results demonstrated that incubation of BV2 and N9 cells with LPS significantly increased TNF-α and IL-1β; or TNF-α, IL-1β, COX2, and NLRP3 mRNA levels, respectively (Figures 3.2.3A, B). No differences were observed in COX2 and NLRP3 mRNA levels in BV2 cells exposed to LPS (Figure 3.2.3A). As expected, miR-335 overexpression by itself did not influence mRNA levels of these cytokines. However, concomitant LPS incubation and miR-335 overexpression significantly decreased the mRNA levels of proinflammatory mediators.

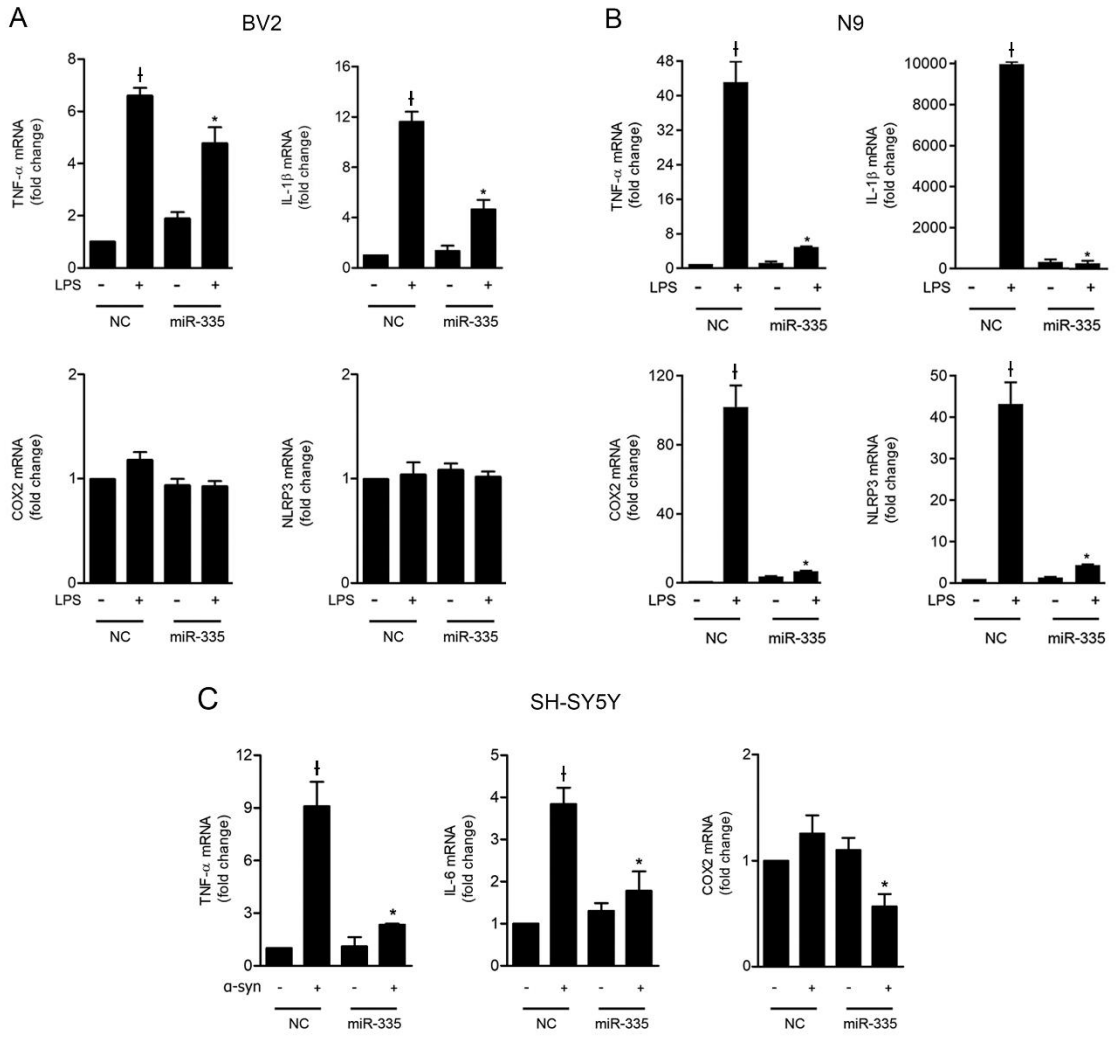

Figure 3.2.3. Modulation of LPS or α-syn-mediated proinflammatory mRNA levels by miR-335. BV2 (A) and N9 (B) cells were transfected with a pre-miR-335 or pre-NC for 24 h, and then stimulated with LPS for additional 24 h. (C) SH-SY5Y cells with or without overexpression of α-syn were transfected with a pre-miR-335 or pre-NC for 24 h. mRNA levels were measured by qRT-PCR. Results are expressed as mean ± SEM from three

independent experiments. ‡$p < 0.01$ vs. NC; *$p < 0.05$ vs. NC overexpressing α-syn or NC exposed to LPS.

In respect to neuronal cells, α-syn overexpression in SH-SY5Y cells significantly increased TNF-α and IL-6 mRNA levels, while no differences were observed in COX2, thereby indicating an α-syn-dependent inflammatory status in these cells (Figure 3.2.3C). Again, miR-335 overexpression alone did not influence the expression of these proinflammatory genes. However, when cells overexpress α-syn, miR-335 increased levels significantly attenuate α-syn-induced TNF-α and IL-6 (Figure 3.2.3C). These results confirm the potential of miR-335 in modulating inflammation in both neuronal and microglial cells.

Then, to further confirm mRNA proinflammatory gene expression and dissect inflammatory signaling pathways modulated by miR-335, we investigated the phosphorylation states of JNK (Thr183/Tyr185), p38 (Thr180/Tyr182), and ERK1/2 (Tyr204), three classic MAPK inflammatory signaling pathways, as well as NF-κB activation, which is a key mediator of inflammatory responses (Hashimoto et al. 2003; Tortarolo et al. 2003; Liu et al. 2017), in BV2 cells exposed to LPS from 30 min up to 24 h. As depicted in Figure 5.4, ERK1/2 pathway was activated at 4 and 6 h of LPS exposure (Figures 5.4 A,B), but not at earlier or later time points (data not shown), as determined by the ratio between phosphorylated and total protein levels. Similarly, NF-κB was strongly activated at 4 and 6 h post LPS, as indirectly determined by the p-IκB/IκB ratio (Figures 3.2.4A,B). p38 and JNK pathways showed no alterations (Figure 3.2.4A). Importantly, transfection of cells with miR-335 alone did not activate these signaling pathways; however, miR-335 overexpression significantly reduced LPS-induced ERK1/2 and NF-κB activation (Figures 3.2.4A,B). To further confirm that the observed decrease in LPS-induced ERK1/2 levels is mediated by miR-335, we determined proinflammatory mRNA levels in BV2 cells after transfection with a plasmid encoding a constitutive active form of MEK1 (MEK1∗), which is the upstream kinase of ERK1/2. Our results showed that expression of MEK1∗ tended to abrogate miR-335 effect, as observed by an increase in TNF-α and IL-1β mRNA levels (Fig. S3.2.3).

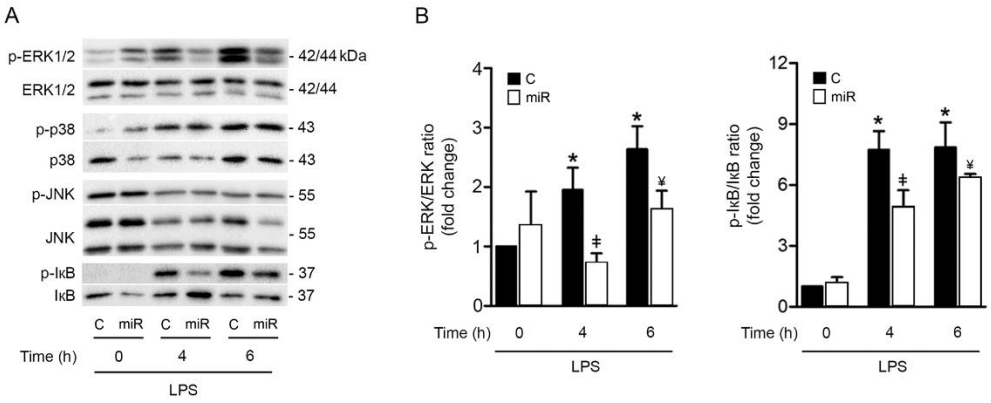

Fig. 3.2.4 Modulation of ERK1/2 and NF-κB activation by miR-335. BV2 cells were transfected with a pre-miR-335 or pre-NC for 24 h and then stimulated with LPS for 4h or 6 h. Representative immunoblots for p-ERK/ERK, p-JNK/JNK, p-p38/p38, and p-IκB/IκB ratios (A) and densitometric analysis of p-ERK/ERK and p-IκB/IκB ratios (B) are presented. Results are presented as mean ± SEM of three independent experiments. **p* < 0.0.5 vs. C 0 h; ǂ*p* < 0.05 vs. LPS 4 h; ¥*p* < 0.05 vs. LPS 6 h.

3.2.4.5. miR-335 directly targets LRRK2 and its overexpression attenuates LRRK2-Wt-driven inflammatory events

Previous *in silico* studies have proposed LRRK2 as a putative target of miR-335, which was further confirmed *in vitro* (Yılmaz S et al. 2016; Patil et al. 2019). Here, using dual-luciferase assay and western blot analysis, we also confirmed that miR-335 directly targets LRRK2 in both BV2 microglial and SH-SY5Y neuroblastoma cells (Figures 3.2.5A–D). In addition, using well-known *in silico* tools including TargetScan and PicTar databases, we found that α-syn 3'-UTR is also a putative target of miR-335 (Fig. S3.2.4). Although LRRK2 pathogenic mutations are linked to dopaminergic cell death, there is also evidence suggesting that LRRK2-Wt overexpression upregulates α-syn levels, thereby influencing the pathological output of LRRK2-related PD (Lin et al. 2009; Carballo-Carbajal et al. 2010). Here, we used BV2 microglial cells co-transfected with LRRK2-Wt expression plasmid and premiR-335, and further incubated with LPS for additional 24 h; and SH-SY5Y neuroblastoma cells, with or without α-syn overexpression co-transfected with LRRK2-Wt and pre-miR-335. Transfection of

BV2 cells with LRRK2-Wt plasmid resulted in a significant increase of LRRK2 protein, which in turn was attenuated by miR-335 overexpression (Fig. 3.2.5D). Additionally, LRRK2-Wt overexpression, with or without concomitant LPS incubation, did not affect cell viability, as observed by MTS and LDH assays (Fig. S3.2.5A). Also, miR-335 overexpression did not induce any alteration in cell viability, in the presence or absence of LRRK2-Wt overexpression (Fig. S3.2.5A). Similar results were observed in SH-SY5Y cells with or without α-syn and concomitant overexpression of LRRK2-Wt (Fig. S3.2.5B).

Finally, the role of LRRK2 in inflammation has been studied since the identification of LRRK2 as one of the genes causing susceptibility for the development of inflammatory diseases. Moreover, recent evidence shows that LRRK2 is elevated in immune cells, including microglia, where it may promote inflammation (Moehle et al. 2012; Gillardon et al. 2012). Thus, we wanted to explore whether LRRK2-Wt overexpression could influence the expression of proinflammatory genes, which may in turn be modulated by miR-335. We used BV2 microglia cells co-transfected with LRRK2-Wt or empty vector plasmid and pre-miR-335 for 24 h, and further incubated with LPS for additional 24 h, or SH-SY5Y cells overexpressing α-syn co-transfected with LRRK2-Wt or empty vector plasmid and pre-miR-335 for 24 h. Here, LRRK2-Wt overexpression significantly increased TNF-α, IL-1β and NLRP3 but not COX2 mRNA levels. Concomitant treatment with LPS further increased the levels of these proinflammatory markers (Figure 3.2.5E). Importantly, miR-335 overexpression significantly reduced TNF-α and IL-1β mRNA levels in both LRRK2-Wt and LRRK2-Wt exposed to LPS conditions (Figure 3.2.5E). Similar results were observed in SH-SY5Y cells, where LRRK2-Wt overexpression significantly increased TNF-α, IL-1β and COX2 mRNA levels with or without α-syn overexpression (Figure 3.2.5F). More importantly, miR-335 overexpression also significantly decreased TNF-α and IL-1β mRNA levels (Figure 3.2.5F). These results confirm the role of miR-335 in protecting microglia and neuronal cells from an inflammatory phenotype.

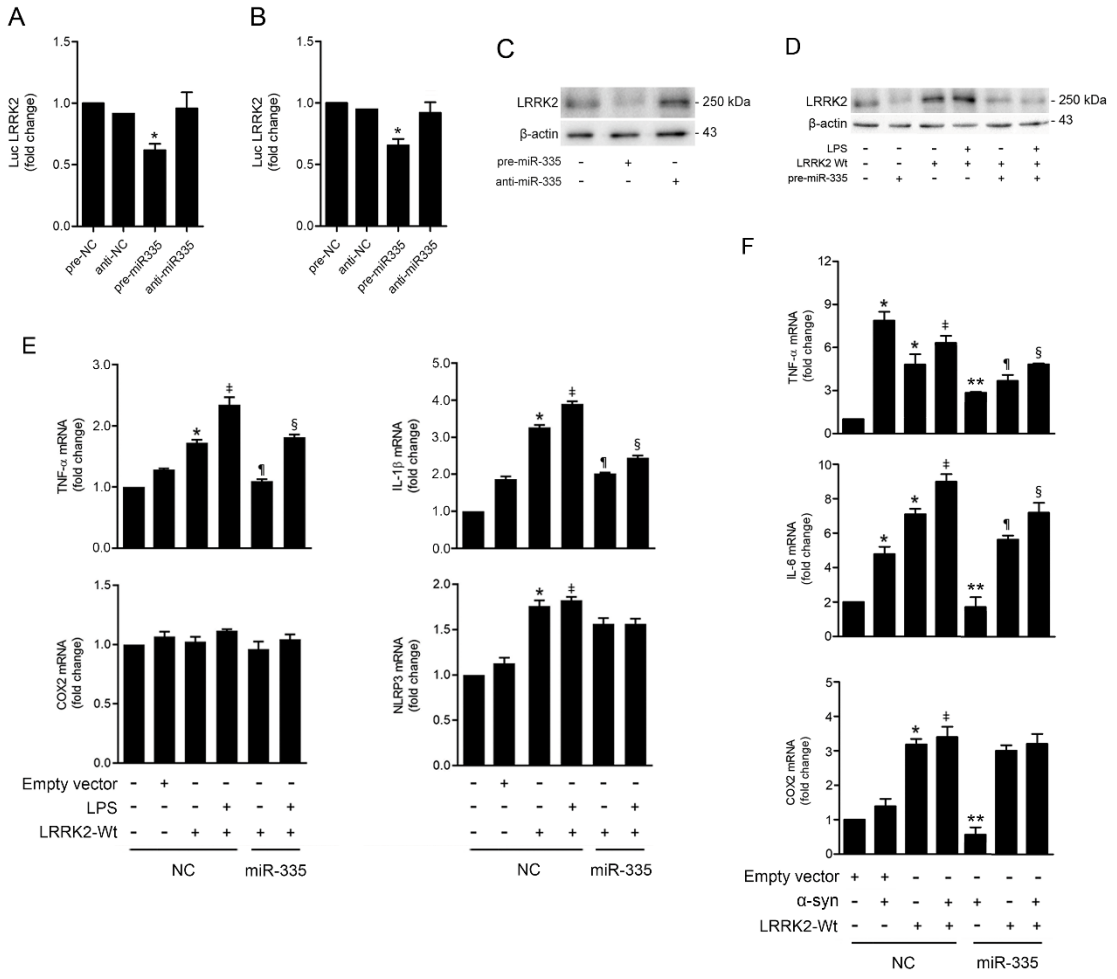

Fig. 3.2.5 MiR-335 directly targets LRRK2. (A) SH-SY5Y cells were co-transfected with a LRRK2 luciferase reporter vector, or negative control, and pre-miR-335/pre-NC; or anti-miR-335/anti-NC for 24 h. (B) BV2 cells were co-transfected with a LRRK2 luciferase reporter vector, or negative control, and pre-miR-335/pre-NC; or anti-miR-335/anti-NC for 24 h. Renilla luciferase signal was used as an internal standard control. Results are presented as mean ± SEM of three independent experiments. **p* < 0.0.5 vs. pre-NC. (C) Representative immunoblots are presented for LRRK2 in SH-SY5Y cells. β-Actin was used as loading control. (D) BV2 cells were co-transfected with a LRRK2-Wt or empty vector plasmid and with a pre-miR-335 or pre-NC for 24 h, and then stimulated with LPS for additional 24 h. Representative immunoblots are presented for LRRK2. β-Actin was used as loading control. (E) Modulation of LRRK2-Wt-induced proinflammatory mRNA levels by miR-335. BV2 cells were co-transfected with a LRRK2-Wt or empty vector plasmid and with a pre-miR-335 or pre-NC for 24 h, and then stimulated with LPS for additional 24 h. TNF-α, IL-1β, COX2, and NLRP3 mRNA levels were measured by qRT-PCR. Results are expressed as mean ± SEM from three independent experiments. **p* <

0.05 vs. empty vector; ǂ$p < 0.05$ vs. empty vector transfected with pre-NC, ¶$p < 0.05$ vs. LRRK2-Wt; §$p < 0.05$ vs. LRRK2-Wt exposed to LPS. (F) Modulation of LRRK2-Wt-induced proinflammatory mRNA levels by miR-335. SH-SY5Y cells with or without overexpression of α-syn were co-transfected with a LRRK2-Wt or empty vector plasmid and with a pre-miR-335 or pre-NC for 24 h. TNF-α, IL-1β, and COX2 mRNA levels were measured by qRT-PCR. Results are expressed as mean ± SEM from three independent experiments. *$p < 0.05$ vs. empty vector; ǂ$p < 0.05$ vs. empty vector transfected with pre-NC, **$p < 0.05$ vs. NC overexpressing α-syn; ¶$p < 0.05$ vs. LRRK2-Wt without α-syn overexpression; §$p < 0.05$ vs. LRRK2-Wt with α-syn overexpression.

3.2.5. Discussion

In this study, we hypothesized that miR-335 plays important roles during inflammation by targeting LRRK2. We first determined the levels of miR-335 in different *in vitro* models and its circulating levels in *in vivo* PD-mimicking experimental models and in PD patients. Recent studies have shown that miR335 may be linked to PD pathogenesis, since we and others have found reduced expression levels in whole blood, PBMCs and serum of PD patients compared with control subjects (Yılmaz S et al. 2016; Martins et al. 2011; Oliveira et al. 2020). In accordance, here we observed that miR-335 is significantly reduced in the sera of both iPD and LRRK2-PD patients as compared with control subjects. Others have suggested that the role of miR-335 in PD pathogenesis is mediated by LRRK2 (Patil et al. 2019; Yılmaz S et al. 2016). In this regard, we confirmed that miR-335 directly targets LRRK2 in BV2 and SHSY5Y cells. Moreover, it has been demonstrated that LRRK2 expression is induced by inflammatory stimuli, such as LPS or IFN-γ in activated microglia, PBMCs and cultured bone marrow-derived macrophages (Moehle et al. 2012; Hakimi et al. 2011; Gardet et al. 2010). LRRK2 protein activation is linked to inflammatory signaling, while no significant differences occur in LRRK2 mRNA levels, which could suggest a post-transcriptional regulation, for instance by miRNAs (Moehle et al. 2012). Here, we showed that BV2 microglial cells stimulated with LPS presented a significant reduction in miR-335 expression levels. Moreover, concomitant overexpression of LRRK2-Wt also contributed to a reduction in the levels of this miRNA, which could indicate a feedback loop where an inflammatory stimulus reduces miR-335

expression, which may in turn promote an increase in LRRK2 protein levels, therefore exacerbating inflammation. In fact, others have shown that in response to TLR4 activation, LRRK2 inhibition, either by small-molecule kinase inhibitors or LRRK2 knockdown, reduces proinflammatory signaling pathways (Moehle et al. 2012). Furthermore, we determined miR-335 expression levels in the sera of mice subjected to a single injection of the MPTP neurotoxin, a well-known trigger of PD-related pathology, and observed that miR-335 was significantly reduced in these mice in comparison with control mice, which may suggest an overall reduction in miR-335 levels in the presence of an inflammatory environment. Indeed, others have demonstrated that MPTP-treated mice present increased expression of TLR4, which is involved in the release of proinflammatory molecules from microglia (Shao et al. 2019; Lofrumento et al. 2011). Overall, these results suggest that the levels of miR-335 decrease in response to inflammatory environments. Thus, it is possible to speculate about the potential role of this miRNA in contributing to an overall reduction of inflammation in animal models of PD-related pathologies.

Considering that miR-335 is reduced in different inflammatory PD models, we tested if elevating the levels of miR-335 could impact on inflammation. Notably, we observed that miR-335 overexpression significantly reduced RIP1 and RIP3 protein levels induced by LPS stimulation in BV2 and N9 microglial cells, while no differences were observed in p-MLKL/MLKL ratio nor in cell viability, indicating that modulation of RIP1/3 by miR-335 did not influence cell death by necroptosis in these models. In fact, some studies have demonstrated that proinflammatory stimulation of macrophages and microglia and consequent RIP1 activation, with or without RIP3 recruitment, could induce the expression of proinflammatory genes, with no MLKL involvement or cell death associated (Christofferson et al. 2012; Ito et al. 2016; Degterev et al. 2019; Ofengeim et al. 2017). Interestingly, no differences in RIP1 and RIP3 were observed in SH-SY5Y cells overexpressing α-syn, thus suggesting that, at least in our conditions, α-syn overexpression is not sufficient for inducing inflammatory-dependent activation of RIP1 and RIP3, or that the cells themselves may not rely as strongly on RIP1/3 signaling as microglial cells. Importantly, LPS stimulation of BV2 and N9 microglial cells as well as α-syn overexpression in SH-SY5Y cells strongly induced the expression of several proinflammatory genes, including TNF-α, IL-

1β, IL-6, COX2, and NLRP3, which was counteracted by miR-335 overexpression, thus highlighting the role of miR-335 as an anti-inflammatory miRNA. These results are in accordance with other studies where miR-335 upregulation was associated with decreased inflammation through the reduction of proinflammatory gene expression, ROS levels and inflammasome activation in a sepsis mice model (Gao et al. 2018). In SH-SY5Y cells, others also demonstrated that miR-335 inhibition results in increased ROS production (De Luna et al. 2020).

Throughout the years, several lines of evidence have proposed that increased proinflammatory gene expression depends on the activation of multiple MAPKs, specially p38, ERK1/2 and JNK, and downstream activation of transcription factors, such as NF-κB. However, the precise mechanisms connecting these events to RIP1 and/or RIP3 activation are still poorly understood (Christofferson et al. 2012; Ito et al. 2016; Zhu et al. 2018). Interestingly, some studies demonstrated that increased LRRK2 protein levels promote ERK1/2 activation, without affecting p38 or JNK signaling pathways (Carballo-Carbajal et al. 2010). Our results are in accordance with these studies since miR-335 overexpression reduced LPS-induced ERK1/2 activation, thereby confirming its role in reducing inflammation which is probably mediated by LRRK2 inhibition. Overall, we observed that stimulation of cells with a proinflammatory stimulus, such as LPS, strongly increases RIP1 and RIP3 protein levels, which may consequently contribute to the activation of ERK1/2 pathway, thus leading to the downstream activation of NF-κB transcription factor, which may contribute to the induction of proinflammatory gene expression (Festjens et al. 2007; Humphries et al. 2015). Importantly, miR-335 demonstrated high anti-inflammatory potential by reducing these inflammatory mechanisms.

After determining the role of miR-335 overexpression in diminishing inflammation mediated by a classical inflammatory stimulus, we hypothesized that miR-335 could also reduce LRRK2-Wt-driven inflammation and/or cell death. LRRK2 has been widely described in the regulation of several inflammatory pathways and its activation associated with neuronal death (Chen et al. 2012). Interestingly, although LRRK2 mutations are commonly linked to neuronal death exacerbation, the role of LRRK2-Wt overexpression is not completely understood, with some studies showing a role in protecting SH-SY5Y cells from

death (Liou et al. 2008), and others indicating a deleterious effect by increasing α-syn levels in HEK293 cells (Carballo-Carbajal et al. 2010). Moreover, in both SH-SY5Y and immune cells, LRRK2-Wt overexpression seems to have other detrimental effects, including mitochondrial fragmentation and inflammation (Wang et al. 2012; Moehle et al. 2012; Berwick et al. 2019; Marker et al. 2012). Our results showed that LRRK2-Wt overexpression did not induce cell death in BV2 nor SH-SY5Y cells. However, LRRK2-Wt overexpression strongly induced proinflammatory gene expression in BV2 microglia and SH-SY5Y neuroblastoma cells, while miR-335 overexpression attenuated this effect.

In conclusion, we have unraveled a novel role for miR-335 during inflammation in PD-like conditions in both microglial and neuronal cells, which are probably but not exclusively dependent on LRRK2 targeting. Here, miR-335 showed to be reduced in different *in vitro* and *in vivo* PD-mimicking models and in PD patients, while its overexpression strongly reduced inflammation induced by either LPS stimulation or LRRK2-Wt overexpression. These observations suggest that miR335 overexpression may contribute to a less pro-inflammatory activation in PD, thereby contributing to attenuate chronic neuroinflammation and PD progression.

3.2.6. Supplementary figures

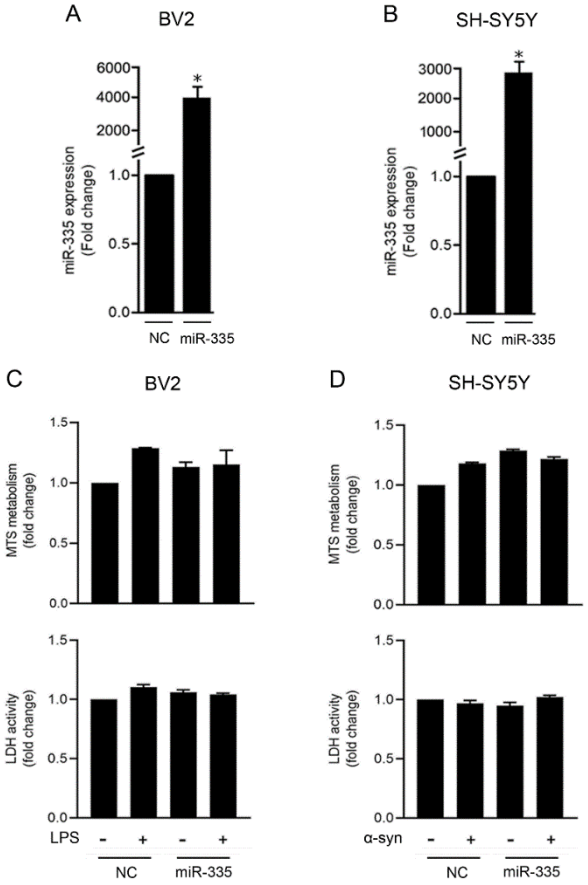

Figure S3.2.1. Modulation of cell viability by miR-335. (A) qRT-PCR analysis of miR-335 in BV2 cells transfected with a pre-miR-335 or pre-NC for 24 h. (B) qRT-PCR analysis of miR-335 in SH-SY5Y cells transfected with a pre-miR-335 or pre-NC for 24 h. (C) BV2 cells were transfected with a pre-miR-335 or pre-NC for 24 h and then stimulated with LPS for additional 24 h. (D) SH-SY5Y cells with or without overexpression of α-syn were transfected with a pre-miR-335 or pre-NC for 24 h. Cell metabolic activity was determined by MTS metabolism assay and cell membrane integrity by LDH activity in the supernatant. Results are presented as mean ± SEM of three independent experiments performed in duplicates and normalized to control cells transfected with pre-NC.

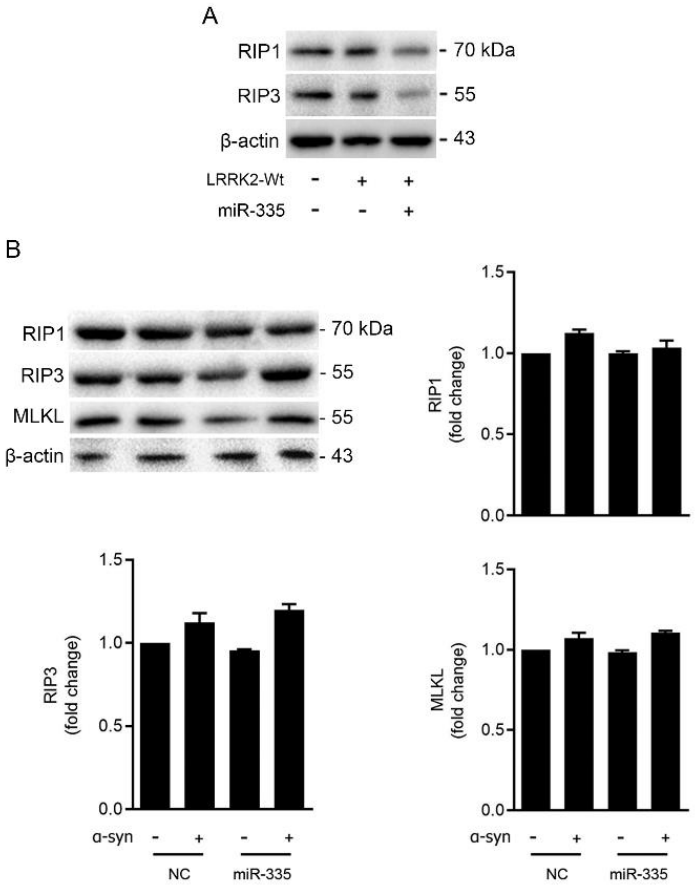

Figure S3.2.2. Modulation of RIP1, RIP3 and MLKL by miR-335. (A) BV2 cells were co-transfected with a LRRK2-Wt or empty vector plasmid and with a pre-miR-335 or pre-NC for 24 h. (B) SH-SY5Y neuroblastoma cells with or without overexpression of α-syn were transfected with pre-miR-335 or pre-NC for 24 h. Total protein extracts were prepared for Western blot analysis of RIP1, RIP3 and MLKL. Representative immunoblots are presented. β-actin was used as loading control. Values are expressed as mean ± SEM of three independent experiments.

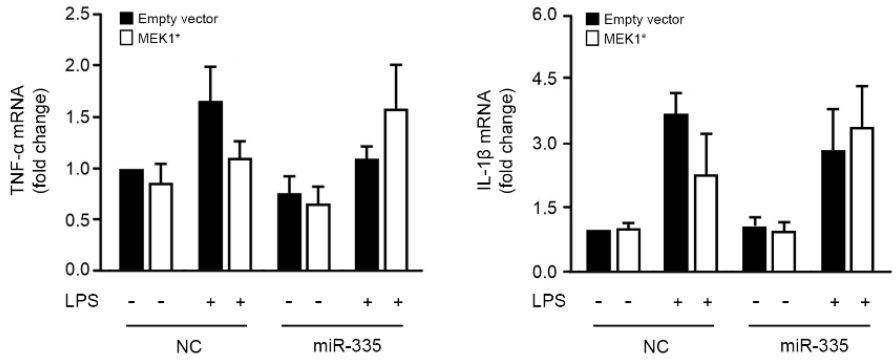

Figure S3.2.3 Modulation of proinflammatory mRNA levels by miR-335. BV2 cells were co-transfected with a plasmid encoding a constitutively active form of MEK1 (MEK1*), or empty vector and pre-miR-335/pre-NC for 24 h, and then stimulated with LPS for additional 24 h. TNF-α and IL-1β mRNA levels were measured by qRT-PCR. Results are expressed as mean ± SEM from two independent experiments.

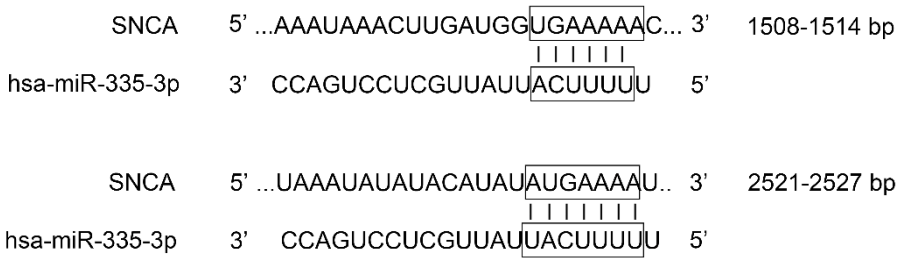

Figure S3.2.4 *In silico* analysis of has-miR-335-3p targeting of α-syn (SNCA) 3'-UTR region using TargetScan and PicTar databases.

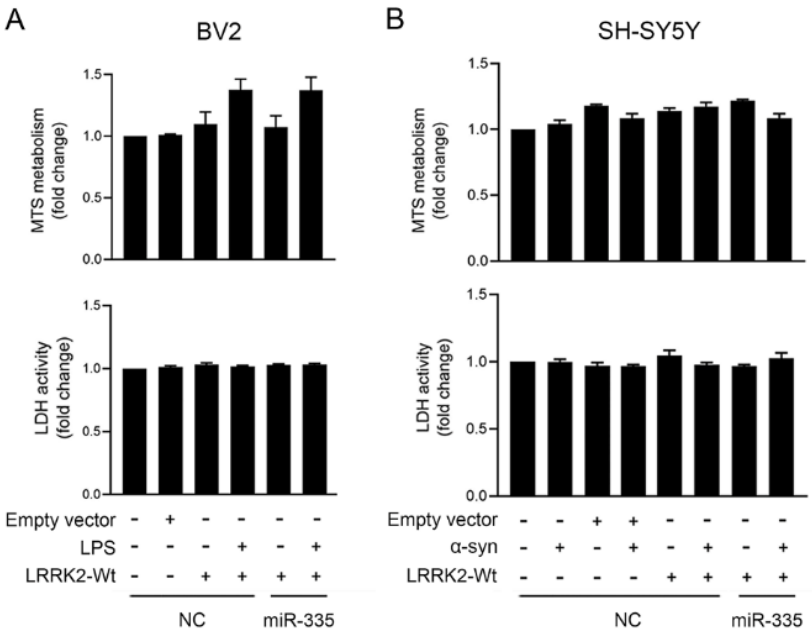

Figure S3.2.5 Modulation of cell viability by LRRK2-Wt. (A) BV2 cells were co-transfected with a LRRK2-Wt or empty vector plasmid and with a pre-miR-335 or pre-NC for 24 h, and then stimulated with LPS for additional 24 h. (B) SH-SY5Y cells overexpressing α-syn were co-transfected with a LRRK2-Wt or empty vector plasmid and with a pre-miR-335 or pre-NC for 24 h. Cell metabolic activity was determined by MTS metabolism assay and cell membrane integrity by LDH activity in the supernatant. Results are presented as mean ± SEM of three independent experiments performed in duplicates and normalized to control cells transfected with pre-NC.

CONCLUDING REMARKS

During the last decades, the epidemiologic developments of neurological diseases have shown that, although the risk of stroke and dementia has declined, the risk of neurodegenerative diseases, including PD, have consistently increased in several high-income countries, especially in North America and western Europe (Rocca 2017, 2018). According to the Global Burden of Disease study, neurological disorders are nowadays the main leading cause of disability worldwide and the second leading cause of global death, with PD being the fastest growing disease (GBD 2017). From 1990 to 2016, PD burden increased to more than a double, affecting 6.1 million people, and it is expected that this trend continues to increase in the next 30 years, attaining more than 12 million patients over the world (GBD 2017; GBD 2019). The increase in life expectancy is widely assumed as the main contributor to the increase in PD burden overtime. Moreover, PD current treatments can only alleviate symptomatic effects of the disease, and there are no available treatments to stop or slow disease progression. In fact, as disease progresses, PD patients face a continuously deterioration in terms of symptom severity, which along with increased aged population strongly impacts life quality and also economic and healthcare costs. In fact, in 2010, data from the United States of America indicated that prolonged disability and healthcare expenses costed approximately $28.8 billion that year, or $45.600 per PD patient, being expected to double until 2040 (Kowal et al. 2013). Therefore, there is an urgent, unmet need for research to focus on delivering novel methodologies for early and effective diagnosis as well as in the identification of novel preventive therapeutic approaches that could revert or at least mitigate disease progression. Overall, a profound understating of the pathological mechanisms involved in PD as well as its aetiology will certainly attest for novel breakthroughs in the field.

The original work presented in this thesis aimed to contribute to the identification of novel potential therapeutic approaches in PD, especially focusing on the discovery of novel necroptosis inhibitors. Moreover, we also intended to identify deregulated miRNAs that may play a role in disease pathogenesis and gain insight on how miRNAs modulation could downregulate inflammatory and/or cell death pathways in PD-mimicking models.

Concerning the discovery of novel small-molecule necroptosis inhibitors, cell-based necroptosis models have been largely used for drug screening

proposes. These cell-based models can be used following different paths: the discovery of novel compounds through modern medicinal strategies; screening of large compound libraries; drug repurposing of already approved drugs and consequent structural optimization; and testing of natural products (Zhuang and Chen 2020). To date, there are several well-established cellular models from different species and tissues widely used to study necroptosis, including L929 murine fibroblasts (Wagner and Schreiber 2016), Jurkat FADD$^{-/-}$ human leukaemic T cell lymphoblasts (Vercammen et al. 1998) and HT29 human colorectal adenocarcinoma cells (He et al. 2009). In our work, we established a novel and robust cell-based model to discover new necroptosis inhibitors, based on the stimulation of BV2 murine microglia cells with the well-known pan-caspase inhibitor, zVAD, and confirmed high necroptosis commitment in this model. Previous evidence have already shown that stimulation of specific cell lines, such as L929, with zVAD, strongly induced necroptosis (Yu et al. 2006; Wu et al. 2011). Here, we characterized an *in vitro* system that allows for compound screening using a CNS cellular type (Fig. 4.1).

Importantly, there are several necroptosis inhibitors identified so far that target key components of the necroptotic signalling cascade, including RIP1, RIP3 or MLKL. However, RIP1 has become the most prominent and studied target for drug development either in the pharmaceutical industry and academic research, mostly due to its crucial role in TNF-α signalling responses and highly flexible kinase structure (Humphries et al. 2015; Chirieleison et al. 2016; Zhuang and Chen 2020). Notably, we identified one hit compound – Oxa12 – that strongly inhibited zVAD-induced necroptosis in BV2 and L929 cell lines. Additional docking studies suggested that Oxa12 most likely prevent necroptosis by inhibiting RIP1 kinase activity. Further characterization into Oxa12 mechanism of action showed that Oxa12 reduces necroptosis-mediated inflammation, by reducing TNF-α mRNA levels and cytokine secretion, which indicates that RIP1 kinase activity might be essential for TNF-α production. In fact, earlier studies from other authors demonstrated that zVAD-induced necroptosis strongly relies

on the production and consequent autocrine secretion of TNF-α (Wu et al. 2011; Hitomi et al. 2008; Christofferson et al. 2012).

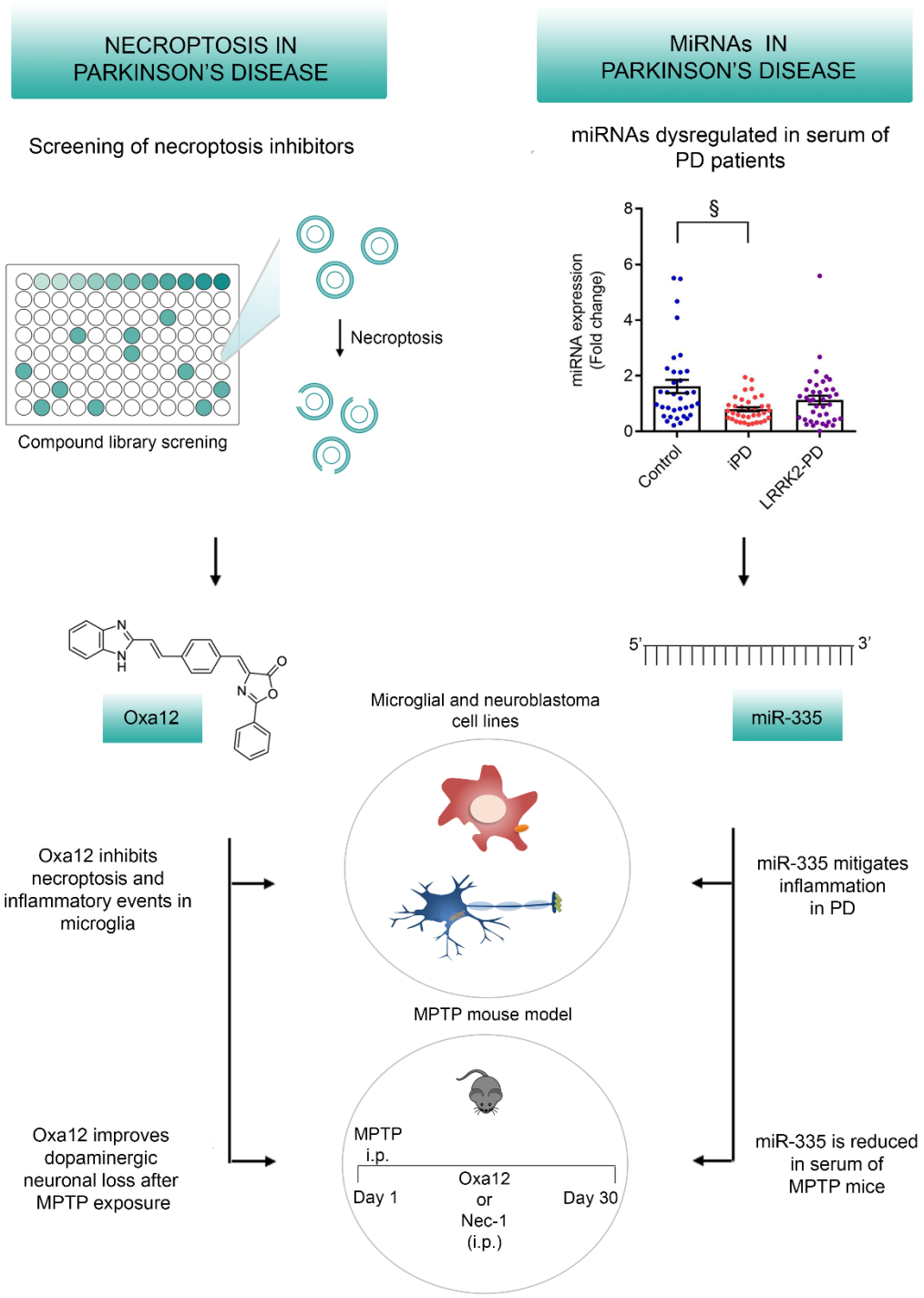

Figure 4.1 Overview of necroptosis and miRNAs in Parkinson's disease. In our first main work, we conducted a phenotypic screening to identify necroptosis inhibitors in a microglial cell line. Oxa12 was identified as a potent necroptosis inhibitor with anti-inflammatory properties. This compound was then validated in the sub-acute MPTP

mouse model, where it improved dopaminergic neuronal loss after MPTP exposure. Moreover, in our second main work, we evaluated which miRNAs from a selected library were dysregulated in the serum of PD patients. From the identified miRNAs, we selected miR-335 that was reduced in the serum of iPD and LRRK2-PD patients. MiRNA-335 was also reduced in the serum of MPTP mice. *In vitro*, miR-335 mitigated inflammation in microglial and neuroblastoma cellular models of PD.

In addition, Oxa12 also showed to markedly reduce inflammation initiated by a classic inflammatory stimulus, without necroptosis commitment. More specifically, Oxa12 reduced TNF-α and IL-1β mRNA levels induced by LPS stimulation, which strongly suggested its anti-inflammatory properties, apart from the role as necroptosis inhibitor. In accordance, earlier studies also proposed anti-inflammatory roles for Nec-1, independently of its necroptosis inhibitor function (Jie et al. 2016). Others have also described that RIP1 activation may promote inflammation in microglia and astrocytes, through production of proinflammatory cytokines (Mifflin et al. 2020). Our results are in accordance with these studies, since Oxa12, probably by inhibiting RIP1, reduces inflammation. Additional treatment of LPS-stimulated BV2 cells with zVAD potentiated inflammation, which was also counteracted by Oxa12.

Previous studies have also indicated that during zVAD-induced necroptosis in L929 cells, JNK activation was responsible for promoting TNF-α gene expression and, consequently, TNF-α cytokine secretion, downstream of RIP1 (Christofferson et al. 2012; Wu et al. 2011). In fact, zVAD appears to activate protein kinase C (PKC), leading to JNK activation and consequent activation of transcription factor AP1, that promotes TNF-α expression (Wu et al. 2011). Moreover, RIP1 is also reported to promote JNK activation by interacting with E3 ubiquitin ligase EDD and cIAP1, which ultimately lead to Sp1-dependent TNF-α transcription (Christofferson et al. 2012). Altogether, TNF-α transcription could translate into increase TNF-α secretion levels, which may promote necroptosis through TNFR activation (Wu et al. 2011). Accordantly, we observed increased JNK activation in BV2 cells treated with zVAD, which correlates with the increase observed in TNF-α gene expression and secretion. Curiously, there is a lack of consensus regarding p38 activation during necroptosis. In fact, while some authors have demonstrated that prolonged p38 activation induces cell

death in various cell lines (Mackay and Mochly-Rosen 2000), others showed that, in L929 cells, this signalling pathway is not activated during necroptosis (Wu et al. 2009). More recently, some studies have shown that in activated macrophages, zVAD-induced necroptosis occurs through ROS-mediated activation of p38 signalling pathway (Koike et al. 2019). Here, we observed p38 activation in zVAD-treated BV2 cells. Furthermore, the role of these two MAPK pathways in inflammation is widely known, thus suggesting that the release of intracellular components by necroptotic cells could induce their activation. More importantly, Oxa12 strongly reduced both JNK and p38 activation, which further indicates the role of these signalling pathways in necroptosis, at least in our conditions. Moreover, no differences were observed in Akt Ser473 phosphorylation. In fact, some authors have shown the key role of Akt during necroptosis by mediating TNF-α synthesis, which seem to be dependent Akt Thr308 phosphorylation (McNamara et al. 2013). Finally, activation of transcription factor NF-κB was also observed in zVAD-treated BV2 cells, which is in accordance with previous studies supporting a role of NF-κB activation in glial cells in mediating inflammatory processes (Camandola and Mattson 2007). Importantly, Oxa12 strongly reduced NF-κB activation, highlighting its effectiveness at reducing inflammatory-associated events.

Based on Oxa12 chemical structure, additional optimizations were performed as an attempt to improve compound solubility and efficacy. From the original in-house library of 58 compounds, 31 of them were screened in zVAD-treated BV2 microglial cells, our optimized cellular model. The remaining 7 compounds were insoluble at tested concentration, being excluded from further studies. Again, we identified Oxa12 as a strong necroptosis inhibitor that prevented necroptosis in ~70% with an EC_{50} value of 0.989 μM. All the other chemical compound modifications showed less activity in inhibiting z-VAD-induced cell death in our model. Importantly, it is crucial to establish structure-activity relationship between the analogues of the same chemotype in order to better understand which is the target-specific and the undesired nonspecific effects (Moffat et al. 2017). Next, we determined whether Oxa12 was included in the CNS drug property space, using a CNS multiparameter optimization (MPO) algorithm. This approach uses six physicochemical parameters of drugs, including lipophilicity, calculated distribution coefficient, molecular weight,

topological polar surface area, number of hydrogen bond doners, and most basic center (pK_a). The CNS MPO scoring has advantages in comparison with hard cut-offs or with the utilization of single parameters to optimize structure-activity relationships by enlarging medicinal chemistry design space through holistic assessment approaches (Wager et al. 2010). Moreover, this tool is designed to predict the absorption, distribution, metabolism, and excretion (ADME) and safety properties suitable for CNS targeting (Wager et al. 2010). We observed a score of 3.6 for Oxa12, which was similar to that determined for other well-known CNS drugs, thus indicating that Oxa12 has a good brain exposure. In addition, the extent of Oxa12 metabolism in mouse liver microsomes was also determined. We showed that Oxa12 has an estimated half-life of 13 min. Importantly, although the original Nec-1 presents a half-life of <5 min, other chemical optimizations of this compound had a half-life of approximately 1 h in mouse microsomal assays (Degterev et al. 2013). Therefore, although Oxa12 estimated half-life may negatively impact the systemic and brain exposure of this compound, our combined analysis of the CNS MPO score and metabolic data confirms that Oxa12 is a good addition to the chemical toolbox of CNS-targeting anti-necroptotic compounds.

Afterwards, we determined the ability of our selected hit to protect dopaminergic neuronal cells from death *in vivo* using the sub-acute MPTP mouse model. Several studies have already reported the involvement of necroptosis in various regimens of MPTP exposure, including in the acute and sub-chronic, as well in the 6-OHDA model (Hu et al. 2019; Oñate et al. 2020; Lin et al. 2020; Iannielli et al. 2018). Here, we used the sub-acute regimen of MPTP exposure, based on a unique injection of MPTP (40 mg/mL), and despite the absence of visible motor deficits, we observed a significant loss of dopaminergic enervation in the SN and striatum, 30 days post-injection, as revealed by a ~50% decrease of TH-positive cells (Fig. 4.1). No markers of necroptosis commitment were observed in these mice, which suggest that necroptosis may not play a prominent role in dopaminergic neurodegeneration, at least in our model. However, Oxa12 was able to protect from MPTP-mediated dopaminergic neuronal death in both SN and striatum. Although others have reported that Nec-1 or Nec-1s administration attenuated dopaminergic neurodegeneration (Iannielli et al. 2018; Lin et al. 2020; Oñate et al. 2020), here, we only observed a tendency of Nec-1s

to protect cells from MPTP-induced neurodegeneration. Additional work is thus needed to understand the concrete role of necroptosis during MPTP-driven neurodegeneration. In fact, others have described that different cell death pathways may be activated in both animal models of PD and PD patients (Lin et al. 2020). In fact, a recent study showed that MPTP-injected RIP3ko or MLKLko mice still present a small number of necrotic neurons (Lin et al. 2020). Moreover, longer exposure times to low MPTP doses seem to influence other cell death pathways, thus suggesting that shorter MPTP exposure may be ideal to detect necroptotic markers and determine the role of necroptosis in the MPTP-driven neurodegeneration. In fact, some authors detected increased levels of RIP1, RIP3 and MLKL in the SN, 7 days after injection, in a MPTP acute intoxication model, followed by a decrease in RIP3 levels until 21 days post-injection (Lin et al. 2020). Interestingly, others could not detect these necroptotic markers at 4, 6 or 30 days after MPTP injection (Dionísio et al. 2019), which could be related to the differences between the MPTP regimens. Therefore, additional work is needed to better understand the contribution of each specific cell death pathway during MPTP-driven neurodegeneration. Moreover, even though the molecular driver may be the same in animal models and humans, MPTP animal models do not completely recapitulate the broad spectrum of PD pathogenic mechanisms and symptoms (Meredith et al. 2011; Moffat et al. 2017).

Overall, necroptosis remains a promising therapeutic target in PD, particularly since inhibition of their molecular effectors has no deleterious effects in organismal homeostasis, contrarily to apoptotic inhibition. However, cell death inhibition may not translate into symptomatic improvement, since the underlying pathological mechanisms of PD including intracellular stress, mitochondrial dysfunction, energy depletion and lysosomal/proteasomal inhibition could still promote neuronal dysfunction through the recruitment of different RCD pathways or even passive necrosis (Poewe et al. 2017). In addition, TH-positive neuronal loss in the SN occurs mainly during the PD prodromal stage, with controlled subsequent neuronal death (Kordower et al. 2013). Thus, there is an urge need for the development of reliable clinical imaging and strong biomarkers for PD, especially during the prodromal phase, to attenuate disease progression at early stages.

Here, we also aimed at discovering a signature of miRNAs that could be used to distinguish PD-diagnosed patients from healthy individuals and, therefore, contribute to better understand PD pathophysiology and improve disease diagnosis (Fig. 4.1). Importantly, we identified a differential pattern of miRNA expression in iPD and LRRK2-PD patients in comparison with control subjects; with miR-146a, miR-335-3p and miR-335-5p being downregulated in PD patients and no significant variation in miR-21, miR-34a, miR-34c and miR-155. Previous studies have already described miR-146a as reduced in PD (Taganov et al. 2006; Caggiu et al. 2018). Importantly, miR-146a negatively regulates inflammation and immunity by interacting with IRAK1 and TRAF6 and attenuating inflammatory responses (Taganov et al. 2006; Caggiu et al. 2018). In fact, increasing evidence points for chronic inflammation as a hallmark and key risk factor for PD aggravation (Caggiu et al. 2018). These data suggest an overall pro-inflammatory environment in PD that may translate into a reduction in anti-inflammatory-like miRNAs, including miR-146a. Regarding miR-335, the existent literature is somehow contradictory, with studies showing a downregulation of this miRNA in whole blood and PBMCs isolated from PD patients (Martins et al. 2011; Yılmaz S et al. 2016), while others demonstrate an upregulation of miR-335 in PD patient serum samples (Patil et al. 2019). Here, we showed that both miR-335-3p and miR-335-5p were significantly reduced in the serum of iPD and LRRK2-PD patients. However, the discrepancy between studies may be attributed to different clinical cohorts used for miRNA extraction and analysis. In that regard, further investigation using larger cohorts could be instrumental to clarify this inconsistency. More importantly, miR-335 was confirmed to target LRRK2 gene *in silico* and *in vitro* (Patil et al. 2019). These results may suggest that a downregulation of miR-335 is PD could contribute to an increase in LRRK2 protein content, and consequently protein activity, which is often observed during PD pathogenesis (Cook et al. 2017). To further dissect this hypothesis, it would be interesting to investigate LRRK2 expression levels in PD samples, including immune cells and/or brain tissue. Interestingly, although we did not find significant differences between miR-155 expression in PD patients and controls; this miR was elevated in LRRK2-PD patients in comparison with iPD patients. In fact, increasing evidence has suggested that LRRK2 has a role in modulating inflammation in microglia (Moehle et al. 2012; Dzamko et al. 2015). Moreover,

LRRK2-PD patients could also present increased peripheral inflammation in comparison with iPD patients (Dzamko et al. 2015; Brockmann et al. 2017). In contrast with other studies (Junker et al. 2009; Miñones-Moyano et al. 2011; Bhattacharjee et al. 2014), we did not observe differences in miR-21, miR-34a and miR-34c expression between PD patients and controls. The variability between different studies could be easily related to the conditions of sample collection and storage, methodological heterogeneity, differences in miRNA normalization strategies, purification protocols, and different biologic samples and cohorts. In addition, some data have also demonstrated that antiparkinsonian medications may influence miRNA expression and expression of their target genes in PD patients. In fact, treatment with L-DOPA as well as deep brain stimulation seem to influence the expression profile of several miRNAs, which may further explain the differences observed among independent studies (Alieva et al. 2015; Margis et al. 2011; Soreq et al. 2013; Soreq et al. 2015).

Finally, based on our own work and that from other authors showing that miR-335 is altered in PD and that this miRNA could target LRRK2 (Martins et al. 2011; Patil et al. 2019), we decided to investigate how miR-335 affected inflammation and/or cell death pathway in PD-mimicking models (Fig. 4.1). Firstly, we proved here that miR-335 directly targets LRRK2, which is in accordance with previous *in silico* and *in vitro* studies (Patil et al. 2019; Yılmaz S et al. 2016). Furthermore, since we and others have shown that miR-335 is reduced in different *in vitro* and *in vivo* PD-mimicking models and in PD patients, we determined whether elevating miR-335 levels could impact on inflammation. Functionally, miR-335 overexpression counteracted LPS-induced inflammation in microglia cells, by decreasing RIP1 and RIP3 protein levels, ERK1/2 and NF-κB activation and proinflammatory gene expression. Some studies have already demonstrated that proinflammatory stimulation of microglia and macrophages and resulting RIP1 activation, may promote MAPK activation and, consequently, transcription factor activation and proinflammatory gene expression, with or without RIP3 recruitment and without cell death and MLKL involvement (Ito et al. 2016; Degterev, Ofengeim, and Yuan 2019; Hashimoto et al. 2003; Ofengeim et al. 2017). In fact, evidence has shown that key mechanisms of neurodegeneration may involve RIP1-mediated cell-autonomous mechanisms in microglial cells, which could lead to proinflammatory cytokine release, and

subsequent axonal degeneration, promoting a feedback loop where DAMPs released increase microglial inflammation and consequently neuronal death in a cell non-autonomous manner (Yuan et al. 2019). In accordance, others demonstrated that RIP1 kinase activity is required for inflammatory gene expression in myeloid cells in mice injected with a sublethal dose of LPS (Najjar et al. 2016). Indeed, RIP1 and RIP3 display several cell death-independent functions, including the regulation of immune responses, inflammasome activation and mitochondrial function, which are dependent on their kinase or scaffolding activities (Moriwaki et al. 2017a; Choi et al. 2019; Yuan et al. 2019). Thus, a better understanding of these functions may elucidate their role during a pathological condition and their targeted therapeutic strategies.

Further, some studies have reported that, in LPS-injected mice, RIP1- and RIP3-induced proinflammatory signalling is mediated by ERK1/2 pathway, without MEK1/2 requirement, their upstream regulators (Najjar et al. 2016). Moreover, others also suggested that increased LRRK2 protein levels promote EKR1/2 activation, without affecting p38 or JNK signalling pathways (Carballo-Carbajal et al. 2010). In accordance, we observed ERK1/2 and NF-κB activation in LPS-stimulated BV2 microglial cells and no differences in p38 and JNK activation. More importantly, LPS-mediated ERK1/2 and NF-κB activation were decreased in miR-335 overexpressing BV2 cells, which confirms miR-335 role in reducing inflammation, probably by targeting LRRK2. However, additional siLRRK2 experiments should still be conducted to further determine if miR-335 protective role in mediated by LRRK2 targeting. Accordantly, some studies have shown that miR-335 upregulation is associated with an overall reduced inflammatory environment (Gao et al. 2018; De Luna et al. 2020). Also, a potential interaction between LRRK2 and ERK pathway was already described in neuronal cells (Plowey et al. 2008; Liou et al. 2008). However, other studies showed activation of the JNK pathway in G2019S-LRRK2-PD patient-derived lymphoblasts, thus suggesting cell-type specific differences in LRRK2 scaffolding and MAPKs signalling interactions. In that regard, to further confirm miR-335 regulation of ERK1/2 pathway, we determined proinflammatory mRNA levels in BV2 cells after transfection with a plasmid encoding a constitutive active form of MEK1 (MEK1*), which is the upstream kinase of ERK1/2. We observed that MEK1* expression tended to abolish the miR-335 effect, thus indicating miR-335

regulation of ERK1/2 pathway. Interestingly, although no differences in RIP1, RIP3 or MLKL were observed in SH-SY5Y cells overexpressing α-syn, miR-335 overexpression counteracted α-syn-induced proinflammatory gene expression, therefore indicating that these cells may not depend on RIP1/3 signalling or, at least in our conditions, α-syn-mediated inflammation is not enough for inducing inflammatory-dependent activation of RIPs.

Additionally, several studies have reported the role of LRRK2 in the regulation of different inflammatory pathways, and its activation associated with neuronal death (Wang et al. 2012). Further, although LRRK2 mutations are usually linked to neuronal death, the role of LRRK2wt is still not completely comprehended, with studies suggesting a role in protecting SH-SY5Y cells from death, and others showing a deleterious effect by elevating α-syn levels in HEK293 cells (Moehle et al. 2012; Liou et al. 2008). Importantly, in neuronal and immune cells, LRRK2wt seems to contribute to mitochondrial fragmentation and inflammation (Hakimi et al. 2011; Berwick et al. 2019; Marker et al. 2012). Further, others have demonstrated that LRRK2wt overexpression in mice did not induce any PD-relevant phenotype (Xu et al. 2012). Concordantly, we observed that LRRK2wt did not influence cell death either in BV2 microglial and SH-SY5Y neuroblastoma cells. However, LRRK2wt overexpression strongly induced proinflammatory gene expression in BV2 microglial cells, which was further counteracted by miR-335 overexpression.

In conclusion, the work developed in this thesis brought novel insights on the discovery of novel small-molecule necroptosis inhibitors, as well as in miRNAs that might be used as promising therapeutic strategies. Moreover, a better understanding of the synergistic functions of necroptosis inhibition and miRNA-based strategies might increase their therapeutic potential for neurodegenerative diseases, including PD.

REFERENCES

Aaes, T. L., Kaczmarek, A., Delvaeye, T., De Craene, B., De Koker, S., Heyndrickx, L., . . . Krysko, D. V. (2016). Vaccination with Necroptotic Cancer Cells Induces Efficient Anti-tumor Immunity. *Cell reports, 15*(2), 274-287. doi:10.1016/j.celrep.2016.03.037

Abderrazak, A., Syrovets, T., Couchie, D., El Hadri, K., Friguet, B., Simmet, T., & Rouis, M. (2015). NLRP3 inflammasome: from a danger signal sensor to a regulatory node of oxidative stress and inflammatory diseases. *Redox Biol, 4*, 296-307. doi:10.1016/j.redox.2015.01.008

Afonso, M. B., Rodrigues, P. M., Carvalho, T., Caridade, M., Borralho, P., Cortez-Pinto, H., . . . Rodrigues, C. M. (2015). Necroptosis is a key pathogenic event in human and experimental murine models of non-alcoholic steatohepatitis. *Clin Sci (Lond), 129*(8), 721-739. doi:10.1042/cs20140732

Åkerblom, M., Sachdeva, R., Barde, I., Verp, S., Gentner, B., Trono, D., & Jakobsson, J. (2012). MicroRNA-124 is a subventricular zone neuronal fate determinant. *J Neurosci, 32*(26), 8879-8889. doi:10.1523/jneurosci.0558-12.2012

Alegre-Abarrategui, J., & Wade-Martins, R. (2009). Parkinson disease, LRRK2 and the endocytic-autophagic pathway. *Autophagy, 5*(8), 1208-1210. doi:10.4161/auto.5.8.9894

Alieva, A., Filatova, E. V., Karabanov, A. V., Illarioshkin, S. N., Limborska, S. A., Shadrina, M. I., & Slominsky, P. A. (2015). miRNA expression is highly sensitive to a drug therapy in Parkinson's disease. *Parkinsonism Relat Disord, 21*(1), 72-74. doi:10.1016/j.parkreldis.2014.10.018

Alvarez-Erviti, L., Seow, Y., Schapira, A. H., Rodriguez-Oroz, M. C., Obeso, J. A., & Cooper, J. M. (2013). Influence of microRNA deregulation on chaperone-mediated autophagy and α-synuclein pathology in Parkinson's disease. *Cell Death Dis, 4*(3), e545. doi:10.1038/cddis.2013.73

Anand, V. S., & Braithwaite, S. P. (2009). LRRK2 in Parkinson's disease: biochemical functions. *Febs j, 276*(22), 6428-6435. doi:10.1111/j.1742-4658.2009.07341.x

Andres-Mateos, E., Mejias, R., Sasaki, M., Li, X., Lin, B. M., Biskup, S., . . . Dawson, V. L. (2009). Unexpected lack of hypersensitivity in LRRK2 knock-out mice to MPTP (1-methyl-4-phenyl-1,2,3,6-tetrahydropyridine). *J Neurosci, 29*(50), 15846-15850. doi:10.1523/jneurosci.4357-09.2009

Anglade, P., Vyas, S., Javoy-Agid, F., Herrero, M. T., Michel, P. P., Marquez, J., . . . Agid, Y. (1997). Apoptosis and autophagy in nigral neurons of patients with Parkinson's disease. *Histol Histopathol, 12*(1), 25-31.

Ascherio, A., LeWitt, P. A., Xu, K., Eberly, S., Watts, A., Matson, W. R., . . . Schwarzschild, M. A. (2009). Urate as a predictor of the rate of clinical decline in Parkinson disease. *Arch Neurol, 66*(12), 1460-1468. doi:10.1001/archneurol.2009.247

Aviles-Olmos, I., Limousin, P., Lees, A., & Foltynie, T. (2013). Parkinson's disease, insulin resistance and novel agents of neuroprotection. *Brain, 136*(Pt 2), 374-384. doi:10.1093/brain/aws009

Barber, T. R., Klein, J. C., Mackay, C. E., & Hu, M. T. M. (2017). Neuroimaging in pre-motor Parkinson's disease. *NeuroImage. Clinical, 15*, 215-227. doi:10.1016/j.nicl.2017.04.011

Bardien, S., Lesage, S., Brice, A., & Carr, J. (2011). Genetic characteristics of leucine-rich repeat kinase 2 (LRRK2) associated Parkinson's disease. *Parkinsonism Relat Disord, 17*(7), 501-508. doi:10.1016/j.parkreldis.2010.11.008

Bartel, D. P. (2004). MicroRNAs: genomics, biogenesis, mechanism, and function. *Cell, 116*(2), 281-297. doi:10.1016/s0092-8674(04)00045-5

Béraud, D., Twomey, M., Bloom, B., Mittereder, A., Ton, V., Neitzke, K., . . . Maguire-Zeiss, K. A. (2011). α-Synuclein Alters Toll-Like Receptor Expression. *Front Neurosci, 5*, 80-80. doi:10.3389/fnins.2011.00080

Berger, S. B., Harris, P., Nagilla, R., Kasparcova, V., Hoffman, S., Swift, B., . . . Gough, P. J. (2015). Characterization of GSK'963: a structurally distinct, potent and selective inhibitor of RIP1 kinase. *Cell Death Discov, 1*, 15009. doi:10.1038/cddiscovery.2015.9

Berghe, T. V., Vanlangenakker, N., Parthoens, E., Deckers, W., Devos, M., Festjens, N., . . . Vandenabeele, P. (2010). Necroptosis, necrosis and secondary necrosis converge on similar cellular disintegration features. *Cell Death & Differentiation, 17*(6), 922-930. doi:10.1038/cdd.2009.184

Bertrand, M. J. M., Lippens, S., Staes, A., Gilbert, B., Roelandt, R., De Medts, J., . . . Vandenabeele, P. (2011). cIAP1/2 are direct E3 ligases conjugating diverse types of ubiquitin chains to receptor interacting proteins kinases 1 to 4 (RIP1-4). *PloS one, 6*(9), e22356-e22356. doi:10.1371/journal.pone.0022356

Berwick, D. C., Heaton, G. R., Azeggagh, S., & Harvey, K. (2019). LRRK2 Biology from structure to dysfunction: research progresses, but the themes remain the same. *Mol Neurodegener, 14*(1), 49. doi:10.1186/s13024-019-0344-2

Betarbet, R., Sherer, T. B., MacKenzie, G., Garcia-Osuna, M., Panov, A. V., & Greenamyre, J. T. (2000). Chronic systemic pesticide exposure reproduces features of Parkinson's disease. *Nat Neurosci, 3*(12), 1301-1306. doi:10.1038/81834

Bhattacharjee, S., Zhao, Y., & Lukiw, W. J. (2014). Deficits in the miRNA-34a-regulated endogenous TREM2 phagocytosis sensor-receptor in Alzheimer's disease (AD); an update. *Front Aging Neurosci, 6*, 116. doi:10.3389/fnagi.2014.00116

Bieri, G., Brahic, M., Bousset, L., Couthouis, J., Kramer, N. J., Ma, R., . . . Gitler, A. D. (2019). LRRK2 modifies α-syn pathology and spread in mouse models and human neurons. *Acta Neuropathol, 137*(6), 961-980. doi:10.1007/s00401-019-01995-0

Bigenzahn, J. W., Fauster, A., Rebsamen, M., Kandasamy, R. K., Scorzoni, S., Vladimer, G. I., . . . Superti-Furga, G. (2016). An Inducible Retroviral Expression System for Tandem Affinity Purification Mass-Spectrometry-Based Proteomics Identifies Mixed Lineage Kinase Domain-like Protein (MLKL) as an Heat Shock Protein 90 (HSP90) Client. *Mol Cell Proteomics, 15*(3), 1139-1150. doi:10.1074/mcp.o115.055350

Billingsley, K. J., Bandres-Ciga, S., Saez-Atienzar, S., & Singleton, A. B. (2018). Genetic risk factors in Parkinson's disease. *Cell Tissue Res, 373*(1), 9-20. doi:10.1007/s00441-018-2817-y

Biosa, A., Trancikova, A., Civiero, L., Glauser, L., Bubacco, L., Greggio, E., & Moore, D. J. (2012). GTPase activity regulates kinase activity and cellular phenotypes of Parkinson's disease-associated LRRK2. *Hum Mol Genet, 22*(6), 1140-1156. doi:10.1093/hmg/dds522

Biskup, S., Moore, D. J., Rea, A., Lorenz-Deperieux, B., Coombes, C. E., Dawson, V. L., . . . West, A. B. (2007). Dynamic and redundant regulation of LRRK2 and LRRK1 expression. *BMC Neurosci, 8*, 102. doi:10.1186/1471-2202-8-102

Blesa, J., & Przedborski, S. (2014). Parkinson's disease: animal models and dopaminergic cell vulnerability. *Front Neuroanat, 8*, 155. doi:10.3389/fnana.2014.00155

Bohgaki, T., Mozo, J., Salmena, L., Matysiak-Zablocki, E., Bohgaki, M., Sanchez, O., . . . Hakem, R. (2011). Caspase-8 inactivation in T cells increases necroptosis and suppresses autoimmunity in Bim-/- mice. *The Journal of cell biology, 195*(2), 277-291. doi:10.1083/jcb.201103053

Bolam, J. P., & Pissadaki, E. K. (2012). Living on the edge with too many mouths to feed: why dopamine neurons die. *Mov Disord, 27*(12), 1478-1483. doi:10.1002/mds.25135

Bonifati, V., Rizzu, P., van Baren, M. J., Schaap, O., Breedveld, G. J., Krieger, E., . . . Heutink, P. (2003). Mutations in the DJ-1 gene associated with autosomal recessive early-onset parkinsonism. *Science, 299*(5604), 256-259. doi:10.1126/science.1077209

Bonnet, M. C., Preukschat, D., Welz, P. S., van Loo, G., Ermolaeva, M. A., Bloch, W., . . . Pasparakis, M. (2011). The adaptor protein FADD protects epidermal keratinocytes from necroptosis in vivo and prevents skin inflammation. *Immunity, 35*(4), 572-582. doi:10.1016/j.immuni.2011.08.014

Booth, H. D. E., Hirst, W. D., & Wade-Martins, R. (2017). The Role of Astrocyte Dysfunction in Parkinson's Disease Pathogenesis. *Trends Neurosci, 40*(6), 358-370. doi:10.1016/j.tins.2017.04.001

Botta-Orfila, T., Morató, X., Compta, Y., Lozano, J. J., Falgàs, N., Valldeoriola, F., . . . Ezquerra, M. (2014). Identification of blood serum micro-RNAs associated with idiopathic and LRRK2 Parkinson's disease. *J Neurosci Res, 92*(8), 1071-1077. doi:10.1002/jnr.23377

Bové, J., & Perier, C. (2012). Neurotoxin-based models of Parkinson's disease. *Neuroscience, 211*, 51-76. doi:10.1016/j.neuroscience.2011.10.057

Braak, H., Del Tredici, K., Rüb, U., de Vos, R. A., Jansen Steur, E. N., & Braak, E. (2003). Staging of brain pathology related to sporadic Parkinson's disease. *Neurobiol Aging, 24*(2), 197-211. doi:10.1016/s0197-4580(02)00065-9

Bravo-San Pedro, J. M., Gómez-Sánchez, R., Pizarro-Estrella, E., Niso-Santano, M., González-Polo, R. A., & Fuentes Rodríguez, J. M. (2012). Parkinson's disease: leucine-rich repeat kinase 2 and autophagy, intimate enemies. *Parkinson's disease, 2012*, 151039-151039. doi:10.1155/2012/151039

Brenner, D., Blaser, H., & Mak, T. W. (2015). Regulation of tumour necrosis factor signalling: live or let die. *Nat Rev Immunol, 15*(6), 362-374. doi:10.1038/nri3834

Brito, H., Marques, V., Afonso, M. B., Brown, D. G., Börjesson, U., Selmi, N., . . . Rodrigues, C. M. P. (2020). Phenotypic high-throughput screening platform identifies novel chemotypes for necroptosis inhibition. *Cell Death Discovery, 6*(1), 6. doi:10.1038/s41420-020-0240-0

Brockmann, K., Schulte, C., Schneiderhan-Marra, N., Apel, A., Pont-Sunyer, C., Vilas, D., . . . Maetzler, W. (2017). Inflammatory profile discriminates clinical subtypes in LRRK2-associated Parkinson's disease. *Eur J Neurol, 24*(2), 427-e426. doi:10.1111/ene.13223

Butovsky, O., Siddiqui, S., Gabriely, G., Lanser, A. J., Dake, B., Murugaiyan, G., . . . Weiner, H. L. (2012). Modulating inflammatory monocytes with a unique microRNA gene signature ameliorates murine ALS. *J Clin Invest, 122*(9), 3063-3087. doi:10.1172/jci62636

Caccamo, A., Branca, C., Piras, I. S., Ferreira, E., Huentelman, M. J., Liang, W. S., . . . Oddo, S. (2017). Necroptosis activation in Alzheimer's disease. *Nat Neurosci, 20*(9), 1236-1246. doi:10.1038/nn.4608

Caggiu, E., Paulus, K., Mameli, G., Arru, G., Sechi, G. P., & Sechi, L. A. (2018). Differential expression of miRNA 155 and miRNA 146a in Parkinson's disease patients. *eNeurologicalSci, 13*, 1-4. doi:10.1016/j.ensci.2018.09.002

Cai, Z., Jitkaew, S., Zhao, J., Chiang, H. C., Choksi, S., Liu, J., . . . Liu, Z. G. (2014). Plasma membrane translocation of trimerized MLKL protein is required for TNF-induced necroptosis. *Nature cell biology, 16*(1), 55-65. doi:10.1038/ncb2883

Camandola, S., & Mattson, M. P. (2007). NF-kappa B as a therapeutic target in neurodegenerative diseases. *Expert Opin Ther Targets, 11*(2), 123-132. doi:10.1517/14728222.11.2.123

Cao, M., Chen, F., Xie, N., Cao, M. Y., Chen, P., Lou, Q., . . . Gao, H. (2018). c-Jun N-terminal kinases differentially regulate TNF- and TLRs-mediated necroptosis through their kinase-dependent and -independent activities. *Cell Death Dis, 9*(12), 1140. doi:10.1038/s41419-018-1189-2

Cao, S., Standaert, D. G., & Harms, A. S. (2012). The gamma chain subunit of Fc receptors is required for alpha-synuclein-induced pro-inflammatory signaling in microglia. *J Neuroinflammation, 9*, 259. doi:10.1186/1742-2094-9-259

Carballo-Carbajal, I., Weber-Endress, S., Rovelli, G., Chan, D., Wolozin, B., Klein, C. L., . . . Kahle, P. J. (2010). Leucine-rich repeat kinase 2 induces alpha-synuclein expression via the extracellular signal-regulated kinase pathway. *Cell Signal, 22*(5), 821-827. doi:10.1016/j.cellsig.2010.01.006

Cardoso, A. L., Guedes, J. R., Pereira de Almeida, L., & Pedroso de Lima, M. C. (2012). miR-155 modulates microglia-mediated immune response by down-regulating SOCS-1 and promoting cytokine and nitric oxide production. *Immunology, 135*(1), 73-88. doi:10.1111/j.1365-2567.2011.03514.x

Castro-Caldas, M., Neves Carvalho, A., Peixeiro, I., Rodrigues, E., Lechner, M. C., & Gama, M. J. (2009). GSTpi expression in MPTP-induced dopaminergic neurodegeneration of C57BL/6 mouse midbrain and striatum. *J Mol Neurosci, 38*(2), 114-127. doi:10.1007/s12031-008-9141-z

Chan, S. L., & Tan, E. K. (2017). Targeting LRRK2 in Parkinson's disease: an update on recent developments. *Expert Opin Ther Targets, 21*(6), 601-610. doi:10.1080/14728222.2017.1323881

Chaudhuri, K. R., & Odin, P. (2010). The challenge of non-motor symptoms in Parkinson's disease. *Prog Brain Res, 184*, 325-341. doi:10.1016/s0079-6123(10)84017-8

Chaudhuri, K. R., & Schapira, A. H. (2009). Non-motor symptoms of Parkinson's disease: dopaminergic pathophysiology and treatment. *Lancet Neurol, 8*(5), 464-474. doi:10.1016/s1474-4422(09)70068-7

Chavez-Valdez, R., Martin, L. J., Flock, D. L., & Northington, F. J. (2012). Necrostatin-1 attenuates mitochondrial dysfunction in neurons and astrocytes following neonatal hypoxia-ischemia. *Neuroscience, 219*, 192-203. doi:10.1016/j.neuroscience.2012.05.002

Chen, C. Y., Weng, Y. H., Chien, K. Y., Lin, K. J., Yeh, T. H., Cheng, Y. P., . . . Wang, H. L. (2012). (G2019S) LRRK2 activates MKK4-JNK pathway and causes degeneration of SN dopaminergic neurons in a transgenic mouse model of PD. *Cell Death Differ, 19*(10), 1623-1633. doi:10.1038/cdd.2012.42

Chen, H., Chan, B. K., Drummond, J., Estrada, A. A., Gunzner-Toste, J., Liu, X., . . . Burdick, D. J. (2012). Discovery of selective LRRK2 inhibitors guided by computational analysis and molecular modeling. *J Med Chem, 55*(11), 5536-5545. doi:10.1021/jm300452p

Chen, J., Chen, Y., & Pu, J. (2018). Leucine-Rich Repeat Kinase 2 in Parkinson's Disease: Updated from Pathogenesis to Potential Therapeutic Target. *Eur Neurol, 79*(5-6), 256-265. doi:10.1159/000488938

Chen, J., Jin, H., Xu, H., Peng, Y., Jie, L., Xu, D., . . . Chen, G. (2019). The Neuroprotective Effects of Necrostatin-1 on Subarachnoid Hemorrhage in Rats Are Possibly Mediated by Preventing Blood-Brain Barrier Disruption and RIP3-Mediated Necroptosis. *Cell Transplant, 28*(11), 1358-1372. doi:10.1177/0963689719867285

Chen, X., Ba, Y., Ma, L., Cai, X., Yin, Y., Wang, K., . . . Zhang, C. Y. (2008). Characterization of microRNAs in serum: a novel class of biomarkers for diagnosis of cancer and other diseases. *Cell Res, 18*(10), 997-1006. doi:10.1038/cr.2008.282

Chen, X., Li, W., Ren, J., Huang, D., He, W. T., Song, Y., . . . Han, J. (2014). Translocation of mixed lineage kinase domain-like protein to plasma membrane leads to necrotic cell death. *Cell Res, 24*(1), 105-121. doi:10.1038/cr.2013.171

Chen, Z. C., Zhang, W., Chua, L. L., Chai, C., Li, R., Lin, L., . . . Tan, E. K. (2017). Phosphorylation of amyloid precursor protein by mutant LRRK2 promotes AICD activity and neurotoxicity in Parkinson's disease. *Sci Signal, 10*(488). doi:10.1126/scisignal.aam6790

Cheng, L. C., Pastrana, E., Tavazoie, M., & Doetsch, F. (2009). miR-124 regulates adult neurogenesis in the subventricular zone stem cell niche. *Nat Neurosci, 12*(4), 399-408. doi:10.1038/nn.2294

Chien, H. F., Figueiredo, T. R., Hollaender, M. A., Tofoli, F., Takada, L. T., Pereira Lda, V., & Barbosa, E. R. (2014). Frequency of the LRRK2 G2019S mutation in late-onset sporadic patients with Parkinson's disease. *Arq Neuropsiquiatr, 72*(5), 356-359. doi:10.1590/0004-282x20140019

Chirieleison, S. M., Kertesy, S. B., & Abbott, D. W. (2016). Synthetic Biology Reveals the Uniqueness of the RIP Kinase Domain. *J Immunol, 196*(10), 4291-4297. doi:10.4049/jimmunol.1502631

Cho, H. J., Liu, G., Jin, S. M., Parisiadou, L., Xie, C., Yu, J., . . . Cai, H. (2013). MicroRNA-205 regulates the expression of Parkinson's disease-related leucine-rich repeat kinase 2 protein. *Hum Mol Genet, 22*(3), 608-620. doi:10.1093/hmg/dds470

Cho, Y. S., Challa, S., Moquin, D., Genga, R., Ray, T. D., Guildford, M., & Chan, F. K. (2009). Phosphorylation-driven assembly of the RIP1-RIP3 complex regulates programmed necrosis and virus-induced inflammation. *Cell, 137*(6), 1112-1123. doi:10.1016/j.cell.2009.05.037

Choi, D. C., Chae, Y. J., Kabaria, S., Chaudhuri, A. D., Jain, M. R., Li, H., . . . Junn, E. (2014). MicroRNA-7 protects against 1-methyl-4-phenylpyridinium-induced cell death by targeting RelA. *J Neurosci, 34*(38), 12725-12737. doi:10.1523/jneurosci.0985-14.2014

Choi, M. E., Price, D. R., Ryter, S. W., & Choi, A. M. K. (2019). Necroptosis: a crucial pathogenic mediator of human disease. *JCI Insight, 4*(15). doi:10.1172/jci.insight.128834

Christofferson, D. E., Li, Y., Hitomi, J., Zhou, W., Upperman, C., Zhu, H., . . . Yuan, J. (2012). A novel role for RIP1 kinase in mediating TNFα production. *Cell Death Dis, 3*(6), e320-e320. doi:10.1038/cddis.2012.64

Chung, J. Y., Lee, S. J., Lee, S. H., Jung, Y. S., Ha, N. C., Seol, W., & Park, B. J. (2011). Direct interaction of α-synuclein and AKT regulates IGF-1 signaling: implication of Parkinson disease. *Neurosignals, 19*(2), 86-96. doi:10.1159/000325028

Cipriani, S., Chen, X., & Schwarzschild, M. A. (2010). Urate: a novel biomarker of Parkinson's disease risk, diagnosis and prognosis. *Biomark Med, 4*(5), 701-712. doi:10.2217/bmm.10.94

Connolly, B. S., & Lang, A. E. (2014). Pharmacological treatment of Parkinson disease: a review. *JAMA, 311*(16), 1670-1683. doi:10.1001/jama.2014.3654

Conos, S. A., Chen, K. W., De Nardo, D., Hara, H., Whitehead, L., Núñez, G., . . . Vince, J. E. (2017). Active MLKL triggers the NLRP3 inflammasome in a cell-intrinsic manner. *Proc Natl Acad Sci U S A, 114*(6), E961-e969. doi:10.1073/pnas.1613305114

Conrad, M., Angeli, J. P., Vandenabeele, P., & Stockwell, B. R. (2016). Regulated necrosis: disease relevance and therapeutic opportunities. *Nat Rev Drug Discov, 15*(5), 348-366. doi:10.1038/nrd.2015.6

Cook, D. A., Kannarkat, G. T., Cintron, A. F., Butkovich, L. M., Fraser, K. B., Chang, J., . . . Tansey, M. G. (2017). LRRK2 levels in immune cells are increased in Parkinson's disease. *npj Parkinson's Disease, 3*(1), 11. doi:10.1038/s41531-017-0010-8

Cookson, M. R. (2010). The role of leucine-rich repeat kinase 2 (LRRK2) in Parkinson's disease. *Nat Rev Neurosci, 11*(12), 791-797. doi:10.1038/nrn2935

Correia Guedes, L., Ferreira, J. J., Rosa, M. M., Coelho, M., Bonifati, V., & Sampaio, C. (2010). Worldwide frequency of G2019S LRRK2 mutation in Parkinson's disease: a systematic review. *Parkinsonism Relat Disord, 16*(4), 237-242. doi:10.1016/j.parkreldis.2009.11.004

Cosín-Tomás, M., Antonell, A., Lladó, A., Alcolea, D., Fortea, J., Ezquerra, M., . . . Kaliman, P. (2017). Plasma miR-34a-5p and miR-545-3p as Early Biomarkers of Alzheimer's Disease: Potential and Limitations. *Mol Neurobiol, 54*(7), 5550-5562. doi:10.1007/s12035-016-0088-8

Cusson-Hermance, N., Khurana, S., Lee, T. H., Fitzgerald, K. A., & Kelliher, M. A. (2005). Rip1 mediates the Trif-dependent toll-like receptor 3- and 4-induced NF-{kappa}B activation but does not contribute to interferon regulatory factor 3 activation. *J Biol Chem, 280*(44), 36560-36566. doi:10.1074/jbc.M506831200

Daher, J. P., Abdelmotilib, H. A., Hu, X., Volpicelli-Daley, L. A., Moehle, M. S., Fraser, K. B., . . . West, A. B. (2015). Leucine-rich Repeat Kinase 2 (LRRK2) Pharmacological Inhibition Abates α-Synuclein Gene-induced Neurodegeneration. *J Biol Chem, 290*(32), 19433-19444. doi:10.1074/jbc.M115.660001

Daher, J. P., Volpicelli-Daley, L. A., Blackburn, J. P., Moehle, M. S., & West, A. B. (2014). Abrogation of α-synuclein-mediated dopaminergic neurodegeneration in LRRK2-deficient rats. *Proc Natl Acad Sci U S A, 111*(25), 9289-9294. doi:10.1073/pnas.1403215111

Damier, P., Hirsch, E. C., Agid, Y., & Graybiel, A. M. (1999). The substantia nigra of the human brain. I. Nigrosomes and the nigral matrix, a compartmental organization based on calbindin D(28K) immunohistochemistry. *Brain, 122 (Pt 8)*, 1421-1436. doi:10.1093/brain/122.8.1421

Danborg, P. B., Simonsen, A. H., Waldemar, G., & Heegaard, N. H. (2014). The potential of microRNAs as biofluid markers of neurodegenerative diseases--a systematic review. *Biomarkers, 19*(4), 259-268. doi:10.3109/1354750x.2014.904001

Daniëls, V., Vancraenenbroeck, R., Law, B. M., Greggio, E., Lobbestael, E., Gao, F., . . . Taymans, J. M. (2011). Insight into the mode of action of the LRRK2 Y1699C pathogenic mutant. *J Neurochem, 116*(2), 304-315. doi:10.1111/j.1471-4159.2010.07105.x

Dannappel, M., Vlantis, K., Kumari, S., Polykratis, A., Kim, C., Wachsmuth, L., . . . Pasparakis, M. (2014). RIPK1 maintains epithelial homeostasis by inhibiting apoptosis and necroptosis. *Nature, 513*(7516), 90-94. doi:10.1038/nature13608

Dauer, W., & Przedborski, S. (2003). Parkinson's disease: mechanisms and models. *Neuron, 39*(6), 889-909. doi:10.1016/s0896-6273(03)00568-3

Davidovich, P., Kearney, C. J., & Martin, S. J. (2014). Inflammatory outcomes of apoptosis, necrosis and necroptosis. *Biol Chem, 395*(10), 1163-1171. doi:10.1515/hsz-2014-0164

Davies, K. A., Tanzer, M. C., Griffin, M. D. W., Mok, Y. F., Young, S. N., Qin, R., . . . Murphy, J. M. (2018). The brace helices of MLKL mediate interdomain communication and oligomerisation to regulate cell death by necroptosis. *Cell Death Differ, 25*(9), 1567-1580. doi:10.1038/s41418-018-0061-3

Davies, P., Hinkle, K. M., Sukar, N. N., Sepulveda, B., Mesias, R., Serrano, G., . . . Melrose, H. L. (2013). Comprehensive characterization and optimization of anti-LRRK2 (leucine-rich repeat kinase 2) monoclonal antibodies. *Biochem J, 453*(1), 101-113. doi:10.1042/bj20121742

De Luna, N., Turon-Sans, J., Cortes-Vicente, E., Carrasco-Rozas, A., Illán-Gala, I., Dols-Icardo, O., . . . Rojas-García, R. (2020). Downregulation of miR-335-5P in Amyotrophic Lateral Sclerosis Can Contribute to Neuronal Mitochondrial Dysfunction and Apoptosis. *Sci Rep, 10*(1), 4308. doi:10.1038/s41598-020-61246-1

Declercq, W., Vanden Berghe, T., & Vandenabeele, P. (2009). RIP kinases at the crossroads of cell death and survival. *Cell, 138*(2), 229-232. doi:10.1016/j.cell.2009.07.006

Degterev, A., Hitomi, J., Germscheid, M., Ch'en, I. L., Korkina, O., Teng, X., . . . Yuan, J. (2008). Identification of RIP1 kinase as a specific cellular target of necrostatins. *Nat Chem Biol, 4*(5), 313-321. doi:10.1038/nchembio.83

Degterev, A., Huang, Z., Boyce, M., Li, Y., Jagtap, P., Mizushima, N., . . . Yuan, J. (2005). Chemical inhibitor of nonapoptotic cell death with therapeutic potential for ischemic brain injury. *Nat Chem Biol, 1*(2), 112-119. doi:10.1038/nchembio711

Degterev, A., Maki, J. L., & Yuan, J. (2013). Activity and specificity of necrostatin-1, small-molecule inhibitor of RIP1 kinase. *Cell Death & Differentiation, 20*(2), 366-366. doi:10.1038/cdd.2012.133

Degterev, A., Ofengeim, D., & Yuan, J. (2019). Targeting RIPK1 for the treatment of human diseases. *Proc Natl Acad Sci U S A, 116*(20), 9714-9722. doi:10.1073/pnas.1901179116

Dermentzaki, G., Politi, K. A., Lu, L., Mishra, V., Pérez-Torres, E. J., Sosunov, A. A., . . . Przedborski, S. (2019). Deletion of Ripk3 Prevents Motor Neuron Death In Vitro but not In Vivo. *eNeuro, 6*(1). doi:10.1523/eneuro.0308-18.2018

Devos, D., Moreau, C., Devedjian, J. C., Kluza, J., Petrault, M., Laloux, C., . . . Bordet, R. (2014). Targeting chelatable iron as a therapeutic modality in Parkinson's disease. *Antioxid Redox Signal, 21*(2), 195-210. doi:10.1089/ars.2013.5593

Dhillon, A. S., Hagan, S., Rath, O., & Kolch, W. (2007). MAP kinase signalling pathways in cancer. *Oncogene, 26*(22), 3279-3290. doi:10.1038/sj.onc.1210421

Di, L., Kerns, E. H., Li, S. Q., & Petusky, S. L. (2006). High throughput microsomal stability assay for insoluble compounds. *Int J Pharm, 317*(1), 54-60. doi:10.1016/j.ijpharm.2006.03.007

Di Maio, R., Hoffman, E. K., Rocha, E. M., Keeney, M. T., Sanders, L. H., De Miranda, B. R., . . . Greenamyre, J. T. (2018). LRRK2 activation in idiopathic Parkinson's disease. *Sci Transl Med, 10*(451). doi:10.1126/scitranslmed.aar5429

Dias, V., Junn, E., & Mouradian, M. M. (2013). The role of oxidative stress in Parkinson's disease. *J Parkinsons Dis, 3*(4), 461-491. doi:10.3233/jpd-130230

Dillon, C. P., Oberst, A., Weinlich, R., Janke, L. J., Kang, T.-B., Ben-Moshe, T., . . . Green, D. R. (2012). Survival function of the FADD-CASPASE-8-cFLIP(L) complex. *Cell reports, 1*(5), 401-407. doi:10.1016/j.celrep.2012.03.010

Dionísio, P. A., Oliveira, S. R., Gaspar, M. M., Gama, M. J., Castro-Caldas, M., Amaral, J. D., & Rodrigues, C. M. P. (2019). Ablation of RIP3 protects from dopaminergic neurodegeneration in experimental Parkinson's disease. *Cell Death Dis, 10*(11), 840. doi:10.1038/s41419-019-2078-z

Dobbs, R. J., Charlett, A., Purkiss, A. G., Dobbs, S. M., Weller, C., & Peterson, D. W. (1999). Association of circulating TNF-alpha and IL-6 with ageing and parkinsonism. *Acta Neurol Scand, 100*(1), 34-41. doi:10.1111/j.1600-0404.1999.tb00721.x

Dondelinger, Y., Declercq, W., Montessuit, S., Roelandt, R., Goncalves, A., Bruggeman, I., . . . Vandenabeele, P. (2014). MLKL compromises plasma membrane integrity by binding to phosphatidylinositol phosphates. *Cell reports, 7*(4), 971-981. doi:10.1016/j.celrep.2014.04.026

Dondelinger, Y., Hulpiau, P., Saeys, Y., Bertrand, M. J. M., & Vandenabeele, P. (2016). An evolutionary perspective on the necroptotic pathway. *Trends Cell Biol, 26*(10), 721-732. doi:10.1016/j.tcb.2016.06.004

Dos Santos, M. C. T., Barreto-Sanz, M. A., Correia, B. R. S., Bell, R., Widnall, C., Perez, L. T., . . . Nogueira da Costa, A. (2018). miRNA-based signatures in cerebrospinal fluid as potential diagnostic tools for early stage Parkinson's disease. *Oncotarget, 9*(25), 17455-17465. doi:10.18632/oncotarget.24736

Doxakis, E. (2010). Post-transcriptional regulation of alpha-synuclein expression by mir-7 and mir-153. *J Biol Chem, 285*(17), 12726-12734. doi:10.1074/jbc.M109.086827

Dzamko, N., Geczy, C. L., & Halliday, G. M. (2015). Inflammation is genetically implicated in Parkinson's disease. *Neuroscience, 302*, 89-102. doi:10.1016/j.neuroscience.2014.10.028

Dzamko, N., Rowe, D. B., & Halliday, G. M. (2016). Increased peripheral inflammation in asymptomatic leucine-rich repeat kinase 2 mutation carriers. *Mov Disord, 31*(6), 889-897. doi:10.1002/mds.26529

Emamzadeh, F. N., & Surguchov, A. (2018). Parkinson's Disease: Biomarkers, Treatment, and Risk Factors. *Front Neurosci, 12*, 612. doi:10.3389/fnins.2018.00612

Etheridge, A., Lee, I., Hood, L., Galas, D., & Wang, K. (2011). Extracellular microRNA: a new source of biomarkers. *Mutat Res, 717*(1-2), 85-90. doi:10.1016/j.mrfmmm.2011.03.004

Farrer, M., Chan, P., Chen, R., Tan, L., Lincoln, S., Hernandez, D., . . . Langston, J. W. (2001). Lewy bodies and parkinsonism in families with parkin mutations. *Ann Neurol, 50*(3), 293-300. doi:10.1002/ana.1132

Fauster, A., Rebsamen, M., Huber, K. V., Bigenzahn, J. W., Stukalov, A., Lardeau, C. H., . . . Superti-Furga, G. (2015). A cellular screen identifies ponatinib and pazopanib as inhibitors of necroptosis. *Cell Death Dis, 6*(5), e1767. doi:10.1038/cddis.2015.130

Fearnley, J. M., & Lees, A. J. (1991). Ageing and Parkinson's disease: substantia nigra regional selectivity. *Brain, 114 (Pt 5)*, 2283-2301. doi:10.1093/brain/114.5.2283

Feoktistova, M., Geserick, P., Kellert, B., Dimitrova, D. P., Langlais, C., Hupe, M., . . . Leverkus, M. (2011). cIAPs block Ripoptosome formation, a RIP1/caspase-8 containing intracellular cell death complex differentially regulated by cFLIP isoforms. *Mol Cell, 43*(3), 449-463. doi:10.1016/j.molcel.2011.06.011

Ferracin, M., Lupini, L., Salamon, I., Saccenti, E., Zanzi, M. V., Rocchi, A., . . . Negrini, M. (2015). Absolute quantification of cell-free microRNAs in cancer patients. *Oncotarget, 6*(16), 14545-14555. doi:10.18632/oncotarget.3859

Festjens, N., Vanden Berghe, T., Cornelis, S., & Vandenabeele, P. (2007). RIP1, a kinase on the crossroads of a cell's decision to live or die. *Cell Death Differ, 14*(3), 400-410. doi:10.1038/sj.cdd.4402085

Fornai, F., Schlüter, O. M., Lenzi, P., Gesi, M., Ruffoli, R., Ferrucci, M., . . . Südhof, T. C. (2005). Parkinson-like syndrome induced by continuous MPTP infusion: convergent roles of the ubiquitin-proteasome system and alpha-synuclein. *Proc Natl Acad Sci U S A, 102*(9), 3413-3418. doi:10.1073/pnas.0409713102

Fragkouli, A., & Doxakis, E. (2014). miR-7 and miR-153 protect neurons against MPP(+)-induced cell death via upregulation of mTOR pathway. *Frontiers in cellular neuroscience, 8*, 182. doi:10.3389/fncel.2014.00182

Fredriksson, A., & Archer, T. (1994). MPTP-induced behavioural and biochemical deficits: a parametric analysis. *J Neural Transm Park Dis Dement Sect, 7*(2), 123-132. doi:10.1007/bf02260967

Fricker, M., Vilalta, A., Tolkovsky, A. M., & Brown, G. C. (2013). Caspase inhibitors protect neurons by enabling selective necroptosis of inflamed microglia. *J Biol Chem, 288*(13), 9145-9152. doi:10.1074/jbc.M112.427880

Friedman, R. C., Farh, K. K., Burge, C. B., & Bartel, D. P. (2009). Most mammalian mRNAs are conserved targets of microRNAs. *Genome Res, 19*(1), 92-105. doi:10.1101/gr.082701.108

Fuchs, Y., & Steller, H. (2011). Programmed cell death in animal development and disease. *Cell, 147*(4), 742-758. doi:10.1016/j.cell.2011.10.033

Gaba, A., Xu, F., Lu, Y., Park, H. S., Liu, G., & Zhou, Y. (2019). The NS1 Protein of Influenza A Virus Participates in Necroptosis by Interacting with MLKL and Increasing Its Oligomerization and Membrane Translocation. *J Virol, 93*(2). doi:10.1128/jvi.01835-18

Gaig, C., Vilas, D., Infante, J., Sierra, M., García-Gorostiaga, I., Buongiorno, M., . . . Tolosa, E. (2014). Nonmotor symptoms in LRRK2 G2019S associated Parkinson's disease. *PloS one, 9*(10), e108982. doi:10.1371/journal.pone.0108982

Gallo, A., Tandon, M., Alevizos, I., & Illei, G. G. (2012). The majority of microRNAs detectable in serum and saliva is concentrated in exosomes. *PLoS One, 7*(3), e30679. doi:10.1371/journal.pone.0030679

Gallo, K. A., & Johnson, G. L. (2002). Mixed-lineage kinase control of JNK and p38 MAPK pathways. *Nat Rev Mol Cell Biol, 3*(9), 663-672. doi:10.1038/nrm906

Galluzzi, L., Vitale, I., Aaronson, S. A., Abrams, J. M., Adam, D., Agostinis, P., . . . Kroemer, G. (2018). Molecular mechanisms of cell death: recommendations of the Nomenclature Committee on Cell Death 2018. *Cell Death & Differentiation, 25*(3), 486-541. doi:10.1038/s41418-017-0012-4

Gan-Or, Z., Leblond, C. S., Mallett, V., Orr-Urtreger, A., Dion, P. A., & Rouleau, G. A. (2015). LRRK2 mutations in Parkinson disease; a sex effect or lack thereof? A meta-analysis. *Parkinsonism Relat Disord, 21*(7), 778-782. doi:10.1016/j.parkreldis.2015.05.002

Gao, H. M., Zhang, F., Zhou, H., Kam, W., Wilson, B., & Hong, J. S. (2011). Neuroinflammation and α-synuclein dysfunction potentiate each other, driving chronic progression of

neurodegeneration in a mouse model of Parkinson's disease. *Environ Health Perspect, 119*(6), 807-814. doi:10.1289/ehp.1003013

Gao, X. L., Li, J. Q., Dong, Y. T., Cheng, E. J., Gong, J. N., Qin, Y. L., . . . An, D. D. (2018). Upregulation of microRNA-335-5p reduces inflammatory responses by inhibiting FASN through the activation of AMPK/ULK1 signaling pathway in a septic mouse model. *Cytokine, 110*, 466-478. doi:10.1016/j.cyto.2018.05.016

Gardet, A., Benita, Y., Li, C., Sands, B. E., Ballester, I., Stevens, C., . . . Podolsky, D. K. (2010). LRRK2 is involved in the IFN-gamma response and host response to pathogens. *J Immunol, 185*(9), 5577-5585. doi:10.4049/jimmunol.1000548

Gaudet, A. D., Fonken, L. K., Watkins, L. R., Nelson, R. J., & Popovich, P. G. (2018). MicroRNAs: Roles in Regulating Neuroinflammation. *Neuroscientist, 24*(3), 221-245. doi:10.1177/1073858417721150

Gehrke, S., Imai, Y., Sokol, N., & Lu, B. (2010). Pathogenic LRRK2 negatively regulates microRNA-mediated translational repression. *Nature, 466*(7306), 637-641. doi:10.1038/nature09191

Gerhard, A., Pavese, N., Hotton, G., Turkheimer, F., Es, M., Hammers, A., . . . Brooks, D. J. (2006). In vivo imaging of microglial activation with [11C](R)-PK11195 PET in idiopathic Parkinson's disease. *Neurobiol Dis, 21*(2), 404-412. doi:10.1016/j.nbd.2005.08.002

Giasson, B. I., Covy, J. P., Bonini, N. M., Hurtig, H. I., Farrer, M. J., Trojanowski, J. Q., & Van Deerlin, V. M. (2006). Biochemical and pathological characterization of Lrrk2. *Ann Neurol, 59*(2), 315-322. doi:10.1002/ana.20791

Gillardon, F., Schmid, R., & Draheim, H. (2012). Parkinson's disease-linked leucine-rich repeat kinase 2(R1441G) mutation increases proinflammatory cytokine release from activated primary microglial cells and resultant neurotoxicity. *Neuroscience, 208*, 41-48. doi:10.1016/j.neuroscience.2012.02.001

Gilsbach, B. K., & Kortholt, A. (2014). Structural biology of the LRRK2 GTPase and kinase domains: implications for regulation. *Front Mol Neurosci, 7*, 32. doi:10.3389/fnmol.2014.00032

Global, regional, and national burden of neurological disorders during 1990-2015: a systematic analysis for the Global Burden of Disease Study 2015. (2017). *Lancet Neurol, 16*(11), 877-897. doi:10.1016/s1474-4422(17)30299-5

Global, regional, and national burden of neurological disorders, 1990-2016: a systematic analysis for the Global Burden of Disease Study 2016. (2019). *Lancet Neurol, 18*(5), 459-480. doi:10.1016/s1474-4422(18)30499-x

Gloeckner, C. J., Kinkl, N., Schumacher, A., Braun, R. J., O'Neill, E., Meitinger, T., . . . Ueffing, M. (2006). The Parkinson disease causing LRRK2 mutation I2020T is associated with increased kinase activity. *Hum Mol Genet, 15*(2), 223-232. doi:10.1093/hmg/ddi439

Gmitterová, K., Heinemann, U., Gawinecka, J., Varges, D., Ciesielczyk, B., Valkovic, P., . . . Zerr, I. (2009). 8-OHdG in cerebrospinal fluid as a marker of oxidative stress in various neurodegenerative diseases. *Neurodegener Dis, 6*(5-6), 263-269. doi:10.1159/000237221

Goetz, C. G., Fahn, S., Martinez-Martin, P., Poewe, W., Sampaio, C., Stebbins, G. T., . . . LaPelle, N. (2007). Movement Disorder Society-sponsored revision of the Unified Parkinson's Disease Rating Scale (MDS-UPDRS): Process, format, and clinimetric testing plan. *Mov Disord, 22*(1), 41-47. doi:10.1002/mds.21198

Gomez Perdiguero, E., Klapproth, K., Schulz, C., Busch, K., Azzoni, E., Crozet, L., . . . Rodewald, H. R. (2015). Tissue-resident macrophages originate from yolk-sac-derived erythro-myeloid progenitors. *Nature, 518*(7540), 547-551. doi:10.1038/nature13989

Gong, Y., Fan, Z., Luo, G., Yang, C., Huang, Q., Fan, K., . . . Liu, C. (2019). The role of necroptosis in cancer biology and therapy. *Mol Cancer, 18*(1), 100. doi:10.1186/s12943-019-1029-8

González-Juarbe, N., Gilley, R. P., Hinojosa, C. A., Bradley, K. M., Kamei, A., Gao, G., . . . Orihuela, C. J. (2015). Pore-Forming Toxins Induce Macrophage Necroptosis during Acute Bacterial Pneumonia. *PLoS Pathog, 11*(12), e1005337. doi:10.1371/journal.ppat.1005337

Goossens, V., Stangé, G., Moens, K., Pipeleers, D., & Grooten, J. (1999). Regulation of tumor necrosis factor-induced, mitochondria- and reactive oxygen species-dependent cell death by the electron flux through the electron transport chain complex I. *Antioxid Redox Signal, 1*(3), 285-295. doi:10.1089/ars.1999.1.3-285

Greggio, E., Zambrano, I., Kaganovich, A., Beilina, A., Taymans, J. M., Daniëls, V., . . . Cookson, M. R. (2008). The Parkinson disease-associated leucine-rich repeat kinase 2 (LRRK2) is a dimer that undergoes intramolecular autophosphorylation. *J Biol Chem, 283*(24), 16906-16914. doi:10.1074/jbc.M708718200

Grootjans, S., Vanden Berghe, T., & Vandenabeele, P. (2017). Initiation and execution mechanisms of necroptosis: an overview. *Cell Death Differ, 24*(7), 1184-1195. doi:10.1038/cdd.2017.65

Gui, Y., Liu, H., Zhang, L., Lv, W., & Hu, X. (2015). Altered microRNA profiles in cerebrospinal fluid exosome in Parkinson disease and Alzheimer disease. *Oncotarget, 6*(35), 37043-37053. doi:10.18632/oncotarget.6158

Guo, H., Omoto, S., Harris, P. A., Finger, J. N., Bertin, J., Gough, P. J., . . . Mocarski, E. S. (2015). Herpes simplex virus suppresses necroptosis in human cells. *Cell Host Microbe, 17*(2), 243-251. doi:10.1016/j.chom.2015.01.003

Guo, L., Gandhi, P. N., Wang, W., Petersen, R. B., Wilson-Delfosse, A. L., & Chen, S. G. (2007). The Parkinson's disease-associated protein, leucine-rich repeat kinase 2 (LRRK2), is an authentic GTPase that stimulates kinase activity. *Exp Cell Res, 313*(16), 3658-3670. doi:10.1016/j.yexcr.2007.07.007

Gutierrez, K. D., Davis, M. A., Daniels, B. P., Olsen, T. M., Ralli-Jain, P., Tait, S. W., . . . Oberst, A. (2017). MLKL Activation Triggers NLRP3-Mediated Processing and Release of IL-1β Independently of Gasdermin-D. *J Immunol, 198*(5), 2156-2164. doi:10.4049/jimmunol.1601757

Haas, T. L., Emmerich, C. H., Gerlach, B., Schmukle, A. C., Cordier, S. M., Rieser, E., . . . Walczak, H. (2009). Recruitment of the linear ubiquitin chain assembly complex stabilizes the TNF-R1 signaling complex and is required for TNF-mediated gene induction. *Mol Cell, 36*(5), 831-844. doi:10.1016/j.molcel.2009.10.013

Hakimi, M., Selvanantham, T., Swinton, E., Padmore, R. F., Tong, Y., Kabbach, G., . . . Schlossmacher, M. G. (2011). Parkinson's disease-linked LRRK2 is expressed in circulating and tissue immune cells and upregulated following recognition of microbial structures. *J Neural Transm (Vienna), 118*(5), 795-808. doi:10.1007/s00702-011-0653-2

Halliday, G. M., & McCann, H. (2010). The progression of pathology in Parkinson's disease. *Ann N Y Acad Sci, 1184*, 188-195. doi:10.1111/j.1749-6632.2009.05118.x

Hänggi, K., Vasilikos, L., Valls, A. F., Yerbes, R., Knop, J., Spilgies, L. M., . . . Wong, W. W.-L. (2017). RIPK1/RIPK3 promotes vascular permeability to allow tumor cell extravasation

independent of its necroptotic function. *Cell Death Dis, 8*(2), e2588-e2588. doi:10.1038/cddis.2017.20

Harris, P. A., Bandyopadhyay, D., Berger, S. B., Campobasso, N., Capriotti, C. A., Cox, J. A., . . . Gough, P. J. (2013). Discovery of Small Molecule RIP1 Kinase Inhibitors for the Treatment of Pathologies Associated with Necroptosis. *ACS Med Chem Lett, 4*(12), 1238-1243. doi:10.1021/ml400382p

Harris, P. A., Berger, S. B., Jeong, J. U., Nagilla, R., Bandyopadhyay, D., Campobasso, N., . . . Bertin, J. (2017). Discovery of a First-in-Class Receptor Interacting Protein 1 (RIP1) Kinase Specific Clinical Candidate (GSK2982772) for the Treatment of Inflammatory Diseases. *J Med Chem, 60*(4), 1247-1261. doi:10.1021/acs.jmedchem.6b01751

Hashimoto, Y., Tsuji, O., Niikura, T., Yamagishi, Y., Ishizaka, M., Kawasumi, M., . . . Nishimoto, I. (2003). Involvement of c-Jun N-terminal kinase in amyloid precursor protein-mediated neuronal cell death. *J Neurochem, 84*(4), 864-877. doi:10.1046/j.1471-4159.2003.01585.x

Hatano, T., Kubo, S., Imai, S., Maeda, M., Ishikawa, K., Mizuno, Y., & Hattori, N. (2007). Leucine-rich repeat kinase 2 associates with lipid rafts. *Hum Mol Genet, 16*(6), 678-690. doi:10.1093/hmg/ddm013

Hattori, N., Tanaka, M., Ozawa, T., & Mizuno, Y. (1991). Immunohistochemical studies on complexes I, II, III, and IV of mitochondria in Parkinson's disease. *Ann Neurol, 30*(4), 563-571. doi:10.1002/ana.410300409

He, S., Liang, Y., Shao, F., & Wang, X. (2011). Toll-like receptors activate programmed necrosis in macrophages through a receptor-interacting kinase-3-mediated pathway. *Proc Natl Acad Sci U S A, 108*(50), 20054-20059. doi:10.1073/pnas.1116302108

He, S., Wang, L., Miao, L., Wang, T., Du, F., Zhao, L., & Wang, X. (2009). Receptor interacting protein kinase-3 determines cellular necrotic response to TNF-alpha. *Cell, 137*(6), 1100-1111. doi:10.1016/j.cell.2009.05.021

He, S., & Wang, X. (2018). RIP kinases as modulators of inflammation and immunity. *Nat Immunol, 19*(9), 912-922. doi:10.1038/s41590-018-0188-x

Healy, D. G., Falchi, M., O'Sullivan, S. S., Bonifati, V., Durr, A., Bressman, S., . . . Wood, N. W. (2008). Phenotype, genotype, and worldwide genetic penetrance of LRRK2-associated Parkinson's disease: a case-control study. *Lancet Neurol, 7*(7), 583-590. doi:10.1016/s1474-4422(08)70117-0

Henn, I. H., Gostner, J. M., Lackner, P., Tatzelt, J., & Winklhofer, K. F. (2005). Pathogenic mutations inactivate parkin by distinct mechanisms. *J Neurochem, 92*(1), 114-122. doi:10.1111/j.1471-4159.2004.02854.x

Herrera, B. M., Lockstone, H. E., Taylor, J. M., Ria, M., Barrett, A., Collins, S., . . . Lindgren, C. M. (2010). Global microRNA expression profiles in insulin target tissues in a spontaneous rat model of type 2 diabetes. *Diabetologia, 53*(6), 1099-1109. doi:10.1007/s00125-010-1667-2

Higashi, S., Biskup, S., West, A. B., Trinkaus, D., Dawson, V. L., Faull, R. L., . . . Emson, P. C. (2007). Localization of Parkinson's disease-associated LRRK2 in normal and pathological human brain. *Brain Res, 1155*, 208-219. doi:10.1016/j.brainres.2007.04.034

Hildebrand, J. M., Tanzer, M. C., Lucet, I. S., Young, S. N., Spall, S. K., Sharma, P., . . . Silke, J. (2014). Activation of the pseudokinase MLKL unleashes the four-helix bundle domain to induce membrane localization and necroptotic cell death. *Proc Natl Acad Sci U S A, 111*(42), 15072-15077. doi:10.1073/pnas.1408987111

Hinkle, K. M., Yue, M., Behrouz, B., Dächsel, J. C., Lincoln, S. J., Bowles, E. E., . . . Melrose, H. L. (2012). LRRK2 knockout mice have an intact dopaminergic system but display alterations in exploratory and motor co-ordination behaviors. *Mol Neurodegener, 7*, 25. doi:10.1186/1750-1326-7-25

Hirayama, M., Nakamura, T., Watanabe, H., Uchida, K., Hama, T., Hara, T., . . . Sobue, G. (2011). Urinary 8-hydroxydeoxyguanosine correlate with hallucinations rather than motor symptoms in Parkinson's disease. *Parkinsonism Relat Disord, 17*(1), 46-49. doi:10.1016/j.parkreldis.2010.11.004

Hirsch, E. C., Vyas, S., & Hunot, S. (2012). Neuroinflammation in Parkinson's disease. *Parkinsonism Relat Disord, 18 Suppl 1*, S210-212. doi:10.1016/s1353-8020(11)70065-7

Hitomi, J., Christofferson, D. E., Ng, A., Yao, J., Degterev, A., Xavier, R. J., & Yuan, J. (2008). Identification of a molecular signaling network that regulates a cellular necrotic cell death pathway. *Cell, 135*(7), 1311-1323. doi:10.1016/j.cell.2008.10.044

Hoehn, M. M., & Yahr, M. D. (1967). Parkinsonism: onset, progression and mortality. *Neurology, 17*(5), 427-442. doi:10.1212/wnl.17.5.427

Hoye, M. L., Koval, E. D., Wegener, A. J., Hyman, T. S., Yang, C., O'Brien, D. R., . . . Miller, T. M. (2017). MicroRNA Profiling Reveals Marker of Motor Neuron Disease in ALS Models. *J Neurosci, 37*(22), 5574-5586. doi:10.1523/jneurosci.3582-16.2017

Hsu, C. H., Chan, D., Greggio, E., Saha, S., Guillily, M. D., Ferree, A., . . . Wolozin, B. (2010). MKK6 binds and regulates expression of Parkinson's disease-related protein LRRK2. *J Neurochem, 112*(6), 1593-1604. doi:10.1111/j.1471-4159.2010.06568.x

Hu, Y. B., Zhang, Y. F., Wang, H., Ren, R. J., Cui, H. L., Huang, W. Y., . . . Wang, G. (2019). miR-425 deficiency promotes necroptosis and dopaminergic neurodegeneration in Parkinson's disease. *Cell Death Dis, 10*(8), 589. doi:10.1038/s41419-019-1809-5

Huang, D., Xu, J., Wang, J., Tong, J., Bai, X., Li, H., . . . Huang, F. (2017). Dynamic Changes in the Nigrostriatal Pathway in the MPTP Mouse Model of Parkinson's Disease. *Parkinson's disease, 2017*, 9349487. doi:10.1155/2017/9349487

Huang, Z., Zhou, T., Sun, X., Zheng, Y., Cheng, B., Li, M., . . . He, C. (2018). Necroptosis in microglia contributes to neuroinflammation and retinal degeneration through TLR4 activation. *Cell Death Differ, 25*(1), 180-189. doi:10.1038/cdd.2017.141

Humphries, F., Yang, S., Wang, B., & Moynagh, P. N. (2015). RIP kinases: key decision makers in cell death and innate immunity. *Cell Death Differ, 22*(2), 225-236. doi:10.1038/cdd.2014.126

Iacono, D., Geraci-Erck, M., Rabin, M. L., Adler, C. H., Serrano, G., Beach, T. G., & Kurlan, R. (2015). Parkinson disease and incidental Lewy body disease: Just a question of time? *Neurology, 85*(19), 1670-1679. doi:10.1212/wnl.0000000000002102

Iannielli, A., Bido, S., Folladori, L., Segnali, A., Cancellieri, C., Maresca, A., . . . Broccoli, V. (2018). Pharmacological Inhibition of Necroptosis Protects from Dopaminergic Neuronal Cell Death in Parkinson's Disease Models. *Cell reports, 22*(8), 2066-2079. doi:10.1016/j.celrep.2018.01.089

Ishikawa, A., & Takahashi, H. (1998). Clinical and neuropathological aspects of autosomal recessive juvenile parkinsonism. *J Neurol, 245*(11 Suppl 3), P4-9. doi:10.1007/pl00007745

Ito, Y., Ofengeim, D., Najafov, A., Das, S., Saberi, S., Li, Y., . . . Yuan, J. (2016). RIPK1 mediates axonal degeneration by promoting inflammation and necroptosis in ALS. *Science, 353*(6299), 603-608. doi:10.1126/science.aaf6803

Jackson-Lewis, V., Jakowec, M., Burke, R. E., & Przedborski, S. (1995). Time course and morphology of dopaminergic neuronal death caused by the neurotoxin 1-methyl-4-phenyl-1,2,3,6-tetrahydropyridine. *Neurodegeneration, 4*(3), 257-269. doi:10.1016/1055-8330(95)90015-2

Jacobsen, A. V., Lowes, K. N., Tanzer, M. C., Lucet, I. S., Hildebrand, J. M., Petrie, E. J., . . . Murphy, J. M. (2016). HSP90 activity is required for MLKL oligomerisation and membrane translocation and the induction of necroptotic cell death. *Cell Death Dis, 7*(1), e2051. doi:10.1038/cddis.2015.386

Jankovic, J. (2008). Parkinson's disease: clinical features and diagnosis. *J Neurol Neurosurg Psychiatry, 79*(4), 368-376. doi:10.1136/jnnp.2007.131045

Jankovic, J., & Aguilar, L. G. (2008). Current approaches to the treatment of Parkinson's disease. *Neuropsychiatr Dis Treat, 4*(4), 743-757. doi:10.2147/ndt.s2006

Javitch, J. A., D'Amato, R. J., Strittmatter, S. M., & Snyder, S. H. (1985). Parkinsonism-inducing neurotoxin, N-methyl-4-phenyl-1,2,3,6 -tetrahydropyridine: uptake of the metabolite N-methyl-4-phenylpyridine by dopamine neurons explains selective toxicity. *Proc Natl Acad Sci U S A, 82*(7), 2173-2177. doi:10.1073/pnas.82.7.2173

Jiang, T., Hoekstra, J., Heng, X., Kang, W., Ding, J., Liu, J., . . . Zhang, J. (2015). P2X7 receptor is critical in α-synuclein--mediated microglial NADPH oxidase activation. *Neurobiol Aging, 36*(7), 2304-2318. doi:10.1016/j.neurobiolaging.2015.03.015

Jie, H., He, Y., Huang, X., Zhou, Q., Han, Y., Li, X., . . . Sun, E. (2016). Necrostatin-1 enhances the resolution of inflammation by specifically inducing neutrophil apoptosis. *Oncotarget, 7*(15), 19367-19381. doi:10.18632/oncotarget.8346

Jin, S., DiPaola, R. S., Mathew, R., & White, E. (2007). Metabolic catastrophe as a means to cancer cell death. *J Cell Sci, 120*(Pt 3), 379-383. doi:10.1242/jcs.03349

Junker, A., Krumbholz, M., Eisele, S., Mohan, H., Augstein, F., Bittner, R., . . . Meinl, E. (2009). MicroRNA profiling of multiple sclerosis lesions identifies modulators of the regulatory protein CD47. *Brain, 132*(Pt 12), 3342-3352. doi:10.1093/brain/awp300

Junn, E., Lee, K.-W., Jeong, B. S., Chan, T. W., Im, J.-Y., & Mouradian, M. M. (2009). Repression of alpha-synuclein expression and toxicity by microRNA-7. *Proc Natl Acad Sci U S A, 106*(31), 13052-13057. doi:10.1073/pnas.0906277106

Kabaria, S., Choi, D. C., Chaudhuri, A. D., Mouradian, M. M., & Junn, E. (2015). Inhibition of miR-34b and miR-34c enhances α-synuclein expression in Parkinson's disease. *FEBS Lett, 589*(3), 319-325. doi:10.1016/j.febslet.2014.12.014

Kachroo, A., & Schwarzschild, M. A. (2012). Adenosine A2A receptor gene disruption protects in an α-synuclein model of Parkinson's disease. *Ann Neurol, 71*(2), 278-282. doi:10.1002/ana.22630

Kaiser, W. J., & Offermann, M. K. (2005). Apoptosis induced by the toll-like receptor adaptor TRIF is dependent on its receptor interacting protein homotypic interaction motif. *J Immunol, 174*(8), 4942-4952. doi:10.4049/jimmunol.174.8.4942

Kaiser, W. J., Sridharan, H., Huang, C., Mandal, P., Upton, J. W., Gough, P. J., . . . Mocarski, E. S. (2013). Toll-like receptor 3-mediated necrosis via TRIF, RIP3, and MLKL. *J Biol Chem, 288*(43), 31268-31279. doi:10.1074/jbc.M113.462341

Kaiser, W. J., Upton, J. W., Long, A. B., Livingston-Rosanoff, D., Daley-Bauer, L. P., Hakem, R., . . . Mocarski, E. S. (2011). RIP3 mediates the embryonic lethality of caspase-8-deficient mice. *Nature, 471*(7338), 368-372. doi:10.1038/nature09857

Kanagaraj, N., Beiping, H., Dheen, S. T., & Tay, S. S. (2014). Downregulation of miR-124 in MPTP-treated mouse model of Parkinson's disease and MPP iodide-treated MN9D cells modulates the expression of the calpain/cdk5 pathway proteins. *Neuroscience, 272*, 167-179. doi:10.1016/j.neuroscience.2014.04.039

Kang, S., Fernandes-Alnemri, T., Rogers, C., Mayes, L., Wang, Y., Dillon, C., . . . Alnemri, E. S. (2015). Caspase-8 scaffolding function and MLKL regulate NLRP3 inflammasome activation downstream of TLR3. *Nature Communications, 6*(1), 7515. doi:10.1038/ncomms8515

Kang, T. B., Yang, S. H., Toth, B., Kovalenko, A., & Wallach, D. (2013). Caspase-8 blocks kinase RIPK3-mediated activation of the NLRP3 inflammasome. *Immunity, 38*(1), 27-40. doi:10.1016/j.immuni.2012.09.015

Karuppagounder, S. S., Xiong, Y., Lee, Y., Lawless, M. C., Kim, D., Nordquist, E., . . . Dawson, V. L. (2016). LRRK2 G2019S transgenic mice display increased susceptibility to 1-methyl-4-phenyl-1,2,3,6-tetrahydropyridine (MPTP)-mediated neurotoxicity. *J Chem Neuroanat, 76*(Pt B), 90-97. doi:10.1016/j.jchemneu.2016.01.007

Kasof, G. M., Prosser, J. C., Liu, D., Lorenzi, M. V., & Gomes, B. C. (2000). The RIP-like kinase, RIP3, induces apoptosis and NF-kappaB nuclear translocation and localizes to mitochondria. *FEBS Lett, 473*(3), 285-291. doi:10.1016/s0014-5793(00)01473-3

Kawai, T., & Akira, S. (2010). The role of pattern-recognition receptors in innate immunity: update on Toll-like receptors. *Nature Immunology, 11*(5), 373-384. doi:10.1038/ni.1863

Kearney, C. J., Cullen, S. P., Tynan, G. A., Henry, C. M., Clancy, D., Lavelle, E. C., & Martin, S. J. (2015). Necroptosis suppresses inflammation via termination of TNF- or LPS-induced cytokine and chemokine production. *Cell Death Differ, 22*(8), 1313-1327. doi:10.1038/cdd.2014.222

Kerr, J. F., Wyllie, A. H., & Currie, A. R. (1972). Apoptosis: a basic biological phenomenon with wide-ranging implications in tissue kinetics. *Br J Cancer, 26*(4), 239-257. doi:10.1038/bjc.1972.33

Kestenbaum, M., & Alcalay, R. N. (2017). Clinical Features of LRRK2 Carriers with Parkinson's Disease. *Adv Neurobiol, 14*, 31-48. doi:10.1007/978-3-319-49969-7_2

Khoo, S. K., Petillo, D., Kang, U. J., Resau, J. H., Berryhill, B., Linder, J., . . . Tan, A. C. (2012). Plasma-based circulating MicroRNA biomarkers for Parkinson's disease. *J Parkinsons Dis, 2*(4), 321-331. doi:10.3233/jpd-012144

Kim, B., Yang, M. S., Choi, D., Kim, J. H., Kim, H. S., Seol, W., . . . Joe, E. H. (2012). Impaired inflammatory responses in murine Lrrk2-knockdown brain microglia. *PloS one, 7*(4), e34693. doi:10.1371/journal.pone.0034693

Kim, S. J., & Li, J. (2013). Caspase blockade induces RIP3-mediated programmed necrosis in Toll-like receptor-activated microglia. *Cell Death Dis, 4*(7), e716. doi:10.1038/cddis.2013.238

Kim, Y. S., Morgan, M. J., Choksi, S., & Liu, Z. G. (2007). TNF-induced activation of the Nox1 NADPH oxidase and its role in the induction of necrotic cell death. *Mol Cell, 26*(5), 675-687. doi:10.1016/j.molcel.2007.04.021

Kitada, T., Asakawa, S., Hattori, N., Matsumine, H., Yamamura, Y., Minoshima, S., . . . Shimizu, N. (1998). Mutations in the parkin gene cause autosomal recessive juvenile parkinsonism. *Nature, 392*(6676), 605-608. doi:10.1038/33416

Kitur, K., Wachtel, S., Brown, A., Wickersham, M., Paulino, F., Peñaloza, H. F., . . . Prince, A. (2016). Necroptosis Promotes Staphylococcus aureus Clearance by Inhibiting Excessive Inflammatory Signaling. *Cell reports, 16*(8), 2219-2230. doi:10.1016/j.celrep.2016.07.039

Klinkenberg, M., Gispert, S., Dominguez-Bautista, J. A., Braun, I., Auburger, G., & Jendrach, M. (2012). Restriction of trophic factors and nutrients induces PARKIN expression. *Neurogenetics, 13*(1), 9-21. doi:10.1007/s10048-011-0303-8

Koike, A., Hanatani, M., & Fujimori, K. (2019). Pan-caspase inhibitors induce necroptosis via ROS-mediated activation of mixed lineage kinase domain-like protein and p38 in classically activated macrophages. *Exp Cell Res, 380*(2), 171-179. doi:10.1016/j.yexcr.2019.04.027

Koo, G.-B., Morgan, M. J., Lee, D.-G., Kim, W.-J., Yoon, J.-H., Koo, J. S., . . . Kim, Y.-S. (2015). Methylation-dependent loss of RIP3 expression in cancer represses programmed necrosis in response to chemotherapeutics. *Cell Research, 25*(6), 707-725. doi:10.1038/cr.2015.56

Kordower, J. H., Olanow, C. W., Dodiya, H. B., Chu, Y., Beach, T. G., Adler, C. H., . . . Bartus, R. T. (2013). Disease duration and the integrity of the nigrostriatal system in Parkinson's disease. *Brain, 136*(Pt 8), 2419-2431. doi:10.1093/brain/awt192

Kouli, A., Horne, C. B., & Williams-Gray, C. H. (2019). Toll-like receptors and their therapeutic potential in Parkinson's disease and α-synucleinopathies. *Brain Behav Immun, 81*, 41-51. doi:10.1016/j.bbi.2019.06.042

Koval, E. D., Shaner, C., Zhang, P., du Maine, X., Fischer, K., Tay, J., . . . Miller, T. M. (2013). Method for widespread microRNA-155 inhibition prolongs survival in ALS-model mice. *Hum Mol Genet, 22*(20), 4127-4135. doi:10.1093/hmg/ddt261

Kowal, S. L., Dall, T. M., Chakrabarti, R., Storm, M. V., & Jain, A. (2013). The current and projected economic burden of Parkinson's disease in the United States. *Mov Disord, 28*(3), 311-318. doi:10.1002/mds.25292

Kurkowska-Jastrzebska, I., Wrońska, A., Kohutnicka, M., Członkowski, A., & Członkowska, A. (1999). The inflammatory reaction following 1-methyl-4-phenyl-1,2,3, 6-tetrahydropyridine intoxication in mouse. *Exp Neurol, 156*(1), 50-61. doi:10.1006/exnr.1998.6993

Langston, J. W. (2017). The MPTP Story. *J Parkinsons Dis, 7*(s1), S11-s19. doi:10.3233/jpd-179006

Langston, J. W., Ballard, P., Tetrud, J. W., & Irwin, I. (1983). Chronic Parkinsonism in humans due to a product of meperidine-analog synthesis. *Science, 219*(4587), 979-980. doi:10.1126/science.6823561

Langston, J. W., Forno, L. S., Tetrud, J., Reeves, A. G., Kaplan, J. A., & Karluk, D. (1999). Evidence of active nerve cell degeneration in the substantia nigra of humans years after 1-methyl-4-phenyl-1,2,3,6-tetrahydropyridine exposure. *Ann Neurol, 46*(4), 598-605. doi:10.1002/1531-8249(199910)46:4<598::aid-ana7>3.0.co;2-f

Laster, S. M., Wood, J. G., & Gooding, L. R. (1988). Tumor necrosis factor can induce both apoptic and necrotic forms of cell lysis. *J Immunol, 141*(8), 2629-2634.

Latz, E., Xiao, T. S., & Stutz, A. (2013). Activation and regulation of the inflammasomes. *Nat Rev Immunol, 13*(6), 397-411. doi:10.1038/nri3452

Lawlor, K. E., Khan, N., Mildenhall, A., Gerlic, M., Croker, B. A., D'Cruz, A. A., . . . Vince, J. E. (2015). RIPK3 promotes cell death and NLRP3 inflammasome activation in the absence of MLKL. *Nat Commun, 6*, 6282. doi:10.1038/ncomms7282

Le, W., Wu, J., & Tang, Y. (2016). Protective Microglia and Their Regulation in Parkinson's Disease. *Front Mol Neurosci, 9*, 89-89. doi:10.3389/fnmol.2016.00089

Lee, E., Hwang, I., Park, S., Hong, S., Hwang, B., Cho, Y., . . . Yu, J.-W. (2019). MPTP-driven NLRP3 inflammasome activation in microglia plays a central role in dopaminergic neurodegeneration. *Cell Death & Differentiation, 26*(2), 213-228. doi:10.1038/s41418-018-0124-5

Lees, A. J. (2007). Unresolved issues relating to the shaking palsy on the celebration of James Parkinson's 250th birthday. *Mov Disord, 22 Suppl 17*, S327-334. doi:10.1002/mds.21684

Leggio, L., Vivarelli, S., L'Episcopo, F., Tirolo, C., Caniglia, S., Testa, N., . . . Iraci, N. (2017). microRNAs in Parkinson's Disease: From Pathogenesis to Novel Diagnostic and Therapeutic Approaches. *Int J Mol Sci, 18*(12). doi:10.3390/ijms18122698

Leung, A. K., & Sharp, P. A. (2010). MicroRNA functions in stress responses. *Mol Cell, 40*(2), 205-215. doi:10.1016/j.molcel.2010.09.027

Levy, O. A., Malagelada, C., & Greene, L. A. (2009). Cell death pathways in Parkinson's disease: proximal triggers, distal effectors, and final steps. *Apoptosis, 14*(4), 478-500. doi:10.1007/s10495-008-0309-3

Li, D., Xu, T., Cao, Y., Wang, H., Li, L., Chen, S., . . . Shen, Z. (2015). A cytosolic heat shock protein 90 and cochaperone CDC37 complex is required for RIP3 activation during necroptosis. *Proc Natl Acad Sci U S A, 112*(16), 5017-5022. doi:10.1073/pnas.1505244112

Li, J., McQuade, T., Siemer, A. B., Napetschnig, J., Moriwaki, K., Hsiao, Y. S., . . . Wu, H. (2012). The RIP1/RIP3 necrosome forms a functional amyloid signaling complex required for programmed necrosis. *Cell, 150*(2), 339-350. doi:10.1016/j.cell.2012.06.019

Li, J., Wang, H., & Rosenberg, P. A. (2009). Vitamin K prevents oxidative cell death by inhibiting activation of 12-lipoxygenase in developing oligodendrocytes. *J Neurosci Res, 87*(9), 1997-2005. doi:10.1002/jnr.22029

Li, J. Q., Tan, L., & Yu, J. T. (2014). The role of the LRRK2 gene in Parkinsonism. *Mol Neurodegener, 9*, 47. doi:10.1186/1750-1326-9-47

Li, S., Zhang, Y., Guan, Z., Li, H., Ye, M., Chen, X., . . . Peng, K. (2020). SARS-CoV-2 triggers inflammatory responses and cell death through caspase-8 activation. *Signal Transduct Target Ther, 5*(1), 235. doi:10.1038/s41392-020-00334-0

Li, X., Patel, J. C., Wang, J., Avshalumov, M. V., Nicholson, C., Buxbaum, J. D., . . . Yue, Z. (2010). Enhanced striatal dopamine transmission and motor performance with LRRK2 overexpression in mice is eliminated by familial Parkinson's disease mutation G2019S. *J Neurosci, 30*(5), 1788-1797. doi:10.1523/jneurosci.5604-09.2010

Li, X., Tan, Y. C., Poulose, S., Olanow, C. W., Huang, X. Y., & Yue, Z. (2007). Leucine-rich repeat kinase 2 (LRRK2)/PARK8 possesses GTPase activity that is altered in familial Parkinson's disease R1441C/G mutants. *J Neurochem, 103*(1), 238-247. doi:10.1111/j.1471-4159.2007.04743.x

Li, X., Yao, X., Zhu, Y., Zhang, H., Wang, H., Ma, Q., . . . Xiong, H. (2019). The Caspase Inhibitor Z-VAD-FMK Alleviates Endotoxic Shock via Inducing Macrophages Necroptosis and Promoting MDSCs-Mediated Inhibition of Macrophages Activation. *Front Immunol, 10*, 1824. doi:10.3389/fimmu.2019.01824

Li, Y., Liu, W., Oo, T. F., Wang, L., Tang, Y., Jackson-Lewis, V., . . . Li, C. (2009). Mutant LRRK2(R1441G) BAC transgenic mice recapitulate cardinal features of Parkinson's disease. *Nat Neurosci, 12*(7), 826-828. doi:10.1038/nn.2349

Li, Y. Y., Cui, J. G., Dua, P., Pogue, A. I., Bhattacharjee, S., & Lukiw, W. J. (2011). Differential expression of miRNA-146a-regulated inflammatory genes in human primary neural, astroglial and microglial cells. *Neurosci Lett, 499*(2), 109-113. doi:10.1016/j.neulet.2011.05.044

Liddelow, S. A., Guttenplan, K. A., Clarke, L. E., Bennett, F. C., Bohlen, C. J., Schirmer, L., . . . Barres, B. A. (2017). Neurotoxic reactive astrocytes are induced by activated microglia. *Nature, 541*(7638), 481-487. doi:10.1038/nature21029

Lin, L. F., Doherty, D. H., Lile, J. D., Bektesh, S., & Collins, F. (1993). GDNF: a glial cell line-derived neurotrophic factor for midbrain dopaminergic neurons. *Science, 260*(5111), 1130-1132. doi:10.1126/science.8493557

Lin, Q.-S., Chen, P., Wang, W.-X., Lin, C.-C., Zhou, Y., Yu, L.-H., . . . Kang, D.-Z. (2020). RIP1/RIP3/MLKL mediates dopaminergic neuron necroptosis in a mouse model of Parkinson disease. *Laboratory Investigation, 100*(3), 503-511. doi:10.1038/s41374-019-0319-5

Lin, S., & Gregory, R. I. (2015). MicroRNA biogenesis pathways in cancer. *Nature Reviews Cancer, 15*(6), 321-333. doi:10.1038/nrc3932

Lin, X., Parisiadou, L., Gu, X. L., Wang, L., Shim, H., Sun, L., . . . Cai, H. (2009). Leucine-rich repeat kinase 2 regulates the progression of neuropathology induced by Parkinson's-disease-related mutant alpha-synuclein. *Neuron, 64*(6), 807-827. doi:10.1016/j.neuron.2009.11.006

Lindström, V., Gustafsson, G., Sanders, L. H., Howlett, E. H., Sigvardson, J., Kasrayan, A., . . . Erlandsson, A. (2017). Extensive uptake of α-synuclein oligomers in astrocytes results in sustained intracellular deposits and mitochondrial damage. *Mol Cell Neurosci, 82*, 143-156. doi:10.1016/j.mcn.2017.04.009

Liou, A. K., Leak, R. K., Li, L., & Zigmond, M. J. (2008). Wild-type LRRK2 but not its mutant attenuates stress-induced cell death via ERK pathway. *Neurobiol Dis, 32*(1), 116-124. doi:10.1016/j.nbd.2008.06.016

Liu, G., & Abraham, E. (2013). MicroRNAs in immune response and macrophage polarization. *Arterioscler Thromb Vasc Biol, 33*(2), 170-177. doi:10.1161/atvbaha.112.300068

Liu, G., Sgobio, C., Gu, X., Sun, L., Lin, X., Yu, J., . . . Cai, H. (2015). Selective expression of Parkinson's disease-related Leucine-rich repeat kinase 2 G2019S missense mutation in midbrain dopaminergic neurons impairs dopamine release and dopaminergic gene expression. *Hum Mol Genet, 24*(18), 5299-5312. doi:10.1093/hmg/ddv249

Liu, J., Huang, D., Xu, J., Tong, J., Wang, Z., Huang, L., . . . Huang, F. (2015). Tiagabine Protects Dopaminergic Neurons against Neurotoxins by Inhibiting Microglial Activation. *Sci Rep, 5*(1), 15720. doi:10.1038/srep15720

Liu, Q., Qiu, J., Liang, M., Golinski, J., van Leyen, K., Jung, J. E., . . . Whalen, M. J. (2014). Akt and mTOR mediate programmed necrosis in neurons. *Cell Death Dis, 5*(2), e1084. doi:10.1038/cddis.2014.69

Liu, T., Zhang, L., Joo, D., & Sun, S.-C. (2017). NF-κB signaling in inflammation. *Signal Transduction and Targeted Therapy, 2*(1), 17023. doi:10.1038/sigtrans.2017.23

Lofrumento, D. D., Saponaro, C., Cianciulli, A., De Nuccio, F., Mitolo, V., Nicolardi, G., & Panaro, M. A. (2011). MPTP-induced neuroinflammation increases the expression of pro-inflammatory cytokines and their receptors in mouse brain. *Neuroimmunomodulation, 18*(2), 79-88. doi:10.1159/000320027

Loria, F., Vargas, J. Y., Bousset, L., Syan, S., Salles, A., Melki, R., & Zurzolo, C. (2017). α-Synuclein transfer between neurons and astrocytes indicates that astrocytes play a role in degradation rather than in spreading. *Acta Neuropathol, 134*(5), 789-808. doi:10.1007/s00401-017-1746-2

Lotharius, J., & Brundin, P. (2002). Pathogenesis of Parkinson's disease: dopamine, vesicles and alpha-synuclein. *Nat Rev Neurosci, 3*(12), 932-942. doi:10.1038/nrn983

Louafi, F., Martinez-Nunez, R. T., & Sanchez-Elsner, T. (2010). MicroRNA-155 targets SMAD2 and modulates the response of macrophages to transforming growth factor-{beta}. *J Biol Chem, 285*(53), 41328-41336. doi:10.1074/jbc.M110.146852

Lule, S., Wu, L., McAllister, L. M., Edmiston, W. J., 3rd, Chung, J. Y., Levy, E., . . . Whalen, M. J. (2017). Genetic Inhibition of Receptor Interacting Protein Kinase-1 Reduces Cell Death and Improves Functional Outcome After Intracerebral Hemorrhage in Mice. *Stroke, 48*(9), 2549-2556. doi:10.1161/strokeaha.117.017702

Mackay, K., & Mochly-Rosen, D. (2000). Involvement of a p38 mitogen-activated protein kinase phosphatase in protecting neonatal rat cardiac myocytes from ischemia. *J Mol Cell Cardiol, 32*(8), 1585-1588. doi:10.1006/jmcc.2000.1194

Mandal, P., Berger, S. B., Pillay, S., Moriwaki, K., Huang, C., Guo, H., . . . Kaiser, W. J. (2014). RIP3 induces apoptosis independent of pronecrotic kinase activity. *Mol Cell, 56*(4), 481-495. doi:10.1016/j.molcel.2014.10.021

Margis, R., Margis, R., & Rieder, C. R. (2011). Identification of blood microRNAs associated to Parkinsonĭs disease. *J Biotechnol, 152*(3), 96-101. doi:10.1016/j.jbiotec.2011.01.023

Marker, D. F., Puccini, J. M., Mockus, T. E., Barbieri, J., Lu, S. M., & Gelbard, H. A. (2012). LRRK2 kinase inhibition prevents pathological microglial phagocytosis in response to HIV-1 Tat protein. *J Neuroinflammation, 9*, 261. doi:10.1186/1742-2094-9-261

Marras, C., & Lang, A. (2013). Parkinson's disease subtypes: lost in translation? *J Neurol Neurosurg Psychiatry, 84*(4), 409-415. doi:10.1136/jnnp-2012-303455

Martins, M., Rosa, A., Guedes, L. C., Fonseca, B. V., Gotovac, K., Violante, S., . . . Oliveira, S. A. (2011). Convergence of miRNA expression profiling, α-synuclein interacton and GWAS in Parkinson's disease. *PloS one, 6*(10), e25443. doi:10.1371/journal.pone.0025443

Mata, I. F., Wedemeyer, W. J., Farrer, M. J., Taylor, J. P., & Gallo, K. A. (2006). LRRK2 in Parkinson's disease: protein domains and functional insights. *Trends Neurosci, 29*(5), 286-293. doi:10.1016/j.tins.2006.03.006

Mayer, R. A., Kindt, M. V., & Heikkila, R. E. (1986). Prevention of the nigrostriatal toxicity of 1-methyl-4-phenyl-1,2,3,6-tetrahydropyridine by inhibitors of 3,4-dihydroxyphenylethylamine transport. *J Neurochem, 47*(4), 1073-1079. doi:10.1111/j.1471-4159.1986.tb00722.x

McGeer, P. L., Itagaki, S., Boyes, B. E., & McGeer, E. G. (1988). Reactive microglia are positive for HLA-DR in the substantia nigra of Parkinson's and Alzheimer's disease brains. *Neurology, 38*(8), 1285-1291. doi:10.1212/wnl.38.8.1285

McNamara, C. R., Ahuja, R., Osafo-Addo, A. D., Barrows, D., Kettenbach, A., Skidan, I., . . . Degterev, A. (2013). Akt Regulates TNFα synthesis downstream of RIP1 kinase activation during necroptosis. *PLoS One, 8*(3), e56576. doi:10.1371/journal.pone.0056576

Meredith, G. E., & Kang, U. J. (2006). Behavioral models of Parkinson's disease in rodents: A new look at an old problem. *Movement Disorders, 21*(10), 1595-1606. doi:https://doi.org/10.1002/mds.21010

Meredith, G. E., & Rademacher, D. J. (2011). MPTP mouse models of Parkinson's disease: an update. *J Parkinsons Dis, 1*(1), 19-33. doi:10.3233/jpd-2011-11023

Meylan, E., Burns, K., Hofmann, K., Blancheteau, V., Martinon, F., Kelliher, M., & Tschopp, J. (2004). RIP1 is an essential mediator of Toll-like receptor 3-induced NF-kappa B activation. *Nat Immunol, 5*(5), 503-507. doi:10.1038/ni1061

Mifflin, L., Ofengeim, D., & Yuan, J. (2020). Receptor-interacting protein kinase 1 (RIPK1) as a therapeutic target. *Nature Reviews Drug Discovery, 19*(8), 553-571. doi:10.1038/s41573-020-0071-y

Migheli, R., Del Giudice, M. G., Spissu, Y., Sanna, G., Xiong, Y., Dawson, T. M., . . . Iaccarino, C. (2013). LRRK2 affects vesicle trafficking, neurotransmitter extracellular level and membrane receptor localization. *PloS one, 8*(10), e77198-e77198. doi:10.1371/journal.pone.0077198

Miklossy, J., Arai, T., Guo, J. P., Klegeris, A., Yu, S., McGeer, E. G., & McGeer, P. L. (2006). LRRK2 expression in normal and pathologic human brain and in human cell lines. *J Neuropathol Exp Neurol, 65*(10), 953-963. doi:10.1097/01.jnen.0000235121.98052.54

Miñones-Moyano, E., Porta, S., Escaramís, G., Rabionet, R., Iraola, S., Kagerbauer, B., . . . Martí, E. (2011). MicroRNA profiling of Parkinson's disease brains identifies early downregulation of miR-34b/c which modulate mitochondrial function. *Hum Mol Genet, 20*(15), 3067-3078. doi:10.1093/hmg/ddr210

Miura, M. (2011). Active participation of cell death in development and organismal homeostasis. *Dev Growth Differ, 53*(2), 125-136. doi:10.1111/j.1440-169X.2010.01228.x

Mochizuki, H., Goto, K., Mori, H., & Mizuno, Y. (1996). Histochemical detection of apoptosis in Parkinson's disease. *J Neurol Sci, 137*(2), 120-123. doi:10.1016/0022-510x(95)00336-z

Moehle, M. S., Webber, P. J., Tse, T., Sukar, N., Standaert, D. G., DeSilva, T. M., . . . West, A. B. (2012). LRRK2 inhibition attenuates microglial inflammatory responses. *J Neurosci, 32*(5), 1602-1611. doi:10.1523/jneurosci.5601-11.2012

Moffat, J. G., Vincent, F., Lee, J. A., Eder, J., & Prunotto, M. (2017). Opportunities and challenges in phenotypic drug discovery: an industry perspective. *Nature Reviews Drug Discovery, 16*(8), 531-543. doi:10.1038/nrd.2017.111

Mollenhauer, B., Locascio, J. J., Schulz-Schaeffer, W., Sixel-Döring, F., Trenkwalder, C., & Schlossmacher, M. G. (2011). α-Synuclein and tau concentrations in cerebrospinal fluid of patients presenting with parkinsonism: a cohort study. *Lancet Neurol, 10*(3), 230-240. doi:10.1016/s1474-4422(11)70014-x

Mompeán, M., Li, W., Li, J., Laage, S., Siemer, A. B., Bozkurt, G., . . . McDermott, A. E. (2018). The Structure of the Necrosome RIPK1-RIPK3 Core, a Human Hetero-Amyloid Signaling Complex. *Cell, 173*(5), 1244-1253.e1210. doi:10.1016/j.cell.2018.03.032

Moore, C. S., Rao, V. T., Durafourt, B. A., Bedell, B. J., Ludwin, S. K., Bar-Or, A., & Antel, J. P. (2013). miR-155 as a multiple sclerosis-relevant regulator of myeloid cell polarization. *Ann Neurol, 74*(5), 709-720. doi:10.1002/ana.23967

Moriwaki, K., Balaji, S., Bertin, J., Gough, P. J., & Chan, F. K.-M. (2017). Distinct Kinase-Independent Role of RIPK3 in CD11c(+) Mononuclear Phagocytes in Cytokine-Induced Tissue Repair. *Cell reports, 18*(10), 2441-2451. doi:10.1016/j.celrep.2017.02.015

Moriwaki, K., Balaji, S., McQuade, T., Malhotra, N., Kang, J., & Chan, F. K. (2014). The necroptosis adaptor RIPK3 promotes injury-induced cytokine expression and tissue repair. *Immunity, 41*(4), 567-578. doi:10.1016/j.immuni.2014.09.016

Moriwaki, K., & Chan, F. K. (2013). RIP3: a molecular switch for necrosis and inflammation. *Genes Dev, 27*(15), 1640-1649. doi:10.1101/gad.223321.113

Moriwaki, K., & Chan, F. K. (2017). The Inflammatory Signal Adaptor RIPK3: Functions Beyond Necroptosis. *Int Rev Cell Mol Biol, 328*, 253-275. doi:10.1016/bs.ircmb.2016.08.007

Mortiboys, H., Johansen, K. K., Aasly, J. O., & Bandmann, O. (2010). Mitochondrial impairment in patients with Parkinson disease with the G2019S mutation in LRRK2. *Neurology, 75*(22), 2017-2020. doi:10.1212/WNL.0b013e3181ff9685

Mosharov, E. V., Larsen, K. E., Kanter, E., Phillips, K. A., Wilson, K., Schmitz, Y., . . . Sulzer, D. (2009). Interplay between cytosolic dopamine, calcium, and alpha-synuclein causes selective death of substantia nigra neurons. *Neuron, 62*(2), 218-229. doi:10.1016/j.neuron.2009.01.033

Murphy, J. M., Czabotar, P. E., Hildebrand, J. M., Lucet, I. S., Zhang, J. G., Alvarez-Diaz, S., . . . Alexander, W. S. (2013). The pseudokinase MLKL mediates necroptosis via a molecular switch mechanism. *Immunity, 39*(3), 443-453. doi:10.1016/j.immuni.2013.06.018

Najjar, M., Saleh, D., Zelic, M., Nogusa, S., Shah, S., Tai, A., . . . Degterev, A. (2016). RIPK1 and RIPK3 Kinases Promote Cell-Death-Independent Inflammation by Toll-like Receptor 4. *Immunity, 45*(1), 46-59. doi:10.1016/j.immuni.2016.06.007

Nalls, M. A., Pankratz, N., Lill, C. M., Do, C. B., Hernandez, D. G., Saad, M., . . . Singleton, A. B. (2014). Large-scale meta-analysis of genome-wide association data identifies six new risk loci for Parkinson's disease. *Nat Genet, 46*(9), 989-993. doi:10.1038/ng.3043

Nandipati, S., & Litvan, I. (2016). Environmental Exposures and Parkinson's Disease. *Int J Environ Res Public Health, 13*(9). doi:10.3390/ijerph13090881

Neumann, J., Bras, J., Deas, E., O'Sullivan, S. S., Parkkinen, L., Lachmann, R. H., . . . Wood, N. W. (2009). Glucocerebrosidase mutations in clinical and pathologically proven Parkinson's disease. *Brain, 132*(Pt 7), 1783-1794. doi:10.1093/brain/awp044

Newton, K., Dugger, D. L., Maltzman, A., Greve, J. M., Hedehus, M., Martin-McNulty, B., . . . Vucic, D. (2016). RIPK3 deficiency or catalytically inactive RIPK1 provides greater benefit than MLKL deficiency in mouse models of inflammation and tissue injury. *Cell Death Differ, 23*(9), 1565-1576. doi:10.1038/cdd.2016.46

Newton, K., Dugger, D. L., Wickliffe, K. E., Kapoor, N., de Almagro, M. C., Vucic, D., . . . Dixit, V. M. (2014). Activity of protein kinase RIPK3 determines whether cells die by necroptosis or apoptosis. *Science, 343*(6177), 1357-1360. doi:10.1126/science.1249361

Nishioka, K., Kefi, M., Jasinska-Myga, B., Wider, C., Vilariño-Güell, C., Ross, O. A., . . . Hentati, F. (2010). A comparative study of LRRK2, PINK1 and genetically undefined familial Parkinson's disease. *J Neurol Neurosurg Psychiatry, 81*(4), 391-395. doi:10.1136/jnnp.2009.185231

Northington, F. J., Chavez-Valdez, R., Graham, E. M., Razdan, S., Gauda, E. B., & Martin, L. J. (2011). Necrostatin decreases oxidative damage, inflammation, and injury after neonatal HI. *J Cereb Blood Flow Metab, 31*(1), 178-189. doi:10.1038/jcbfm.2010.72

Nuzziello, N., & Liguori, M. (2019). The MicroRNA Centrism in the Orchestration of Neuroinflammation in Neurodegenerative Diseases. *Cells, 8*(10). doi:10.3390/cells8101193

O'Donnell, M. A., Perez-Jimenez, E., Oberst, A., Ng, A., Massoumi, R., Xavier, R., . . . Ting, A. T. (2011). Caspase 8 inhibits programmed necrosis by processing CYLD. *Nature cell biology, 13*(12), 1437-1442. doi:10.1038/ncb2362

Oberst, A., Dillon, C. P., Weinlich, R., McCormick, L. L., Fitzgerald, P., Pop, C., . . . Green, D. R. (2011). Catalytic activity of the caspase-8-FLIP(L) complex inhibits RIPK3-dependent necrosis. *Nature, 471*(7338), 363-367. doi:10.1038/nature09852

Ofengeim, D., Ito, Y., Najafov, A., Zhang, Y., Shan, B., DeWitt, J. P., . . . Yuan, J. (2015). Activation of necroptosis in multiple sclerosis. *Cell reports, 10*(11), 1836-1849. doi:10.1016/j.celrep.2015.02.051

Ofengeim, D., Mazzitelli, S., Ito, Y., DeWitt, J. P., Mifflin, L., Zou, C., . . . Yuan, J. (2017). RIPK1 mediates a disease-associated microglial response in Alzheimer's disease. *Proc Natl Acad Sci U S A, 114*(41), E8788-e8797. doi:10.1073/pnas.1714175114

Ofengeim, D., & Yuan, J. (2013). Regulation of RIP1 kinase signalling at the crossroads of inflammation and cell death. *Nat Rev Mol Cell Biol, 14*(11), 727-736. doi:10.1038/nrm3683

Ogata, A., Tashiro, K., Nukuzuma, S., Nagashima, K., & Hall, W. W. (1997). A rat model of Parkinson's disease induced by Japanese encephalitis virus. *J Neurovirol, 3*(2), 141-147. doi:10.3109/13550289709015803

Oliveira, S. R., Dionísio, P. A., Brito, H., Franco, L., Rodrigues, C. A. B., Guedes, R. C., . . . Rodrigues, C. M. P. (2018). Phenotypic screening identifies a new oxazolone inhibitor of necroptosis and neuroinflammation. *Cell Death Discovery, 4*(1), 65. doi:10.1038/s41420-018-0067-0

Oliveira, S. R., Dionísio, P. A., Correia Guedes, L., Gonçalves, N., Coelho, M., Rosa, M. M., . . . Rodrigues, C. M. P. (2020). Circulating Inflammatory miRNAs Associated with Parkinson's Disease Pathophysiology. *Biomolecules, 10*(6). doi:10.3390/biom10060945

Oñate, M., Catenaccio, A., Salvadores, N., Saquel, C., Martinez, A., Moreno-Gonzalez, I., . . . Court, F. A. (2020). The necroptosis machinery mediates axonal degeneration in a model of Parkinson disease. *Cell Death Differ, 27*(4), 1169-1185. doi:10.1038/s41418-019-0408-4

Orozco, S. L., Daniels, B. P., Yatim, N., Messmer, M. N., Quarato, G., Chen-Harris, H., . . . Oberst, A. (2019). RIPK3 Activation Leads to Cytokine Synthesis that Continues after Loss of Cell Membrane Integrity. *Cell reports, 28*(9), 2275-2287.e2275. doi:10.1016/j.celrep.2019.07.077

Ouchi, Y., Yoshikawa, E., Sekine, Y., Futatsubashi, M., Kanno, T., Ogusu, T., & Torizuka, T. (2005). Microglial activation and dopamine terminal loss in early Parkinson's disease. *Ann Neurol, 57*(2), 168-175. doi:10.1002/ana.20338

Ousingsawat, J., Cabrita, I., Wanitchakool, P., Sirianant, L., Krautwald, S., Linkermann, A., . . . Kunzelmann, K. (2017). Ca(2+) signals, cell membrane disintegration, and activation of TMEM16F during necroptosis. *Cell Mol Life Sci, 74*(1), 173-181. doi:10.1007/s00018-016-2338-3

Paisán-Ruíz, C., Jain, S., Evans, E. W., Gilks, W. P., Simón, J., van der Brug, M., . . . Singleton, A. B. (2004). Cloning of the gene containing mutations that cause PARK8-linked Parkinson's disease. *Neuron, 44*(4), 595-600. doi:10.1016/j.neuron.2004.10.023

Paisán-Ruiz, C., Lewis, P. A., & Singleton, A. B. (2013). LRRK2: cause, risk, and mechanism. *J Parkinsons Dis, 3*(2), 85-103. doi:10.3233/jpd-130192

Papkovskaia, T. D., Chau, K. Y., Inesta-Vaquera, F., Papkovsky, D. B., Healy, D. G., Nishio, K., . . . Cooper, J. M. (2012). G2019S leucine-rich repeat kinase 2 causes uncoupling protein-mediated mitochondrial depolarization. *Hum Mol Genet, 21*(19), 4201-4213. doi:10.1093/hmg/dds244

Paraskevopoulou, M. D., Georgakilas, G., Kostoulas, N., Vlachos, I. S., Vergoulis, T., Reczko, M., . . . Hatzigeorgiou, A. G. (2013). DIANA-microT web server v5.0: service integration into miRNA functional analysis workflows. *Nucleic Acids Res, 41*(Web Server issue), W169-173. doi:10.1093/nar/gkt393

Parnetti, L., Chiasserini, D., Persichetti, E., Eusebi, P., Varghese, S., Qureshi, M. M., . . . Calabresi, P. (2014). Cerebrospinal fluid lysosomal enzymes and alpha-synuclein in Parkinson's disease. *Mov Disord, 29*(8), 1019-1027. doi:10.1002/mds.25772

Parnetti, L., Gaetani, L., Eusebi, P., Paciotti, S., Hansson, O., El-Agnaf, O., . . . Calabresi, P. (2019). CSF and blood biomarkers for Parkinson's disease. *Lancet Neurol, 18*(6), 573-586. doi:10.1016/s1474-4422(19)30024-9

Pasinetti, G. M. (2012). Role of Personalized Medicine in the Identification and Characterization of Parkinson's Disease in Asymptomatic Subjects. *J Alzheimers Dis Parkinsonism, 2*(3). doi:10.4172/2161-0460.1000e118

Pasparakis, M., & Vandenabeele, P. (2015). Necroptosis and its role in inflammation. *Nature, 517*(7534), 311-320. doi:10.1038/nature14191

Patil, K. S., Basak, I., Dalen, I., Hoedt, E., Lange, J., Lunde, K. A., . . . Møller, S. G. (2019). Combinatory microRNA serum signatures as classifiers of Parkinson's disease. *Parkinsonism Relat Disord, 64*, 202-210. doi:10.1016/j.parkreldis.2019.04.010

Paumier, K. L., Sukoff Rizzo, S. J., Berger, Z., Chen, Y., Gonzales, C., Kaftan, E., . . . Dunlop, J. (2013). Behavioral characterization of A53T mice reveals early and late stage deficits related to Parkinson's disease. *PloS one, 8*(8), e70274. doi:10.1371/journal.pone.0070274

Perier, C., Bové, J., & Vila, M. (2012). Mitochondria and programmed cell death in Parkinson's disease: apoptosis and beyond. *Antioxid Redox Signal, 16*(9), 883-895. doi:10.1089/ars.2011.4074

Petersen, S. L., Chen, T. T., Lawrence, D. A., Marsters, S. A., Gonzalvez, F., & Ashkenazi, A. (2015). TRAF2 is a biologically important necroptosis suppressor. *Cell Death Differ, 22*(11), 1846-1857. doi:10.1038/cdd.2015.35

Petrie, E. J., Czabotar, P. E., & Murphy, J. M. (2019). The Structural Basis of Necroptotic Cell Death Signaling. *Trends in Biochemical Sciences, 44*(1), 53-63. doi:https://doi.org/10.1016/j.tibs.2018.11.002

Petrie, E. J., Sandow, J. J., Jacobsen, A. V., Smith, B. J., Griffin, M. D. W., Lucet, I. S., . . . Murphy, J. M. (2018). Conformational switching of the pseudokinase domain promotes human MLKL tetramerization and cell death by necroptosis. *Nature Communications, 9*(1), 2422. doi:10.1038/s41467-018-04714-7

Petrie, E. J., Sandow, J. J., Lehmann, W. I. L., Liang, L. Y., Coursier, D., Young, S. N., . . . Murphy, J. M. (2019). Viral MLKL Homologs Subvert Necroptotic Cell Death by Sequestering Cellular RIPK3. *Cell reports, 28*(13), 3309-3319.e3305. doi:10.1016/j.celrep.2019.08.055

Pissadaki, E. K., & Bolam, J. P. (2013). The energy cost of action potential propagation in dopamine neurons: clues to susceptibility in Parkinson's disease. *Front Comput Neurosci, 7*, 13. doi:10.3389/fncom.2013.00013

Plowey, E. D., Cherra, S. J., 3rd, Liu, Y. J., & Chu, C. T. (2008). Role of autophagy in G2019S-LRRK2-associated neurite shortening in differentiated SH-SY5Y cells. *J Neurochem, 105*(3), 1048-1056. doi:10.1111/j.1471-4159.2008.05217.x

Poewe, W., Seppi, K., Tanner, C. M., Halliday, G. M., Brundin, P., Volkmann, J., . . . Lang, A. E. (2017). Parkinson disease. *Nat Rev Dis Primers, 3*, 17013. doi:10.1038/nrdp.2017.13

Polymeropoulos, M. H., Lavedan, C., Leroy, E., Ide, S. E., Dehejia, A., Dutra, A., . . . Nussbaum, R. L. (1997). Mutation in the alpha-synuclein gene identified in families with Parkinson's disease. *Science, 276*(5321), 2045-2047. doi:10.1126/science.276.5321.2045

Pong, K., Doctrow, S. R., Huffman, K., Adinolfi, C. A., & Baudry, M. (2001). Attenuation of staurosporine-induced apoptosis, oxidative stress, and mitochondrial dysfunction by synthetic superoxide dismutase and catalase mimetics, in cultured cortical neurons. *Exp Neurol, 171*(1), 84-97. doi:10.1006/exnr.2001.7747

Ponomarev, E. D., Veremeyko, T., & Weiner, H. L. (2013). MicroRNAs are universal regulators of differentiation, activation, and polarization of microglia and macrophages in normal and diseased CNS. *Glia, 61*(1), 91-103. doi:10.1002/glia.22363

Porras, G., Li, Q., & Bezard, E. (2012). Modeling Parkinson's disease in primates: The MPTP model. *Cold Spring Harbor perspectives in medicine, 2*(3), a009308-a009308. doi:10.1101/cshperspect.a009308

Postuma, R. B., Berg, D., Stern, M., Poewe, W., Olanow, C. W., Oertel, W., . . . Deuschl, G. (2015). MDS clinical diagnostic criteria for Parkinson's disease. *Mov Disord, 30*(12), 1591-1601. doi:10.1002/mds.26424

Prajapati, P., Sripada, L., Singh, K., Bhatelia, K., Singh, R., & Singh, R. (2015). TNF-α regulates miRNA targeting mitochondrial complex-I and induces cell death in dopaminergic cells. *Biochim Biophys Acta, 1852*(3), 451-461. doi:10.1016/j.bbadis.2014.11.019

Pringsheim, T., Jette, N., Frolkis, A., & Steeves, T. D. (2014). The prevalence of Parkinson's disease: a systematic review and meta-analysis. *Mov Disord, 29*(13), 1583-1590. doi:10.1002/mds.25945

Qin, L., Wu, X., Block, M. L., Liu, Y., Breese, G. R., Hong, J. S., . . . Crews, F. T. (2007). Systemic LPS causes chronic neuroinflammation and progressive neurodegeneration. *Glia, 55*(5), 453-462. doi:10.1002/glia.20467

Quarato, G., Guy, C. S., Grace, C. R., Llambi, F., Nourse, A., Rodriguez, D. A., . . . Green, D. R. (2016). Sequential Engagement of Distinct MLKL Phosphatidylinositol-Binding Sites Executes Necroptosis. *Mol Cell, 61*(4), 589-601. doi:10.1016/j.molcel.2016.01.011

Raju, S., Whalen, D. M., Mengistu, M., Swanson, C., Quinn, J. G., Taylor, S. S., . . . Shaw, A. S. (2018). Kinase domain dimerization drives RIPK3-dependent necroptosis. *Sci Signal, 11*(544). doi:10.1126/scisignal.aar2188

Ramirez, A., Heimbach, A., Gründemann, J., Stiller, B., Hampshire, D., Cid, L. P., . . . Kubisch, C. (2006). Hereditary parkinsonism with dementia is caused by mutations in ATP13A2, encoding a lysosomal type 5 P-type ATPase. *Nat Genet, 38*(10), 1184-1191. doi:10.1038/ng1884

Ramonet, D., Daher, J. P. L., Lin, B. M., Stafa, K., Kim, J., Banerjee, R., . . . Moore, D. J. (2011). Dopaminergic neuronal loss, reduced neurite complexity and autophagic abnormalities in transgenic mice expressing G2019S mutant LRRK2. *PloS one, 6*(4), e18568-e18568. doi:10.1371/journal.pone.0018568

Ransom, B. R., Kunis, D. M., Irwin, I., & Langston, J. W. (1987). Astrocytes convert the parkinsonism inducing neurotoxin, MPTP, to its active metabolite, MPP+. *Neurosci Lett, 75*(3), 323-328. doi:10.1016/0304-3940(87)90543-x

Rawal, N., Parish, C., Castelo-Branco, G., & Arenas, E. (2007). Inhibition of JNK increases survival of transplanted dopamine neurons in Parkinsonian rats. *Cell Death Differ, 14*(2), 381-383. doi:10.1038/sj.cdd.4402010

Re, D. B., Le Verche, V., Yu, C., Amoroso, M. W., Politi, K. A., Phani, S., . . . Przedborski, S. (2014). Necroptosis drives motor neuron death in models of both sporadic and familial ALS. *Neuron, 81*(5), 1001-1008. doi:10.1016/j.neuron.2014.01.011

Refolo, V., & Stefanova, N. (2019). Neuroinflammation and Glial Phenotypic Changes in Alpha-Synucleinopathies. *Frontiers in cellular neuroscience, 13*, 263-263. doi:10.3389/fncel.2019.00263

Reichling, L. J., & Riddle, S. M. (2009). Leucine-rich repeat kinase 2 mutants I2020T and G2019S exhibit altered kinase inhibitor sensitivity. *Biochem Biophys Res Commun, 384*(2), 255-258. doi:10.1016/j.bbrc.2009.04.098

Remijsen, Q., Goossens, V., Grootjans, S., Van den Haute, C., Vanlangenakker, N., Dondelinger, Y., . . . Vandenabeele, P. (2014). Depletion of RIPK3 or MLKL blocks TNF-driven necroptosis and switches towards a delayed RIPK1 kinase-dependent apoptosis. *Cell Death Dis, 5*(1), e1004. doi:10.1038/cddis.2013.531

Rickard, J. A., O'Donnell, J. A., Evans, J. M., Lalaoui, N., Poh, A. R., Rogers, T., . . . Silke, J. (2014). RIPK1 regulates RIPK3-MLKL-driven systemic inflammation and emergency hematopoiesis. *Cell, 157*(5), 1175-1188. doi:10.1016/j.cell.2014.04.019

Rickle, A., Bogdanovic, N., Volkman, I., Winblad, B., Ravid, R., & Cowburn, R. F. (2004). Akt activity in Alzheimer's disease and other neurodegenerative disorders. *Neuroreport, 15*(6), 955-959. doi:10.1097/00001756-200404290-00005

Robinson, N., McComb, S., Mulligan, R., Dudani, R., Krishnan, L., & Sad, S. (2012). Type I interferon induces necroptosis in macrophages during infection with Salmonella enterica serovar Typhimurium. *Nat Immunol, 13*(10), 954-962. doi:10.1038/ni.2397

Rocca, W. A. (2017). Time, Sex, Gender, History, and Dementia. *Alzheimer Dis Assoc Disord, 31*(1), 76-79. doi:10.1097/wad.0000000000000187

Rocca, W. A. (2018). The burden of Parkinson's disease: a worldwide perspective. *Lancet Neurol, 17*(11), 928-929. doi:10.1016/s1474-4422(18)30355-7

Rodrigues, C. A. B., Mariz, I. F. A., Maçôas, E. M. S., Afonso, C. A. M., & Martinho, J. M. G. (2012). Two-photon absorption properties of push–pull oxazolones derivatives. *Dyes and Pigments, 95*(3), 713-722. doi:https://doi.org/10.1016/j.dyepig.2012.06.005

Rodrigues, C. A. B., Mariz, I. F. A., Maçôas, E. M. S., Afonso, C. A. M., & Martinho, J. M. G. (2013). Unsaturated oxazolones as nonlinear fluorophores. *Dyes and Pigments, 99*(3), 642-652. doi:https://doi.org/10.1016/j.dyepig.2013.06.012

Rodriguez, D. A., Weinlich, R., Brown, S., Guy, C., Fitzgerald, P., Dillon, C. P., . . . Green, D. R. (2016). Characterization of RIPK3-mediated phosphorylation of the activation loop of MLKL during necroptosis. *Cell Death Differ, 23*(1), 76-88. doi:10.1038/cdd.2015.70

Ros, U., Peña-Blanco, A., Hänggi, K., Kunzendorf, U., Krautwald, S., Wong, W. W., & García-Sáez, A. J. (2017). Necroptosis Execution Is Mediated by Plasma Membrane Nanopores Independent of Calcium. *Cell reports, 19*(1), 175-187. doi:10.1016/j.celrep.2017.03.024

Roser, A. E., Caldi Gomes, L., Schünemann, J., Maass, F., & Lingor, P. (2018). Circulating miRNAs as Diagnostic Biomarkers for Parkinson's Disease. *Front Neurosci, 12*, 625. doi:10.3389/fnins.2018.00625

Ross, G. W., & Petrovitch, H. (2001). Current evidence for neuroprotective effects of nicotine and caffeine against Parkinson's disease. *Drugs Aging, 18*(11), 797-806. doi:10.2165/00002512-200118110-00001

Rubio-Perez, J. M., & Morillas-Ruiz, J. M. (2012). A review: inflammatory process in Alzheimer's disease, role of cytokines. *ScientificWorldJournal, 2012*, 756357. doi:10.1100/2012/756357

Saba, R., Goodman, C. D., Huzarewich, R. L. C. H., Robertson, C., & Booth, S. A. (2008). A miRNA signature of prion induced neurodegeneration. *PloS one, 3*(11), e3652-e3652. doi:10.1371/journal.pone.0003652

Sahab, Z. J., Semaan, S. M., & Sang, Q. X. (2007). Methodology and applications of disease biomarker identification in human serum. *Biomark Insights, 2*, 21-43.

Saleh, D., Najjar, M., Zelic, M., Shah, S., Nogusa, S., Polykratis, A., . . . Degterev, A. (2017). Kinase Activities of RIPK1 and RIPK3 Can Direct IFN-β Synthesis Induced by Lipopolysaccharide. *J Immunol, 198*(11), 4435-4447. doi:10.4049/jimmunol.1601717

Saporito, M. S., Thomas, B. A., & Scott, R. W. (2000). MPTP activates c-Jun NH(2)-terminal kinase (JNK) and its upstream regulatory kinase MKK4 in nigrostriatal neurons in vivo. *J Neurochem, 75*(3), 1200-1208. doi:10.1046/j.1471-4159.2000.0751200.x

Satake, W., Nakabayashi, Y., Mizuta, I., Hirota, Y., Ito, C., Kubo, M., . . . Toda, T. (2009). Genome-wide association study identifies common variants at four loci as genetic risk factors for Parkinson's disease. *Nat Genet, 41*(12), 1303-1307. doi:10.1038/ng.485

Sato, S., Mizuno, Y., & Hattori, N. (2005). Urinary 8-hydroxydeoxyguanosine levels as a biomarker for progression of Parkinson disease. *Neurology, 64*(6), 1081-1083. doi:10.1212/01.Wnl.0000154597.24838.6b

Satterlee, J. S., Barbee, S., Jin, P., Krichevsky, A., Salama, S., Schratt, G., & Wu, D. Y. (2007). Noncoding RNAs in the brain. *J Neurosci, 27*(44), 11856-11859. doi:10.1523/jneurosci.3624-07.2007

Scalzo, P., Kümmer, A., Bretas, T. L., Cardoso, F., & Teixeira, A. L. (2010). Serum levels of brain-derived neurotrophic factor correlate with motor impairment in Parkinson's disease. *J Neurol, 257*(4), 540-545. doi:10.1007/s00415-009-5357-2

Schaar, D. G., Sieber, B. A., Dreyfus, C. F., & Black, I. B. (1993). Regional and cell-specific expression of GDNF in rat brain. *Exp Neurol, 124*(2), 368-371. doi:10.1006/exnr.1993.1207

Schapira, A. H., Cooper, J. M., Dexter, D., Clark, J. B., Jenner, P., & Marsden, C. D. (1990). Mitochondrial complex I deficiency in Parkinson's disease. *J Neurochem, 54*(3), 823-827. doi:10.1111/j.1471-4159.1990.tb02325.x

Schenk, B., & Fulda, S. (2015). Reactive oxygen species regulate Smac mimetic/TNFα-induced necroptotic signaling and cell death. *Oncogene, 34*(47), 5796-5806. doi:10.1038/onc.2015.35

Schildknecht, S., Pape, R., Meiser, J., Karreman, C., Strittmatter, T., Odermatt, M., . . . Leist, M. (2015). Preferential Extracellular Generation of the Active Parkinsonian Toxin MPP+ by Transporter-Independent Export of the Intermediate MPDP+. *Antioxid Redox Signal, 23*(13), 1001-1016. doi:10.1089/ars.2015.6297

Schrag, A., & Schott, J. M. (2006). Epidemiological, clinical, and genetic characteristics of early-onset parkinsonism. *Lancet Neurol, 5*(4), 355-363. doi:10.1016/s1474-4422(06)70411-2

Schulze-Osthoff, K., Bakker, A. C., Vanhaesebroeck, B., Beyaert, R., Jacob, W. A., & Fiers, W. (1992). Cytotoxic activity of tumor necrosis factor is mediated by early damage of mitochondrial functions. Evidence for the involvement of mitochondrial radical generation. *J Biol Chem, 267*(8), 5317-5323.

Schwarzschild, M. A., Schwid, S. R., Marek, K., Watts, A., Lang, A. E., Oakes, D., . . . Ondrasik, J. (2008). Serum urate as a predictor of clinical and radiographic progression in Parkinson disease. *Arch Neurol, 65*(6), 716-723. doi:10.1001/archneur.2008.65.6.nct70003

Schwienbacher, C., Foco, L., Picard, A., Corradi, E., Serafin, A., Panzer, J., . . . Hicks, A. A. (2017). Plasma and White Blood Cells Show Different miRNA Expression Profiles in Parkinson's Disease. *J Mol Neurosci, 62*(2), 244-254. doi:10.1007/s12031-017-0926-9

Schworer, S. A., Smirnova, II, Kurbatova, I., Bagina, U., Churova, M., Fowler, T., . . . Poltorak, A. (2014). Toll-like receptor-mediated down-regulation of the deubiquitinase cylindromatosis (CYLD) protects macrophages from necroptosis in wild-derived mice. *J Biol Chem, 289*(20), 14422-14433. doi:10.1074/jbc.M114.547547

Scian, M. J., Maluf, D. G., David, K. G., Archer, K. J., Suh, J. L., Wolen, A. R., . . . Mas, V. (2011). MicroRNA profiles in allograft tissues and paired urines associate with chronic allograft dysfunction with IF/TA. *Am J Transplant, 11*(10), 2110-2122. doi:10.1111/j.1600-6143.2011.03666.x

Seo, J., Kim, M. W., Bae, K. H., Lee, S. C., Song, J., & Lee, E. W. (2019). The roles of ubiquitination in extrinsic cell death pathways and its implications for therapeutics. *Biochem Pharmacol, 162*, 21-40. doi:10.1016/j.bcp.2018.11.012

Seo, J., Lee, E. W., Sung, H., Seong, D., Dondelinger, Y., Shin, J., . . . Song, J. (2016). CHIP controls necroptosis through ubiquitylation- and lysosome-dependent degradation of RIPK3. *Nature cell biology, 18*(3), 291-302. doi:10.1038/ncb3314

Serafin, A., Foco, L., Zanigni, S., Blankenburg, H., Picard, A., Zanon, A., . . . Schwienbacher, C. (2015). Overexpression of blood microRNAs 103a, 30b, and 29a in L-dopa-treated patients with PD. *Neurology, 84*(7), 645-653. doi:10.1212/wnl.0000000000001258

Shao, Q. H., Chen, Y., Li, F. F., Wang, S., Zhang, X. L., Yuan, Y. H., & Chen, N. H. (2019). TLR4 deficiency has a protective effect in the MPTP/probenecid mouse model of Parkinson's disease. *Acta Pharmacol Sin, 40*(12), 1503-1512. doi:10.1038/s41401-019-0280-2

Sharma, S., Bandopadhyay, R., Lashley, T., Renton, A. E., Kingsbury, A. E., Kumaran, R., . . . Holton, J. L. (2011). LRRK2 expression in idiopathic and G2019S positive Parkinson's disease subjects: a morphological and quantitative study. *Neuropathol Appl Neurobiol, 37*(7), 777-790. doi:10.1111/j.1365-2990.2011.01187.x

Shigehara, K., Yokomuro, S., Ishibashi, O., Mizuguchi, Y., Arima, Y., Kawahigashi, Y., . . . Uchida, E. (2011). Real-time PCR-based analysis of the human bile microRNAome identifies miR-9 as a potential diagnostic biomarker for biliary tract cancer. *PloS one, 6*(8), e23584. doi:10.1371/journal.pone.0023584

Shivdasani, R. A. (2006). MicroRNAs: regulators of gene expression and cell differentiation. *Blood, 108*(12), 3646-3653. doi:10.1182/blood-2006-01-030015

Soreq, L., Salomonis, N., Bronstein, M., Greenberg, D. S., Israel, Z., Bergman, H., & Soreq, H. (2013). Small RNA sequencing-microarray analyses in Parkinson leukocytes reveal deep brain stimulation-induced splicing changes that classify brain region transcriptomes. *Front Mol Neurosci, 6*, 10. doi:10.3389/fnmol.2013.00010

Soreq, L., Salomonis, N., Guffanti, A., Bergman, H., Israel, Z., & Soreq, H. (2015). Whole transcriptome RNA sequencing data from blood leukocytes derived from Parkinson's disease patients prior to and following deep brain stimulation treatment. *Genom Data, 3*, 57-60. doi:10.1016/j.gdata.2014.11.009

Stefani, A., Cerroni, R., Mazzone, P., Liguori, C., Di Giovanni, G., Pierantozzi, M., & Galati, S. (2019). Mechanisms of action underlying the efficacy of deep brain stimulation of the subthalamic nucleus in Parkinson's disease: central role of disease severity. *Eur J Neurosci, 49*(6), 805-816. doi:10.1111/ejn.14088

Sternberg, E. J., Alcalay, R. N., Levy, O. A., & Louis, E. D. (2013). Postural and Intention Tremors: A Detailed Clinical Study of Essential Tremor vs. Parkinson's Disease. *Front Neurol, 4*, 51. doi:10.3389/fneur.2013.00051

Streit, W. J., Mrak, R. E., & Griffin, W. S. T. (2004). Microglia and neuroinflammation: a pathological perspective. *J Neuroinflammation, 1*(1), 14-14. doi:10.1186/1742-2094-1-14

Su, X., Maguire-Zeiss, K. A., Giuliano, R., Prifti, L., Venkatesh, K., & Federoff, H. J. (2008). Synuclein activates microglia in a model of Parkinson's disease. *Neurobiol Aging, 29*(11), 1690-1701. doi:10.1016/j.neurobiolaging.2007.04.006

Su, X., Wang, H., Kang, D., Zhu, J., Sun, Q., Li, T., & Ding, K. (2015). Necrostatin-1 ameliorates intracerebral hemorrhage-induced brain injury in mice through inhibiting RIP1/RIP3 pathway. *Neurochem Res, 40*(4), 643-650. doi:10.1007/s11064-014-1510-0

Sun, L., Wang, H., Wang, Z., He, S., Chen, S., Liao, D., . . . Wang, X. (2012). Mixed lineage kinase domain-like protein mediates necrosis signaling downstream of RIP3 kinase. *Cell, 148*(1-2), 213-227. doi:10.1016/j.cell.2011.11.031

Sun, X., Lee, J., Navas, T., Baldwin, D. T., Stewart, T. A., & Dixit, V. M. (1999). RIP3, a novel apoptosis-inducing kinase. *J Biol Chem, 274*(24), 16871-16875. doi:10.1074/jbc.274.24.16871

Sureshbabu, A., Patino, E., Ma, K. C., Laursen, K., Finkelsztein, E. J., Akchurin, O., . . . Choi, M. E. (2018). RIPK3 promotes sepsis-induced acute kidney injury via mitochondrial dysfunction. *JCI insight, 3*(11). doi:10.1172/jci.insight.98411

Surmeier, D. J., Guzman, J. N., Sanchez, J., & Schumacker, P. T. (2012). Physiological phenotype and vulnerability in Parkinson's disease. *Cold Spring Harbor perspectives in medicine, 2*(7), a009290-a009290. doi:10.1101/cshperspect.a009290

Surmeier, D. J., Obeso, J. A., & Halliday, G. M. (2017). Selective neuronal vulnerability in Parkinson disease. *Nature Reviews Neuroscience, 18*(2), 101-113. doi:10.1038/nrn.2016.178

Taganov, K. D., Boldin, M. P., Chang, K. J., & Baltimore, D. (2006). NF-kappaB-dependent induction of microRNA miR-146, an inhibitor targeted to signaling proteins of innate immune responses. *Proc Natl Acad Sci U S A, 103*(33), 12481-12486. doi:10.1073/pnas.0605298103

Tait, S. W., Oberst, A., Quarato, G., Milasta, S., Haller, M., Wang, R., . . . Green, D. R. (2013). Widespread mitochondrial depletion via mitophagy does not compromise necroptosis. *Cell reports, 5*(4), 878-885. doi:10.1016/j.celrep.2013.10.034

Takahashi, N., Duprez, L., Grootjans, S., Cauwels, A., Nerinckx, W., DuHadaway, J. B., . . . Vandenabeele, P. (2012). Necrostatin-1 analogues: critical issues on the specificity, activity and in vivo use in experimental disease models. *Cell Death Dis, 3*(11), e437. doi:10.1038/cddis.2012.176

Takekawa, M., Tatebayashi, K., & Saito, H. (2005). Conserved docking site is essential for activation of mammalian MAP kinase kinases by specific MAP kinase kinase kinases. *Mol Cell, 18*(3), 295-306. doi:10.1016/j.molcel.2005.04.001

Tang, Y., & Le, W. (2016). Differential Roles of M1 and M2 Microglia in Neurodegenerative Diseases. *Mol Neurobiol, 53*(2), 1181-1194. doi:10.1007/s12035-014-9070-5

Tanzer, M. C., Matti, I., Hildebrand, J. M., Young, S. N., Wardak, A., Tripaydonis, A., . . . Murphy, J. M. (2016). Evolutionary divergence of the necroptosis effector MLKL. *Cell Death Differ, 23*(7), 1185-1197. doi:10.1038/cdd.2015.169

Tatton, N. A., & Kish, S. J. (1997). In situ detection of apoptotic nuclei in the substantia nigra compacta of 1-methyl-4-phenyl-1,2,3,6-tetrahydropyridine-treated mice using terminal deoxynucleotidyl transferase labelling and acridine orange staining. *Neuroscience, 77*(4), 1037-1048. doi:10.1016/s0306-4522(96)00545-3

Tatton, N. A., Maclean-Fraser, A., Tatton, W. G., Perl, D. P., & Olanow, C. W. (1998). A fluorescent double-labeling method to detect and confirm apoptotic nuclei in Parkinson's disease. *Ann Neurol, 44*(3 Suppl 1), S142-148. doi:10.1002/ana.410440721

Taymans, J. M., Van den Haute, C., & Baekelandt, V. (2006). Distribution of PINK1 and LRRK2 in rat and mouse brain. *J Neurochem, 98*(3), 951-961. doi:10.1111/j.1471-4159.2006.03919.x

Teng, X., Degterev, A., Jagtap, P., Xing, X., Choi, S., Denu, R., . . . Cuny, G. D. (2005). Structure-activity relationship study of novel necroptosis inhibitors. *Bioorg Med Chem Lett, 15*(22), 5039-5044. doi:10.1016/j.bmcl.2005.07.077

Teunissen, C. E., Tumani, H., Engelborghs, S., & Mollenhauer, B. (2014). Biobanking of CSF: international standardization to optimize biomarker development. *Clin Biochem, 47*(4-5), 288-292. doi:10.1016/j.clinbiochem.2013.12.024

Thévenet, J., Pescini Gobert, R., Hooft van Huijsduijnen, R., Wiessner, C., & Sagot, Y. J. (2011). Regulation of LRRK2 expression points to a functional role in human monocyte maturation. *PloS one, 6*(6), e21519. doi:10.1371/journal.pone.0021519

Thomas, B., & Beal, M. F. (2007). Parkinson's disease. *Hum Mol Genet, 16 Spec No. 2*, R183-194. doi:10.1093/hmg/ddm159

Thome, A. D., Harms, A. S., Volpicelli-Daley, L. A., & Standaert, D. G. (2016). microRNA-155 Regulates Alpha-Synuclein-Induced Inflammatory Responses in Models of Parkinson Disease. *J Neurosci, 36*(8), 2383-2390. doi:10.1523/jneurosci.3900-15.2016

Tillerson, J. L., & Miller, G. W. (2003). Grid performance test to measure behavioral impairment in the MPTP-treated-mouse model of parkinsonism. *J Neurosci Methods, 123*(2), 189-200. doi:10.1016/s0165-0270(02)00360-6

Titze de Almeida, S. S., Horst, C. H., Soto-Sánchez, C., Fernandez, E., & Titze de Almeida, R. (2018). Delivery of miRNA-Targeted Oligonucleotides in the Rat Striatum by Magnetofection with Neuromag(®). *Molecules, 23*(7). doi:10.3390/molecules23071825

Tokuda, T., Qureshi, M. M., Ardah, M. T., Varghese, S., Shehab, S. A., Kasai, T., . . . El-Agnaf, O. M. (2010). Detection of elevated levels of α-synuclein oligomers in CSF from patients with Parkinson disease. *Neurology, 75*(20), 1766-1772. doi:10.1212/WNL.0b013e3181fd613b

Tokuda, T., Salem, S. A., Allsop, D., Mizuno, T., Nakagawa, M., Qureshi, M. M., . . . El-Agnaf, O. M. (2006). Decreased alpha-synuclein in cerebrospinal fluid of aged individuals and subjects with Parkinson's disease. *Biochem Biophys Res Commun, 349*(1), 162-166. doi:10.1016/j.bbrc.2006.08.024

Tolosa, E., Vila, M., Klein, C., & Rascol, O. (2020). LRRK2 in Parkinson disease: challenges of clinical trials. *Nat Rev Neurol, 16*(2), 97-107. doi:10.1038/s41582-019-0301-2

Tolosa, E., Wenning, G., & Poewe, W. (2006). The diagnosis of Parkinson's disease. *Lancet Neurol, 5*(1), 75-86. doi:10.1016/s1474-4422(05)70285-4

Tomac, A., Lindqvist, E., Lin, L. F. H., Ögren, S. O., Young, D., Hoffer, B. J., & Olson, L. (1995). Protection and repair of the nigrostriatal dopaminergic system by GDNF in vivo. *Nature, 373*(6512), 335-339. doi:10.1038/373335a0

Tong, Y., Yamaguchi, H., Giaime, E., Boyle, S., Kopan, R., Kelleher, R. J., 3rd, & Shen, J. (2010). Loss of leucine-rich repeat kinase 2 causes impairment of protein degradation pathways, accumulation of alpha-synuclein, and apoptotic cell death in aged mice. *Proc Natl Acad Sci U S A, 107*(21), 9879-9884. doi:10.1073/pnas.1004676107

Tortarolo, M., Veglianese, P., Calvaresi, N., Botturi, A., Rossi, C., Giorgini, A., . . . Bendotti, C. (2003). Persistent activation of p38 mitogen-activated protein kinase in a mouse model of familial amyotrophic lateral sclerosis correlates with disease progression. *Mol Cell Neurosci, 23*(2), 180-192. doi:10.1016/s1044-7431(03)00022-8

Torti, M., Vacca, L., & Stocchi, F. (2018). Istradefylline for the treatment of Parkinson's disease: is it a promising strategy? *Expert Opin Pharmacother, 19*(16), 1821-1828. doi:10.1080/14656566.2018.1524876

Trajkovski, M., Hausser, J., Soutschek, J., Bhat, B., Akin, A., Zavolan, M., . . . Stoffel, M. (2011). MicroRNAs 103 and 107 regulate insulin sensitivity. *Nature, 474*(7353), 649-653. doi:10.1038/nature10112

Tsika, E., & Moore, D. J. (2012). Mechanisms of LRRK2-mediated neurodegeneration. *Curr Neurol Neurosci Rep, 12*(3), 251-260. doi:10.1007/s11910-012-0265-8

Tysnes, O. B., & Storstein, A. (2017). Epidemiology of Parkinson's disease. *J Neural Transm (Vienna), 124*(8), 901-905. doi:10.1007/s00702-017-1686-y

Ungerstedt, U. (1968). 6-Hydroxy-dopamine induced degeneration of central monoamine neurons. *Eur J Pharmacol, 5*(1), 107-110. doi:10.1016/0014-2999(68)90164-7

Upton, J. W., Kaiser, W. J., & Mocarski, E. S. (2010). Virus inhibition of RIP3-dependent necrosis. *Cell Host Microbe, 7*(4), 302-313. doi:10.1016/j.chom.2010.03.006

Upton, J. W., Kaiser, W. J., & Mocarski, E. S. (2012). DAI/ZBP1/DLM-1 complexes with RIP3 to mediate virus-induced programmed necrosis that is targeted by murine cytomegalovirus vIRA. *Cell Host Microbe, 11*(3), 290-297. doi:10.1016/j.chom.2012.01.016

Valente, E. M., Abou-Sleiman, P. M., Caputo, V., Muqit, M. M., Harvey, K., Gispert, S., . . . Wood, N. W. (2004). Hereditary early-onset Parkinson's disease caused by mutations in PINK1. *Science, 304*(5674), 1158-1160. doi:10.1126/science.1096284

Van den Hove, D. L., Kompotis, K., Lardenoije, R., Kenis, G., Mill, J., Steinbusch, H. W., . . . Rutten, B. P. (2014). Epigenetically regulated microRNAs in Alzheimer's disease. *Neurobiol Aging, 35*(4), 731-745. doi:10.1016/j.neurobiolaging.2013.10.082

Vandenabeele, P., Galluzzi, L., Vanden Berghe, T., & Kroemer, G. (2010). Molecular mechanisms of necroptosis: an ordered cellular explosion. *Nat Rev Mol Cell Biol, 11*(10), 700-714. doi:10.1038/nrm2970

Vandenabeele, P., Grootjans, S., Callewaert, N., & Takahashi, N. (2013). Necrostatin-1 blocks both RIPK1 and IDO: consequences for the study of cell death in experimental disease models. *Cell Death Differ, 20*(2), 185-187. doi:10.1038/cdd.2012.151

Venderova, K., & Park, D. S. (2012). Programmed cell death in Parkinson's disease. *Cold Spring Harbor perspectives in medicine, 2*(8), a009365. doi:10.1101/cshperspect.a009365

Vercammen, D., Brouckaert, G., Denecker, G., Van de Craen, M., Declercq, W., Fiers, W., & Vandenabeele, P. (1998). Dual signaling of the Fas receptor: initiation of both apoptotic and necrotic cell death pathways. *J Exp Med, 188*(5), 919-930. doi:10.1084/jem.188.5.919

Vilas, D., Sharp, M., Gelpi, E., Genís, D., Marder, K. S., Cortes, E., . . . Alcalay, R. N. (2018). Clinical and neuropathological features of progressive supranuclear palsy in Leucine rich repeat kinase (LRRK2) G2019S mutation carriers. *Mov Disord, 33*(2), 335-338. doi:10.1002/mds.27225

Visvanathan, J., Lee, S., Lee, B., Lee, J. W., & Lee, S.-K. (2007). The microRNA miR-124 antagonizes the anti-neural REST/SCP1 pathway during embryonic CNS development. *Genes & development, 21*(7), 744-749. doi:10.1101/gad.1519107

Vitner, E. B., Salomon, R., Farfel-Becker, T., Meshcheriakova, A., Ali, M., Klein, A. D., . . . Futerman, A. H. (2014). RIPK3 as a potential therapeutic target for Gaucher's disease. *Nat Med, 20*(2), 204-208. doi:10.1038/nm.3449

Wager, T. T., Hou, X., Verhoest, P. R., & Villalobos, A. (2010). Moving beyond Rules: The Development of a Central Nervous System Multiparameter Optimization (CNS MPO) Approach To Enable Alignment of Druglike Properties. *ACS Chemical Neuroscience, 1*(6), 435-449. doi:10.1021/cn100008c

Wager, T. T., Hou, X., Verhoest, P. R., & Villalobos, A. (2016). Central Nervous System Multiparameter Optimization Desirability: Application in Drug Discovery. *ACS Chemical Neuroscience, 7*(6), 767-775. doi:10.1021/acschemneuro.6b00029

Wagner, B. K., & Schreiber, S. L. (2016). The Power of Sophisticated Phenotypic Screening and Modern Mechanism-of-Action Methods. *Cell Chem Biol, 23*(1), 3-9. doi:10.1016/j.chembiol.2015.11.008

Wahid, F., Shehzad, A., Khan, T., & Kim, Y. Y. (2010). MicroRNAs: synthesis, mechanism, function, and recent clinical trials. *Biochim Biophys Acta, 1803*(11), 1231-1243. doi:10.1016/j.bbamcr.2010.06.013

Wan, N., & Lin, G. (2016). Parkinson's Disease and Pesticides Exposure: New Findings From a Comprehensive Study in Nebraska, USA. *J Rural Health, 32*(3), 303-313. doi:10.1111/jrh.12154

Wang, C., Cai, Y., Gu, Z., Ma, J., Zheng, Z., Tang, B. S., . . . Chan, P. (2014). Clinical profiles of Parkinson's disease associated with common leucine-rich repeat kinase 2 and glucocerebrosidase genetic variants in Chinese individuals. *Neurobiol Aging, 35*(3), 725.e721-726. doi:10.1016/j.neurobiolaging.2013.08.012

Wang, D., Xu, L., Lv, L., Fan, Y., Zhang, D-F., Bi, R., Yu, D., Zhang, W., Li, X-A., Li, Y-Y., Yao, Y.G. (2015). Association of the LRRK2 genetic polymorphisms with leprosy in Han Chinese from Southwest China. *Genes Immun, 16*(2), 112-9. doi: 10.1038/gene.2014.72

Wang, H., Sun, L., Su, L., Rizo, J., Liu, L., Wang, L. F., . . . Wang, X. (2014). Mixed lineage kinase domain-like protein MLKL causes necrotic membrane disruption upon phosphorylation by RIP3. *Mol Cell, 54*(1), 133-146. doi:10.1016/j.molcel.2014.03.003

Wang, L., Du, F., & Wang, X. (2008). TNF-alpha induces two distinct caspase-8 activation pathways. *Cell, 133*(4), 693-703. doi:10.1016/j.cell.2008.03.036

Wang, P., Hou, J., Lin, L., Wang, C., Liu, X., Li, D., . . . Cao, X. (2010). Inducible microRNA-155 feedback promotes type I IFN signaling in antiviral innate immunity by targeting suppressor of cytokine signaling 1. *J Immunol, 185*(10), 6226-6233. doi:10.4049/jimmunol.1000491

Wang, X., McCullough, K. D., Franke, T. F., & Holbrook, N. J. (2000). Epidermal growth factor receptor-dependent Akt activation by oxidative stress enhances cell survival. *J Biol Chem, 275*(19), 14624-14631. doi:10.1074/jbc.275.19.14624

Wang, X., Yan, M. H., Fujioka, H., Liu, J., Wilson-Delfosse, A., Chen, S. G., . . . Zhu, X. (2012). LRRK2 regulates mitochondrial dynamics and function through direct interaction with DLP1. *Hum Mol Genet, 21*(9), 1931-1944. doi:10.1093/hmg/dds003

Wang, Z., Jiang, H., Chen, S., Du, F., & Wang, X. (2012). The mitochondrial phosphatase PGAM5 functions at the convergence point of multiple necrotic death pathways. *Cell, 148*(1-2), 228-243. doi:10.1016/j.cell.2011.11.030

Waragai, M., Nakai, M., Wei, J., Fujita, M., Mizuno, H., Ho, G., . . . Hashimoto, M. (2007). Plasma levels of DJ-1 as a possible marker for progression of sporadic Parkinson's disease. *Neurosci Lett, 425*(1), 18-22. doi:10.1016/j.neulet.2007.08.010

Watson, M. B., Richter, F., Lee, S. K., Gabby, L., Wu, J., Masliah, E., . . . Chesselet, M. F. (2012). Regionally-specific microglial activation in young mice over-expressing human wildtype alpha-synuclein. *Exp Neurol, 237*(2), 318-334. doi:10.1016/j.expneurol.2012.06.025

Webber, P. J., & West, A. B. (2009). LRRK2 in Parkinson's disease: function in cells and neurodegeneration. *Febs j, 276*(22), 6436-6444. doi:10.1111/j.1742-4658.2009.07342.x

Weber, J. A., Baxter, D. H., Zhang, S., Huang, D. Y., Huang, K. H., Lee, M. J., . . . Wang, K. (2010). The microRNA spectrum in 12 body fluids. *Clin Chem, 56*(11), 1733-1741. doi:10.1373/clinchem.2010.147405

West, A. B. (2017). Achieving neuroprotection with LRRK2 kinase inhibitors in Parkinson disease. *Exp Neurol, 298*(Pt B), 236-245. doi:10.1016/j.expneurol.2017.07.019

Winter, J., Jung, S., Keller, S., Gregory, R. I., & Diederichs, S. (2009). Many roads to maturity: microRNA biogenesis pathways and their regulation. *Nature cell biology, 11*(3), 228-234. doi:10.1038/ncb0309-228

Wu, J., Huang, Z., Ren, J., Zhang, Z., He, P., Li, Y., . . . Han, J. (2013). Mlkl knockout mice demonstrate the indispensable role of Mlkl in necroptosis. *Cell Research, 23*(8), 994-1006. doi:10.1038/cr.2013.91

Wu, X. N., Yang, Z. H., Wang, X. K., Zhang, Y., Wan, H., Song, Y., . . . Han, J. (2014). Distinct roles of RIP1-RIP3 hetero- and RIP3-RIP3 homo-interaction in mediating necroptosis. *Cell Death Differ, 21*(11), 1709-1720. doi:10.1038/cdd.2014.77

Wu, Y. T., Tan, H. L., Huang, Q., Ong, C. N., & Shen, H. M. (2009). Activation of the PI3K-Akt-mTOR signaling pathway promotes necrotic cell death via suppression of autophagy. *Autophagy, 5*(6), 824-834. doi:10.4161/auto.9099

Wu, Y. T., Tan, H. L., Huang, Q., Sun, X. J., Zhu, X., & Shen, H. M. (2011). zVAD-induced necroptosis in L929 cells depends on autocrine production of TNFα mediated by the PKC-MAPKs-AP-1 pathway. *Cell Death Differ, 18*(1), 26-37. doi:10.1038/cdd.2010.72

Xia, B., Fang, S., Chen, X., Hu, H., Chen, P., Wang, H., & Gao, Z. (2016). MLKL forms cation channels. *Cell Res, 26*(5), 517-528. doi:10.1038/cr.2016.26

Xie, T., Peng, W., Liu, Y., Yan, C., Maki, J., Degterev, A., . . . Shi, Y. (2013). Structural basis of RIP1 inhibition by necrostatins. *Structure, 21*(3), 493-499. doi:10.1016/j.str.2013.01.016

Xie, T., Peng, W., Yan, C., Wu, J., Gong, X., & Shi, Y. (2013). Structural insights into RIP3-mediated necroptotic signaling. *Cell reports, 5*(1), 70-78. doi:10.1016/j.celrep.2013.08.044

Xu, Q., Shenoy, S., & Li, C. (2012). Mouse models for LRRK2 Parkinson's disease. *Parkinsonism Relat Disord, 18 Suppl 1*, S186-189. doi:10.1016/s1353-8020(11)70058-x

Xu, X., Chua, C. C., Kong, J., Kostrzewa, R. M., Kumaraguru, U., Hamdy, R. C., & Chua, B. H. (2007). Necrostatin-1 protects against glutamate-induced glutathione depletion and caspase-independent cell death in HT-22 cells. *J Neurochem, 103*(5), 2004-2014. doi:10.1111/j.1471-4159.2007.04884.x

Yang, H., Ma, Y., Chen, G., Zhou, H., Yamazaki, T., Klein, C., . . . Kroemer, G. (2016). Contribution of RIP3 and MLKL to immunogenic cell death signaling in cancer chemotherapy. *Oncoimmunology, 5*(6), e1149673. doi:10.1080/2162402x.2016.1149673

Yang, Z., Wang, Y., Zhang, Y., He, X., Zhong, C. Q., Ni, H., . . . Han, J. (2018). RIP3 targets pyruvate dehydrogenase complex to increase aerobic respiration in TNF-induced necroptosis. *Nature cell biology, 20*(2), 186-197. doi:10.1038/s41556-017-0022-y

Yatim, N., Jusforgues-Saklani, H., Orozco, S., Schulz, O., Barreira da Silva, R., Reis e Sousa, C., . . . Albert, M. L. (2015). RIPK1 and NF-κB signaling in dying cells determines cross-priming of $CD8^+$ T cells. *Science, 350*(6258), 328-334. doi:10.1126/science.aad0395

Ye, Y. C., Yu, L., Wang, H. J., Tashiro, S., Onodera, S., & Ikejima, T. (2011). TNFα-induced necroptosis and autophagy via supression of the p38-NF-κB survival pathway in L929 cells. *J Pharmacol Sci, 117*(3), 160-169. doi:10.1254/jphs.11105fp

Yeh, W. C., de la Pompa, J. L., McCurrach, M. E., Shu, H. B., Elia, A. J., Shahinian, A., . . . Mak, T. W. (1998). FADD: essential for embryo development and signaling from some, but not all, inducers of apoptosis. *Science, 279*(5358), 1954-1958. doi:10.1126/science.279.5358.1954

Yılmaz S, G., Geyik, S., Neyal, A. M., Soko, N. D., Bozkurt, H., & Dandara, C. (2016). Hypothesis: Do miRNAs Targeting the Leucine-Rich Repeat Kinase 2 Gene (LRRK2) Influence Parkinson's Disease Susceptibility? *Omics, 20*(4), 224-228. doi:10.1089/omi.2016.0040

Yoshikawa, M., Saitoh, M., Katoh, T., Seki, T., Bigi, S. V., Shimizu, Y., . . . Yogo, T. (2018). Discovery of 7-Oxo-2,4,5,7-tetrahydro-6 H-pyrazolo[3,4- c]pyridine Derivatives as Potent, Orally Available, and Brain-Penetrating Receptor Interacting Protein 1 (RIP1) Kinase Inhibitors: Analysis of Structure-Kinetic Relationships. *J Med Chem, 61*(6), 2384-2409. doi:10.1021/acs.jmedchem.7b01647

Yu, J. Y., Chung, K. H., Deo, M., Thompson, R. C., & Turner, D. L. (2008). MicroRNA miR-124 regulates neurite outgrowth during neuronal differentiation. *Exp Cell Res, 314*(14), 2618-2633. doi:10.1016/j.yexcr.2008.06.002

Yu, L., Wan, F., Dutta, S., Welsh, S., Liu, Z., Freundt, E., . . . Lenardo, M. (2006). Autophagic programmed cell death by selective catalase degradation. *Proc Natl Acad Sci U S A, 103*(13), 4952-4957. doi:10.1073/pnas.0511288103

Yu, P. W., Huang, B. C. B., Shen, M., Quast, J., Chan, E., Xu, X., . . . Luo, Y. (1999). Identification of RIP3, a RIP-like kinase that activates apoptosis and NFκB. *Current Biology, 9*(10), 539-S533. doi:https://doi.org/10.1016/S0960-9822(99)80239-5

Yuan, J., Amin, P., & Ofengeim, D. (2019). Necroptosis and RIPK1-mediated neuroinflammation in CNS diseases. *Nat Rev Neurosci, 20*(1), 19-33. doi:10.1038/s41583-018-0093-1

Yuan, Y., Sun, J., Zhao, M., Hu, J., Wang, X., Du, G., & Chen, N. H. (2010). Overexpression of alpha-synuclein down-regulates BDNF expression. *Cell Mol Neurobiol, 30*(6), 939-946. doi:10.1007/s10571-010-9523-y

Yun, S. P., Kam, T.-I., Panicker, N., Kim, S., Oh, Y., Park, J.-S., . . . Ko, H. S. (2018). Block of A1 astrocyte conversion by microglia is neuroprotective in models of Parkinson's disease. *Nature Medicine, 24*(7), 931-938. doi:10.1038/s41591-018-0051-5

Zhang, D. W., Shao, J., Lin, J., Zhang, N., Lu, B. J., Lin, S. C., . . . Han, J. (2009). RIP3, an energy metabolism regulator that switches TNF-induced cell death from apoptosis to necrosis. *Science, 325*(5938), 332-336. doi:10.1126/science.1172308

Zhang, W., Wang, T., Pei, Z., Miller, D. S., Wu, X., Block, M. L., . . . Zhang, J. (2005). Aggregated alpha-synuclein activates microglia: a process leading to disease progression in Parkinson's disease. *Faseb j, 19*(6), 533-542. doi:10.1096/fj.04-2751com

Zhang, X., Fan, C., Zhang, H., Zhao, Q., Liu, Y., Xu, C., . . . Zhang, H. (2016). MLKL and FADD Are Critical for Suppressing Progressive Lymphoproliferative Disease and Activating the NLRP3 Inflammasome. *Cell reports, 16*(12), 3247-3259. doi:10.1016/j.celrep.2016.06.103

Zhang, Y., Su, S. S., Zhao, S., Yang, Z., Zhong, C.-Q., Chen, X., . . . Han, J. (2017). RIP1 autophosphorylation is promoted by mitochondrial ROS and is essential for RIP3 recruitment into necrosome. *Nature Communications, 8*(1), 14329. doi:10.1038/ncomms14329

Zhao, H. T., John, N., Delic, V., Ikeda-Lee, K., Kim, A., Weihofen, A., . . . Volpicelli-Daley, L. A. (2017). LRRK2 Antisense Oligonucleotides Ameliorate α-Synuclein Inclusion Formation in a Parkinson's Disease Mouse Model. *Mol Ther Nucleic Acids, 8*, 508-519. doi:10.1016/j.omtn.2017.08.002

Zhao, J., Jitkaew, S., Cai, Z., Choksi, S., Li, Q., Luo, J., & Liu, Z. G. (2012). Mixed lineage kinase domain-like is a key receptor interacting protein 3 downstream component of TNF-

induced necrosis. *Proc Natl Acad Sci U S A, 109*(14), 5322-5327. doi:10.1073/pnas.1200012109

Zhao, X. M., Chen, Z., Zhao, J. B., Zhang, P. P., Pu, Y. F., Jiang, S. H., . . . Zhang, S. Q. (2016). Hsp90 modulates the stability of MLKL and is required for TNF-induced necroptosis. *Cell Death Dis, 7*(2), e2089. doi:10.1038/cddis.2015.390

Zhou, T., Wang, Q., Phan, N., Ren, J., Yang, H., Feldman, C. C., . . . Liu, B. (2019). Identification of a novel class of RIP1/RIP3 dual inhibitors that impede cell death and inflammation in mouse abdominal aortic aneurysm models. *Cell Death Dis, 10*(3), 226. doi:10.1038/s41419-019-1468-6

Zhou, W., & Yuan, J. (2014). Necroptosis in health and diseases. *Semin Cell Dev Biol, 35*, 14-23. doi:10.1016/j.semcdb.2014.07.013

Zhou, Y., Lu, M., Du, R.-H., Qiao, C., Jiang, C.-Y., Zhang, K.-Z., . . . Hu, G. (2016). MicroRNA-7 targets Nod-like receptor protein 3 inflammasome to modulate neuroinflammation in the pathogenesis of Parkinson's disease. *Molecular Neurodegeneration, 11*, 28-28. doi:10.1186/s13024-016-0094-3

Zhu, K., Liang, W., Ma, Z., Xu, D., Cao, S., Lu, X., . . . Yuan, J. (2018). Necroptosis promotes cell-autonomous activation of proinflammatory cytokine gene expression. *Cell Death Dis, 9*(5), 500. doi:10.1038/s41419-018-0524-y

Zhu, M., Cortese, G. P., & Waites, C. L. (2018). Parkinson's disease-linked Parkin mutations impair glutamatergic signaling in hippocampal neurons. *BMC Biol, 16*(1), 100. doi:10.1186/s12915-018-0567-7

Zhu, S., Zhang, Y., Bai, G., & Li, H. (2011). Necrostatin-1 ameliorates symptoms in R6/2 transgenic mouse model of Huntington's disease. *Cell Death Dis, 2*(1), e115. doi:10.1038/cddis.2010.94

Zhuang, C., & Chen, F. (2020). Small-Molecule Inhibitors of Necroptosis: Current Status and Perspectives. *J Med Chem, 63*(4), 1490-1510. doi:10.1021/acs.jmedchem.9b01317

Ziemssen, T., Akgün, K., & Brück, W. (2019). Molecular biomarkers in multiple sclerosis. *J Neuroinflammation, 16*(1), 272. doi:10.1186/s12974-019-1674-2

Zimprich, A., Biskup, S., Leitner, P., Lichtner, P., Farrer, M., Lincoln, S., . . . Gasser, T. (2004). Mutations in LRRK2 cause autosomal-dominant parkinsonism with pleomorphic pathology. *Neuron, 44*(4), 601-607. doi:10.1016/j.neuron.2004.11.005

ACKNOWLEDGEMENTS

Durante estes anos de doutoramento tive a oportunidade de conhecer pessoas incríveis, que sempre me apoiaram e permitiram crescer e aprender enquanto pessoa e cientista. Aproveito, por isso, para agradecer a todos de um modo geral e a alguns em particular.

Em primeiro lugar, agradeço profundamente à Professora Cecília Rodrigues, orientadora desta tese, por todo o seu apoio ao longo deste projeto e pela constante disponibilidade para discutir e encorajar sobre o melhor caminho a seguir.

Um especial obrigado à Joana Amaral, coorientadora desta tese, pela enorme paciência, compreensão, ajuda e espírito crítico com que sempre me ouviste e ajudaste. Agradeço por toda a orientação ao longo destes anos e por teres sempre uma solução possível para os problemas que foram surgindo. Obrigada Joana!

Deixo também um obrigado ao Professor Doutor Félix Carvalho, pelo seu papel de coorientador ao longo do desenvolvimento deste trabalho.

Agradeço também ao Pedro Dionísio, por teres desbravado com tanta sabedoria o caminho que acabei por também percorrer. Um grande obrigado por teres estado sempre presente, disponível e disposto a ajudar em tudo. Afinal, vamos sempre ter aquele fatídico mês de Agosto, não é? 😊

Um enorme obrigado a todos os elementos do grupo Cellular Function and Therapeutic Targeting, por me terem recebido com tanta simpatia e alegria. Agradeço aos “pós-Docs” Rui e Susana, por toda a acessibilidade e disponibilidade que sempre mostraram para ajudar e esclarecer qualquer dúvida que fosse surgindo. Um obrigado também à Professora Maria João Gama, à Professora Elsa, à Professora Margarida Castro-Caldas, à Maria João Nunes e à Andreia Carvalho, por todas as sugestões e críticas construtivas que me deram ao longo destes anos e que tanto ajudaram no meu trabalho.

Um grande agradecimento fica também aqui aos ex-membros CellFun, Diane Aurore, Maria Ribeiro, Pedro Rodrigues, Hugo Brito e Cláudia, por todos os conselhos, simpatia, espírito de ajuda e boa disposição. Um enorme obrigado a todos os ainda-membros CellFun, André Santos, André Simão, Vanda, Miguel, Sónia, Rita, Vivane e Tawidul, pelo constante bom ambiente que sempre se viveu no laboratório e pelos divertidos almoços, sempre cheios de animação.

Agradeço também aos meus queridos amigos bairradinos, por me terem enchido de boa disposição e permitido recarregar energias durante os fins de semana destes últimos anos :p Um grande beijinho de obrigada!

Um gigante gigante gigante obrigada ao João, por teres estado sempre disponível para me ouvir ao longo de todo este tempo, por todo o incentivo e por todos os momentos que partilhamos. Obrigada por todo o apoio e palavras de força, em especial neste último ano, que o tornaram sem dúvida mais fácil. Obrigada por tudo, e o resto tu sabes 😊

Por último, deixo um especial agradecimento à minha família e, em particular, à minha Mãe, por todo o amor, apoio e dedicação, ao longo de toda a minha vida, que me permitiu alcançar tanto. Obrigada pela paciência, por teres sempre uma palavra de motivação e por me ouvires sempre que preciso! Obrigada!